Fotocatalisadores e adsorventes contendo caulinita e laponita aplicados na depuração de contaminantes orgânicos e síntese de metaloftalocianina via caulinita/nitroftalonitrilo como precursores.

Fotocatalizadores y adsorbentes basados en caolinita y laponita aplicados en la depuración de contaminantes orgánicos y en la síntesis de metaloftalocianina vía precursores caolinita/nitroftalonitrilo.

Tiago Honorato da Silva

UNIVERSIDADE DE FRANCA/
UNIVERSIDAD DE SALAMANCA

Franca 2019

Fotocatalisadores e adsorventes contendo caulinita e laponita aplicados na depuração de contaminantes orgânicos e síntese de metaloftalocianina via caulinita/nitroftalonitrilo como precursores.

Fotocatalizadores y adsorbentes basados en caolinita y laponita aplicados en la depuración de contaminantes orgánicos y en la síntesis de metaloftalocianina vía precursores caolinita/nitroftalonitrilo.

Tese apresentada pelo Bacharel em Engenharia Química **D Tiago Honorato da Silva** para obter o Título de Doutor em Ciências Químicas

Tesis presentada por el Licenciado en Ingeniería Química **D. Tiago Honorato da Silva** para optar al Grado de Doctor en Ciencias Químicas

Franca, 31 de maio de 2019

Salamanca, 31 de mayo de 2019

Tiago Honorato da Silva

Emerson Henrique de Faria, Professor de Química da Universidade de Franca, Brasil, e Miguel Ángel Vicente Rodríguez, Catedrático de Química Inorgânica da Universidade de Salamanca, Espanha, como orientadores do trabalho intitulado “Fotocatalisadores e adsorventes contendo caulinita e laponita aplicados na depuração de contaminantes orgânicos e síntese de metaloftalocianina via caulinita/nitroftalonitrilo como precursores”.

AFIRMAM:

Este trabalho foi realizado pelo Bacharel em Engenharia Química D Tiago Honorato da Silva para se candidatar ao Doutorado em Química, dentro dos Programas de Doutorado “Ciências – Universidade de Franca, Brasil” e “Ciência e Tecnologia Química – Universidad de Salamanca, Espanha”. Considerando que constitui um trabalho de pesquisa original, está completo e cumpre todos os requisitos exigidos para a defesa pública, autorizando sua apresentação.

Franca, 31 de maio de 2019
Salamanca, 31 de mayo de 2019

Emerson Henrique de Faria

Miguel Ángel Vicente Rodríguez

Emerson Henrique de Faria, Profesor de Química de la Universidad de Franca, Brasil, y Miguel Ángel Vicente Rodríguez, Catedrático de Química Inorgánica de la Universidad de Salamanca, España, como orientadores del trabajo titulado “Fotocatalizadores y adsorbentes que contienen caulinita y laponita aplicados en la depuración de contaminantes orgánicos y síntesis de metaloftalocianina vía caulinita/nitroftalonitrilo como precursores”.

HACEN CONSTAR

Este trabajo fue realizado por el Licenciado en Ingeniería Química D Tiago Honorato da Silva para optar al Doctorado en Química, dentro de los Programas de Doctorado "Ciências - Universidad de Franca, Brasil" y "Ciencia y Tecnología Química - Universidad de Salamanca, España". Considerando que constituye un trabajo de investigación original, está completo y cumple todos los requisitos exigidos para la defensa pública, autorizando su presentación.

Franca, 31 de maio de 2019
Salamanca, 31 de mayo de 2019

Emerson Henrique de Faria Miguel Ángel Vicente Rodríguez

AUTORIZAÇÃO DOS ORIENTADORES

A presente Tese de Doutorado é apresentada no formato de um compilado artigos/publicações. Os orientadores desta Tese de Doutorado autorizam sua apresentação nesse formado de um compilado artigos/publicações.

Emerson Henrique de Faria

Miguel Ángel Vicente Rodríguez

RELATÓRIO DA COMISSÃO ACADÊMICA DO PROGRAMA DE DOUTORADO

A Comissão Acadêmica do Programa de Doutorado Ciências e Tecnologias Químicas emite informe positivo sobre a alteração do título e sobre a apresentação no formato de um compilado de artigos/publicações desta Tese de Doutorado

Encarnación Rodríguez Gonzalo (Presidenta de la Comisión)

RELATÓRIO DA COMISSÃO DE DOUTORATO E PÓS-GRADUAÇÃO DA UNIVERSIDADE

A comissão de Doutorado e Pós-Graduação da Universidade de Salamanca emite informe positivo sobre a alteração do título e sobre a apresentação no formato de um compilado de artigos/publicações desta Tese de Doutorado

AUTORIZACIÓN DE LOS CODIRECTORES

La presente Tesis Doctoral se presenta en el formato de compendio de artículos/publicaciones. Los codirectores de esta Tesis Doctoral autorizamos su presentación en el formato de compendio de artículos/publicaciones.

Emerson Henrique de Faria

Miguel Ángel Vicente Rodríguez

INFORME DE LA COMISIÓN ACADÉMICA DEL PROGRAMA DE DOCTORADO

La Comisión Académica del Programa de Doctorado Ciencia y Tecnología Químicas emite informe positivo sobre el cambio de título y sobre la presentación en el formato de compendio de artículos/publicaciones de esta Tesis Doctoral.

Encarnación Rodríguez Gonzalo (Presidenta de la Comisión)

INFORME DE LA COMISIÓN DE DOCTORADO Y POSGRADO DE LA UNIVERSIDAD

La Comisión de Doctorado y Posgrado de la Universidad de Salamanca emite informe positivo sobre el cambio de título y sobre la presentación en el formato de compendio de artículos/publicaciones de esta Tesis Doctoral.

A presente Tese de Doutorado intitulada “Fotocatalisadores e adsorventes contendo caulinita e laponita aplicados na depuração de contaminantes orgânicos e síntese de metaloftalocianina via caulinita/nitroftalonitrilo como precursores”, elaborado pelo Bacharel em Engenharia Química Tiago Honorato da Silva e que constitui sua Tese de Doutorado para obter o grau de Doutor em Ciências, foi escrita no formato de um compilado de artigos originais de investigação, publicados em revistas científicas de prestígio e indexadas na edição científica do *Journal Citation Reports.*

E para este fim, os artigos originais exigidos, seu título, autores e sua afiliação, juntamente com a referência completa da revista científica onde foram publicados, estão listados abaixo:

La presente Tesis Doctoral titulada “Fotocatalizadores y adsorbentes que contienen caolinita y laponita aplicados en la depuración de contaminantes orgánicos y síntesis de metaloftalocianina vía caulinita/nitroftalonitrilo como precursores”, elaborada por el Licenciado Tiago Honorato da Silva y que constituye su Tesis Doctoral para optar al grado de Doctor en Ciencias, ha sido redactada en el formato de compendio de artículos originales de investigación publicados en revistas científicas de prestigio e indexadas en la edición científica del *Journal Citation Reports*.

Y para que así conste se recogen a continuación los artículos originales requeridos, su título, autores y afiliación de los mismos, junto con la referencia completa de la revista científica donde fueron publicados:

New strategies for synthesis and immobilization of methalophtalocyanines onto kaolinite: Preparation, characterization and chemical stability evaluation

Dyes and Pigments 134 (2016) 41-50
DOI: 10.1016/j.dyepig.2016.06.044

Tiago Honorato da Silva[a], Thalita F.M. de Souza[b], Anderson Orzari Ribeiro[b], Paulo Sergio Calefi[c], Katia Jorge Ciuffi[a], Eduardo Jose Nassar[a], Eduardo Ferreira Molina[a], Peter Hamer[d], Emerson Henrique de Faria[a]

[a] *Grupo de Pesquisa em Materiais Lamelares Híbridos -GPMatLam e Universidade de Franca, Av. Dr. Armando Salles Oliveira, Pq. Universitário, 201, CEP 14404-600, Franca, SP, Brazil*

[b] *Centro de Ciências Naturais e Humanas, Universidade Federal do ABC – UFABC, R. Santa Adélia 166, 09210-170, Santo André, SP, Brazil*

[c] *Instituto Federal de Educação, Ciência e Tecnologia de São Paulo – IFSP, Campus Sertãozinho, Rua Américo Ambrósio, Jd. Canaã, 269, CEP, ~ 14169-263, Sertãozinho, SP, Brazil*

[d] *Instituto de Química, UNESP-Universidade Estadual Paulista, 14800-900, Araraquara, SP, Brazil*

Laponite functionalized with biuret and melamine: Application to adsorption of antibiotic trimethoprim.

Microporous and Mesoporous Materials 253 (2017) 112-122

DOI: 10.1016/j.micromeso.2017.06.047

Beatriz Gonzalez[a], Tiago H. da Silva[b], Katia J. Ciuffi[b], Miguel A. Vicente[a], Raquel Trujillano[a], Vicente Rives[a], Emerson H. de Faria[b], Sophia A. Korili[c], Antonio Gil[c]

[a] *GIR-QUESCAT, Departamento de Química Inorganica, Universidad de Salamanca, 37008 Salamanca, Spain*

[b] *Universidade de Franca, Av. Dr. Armando Salles Oliveira, Parque Universitario, 201, 14404-600, Franca, SP, Brazil*

[c] *Departamento de Química Aplicada, Edificio de los Acebos, Universidad Pública de Navarra, Campus Arrosadía, 31006 Pamplona, Spain*

Kaolinite/TiO_2/cobalt(II) tetracarboxymetallophthalocyanine Nanocomposites as Heterogeneous Photocatalysts for Decomposition of Organic Pollutants Trimethoprim, Caffeine and Prometryn.

Journal of the Brazilian Chemical Society Vol. 00, No. 00, 1-14, 2019

DOI: 10.21577/0103-5053.20190178

Tiago H. da Silva[a], Anderson Orzari Ribeiro[b], Eduardo J. Nassar[a], Raquel Trujillano[c], Vicente Rives[c], Miguel A. Vicente[c], Emerson H. de Faria[a], Katia J. Ciuffi[a]

[a] *Universidade de Franca, Av. Dr. Armando Salles Oliveira, 201, Pq. Universitário CEP 14404-600 Franca-SP-Brazil*

[b] *Centro de Ciências Naturais e Humanas, Universidade Federal do ABC, 09210-170, Santo André, SP, Brazil*

[c] *GIR-QUESCAT, Departamento de Química Inorgánica. Universidad de Salamanca, 37008-Salamanca, Spain*

Dedico a Deus;

Aos meus pais Décio Andrade da Silva e Janei Adriana Honorato de Andrade, pela dedicação, carinho e peço desculpas pelas faltas em alguns momentos, mas foi para alcançarmos o objetivo traçado.

Aos meus familiares, amigos e colegas de trabalho... Vocês foram responsáveis por essa conquista, sem exceções.

Peça Felicidade

Gabriela Melim

Hoje vamos desejar o bem
Sem olhar a quem
Acabar com a solidão
No ato de estender a mão

Peça tudo o que você quiser
Acredite na sua fé
Paz, saúde, vigor, sucesso
Alegria, esperança, amor

Aproveite todas as sensações
Sinta a chuva te molhar
E quando o sol chegar
Deixa esquentar

Tenha dentro do seu coração
Pureza e verdade
O que você transmitir
Volta com intensidade

Quando não souber o que pedir
Peça felicidade
Quando não souber o que doar
Doe sua metade

E depois
Vai sentir a energia
E satisfação de ver nascer um novo dia

Agradecimentos

Agradeço a todos que contribuíram para realização desse sonho, seja no âmbito profissional, pessoal e acadêmico, pois “quem caminha sozinho pode até chegar mais rápido, mas aquele que caminha acompanhado, com certeza vai mais longe” – Clarice Lispector.

Desta maneira alguns nomes são inevitáveis à citação. Meus pais, Décio Andrade da Silva e Janei Adriana Honorato de Andrade, pelo apoio incondicional, amizade, conselhos e incentivo total na construção desse trabalho. Estendo o agradecimento a toda minha família pelo apoio, mesmo não entendendo ou concordando com vários passos durante a caminhada.

Aos colegas de laboratório de pesquisa Sol Gel, agradeço todos os momentos juntos, de apoio, discussões científicas, brincadeiras, risos, puxões de orelhas, enfim, todos os momentos que serviram para construir relacionamentos que vão além de um laboratório, amizades que serão eternas. Em especial, gostaria de agradecer ao Breno e à Larissa, pois caminhamos juntos e sempre me auxiliaram no que precisei.

Aos meus amigos de trabalho, professor Dr. Gustavo Ricci e às professoras Dra. Emiliane e Dra. Liziane, pela amizade, apoio, carinho. Obrigado por fazer parte não somente do círculo profissional, mas também pessoal.

Aos professores do grupo, Prof. Dr. Lucas A. Rocha e Prof. Dr. Eduardo J. Nassar, por compartilharem ensinamentos científicos e pessoais. À Profa. Dra. Katia J. Ciuffi, pela confiança na proposta de um doutorado sanduíche e posterior acordo de cotutela, meu muito obrigado.

Ao meu orientador Prof. Dr. Emerson H. de Faria, pela amizade vinda de outrora, pela confiança e pelo apoio também no processo do doutorado sanduíche, paciência e compreensão em alguns atrasos. Enfim, vocês contribuíram imensamente para a minha formação profissional e pessoal, meu muito obrigado.

Agradeço ao Prof. Dr. Miguel A. V. Rodríguez pelo aceite e recepção no laboratório de “Química del Estado Sólido, Materiales y Catálisis Heterogénea GIR – QUESCAT” da Universidad de Salamanca, Espanha, estendendo meu agradecimento a todos os professores do grupo.

Ao caríssimo Prof. Marco A. Verzola, ex-coordenador dos cursos de química da Universidade de Franca, que permitiu e apoiou o desenvolver do doutorado, contribuindo para a obtenção da bolsa institucional (UNIFRAN) e com o afastamento para a realização do doutorado sanduíche.

À Universidade de Franca – UNIFRAN, por conceder a bolsa de estudos institucional e a liberação para a estância na Universidad de Salamanca, Espanha, para o doutorado sanduíche.

Gostaria de agradecer, em especial, às Universidades de Franca e Salamanca, pelo acordo institucional bilateral entre ambas, que possibilitou firmar e realizar a tese de doutorado em regime de cotutela, desde seu desenvolvimento até a avaliação na defesa, compartilhando as responsabilidades e avaliações dos correspondentes programas de doutorado.

Agradeço também às agências que fomentam e apoiam as pesquisas.

- O presente trabalho foi realizado com apoio da Coordenação de Aperfeiçoamento de Pessoal de Nível Superior - Brasil (CAPES) - Código de Financiamento 001;
- Fundação de Amparo à Pesquisa do Estado de São Paulo (FAPESP);
- Conselho Nacional de Desenvolvimento Científico e Tecnológico (CNPq).

Acknowledgements Article I

The authors thank a Cooperation Grant jointly financed by Universidad de Salamanca (Spain) and FAPESP (Brasil, 2016/50322-2). This study was financed in part by the Coordenação de Aperfeiçoamento de Pessoal de Nível Superior - Brasil (CAPES) - Finance Code 001. The Brazilian group acknowledges the support from the Brazilian research funding agencies Fundação de Amparo à Pesquisa do Estado de São Paulo (FAPESP) (2017/15482-1,2016/01501–1), CAPES (317/15 and 0274-16) and Conselho Nacional de Desenvolvimento Científico e Tecnológico (CNPq) (305398/2015-6, 302668/2017-9, 311767/2015-0).

Acknowledgments Article II

This work has been carried out in the frame of a Spain–Brazil Interuniversity Cooperation Grant, financed by MEC (PHBP14/00003) and CAPES (317/15 and 0274-16) and a Cooperation Grant from Universidad de Salamanca and FAPESP (2016/50322-2). The Spanish authors thank financial support from *Agencia Estatal de Investigación, AEI* (Spanish Ministry of Economy and Competitiveness, MINECO) and the European Regional Development Fund, ERDF (grant MAT2013–47811–C2–R). The Brazilian group thanks support from Brazilian Research funding agencies FAPESP (2013/19523–3) CAPES and CNPq.

Acknowledgements Article III

The authors thank the Brazilian funding agencies FAPESP (2013/19523-3), CAPES, and CNPq and Prof. Tiago Venâncio (Universidade Federal de São Carlos) for assistance with ^{27}Al nuclear magnetic resonance analyses.

Sumário

SIGLAS E ABREVIATURAS

INTRODUÇÃO

POEs	Poluentes Orgânicos Emergentes
POAs	Processos Oxidativos Avançados
UV/Vis	Radiação ultravioleta/visível
MPCs	Metaloftalocianina
LUMO	Orbital molecular mais baixo desocupado
HOMO	Orbital molecular mais alto ocupado

ARTIGO I

EOPs	Poluentes orgânicos emergentes
TMP	Trimetoprim
CFF	Cafeína
PMT	Prometrina
AOP	Processos de oxidação avançados
Kaol	Caulinita purificada
CAR	Compósito obtido por rota ácida
CBR	Compósito obtido por rota básica
CoMPc	Tetracarboxiftalocianina de cobalto (II)
CAR-CoMPc	Compósito obtido por rota ácida com CoMPC
CBR-CoMPc	Compósito obtido por rota básica com CoMPC
BET	Análise de área superficial e porosidade
DTA-TGA	Análise térmica – TGA
	Análise térmica diferencial – DTA
FTIR	Espectroscopia de absorção molecular no infravermelho
ICP-MS	Espectrometria de absorção atômica com plasma induzido
PXRD	Difratometria de raios X

ARTIGO II

BET	Análise de área superficial e porosidade
Biu	Biureto
ClPTES	(3-cloropropil)trietoxisilano
CNP	Compósito polímero-argila
DTA-TGA	Análise térmica – TGA
	Análise térmica diferencial – DTA
FTIR	Espectroscopia de absorção molecular no infravermelho
ICP	Espectrometria de absorção atômica com plasma induzido
Lap	Laponita
Lap-Biu	Laponita funcionalizada com biureto por rota não aquosa
Lap-BiuH	Laponita funcionalizada com melamina por rota aquosa
Lap-Mel	Laponita funcionalizada com melamina por rota não aquosa
Lap-MelH	Laponita funcionalizada com melamina por rota aquosa
Mel	Melamina
PXRD	Difratometria de raios X
SEM	Microscopia eletrônica de Varredura
TMP	Trimetoprim

ARTIGO III

DMSO	Dimetilsulfóxido
KaDMSO	Caulinita intercalada com dimetilsulfóxido
$PCNO_2$	4-nitroftalonitrilo
$KaPCNO_2$	Caulinita funcionalizada com 4-nitroftlonitrilo
Al(III)TNMPC	Tetranitroftalocianina de alumínio (III)
PXRD	Difratometria de raios X
NMR	Ressonância magnética nuclear
FTIR	Espectroscopia de absorção molecular no infravermelho
UV/Vis	Espectroscopia de absorção molecular no ultravioleta/visível
XPS	Espectroscopia de fotoelétrons excitados por raios X
TG/DTG/DTA	Análise térmica – TG Derivada da Análise térmica – DTG Análise térmica diferencial – DTA

Resumo

O grande desafio da atualidade é a obtenção de materiais multifuncionais que sejam aplicados a inúmeros processos, destacando processos que envolvam descontaminação ambiental de corpos hídricos. Nesse contexto, esta Tese de Doutorado se apresenta em um formato de um compilado de artigos originais de investigação, publicados em revistas científicas de prestígio e indexadas na edição científica do *Journal Citation Reports.* O Artigo I apresenta a obtenção de compósitos, preparados pelo método sol-gel, utilizando caulinita, TiO_2 e tetracarboxiftalocianina de cobalto (II), mediante duas rotas sintéticas, ácida e básica, para estudar as diferenças dos materiais obtidos. Os materiais obtidos foram devidamente caracterizados e aplicados em processos de oxidação (degradação) de trimetoprim, cafeína e prometrina. Os resultados demonstram que houve degradação moderada de trimetoprim (30%) e prometrina (54%), e elevado para cafeína (90%). Foi verificada por espectrometria de massas, a obtenção de produtos intermediários de degradação em todos os casos. O Artigo II apresenta os resultados da funcionalização da laponita com ClPTES e dois compostos aminados, melamina e biureto, por duas rotas sintéticas: uma rota não aquosa (utilizando tolueno como solvente) e uma rota aquosa. Os materiais obtidos foram caracterizados e aplicados em processos de adsorção de trimetoprim. Os resultados demonstram que os materiais obtidos têm elevada afinidade com o composto orgânico, atingindo 80% de remoção. Também há um viés importante nos processos industriais, que são processos com menor gasto energético e de reagentes, que vão de acordo com os preceitos de química verde e sustentável. Nesse sentido, são apresentados no Artigo III os resultados da síntese de metaloftalocianina e sua imobilização em caulinita em uma única etapa reacional. O material foi caracterizado, confirmando a síntese e a imobilização da metaloftalocianina na caulinita por espectroscopia fotoelétrica de raios X (XPS) e ressonância magnética nuclear (RMN). A ftalocianina formada é composta por Al(III) dissolvido da lamela da caulinita. Este processo constitui uma nova rota sintética para essas macromoléculas (metaloftalocianinas), abrindo novas perspectivas de síntese.

Resumen

El principal desafío hoy en día es obtener materiales multifuncionales que se apliquen a numerosos procesos, destacando los procesos que involucran la descontaminación ambiental de los cuerpos de agua. En este contexto, esta Tesis Doctoral se presenta en un formato de compendio de artículos originales de investigación publicados en revistas científicas de prestigio e indexadas en la edición científica del *Journal Citation Reports*. El artículo I presenta la obtención de composites, preparados por el método sol-gel, utilizando caolinita, TiO_2 y tetracarboxiftalocianina de cobalto (II), por dos rutas sintéticas, ácida y básica, para estudiar las diferencias de los materiales obtenidos. Los materiales obtenidos fueron debidamente caracterizados y aplicados en procesos de oxidación (degradación) de trimetoprim, cafeína y prometrina. Los resultados demostraron que hubo una degradación moderada de trimetoprim (30%) y prometrina (54%), y elevada para la cafeína (90%). La obtención de productos intermediarios de degradación fue verificada en todos los casos por espectrometría de masas. El artículo II presenta los resultados de la funcionalización de laponita con ClPTES y dos materiales aminados, melamina y biuret, por dos rutas sintéticas: una ruta no acuosa (utilizando tolueno como disolvente) y una ruta acuosa. Los materiales obtenidos fueron caracterizados y aplicados en procesos de adsorción de trimetoprim. Los resultados demostraron que los materiales obtenidos tienen una elevada afinidad hacia el compuesto orgánico, alcanzando el 80% de eliminación. Otro objetivo importante de los procesos industriales es la realización de dichos procesos con menor gasto energético y de reactivos, lo cual va en consonancia con los preceptos de la química verde y sostenible. En este sentido, en el artículo III se presentan resultados de la síntesis de metaloftalocianina y su inmovilización en caolinita en una única etapa de reacción. El material fue caracterizado, confirmando la síntesis e inmovilización de la metaloftalocianina en la caolinita por espectroscopia fotoeléctrica de rayos X (XPS) y resonancia magnética nuclear (RMN). La ftalocianina formada está compuesta de Al (III) disuelto de la lámina de caolinita. Este proceso constituye una nueva ruta sintética para estas macromoléculas (metaloftalocianinas), abriendo nuevas perspectivas de síntesis.

Abstract

The main challenge today is to obtain multifunctional materials that are applied to numerous processes, highlighting the processes that involve the environmental decontamination of water bodies. In this context, this Doctoral Thesis is presented in a compilation format of original research articles published in prestigious scientific journals and indexed in the scientific edition of the Journal Citation Reports. Article I presents the obtaining of composites prepared by the sol-gel method, using kaolinite, TiO_2 and cobalt(II) tetracarboxyphthalocyanine. The materials obtained were duly characterized and applied in oxidation processes (degradation) of trimethoprim, caffeine and prometryn. The results showed that there was a moderate degradation of trimethoprim (30%) and prometryne (54%), and high for caffeine (90%). The obtaining of degradation byproducts was verified in all cases by mass spectrometry. Article II presents the results of the aminosilanization of laponite with ClPTES and melamine or biuret by two synthetic routes. The materials obtained were characterized and applied in trimethoprim adsorption processes. The results showed that the materials obtained have a high affinity towards the organic compound, reaching 80% elimination. Another important objective of industrial processes is to carry out these processes with lower energy and reagents expenditure, which is consistent with the precepts of green and sustainable chemistry. In this sense, Article III presents results of the synthesis of metalophthalocyanine and its immobilization in kaolinite in a single stage of reaction. The material was characterized, confirming the synthesis and immobilization of the metalophthalocyanine in the kaolinite by X-ray photoelectric spectroscopy (XPS) and nuclear magnetic resonance (NMR). The phthalocyanine formed is composed of Al (III) dissolved from the kaolinite coverslip. This process constitutes a new synthetic route for these macromolecules (metallophthalocyanines), opening new perspectives of synthesis

Introdução

O crescimento da produção industrial e da urbanização proporcionou melhorias nas condições de vida da população, inserindo no mercado uma ampla variedade de compostos químicos utilizados nos setores alimentícios, de saúde e transporte, porém, por outro lado, isso também contribui para aumentar a geração de resíduos, oriundos de etapas que englobam todo o processo produtivo, que inevitavelmente são despejados em corpos hídricos. Assim, processos de tratamento de água são cada dia mais desafiadores, pois há a necessidade de otimização de processos e tecnologias para evitar a geração de riscos à saúde humana e garantir a sustentabilidade ambiental. Problemáticas referentes à água são de fato compreendidas e controladas por meio da detecção aprimorada, sistemas de monitoramento específicos e do maior conhecimento dos efeitos ambientais, toxicológicos e biológicos desses compostos (Teodosiu et al., 2018). Com esse ritmo acelerado da industrialização, as previsões estatísticas mostram que milhares de pessoas que vivem em regiões áridas serão definitivamente confrontadas com a escassez de água limpa em 2025 (Pi et al., 2017).

A relevância do setor para a economia é gigantesca como, por exemplo, as estimativas mais recentes do mercado são de US $ 29 bilhões para pesticidas no mundo todo, US $ 1900 bilhões para produtos químicos industriais em economias emergentes, US $ 760 bilhões para consumo farmacêutico global e US $ 2300 bilhões para produtos químicos industriais de países em desenvolvimento (Peng et al., 2018). Em contrapartida, a preocupação ambiental também deveria ter a relevância nas mesmas proporções.

Entre milhões de substâncias conhecidas, mais de 150.000 substâncias são produzidas em quantidades superiores a 10t/ano segundo o REACH[I], que podem entrar no ambiente e penetrar eventualmente na cadeia alimentar, causando algum distúrbio nesses meios. O entendimento do potencial prejuízo ao meio ambiente e/ou à saúde humana que essas substâncias representam é um dos maiores desafios para a pesquisa ambiental atual. A base de dados NORMAN Network (Norman, 2017) de substâncias emergentes apresenta mais de 700 substâncias contaminantes ambientais não regulamentadas que tem efeitos potencialmente prejudiciais. O esquema de priorização NORMAN classifica compostos com base em sua

[I] O REACH (Registration, Evaluation, Authorisation and Restriction of Chemicals) é um regulamento da União Europeia aprovado com o objetivo de melhorar a proteção da saúde humana e do ambiente face aos riscos que podem resultar dos produtos químicos e, simultaneamente, de fomentar, a competitividade da indústria química da União Europeia.

ocorrência e nenhuma das substâncias é descartada da priorização devido à falta de dados de monitoramento ou toxicidade. As categorias de substâncias são definidas levando alguns fatores em consideração, tais como, maior ocorrência, dados de toxicidade e desempenho analítico. Cada um dos parâmetros básicos (ocorrência, toxicidade e uso) e numerosos subparâmetros (por exemplo, substância é um disruptor endócrino, pertencente à categoria de persistente, bioacumulativo [II] e tóxico) tem um fator de "peso" contribuindo para a classificação final (Geissen et al., 2015; Vrana et al., 2016).

Economias emergentes, como China, Índia e Brasil, começaram a liderar a fabricação e o uso de produtos químicos sintéticos. No entanto, iniciativas recentes reconheceram que informações insuficientes estão disponíveis para avaliar os impactos ambientais de substâncias químicas sintéticas nessas áreas. O aumento da liberação de substâncias químicas sintéticas em corpos hídricos agrava a preocupação com a saúde dos seres humanos e dos ecossistemas aquáticos (Peng et al., 2018).

Muitos desses compostos químicos adéquam-se em uma classificação e se tornaram de grande interesse em pesquisas nos últimos anos, tais como, os poluentes orgânicos emergentes (POEs): compostos que são resistentes a processos químicos, biológicos e fotolíticos de degradação, são estáveis, persistentes, bioacumuláveis e podem afetar toda a cadeia alimentar, e promover riscos à saúde humana e meio ambiente (Lorenzo et al., 2018; Peng et al., 2018). Alguns exemplos de POEs são pesticidas, produtos farmacêuticos, produtos de higiene pessoal, detergentes, subprodutos de desinfecção, drogas, dentre outros.

A Tabela 1 apresenta informações e dados relevantes dos POEs utilizados no trabalho (Kudlek, 2017; Petrie et al., 2015; Pi et al., 2017). Informações complementares, propriedades farmacológicas, registro e legislação são bem listados em agências regulamentadoras internacionais como EC-EU, n.d.; EPA, n.d.; PubChem, n.d.[III].

[II] Bioacumulação: fenômeno pelo qual oscompostos químicos são absorvidos pelo organismo, não sendo metabolizadas nem excretadas pelo mesmo, consequentemente acumulando e alcançando concentrações maiores do que no meio.

[III] EPA (United States Environmental Protection Agency); PubChem (Open Chemistry Database), EC-EU (European Commission Health and Food Safety).

Tabela 1: Informações quantitativas dos POEs utilizados nesse trabalho (Drugbank, n.d.; Kudlek, 2017; Lamastra et al., 2016; Petrie et al., 2015).

POEs	Grupo	Solubilidade em água a 25°C (mg/L)	Notas
Prometrina	Pesticida	33	Carcinogênico Limite para água potável: 28µg/L Ecotóxico – ppb* Não aprovado na União Europeia
Trimetoprim	Farmacêutico	400	Combinação com Sulfametoxazol Tóxico para vida aquática LD_{50} = 4850 (via oral em ratos)
Cafeína	Indicador Humano	21600	Aditivo alimentar; aromatizante Estimulante do sistema nervoso central Potencial arritmogênico 80% metabolizado Psicoestimulante mais utilizado no mundo

*ppb – partes por bilhão

A preocupação com os POEs apresenta um crescente impacto nas pesquisas e trabalhos publicados referentes ao tema (Geissen et al., 2015; González et al., 2017a; Peng et al., 2018; Teodosiu et al., 2018). Em pesquisa realizada em base de dados internacionais, utilizando as palavras-chave *"emerging organic pollutants"*, é possível observar a crescente publicação de trabalhos nos últimos 20 anos. O gráfico a seguir (Figura 1) apresenta os resultados da busca na base de dados SCOPUS (www.scopus.com) e pode-se observar a relevância da problemática quando se envolve contaminação hídrica por POEs.

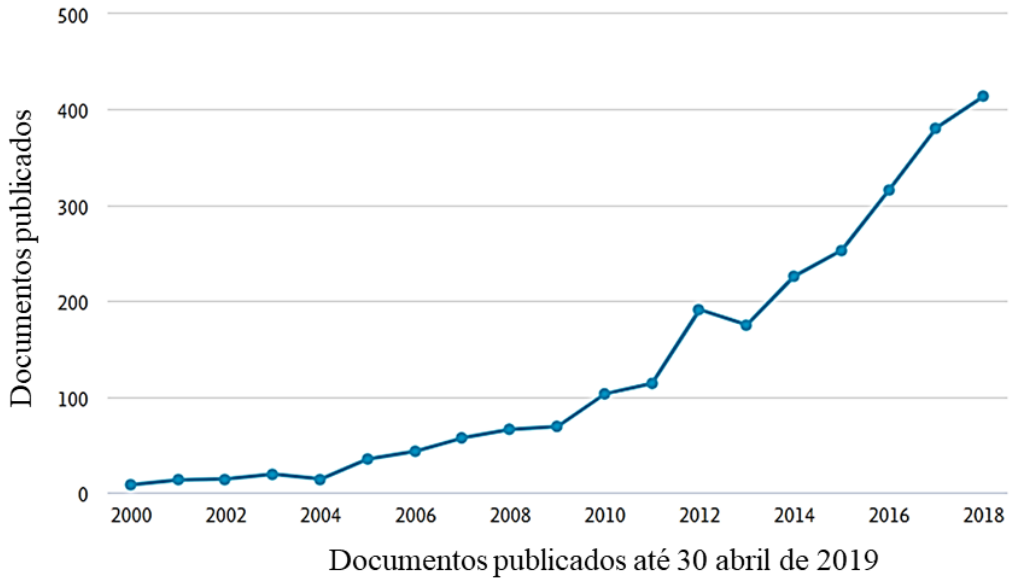

Figura 1: Publicações sobre POEs desde o ano 2000.

Desse modo, não somente há a preocupação em pesquisar o quanto há de contaminantes em sistemas aquáticos, mas também há a necessidade de procurar medidas preventivas ou processos de descontaminação ambiental para recuperação hídrica.

Convencionalmente, tratamentos de água baseiam-se em processos biológicos (biodegradação) e ou processos físico-químicos (floculação, cloração e ozonização) com posteriores processos de separação, como sedimentação/decantação, filtração e adsorção, porém esses processos não são suficientes para completa remoção desses contaminantes, sendo necessários processos com tecnologias mais avançadas (Bokare and Choi, 2014; Rodriguez et al., 2017; Teodosiu et al., 2018).

Vislumbrando medidas para melhorar a eficiência de alguns processos, surge como alternativa a utilização de materiais nanohíbridos orgânico-inorgânico, compósitos e nanocompósitos para aperfeiçoamento de técnicas para remoção desses contaminantes, como processos de oxidação avançados e adsorção.

Processos oxidativos avançados

Os processos oxidativos avançados (POAs) consistem em grupos de tecnologias que foram usados com sucesso no tratamento de água e esgoto nas últimas décadas, que envolvem ozonização direta, ozônio e/ou H_2O_2 combinados com radiação ultravioleta/visível (UV/Vis), Fenton, foto-Fenton, catálise/fotocatálise, eletrólise, dentre outros. Os POAs baseiam-se na produção de radicais hidroxila ($HO^{\bullet}$), sendo este um dos oxidantes mais fortes, com potencial

de oxidação + 2,8V, podendo ser usado para processos de remoção/degradação de POEs. A produção de radical hidroxila pode ser alcançada por muitas vias, permitindo a escolha mais adequada do POA, maximizando os efeitos de acordo com o processo de tratamento hídrico necessário e, processos fotoquímicos [IV] têm gerado grande interesse, pois oferecem a possibilidade de utilização de radiações com comprimentos de ondas específicos, como por exemplo, lâmpadas de mercúrio de 8, 125 e 400W, variando comprimento de onda entre 305 a 366nm, além da utilização da radiação solar, energia natural e renovável, juntamente a compostos semicondutores[V] capazes de gerar esses radicais $HO^{\bullet}$ (Arnab et al., 2014; Byrne et al., 2018; González et al., 2018; Molinari et al., 2017; Teodosiu et al., 2018; Wang et al., 2015).

Os processos fotoquímicos baseiam-se na irradiação de energia luminosa (artificial ou natural) sob um complexo metálico (como por exemplo, um semicondutor), bombardeando fótons em sua superfície excitando os elétrons da banda de valência; se a energia desses fótons for maior do que a energia do *band gap*[VI] esses elétrons "carregados" saltam para a banda de condução deixando um vazio positivo (buraco) na banda de valência; os elétrons da banda de condução tem a capacidade de reagir com o oxigênio (O_2) gerando radicais superóxidos ($\dot{O}_2^-$) ou radicais hidroperóxidos ($HOO\bullet$), espécies essas que são altamente reativas e são então utilizadas nos processos de degradação de poluentes mineralizando parcialmente ou completamente. Paralelamente, outra reação no processo fotocatalítico está em andamento, onde ocorre a oxidação da água nos vazios positivos da banda de valência, gerando radicais hidroxilas ($HO^{\bullet}$) e íons hidrogênio (H^+) que reagem com os poluentes promovendo também a mineralização (Byrne et al., 2018; Szczepanik, 2017). O processo descrito é apresentado a seguir na Figura 2.

[IV] Fotoquímica: estudo das reações químicas provocadas pela incidência de radiação eletromagnética.
[V] Semicondutor: materiais que apresentam propriedades de condução elétrica intermediárias entre aquelas inerentes aos isolantes e aos condutores.
[VI] *Band Gap*: Energia necessária para que o elétron efetue a transição da banda de valência para a banda de condução.

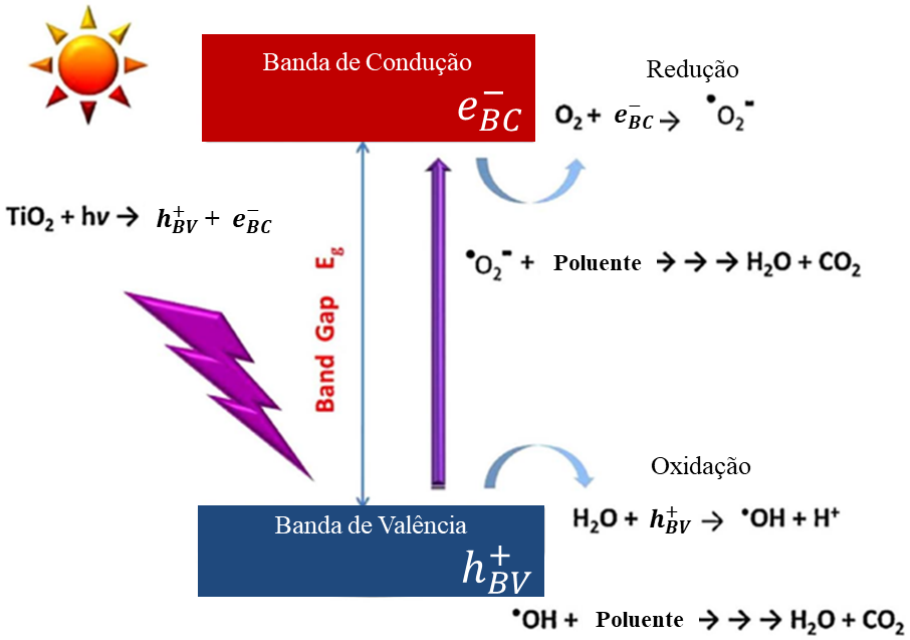

Figura 2: Mecanismo da fotocatálise (adaptado de Byrne et al., 2018).

Entre os fotocatalisadores, o dióxido de titânio (TiO_2) ganha particular interesse nos processos de degradação de poluentes orgânicos sob radiação UV/Vis, devido à algumas características e propriedades físico-químicas como: sua natureza heterogênea, que oferece a possibilidade de reutilização dos fotocatalisadores, fotoestabilidade, não toxicidade, elevada atividade, biocompatibilidade e custo relativamente baixo (Barbosa et al., 2015; Chen et al., 2014). Apesar de todos os benefícios do uso do TiO_2 como fotocatalisador, há algumas desvantagens em sua utilização: baixa eficiência energética, com *band gap* de 3,2eV, sob radiação ultravioleta (<390nm) que corresponde apenas a aproximadamente 4% da radiação solar (Byrne et al., 2018); forte tendência das partículas de TiO_2 se agregarem em partículas aglomeradas, aumentando assim o tamanho, limitando o acesso aos sítios de degradação e, consequentemente, diminuindo a eficiência fotocatalítica (Papoulis et al., 2018).

Para superar e diminuir os efeitos dessas desvantagens, algumas abordagens vêm sendo estudadas, tais como ampliar a faixa de absorção para a região visível, com o depósito na superfície utilizando moléculas que tenham elevado coeficiente de absortividade molecular nessa região, como porfirinas (Huang et al., 2009; Lü et al., 2017; Min et al., 2019; Zajac et al., 2016), facilitando a transferência eletrônica e a dispersão de partículas de TiO_2 sobre superfícies de argilominerais para reduzir a aglomeração e facilitar a recuperação (Barbosa et al., 2015; Bethi et al., 2016; González et al., 2018; Papoulis et al., 2018; Stathatos et al., 2012).

Na tentativa de diminuir essas desvantagens, Min et al., 2019 demonstram que a incorporação de porfirinas na superfície de TiO_2 melhora a eficiência de degradação do corante azul de metileno. Os autores apresentam resultados de eficiência de degradação em 70% do corante em um tempo de 30 minutos. O estudo foi realizado utilizando porfirina substituída base livre e uma metalada com zinco, verificando a influência desses parâmetros tanto no processo de incorporação no TiO_2 quanto na eficiência dos processos. Os autores observaram que a melhor eficiência foi do composto que utiliza a porfirina metalada tetrasubstituída incorporada no TiO_2.

A Figura 3 apresenta um possível mecanismo da degradação fotocatalítica que os autores propõem, onde além do TiO_2 absorver radiação UV/Vis (presente na luz solar), a porfirina absorve radiação visível, acontecendo os processos de excitação e a transferência de elétrons para a banda de condução do semicondutor (TiO_2) (Min et al., 2019).

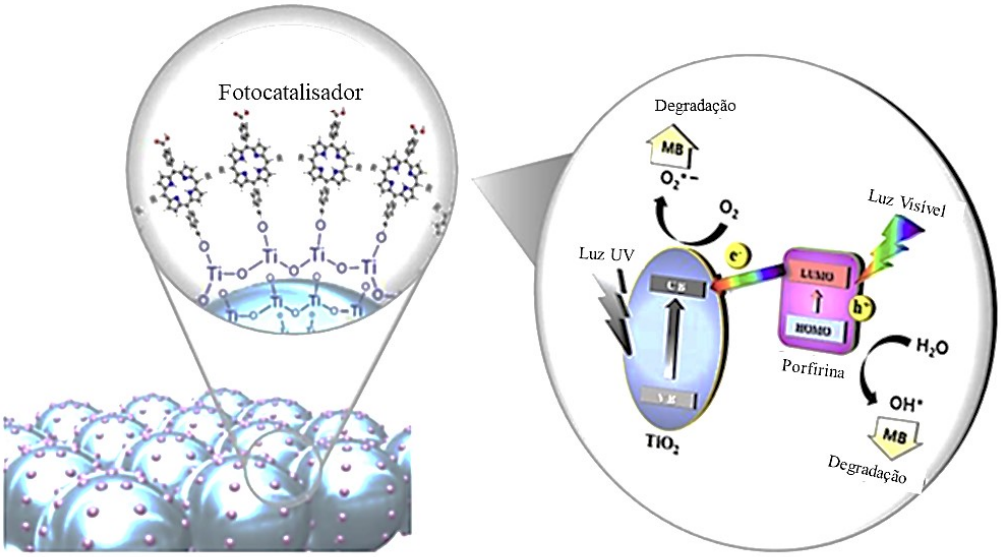

Figura 3: Possível mecanismo da degradação fotocatalítica (adaptado Min et al., 2019).

Analisando os resultados apresentados pelos autores, observa-se a influência da quantidade de grupos cromóforos[VII] na eficiência do processo de degradação, devido à maior absortividade pela porfirina que após absorver a luz solar irradiada, transfere para o titânio, maximizando os efeitos fotoquímicos do sistema TiO_2/porfirina. Isso abre precedentes para outros compostos serem utilizados como fotosensibilizadores, como por exemplo, metaloftalocianinas.

[VII] Cromóforo: grupos funcionais capazes de absorver radiação eletromagnética em determinadas faixas do espectro eletromagnético; parte ou conjunto de átomos de uma molécula responsável por sua cor.

Metaloftalocianinas (MPC) são complexos metálicos muito estáveis, e várias propriedades contribuem para sua versatilidade, incluindo alta estabilidade térmica e físico-química. Seus 18 elétrons π favorecem a alta densidade eletrônica, sendo possível observar bandas de maior intensidade (bandas Q) entre 550 e 800 nm, devido às transições $\pi - \pi^*$ ($a_{1_u} \rightarrow e_g$). Bandas de menor intensidade e mais energéticas (Soret ou B) são observadas entre 300 e 500 nm, originadas das transições $a_{2_u} \rightarrow e_g$ (Ebrahimian et al., 2014; Pirbazari, 2015). A Figura 4 apresenta um esquema dos níveis de energia para as metaloftalocianinas.

Assim, a espectroscopia de absorção molecular na região UV/Vis é importante para caracterizações e entendimentos do comportamento dessas macromoléculas, pois a energia envolvida no processo de emissão do UV/Vis não é suficiente para promover elétrons mais internos ou próximos do núcleo para estados mais excitados. Essas transições eletrônicas ocorrem nos orbitais de fronteiras HOMO (*highest occupied molecular orbital*) – LUMO (*lowest unoccupied molecular orbital*) destas moléculas, onde elétrons são excitados e promovidos do orbital HOMO para o orbital LUMO, sendo esses orbitais de grande importância para a reatividade das metaloftalocianinas (Pereira et al., 2016; Santos, 2016).

Em sistemas híbridos, compostos, por exemplo, por semicondutores e metaloftalocianinas, os elétrons excitados para o orbital LUMO podem ter a capacidade de se transferir para outros níveis de energia, ao invés de retornar diretamente para seu estado fundamental, promovendo assim processos de transferência de carga. O processo de transferência de carga e geração de espécies oxidantes ocorre nas seguintes etapas: (I) absorção da radiação pela metaloftalocianina – processo de excitação HOMO-LUMO; (II) disponibilidade de elétrons no orbital LUMO, que são injetados no semicondutor (TiO_2), geralmente na banda de condução (estado excitado do semicondutor); (III) o processo resulta na produção de espécies como (O_2^-) e ($HO^\bullet$) (Ebrahimian et al., 2014; Kadish et al., 1999; Min et al., 2019; Pirbazari, 2015; Sevim, 2017; Sun et al., 2013; Urbani et al., 2014).

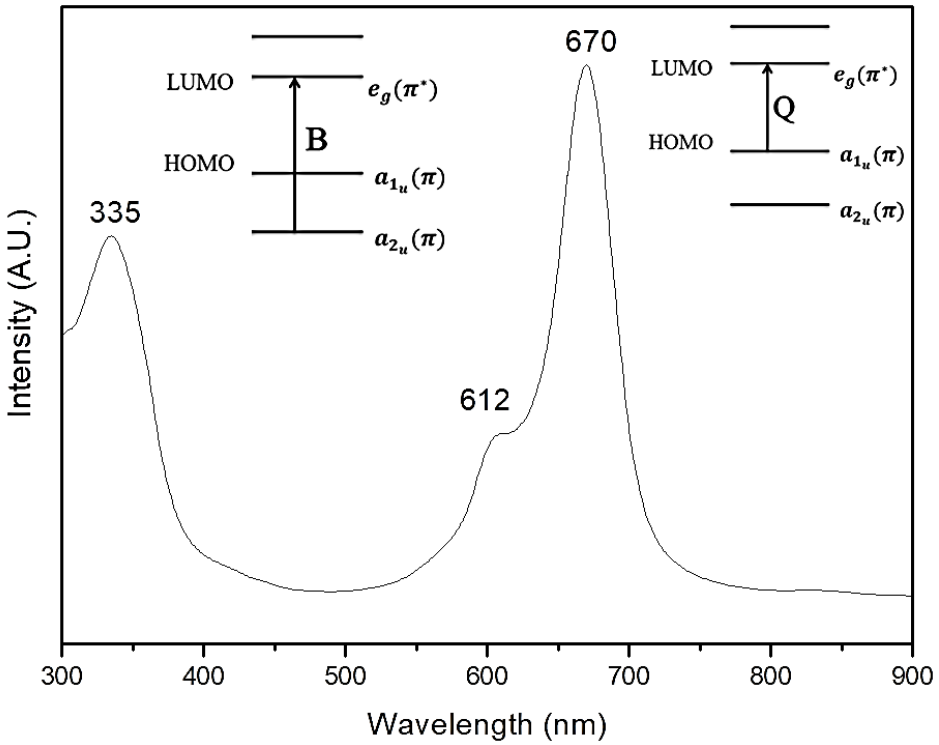

Figura 4: Esquema dos níveis de energia das metaloftalocianinas (Adaptado de Kadish et al., 1999).

Mesgari et al., 2012 apresentam resultados da dopagem de nanopartículas de TiO_2 com ftalocianina para alterar positivamente as propriedades fotocatalíticas do material. Os autores relatam que foram promovidas melhorias nas atividades do material, para a degradação do alaranjado de metila aumentou de aproximadamente 20% (TiO_2) para aproximadamente 80% (ftalocianina/TiO_2), de forma que a maior mudança positiva para o processo de fotocatálise, foi a utilização de radiação no visível (representação na Figura 5) para promover a ativação fotofísica do material, pois houve a diminuição da energia do *band gap* de 3,26 para 2,26eV, para TiO_2 e ftalocianina/TiO_2, respectivamente.

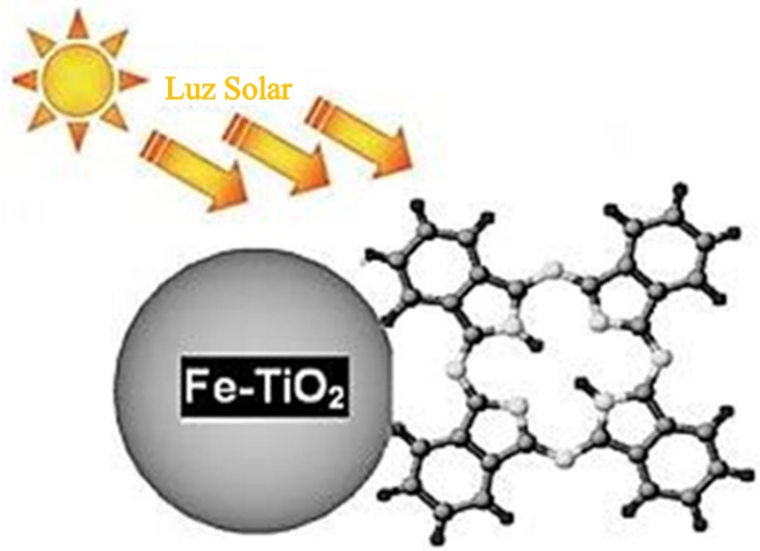

Figura 5: Representação do aproveitamento da luz solar para ativação do fotocatalisador (adaptado de Mesgari et al., 2012).

A outra desvantagem, como dito anteriormente, pode ser superada pela dispersão de TiO_2 em superfícies de argilominerais. Argilominerais se destacam para esses processos reacionais com TiO_2, pois apresentam propriedades físico-químicas estáveis; possibilitam a adsorção de substâncias orgânicas em sua superfície, passo que pode necessário para processos fotocatalíticos; diferentes morfologias podem agregar diferentes propriedades, como argilominerais tubulares, fibrosos e lamelares (Barbosa et al., 2015; Papoulis et al., 2018; Szczepanik, 2017).

Nesse sentido, Papoulis et al., 2018 apresentam resultados da incorporação de partículas de titânio em haloisita e sepiolita para degradação de paracetamol, tetraciclina e rodamina-B (RhB). Os autores relatam que os materiais baseados em sepiolita/TiO_2 mostraram melhores atividades na degradação de paracetamol e tetraciclina, comparados ao Degussa P25 (padrão comercial). Além disso, todos os nanocompósitos apresentaram atividades superiores para a decomposição de RhB. Isso demonstra que a dispersão de partículas de titânio (Figura 6) sobre a superfície dos argilominerais promoveu melhorias na atividade fotocatalítica.

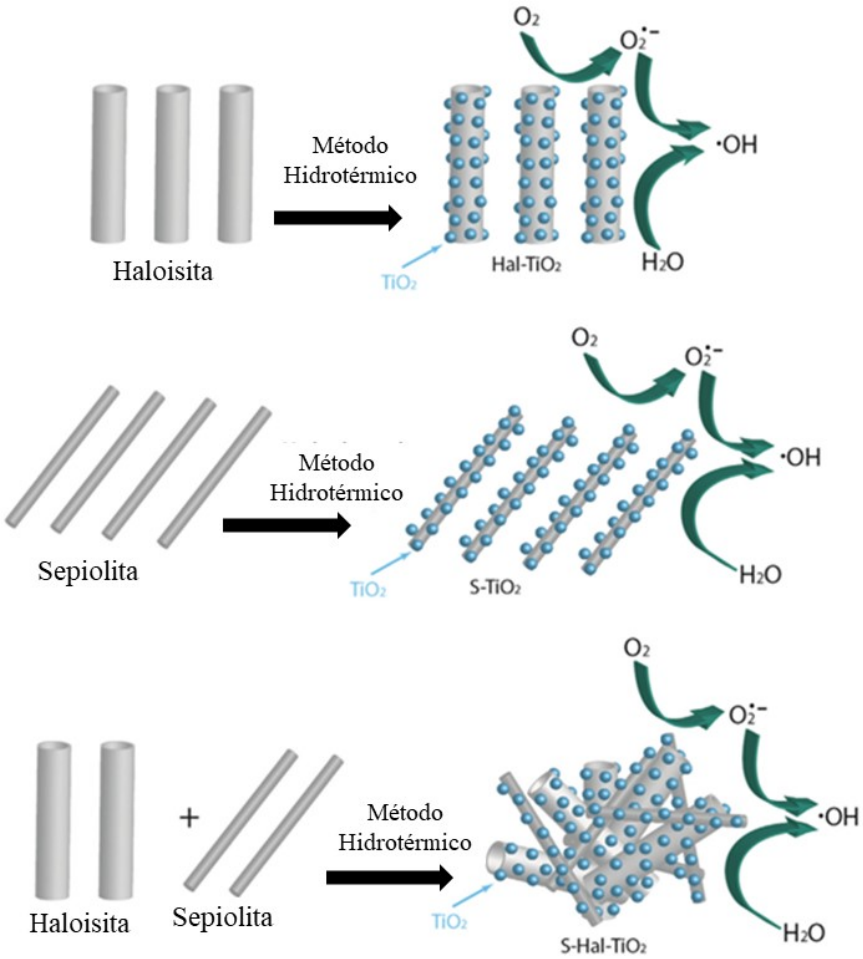

Figura 6: Ilustração esquemática da formação dos compósitos fotocatalíticos TiO_2/argilomineral (haloisita e sepiolita) (adaptado de (Papoulis et al., 2018)).

Barbosa et al., 2015 apresentam resultados da síntese para imobilização de TiO_2 em outro argilomineral, a caulinita, para promover melhorias nas propriedades, associando a eficiência fotoquímica do dióxido de titânio, com as propriedades físico-químicas da caulinita. Os compósitos obtidos foram submetidos à calcinação em diferentes temperaturas para obtenção das diferentes fases do TiO_2, anatase, rutilo e bruquita (Figura 7). Os autores relatam eficiência frente à degradação de corantes industriais azul de metileno e alaranjado de metila II, sendo que todos os compostos obtidos à base de caulinita-TiO_2 apresentaram resultados fotocatalíticos melhores que o TiO_2 comercial (Degussa P25).

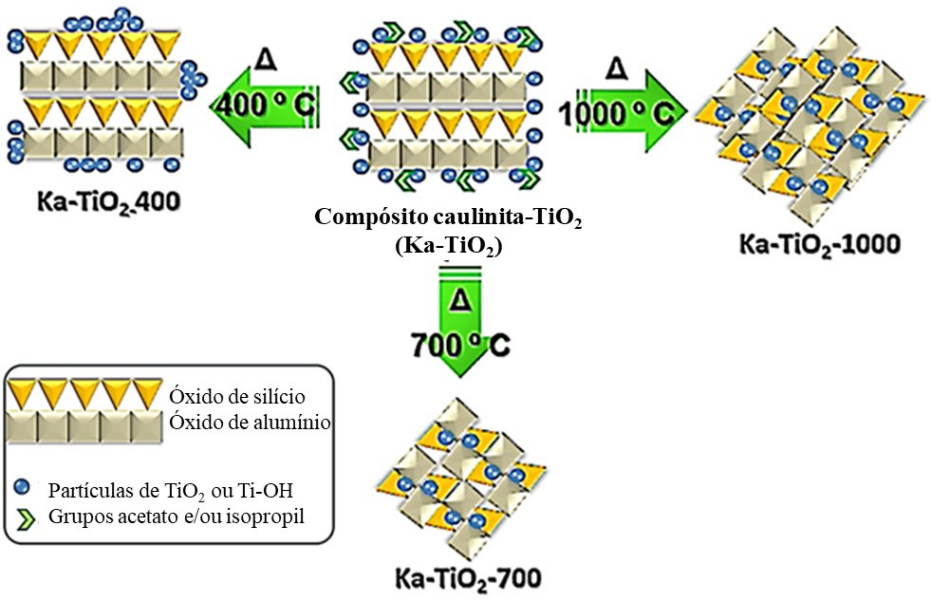

Figura 7: Esquema representativo da obtenção dos compósitos (adaptado de Barbosa et al., 2015).

Dentre o apresentado pelos autores, conclui-se que a imobilização de TiO_2 sobre superfície de argilominerais promove melhorias nos processos fotoquímicos, como maior dispersão das partículas de titânio, evitando a aglomeração, e essas modificações melhoraram os resultados de fotocatálise quando comparados ao padrão comercial.

Adsorção

Os processos de adsorção aparecem como alternativas para a remoção de POEs devido à sua alta eficiência, seletividade, baixo custo, simplicidade e a possibilidade de reutilizar e reciclar o adsorvente (Marçal et al., 2015; Martín et al., 2018).

A adsorção (Figura 8) ocorre sempre que uma superfície sólida é exposta a um gás ou líquido, sendo definida como: o enriquecimento de material ou aumento da densidade do fluido na vizinhança de uma interface, que é influenciada pela extensão da área superficial, tamanho dos poros e partículas. Alguns adsorventes são utilizados em grande escala como dessecantes, catalisadores ou suportes de catalisadores; outros são usados para a separação de gases, a purificação de líquidos e o controle da poluição (Rouquerol et al., 1999).

A adsorção é provocada pelas interações entre o sólido e as moléculas na fase fluida. Dois tipos de interações podem ser observados nos processos de adsorção: as de origem física (fisissorção) ou química (quimissorção) (Rouquerol et al., 1999):

I. Fisissorção: fenômeno geral com um grau de especificidade relativamente baixo; forças de fisissorção são as mesmas responsáveis pela condensação dos vapores e os desvios do comportamento do gás ideal, em altas pressões relativas, geralmente leva a formação de multicamadas.

II. Quimissorção: dependente da reatividade do adsorvente e adsorvato; forças são essencialmente aquelas responsáveis pela formação de compostos químicos (geralmente ligações covalentes), compostos são ligados a partes reativas da superfície (sítios de adsorção) e a adsorção é necessariamente confinada a monocamadas.

Assim a interação entre adsorvente e adsorvato se dá à medida que moléculas se aproximam de uma superfície sólida, estabelecendo um equilíbrio entre as forças intermoleculares de atração e repulsão. Quando algumas moléculas já estão adsorvidas na superfície do sólido, podem ocorrer processos de interação adsorvente-adsorvente e adsorvente-adsorvato, nos sítios disponíveis para tais interações (Rouquerol et al., 1999). Consequentemente, toda aplicação prática e industrial da técnica de adsorção está baseada no desenvolvimento de adsorventes que contenham propriedades texturais bem delineadas, mais especificamente altas áreas superficiais e volumes de poros.

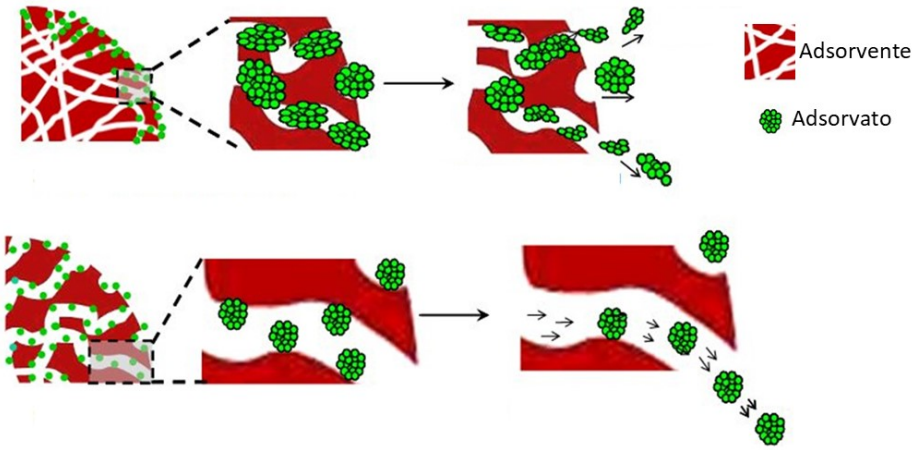

Figura 8: Esquema demonstrativo do processo de adsorção (adaptado de Yu et al., 2014).

Nesse sentido, alguns autores apresentam a utilização de argilominerais como suportes para obtenção de adsorventes com as devidas características desejadas.

Marçal et al., 2015 expõem resultados para a utilização de saponita modificada com 3-aminopropiltrietoxissilano (APTS) e n-hexadeciltrimetilamônio (CTA) como adsorvente de

cafeína. Os autores informam que a modificação da saponita foi crucial para interação dos materiais adsorventes com o adsorvato e que a modificação com APTS apresentou a maior afinidade pela cafeína, obtendo resultados para o máximo de adsorção de 80,54 mg/g em 4 horas. Os autores ainda informam que a saponita natural não apresentou resultados significantes para a adsorção, confirmando a importância de sua modificação.

González et al., 2017b retratam resultados da utilização de outro argilomineral, a montmorilonita, como adsorvente de trimetoprim (antibiótico utilizado para tratamento de infecções urinárias). Os autores promoveram processos de pilarização[VIII] da montmorilonita, com titânio e dopagem com cátions apropriados, a fim de melhorar as propriedades adsortivas do argilomineral. Os melhores resultados observados pelos autores foram os materiais baseados em montmorilonita/titânio/(ferro ou crômio) que apresentaram porcentagens de adsorção próximas a 75% de remoção, em tempos relativamente pequenos, 5 e 10 minutos, quando comparados a montmorilonita natural, que para atingir a mesma relação de remoção necessitou de 150 minutos. Essa diminuição drástica no tempo de adsorção comprova que processos de modificação promoveram melhorias significativas nas propriedades de adsorção.

Martín et al., 2018 avaliaram a capacidade de adsorção de mica modificada, para uma sequência de poluentes orgânicos das mais diferentes naturezas, como produtos farmacêuticos, surfactantes, compostos perfluoroalquílicos e conservantes, totalizado 18 compostos. Os autores avaliaram e compararam os resultados da adsorção desses compostos em mica e mica organicamente modificada com octadecilmina primária. Os resultados apresentados demonstram claramente que a modificação alterou positivamente as propriedades de adsorção do argilomineral. Para a mica sem modificação, os resultados foram taxas de remoção entre 8 e 97% após 7 dias de reação, e que alguns compostos perfluoroalquílicos e farmacêuticos não foram adsorvidos. Já para a mica modificada, as taxas de remoção observadas foram de 70 a 100%, decorridos apenas 24 horas.

A Tabela 2 apresenta dados sumarizados de alguns materiais baseados em matrizes inorgânicas que foram aplicados em processos de fotocatálise e adsorção para remediação ambiental estudando POEs. Nessa tabela, salienta-se a utilização de matrizes inorgânicas, especialmente argilominerais, destacando a importância dessa classe de materiais e abrindo uma gama de utilizações para infinitos fins, quando se busca agregar propriedades fotocatalíticas e adsorventes em compostos já conhecidos.

[VIII] Pilarização: consiste na intercalação de policatiônicos metálicos, seguido de calcinação.

Tabela 2: Principais meios de PAO e Adsorção com argilas aplicadas em POEs

Fotocatalisador	Adsorvente	Composto orgânico	Notas	Referências
Haloisita/Sepiolita/TiO_2		Paracetamol	41% de degradação	(Papoulis et al., 2018)
		Tetraciclina	58% de degradação	
			Lâmpada de mercúrio, 400W, $\lambda_{máx} = 365\text{nm}$	
Heteroestruturas de ZnO-Al_2O_3 dopado com Mg		Cafeína	98,9% de degradação	(Elhalil et al., 2018)
			Lâmpada de mercúrio, 400W	
			Fluxo de O_2	
Caulinita/TiO_2		D-limoneno	Luz Ultravioleta ($\lambda_{máx} = 360$ nm)	(Kibanova et al., 2009; Szczepanik, 2017)
			Propriedades comparadas à TiO_2	
	Saponita	Cafeína	Temperatura ambiente	(Marçal et al., 2015)
			Máximo de adsorção 80,54 mg/g	
			$\sim 240\ min$	
	Nanotubos de carbono	Licomicina/Sulfametoxazol	90% de remoção	(Kim et al., 2014; Zhao et al., 2018)
			Temperatura 20°C	
			Máximo de adsorção 45,8 mg/g	
	Montmorilonita	Trimetoprim	Temperatura ambiente	(González et al., 2017b)
			75% de remoção $\sim 10min$	

Argilominerais

Caulinita

A caulinita é um argilomineral do tipo 1:1 (tipo TO), cuja estrutura é formada a partir da junção de folhas com átomos de silício coordenados tetraedricamente, T, com a gibbsita (folhas com átomos de alumínio coordenados octaedricamente, O) (Cheng et al., 2012; Gardolinski et al., 2003; Machado et al., 2012). A estrutura da caulinita (Figura 9) se mantém coesa pelo compartilhamento de átomos de oxigênio comuns a ambas as folhas (TO ou lamela), cuja fórmula mínima é $Al_2Si_2O_5(OH)_4$ (de Faria et al., 2009; Dedzo and Detellier, 2014; Gräfe et al., 2007).

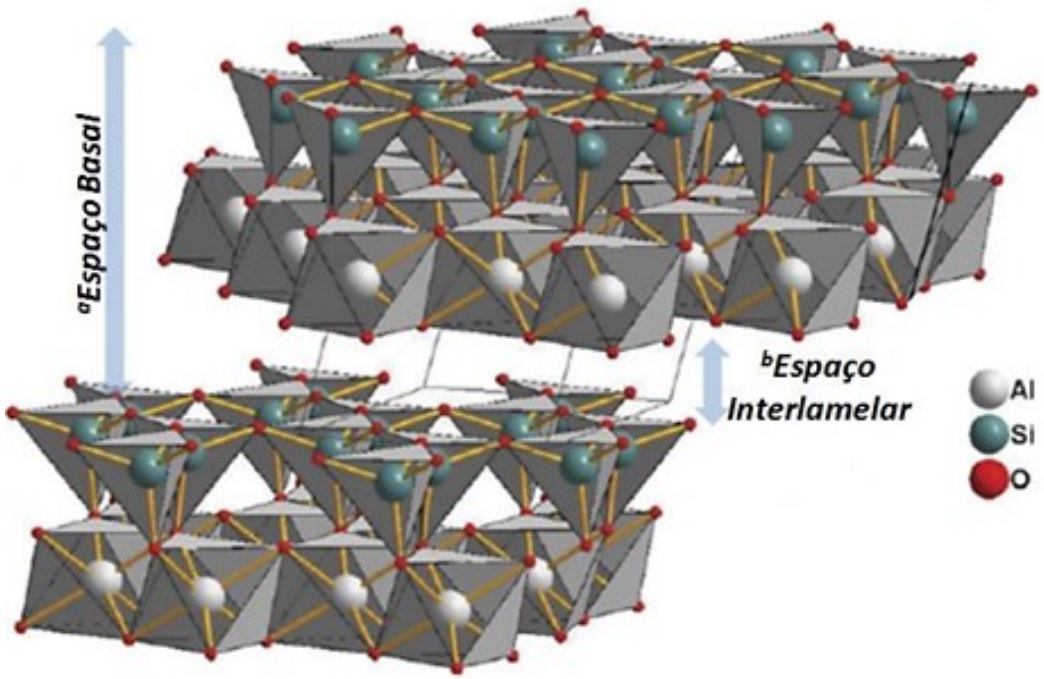

Figura 9: Estrutura idealizada de uma cela unitária de um cristal de caulinita (Faria, 2011) (adaptado de Gräfe et al., 2007).

A caulinita pode ser utilizada como suporte para uma série de processos visando à obtenção de nanomateriais com propriedades para remediação ambiental frente a POEs. A Tabela 3 apresenta alguns desses resultados da literatura explorando a descontaminação/degradação de POEs.

Tabela 3: Nanomateriais baseados em caulinita para remediação ambiental – POEs.

POE (classificação)	Condições experimentais	Resultados	Referência
Ciprofloxacina Antibiótico	Estudo de equilíbrio: 1g de caulinita/10mL solução POE 0,1-2,0mM Estudo cinético: variação do tempo de 15 a 1440 minutos, pH=3,5 Estudo da variação do pH de 3 a 11	Capacidade de adsorção: ~ 10mmol/kg – pH 3,5 ~ 20mmol/kg – pH 5-10 A adsorção é influenciada pelo pH A taxa inicial de adsorção rápida elevada, indicando ser um bom adsorvente para remoção de contaminantes.	(Li et al., 2011)
Triclosan Farmacêutico	Estudo de equilíbrio: 1g/L de caulinita/50mL solução POE 60mg/L Estudo cinético: variação do tempo de 6 a 24 horas Estudo da influência de ácido húmico	Melhores resultados de adsorção em meios ácidos Maior afinidade entre o triclosan e a argila com maior concentração de ácido húmico – fator para adsorção do POE em solos Capacidade de adsorção: ~ 6,4 mg/g – pH 3 Elevando o caráter iônico superfícial da caulinita: ~ 24,66 mg/g	(Behera et al., 2010)
Ciprofloxacina Antibiótico	Atividade fotocatalitica sob radiação UV (lâmpada de mercúrio 300W), solar (lâmpada de Xenon – 50mW/cm²) e visível (lâmpada de Xenon equipada com filtro de 400mn – 90mW/cm²) Influência de atmosfera de nitrogênio	O compósito caulinita/TiO_2 sob atmosfera de nitrogênio apresentou resultados melhores que o atmosfera ambiente O compósito apresentou resultados 7, 2,54 e 3,13 vezes maior que o TiO_2 sob luz UV, solar e visível, respectivamente.	(Li et al., 2018)

Laponita

A laponita é um silicato sintético semelhante em estrutura e composição ao mineral hectorita, que pertence ao grupo das esmectitas, que são argilominerais do tipo 2:1 ou TOT, constituídos por duas folhas com átomos de silício coordenados tetraedricamente e uma folha com átomos de magnésio coordenados octaedricamente, podendo ocorrer à substituição isomórfica de alguns cátions de magnésio com cátions de lítio na folha central, bem como a presença de algumas posições livres, dá origem a uma carga negativa parcial, que é balanceada por cátions sódio. A laponita possui fórmula $Na^{+}_{0,7}[Si_8Mg_{5,5}Li_{0,3}]O_{20}(OH)_4]^{0,7-}$ e tem sua representação demonstrada na Figura 10 (Borsacchi et al., 2007).

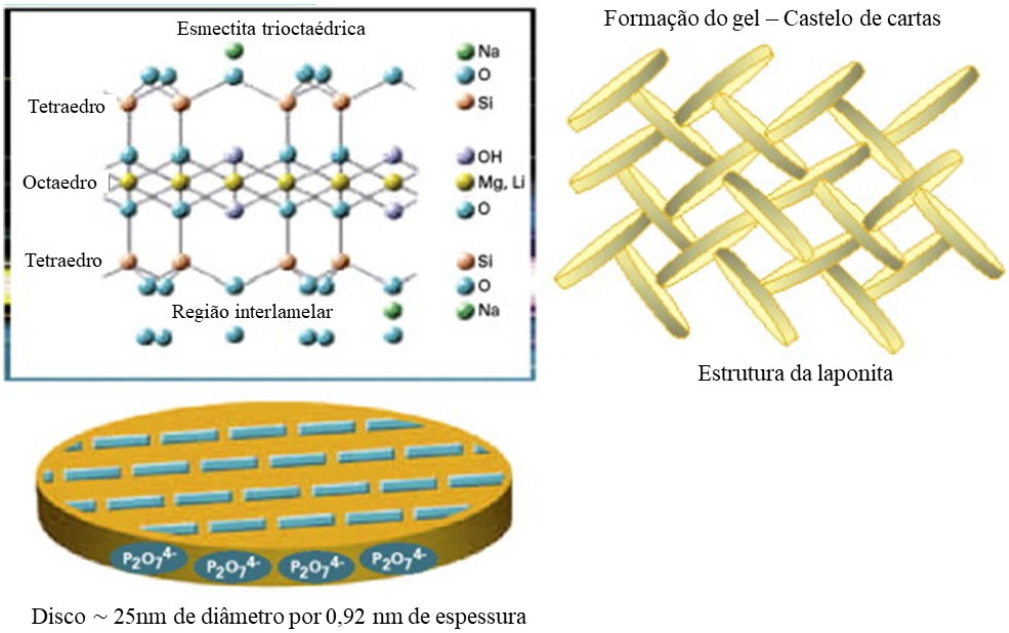

Figura 10: Estrutura de um argilomineral 2:1 (adaptado de Cummins, 2007).

A laponita pode ser utilizada como suporte para uma série de processos visando à obtenção de nanomateriais com propriedades para remediação ambiental frente a alguns compostos orgânicos. A Tabela 4 apresenta alguns desses resultados da literatura para remoção de compostos que podem afetar o meio ambiente.

Tabela 4: Nanomateriais baseados em laponita para remediação ambiental – POEs.

POE	Condições experimentais	Resultados	Referência
Fenol	Radiação UV (UV-C, 15W, λ=254nm; UV-A, 40W, λ=365nm) Utilização de H_2O_2 50 mmol/L $1g_{catalisador}$/solução 1 mmol/L POE Tratamento térmico – 250, 350, 450 e 550°C	Todos materiais apresentam atividade fotocatalítica. Material a 350°C apresentou melhor atividade catalítica (processo foto-Fenton) quando irradiado com a lâmpada UV-C, 15W, λ=254nm em um pH = 3.	(Iurascu et al., 2009)
Ciprofloxacina	Lâmpada de Mercurio – 125W Utiliazação de H_2O_2 Mineralização de solução de 0,15mM de Ciprofloxacina a 298K	Conversão completa de 0,15mM de Ciprofloxacina (60 mM H_2O_2, 1g/L FeLap-RD e pH = 3)	(Bobu et al., 2008)
Albumina (BSA*)	$1\ mg_{sólido}/1mL_{solução}$ 100 mg/L BSA Controle de pH Período de 24h Estudo cinetico e de equilíbrio	Laponita aumentou a capacidade de adsorção, comparado ao sistema quitosana/polivinil álcool isolado Dessorção da BSA sob condições de solução tampão pH = 8 Quantidade máxima de adsorção 240,5 mg/g	(Mahdavinia et al., 2018)
Trimetoprim		Artigo II desta Tese	(González et al., 2017a)

* Bovine serum albumin – albumina do soro bovino.

Metaloftalocianinas

A tese também retrata síntese de metaloftalocianinas mediante uma nova rota sintética sua imobilização em caulinita. Esse tema foi abordado anteriormente, porém de maneira parcial, explanando de suas características eletrônicas. A seguir é abordado suas características reacionais, no processo de obtenção dessas macromoléculas.

O primeiro indício das ftalocianinas foi no início do século XX, em 1907, por Braun e Tcherniac que observaram a formação de um sólido escuro e insolúvel na preparação de 2-cianobenzamida; em 1927, Von der Wied e Diesbach observaram a formação de um sólido de coloração azul intensa na reação de 1,2-dibromobenzeno com cianeto de cobre com piridina em refluxo; e em aproximadamente 1930, Linstead e Robertson começaram a caracterizar esses compostos, pois durante a produção industrial de ftalimida, a partir de anidrido ftálico, ocorreu a formação acidental de um composto azul-esverdeado de alta estabilidade térmica (ftalocianinato de cobre (II)) (Mack and Kobayashi, 2011). Essa descoberta acidental dos complexos metálicos de ftalocianinas (metaloftalocianinas) se tornara uma das mais importantes descobertas para a classe de pigmentos até os dias atuais. Suas propriedades físico-químicas despertaram interesse também em diversos setores tais como: eletrofotografia (Weiss, 2016), eletrocatálise (Brown and Schoenfisch, 2018) e terapia fotodinâmica (Kaya et al., 2018).

As MPCs são macrociclos aromáticos simétricos formados por anéis benzopirrólicos unidos por ligações de nitrogênio (Figura 11), formando uma conjugação de elétrons π que propicia elevado coeficiente de absortividade na região do ultravioleta/visível, configuração eletrônica estável e ótimas propriedades ópticas (Dumoulin et al., 2010; Marzouk et al., 2018; Nyokong and Antunes, 2010). Em geral, a síntese de metaloftalocianinas pode ser realizada empregando o método de ciclotetramerização de precursores derivados do 1,2-dicianobenzeno, ftalimidas, anidrido ftálico, ftaloimida e outros (Figura 11) (Do Nascimento et al., 2013; Gürek; and Hirel, 2011; Lukyanets and Nemykin, 2010; Mack and Kobayashi, 2011).

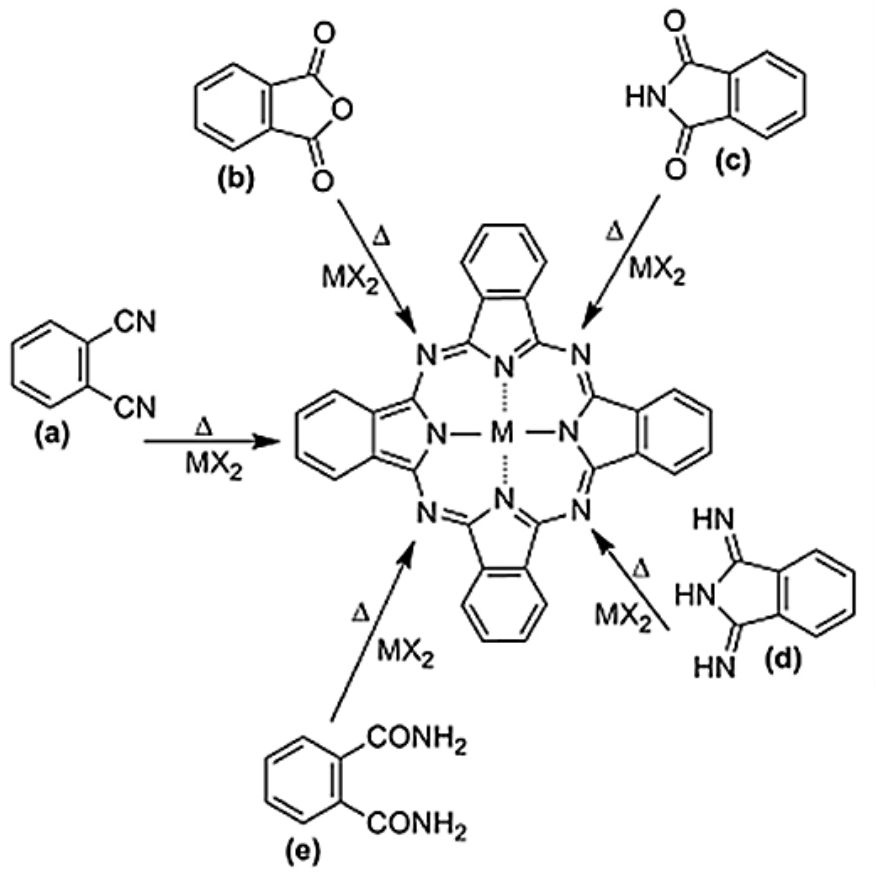

Figura 11: Alguns precursores das metaloftalocianinas incluindo (a) ftalonitrilos, (b) anidrido ftálico, (c) ftaloimidas, (d) 1,3-diiminoisoindolinas e (e) ftaloamidas (adaptado de (Mack and Kobayashi, 2011)) e o macrociclo ftalocianínico.

Desta forma, pesquisadores buscam incessantemente adaptar melhorias nos processos de obtenção de MPCs, com o objetivo de realizar processos com menores gastos energéticos e com menor prejuízo ao meio ambiente. Métodos desenvolvidos para a síntese de metaloftalocianinas envolvem reações que necessitam de moderadas temperaturas, solvente durante a síntese e na maioria dos casos, estas condições levam a produtos que necessitam de processos de purificação (Gürek; and Hirel, 2011; Kaya et al., 2018; Wong et al., 2017). A Tabela 5 a seguir sumariza alguns processos de sínteses.

Tabela 5: Condições reacionais de algumas sínteses na obtenção de metaloftalocianinas

Referência	Temperatura	Notas
(Shaposhnikov et al., 2005)	180-220°C	Síntese de metaloftalocianinas tetrassubstituídas (halogênio, grupos nitro, amino, hidroxi, ciano e terc-butila); Síntese utilizando cloretos metálicos dos grupos III e IV, solventes orgânicos, por exemplo: dimetilformamida; Purificação por Soxhlet utilizando benzeno, etanol ou acetona como solvente.
(Kaya et al., 2018)	130-160°C	Síntese de ftalocianina base livre e metaloftalocianina de zinco (II) e cobalto (II); Utilização de 1,8-diazabiciclo[5.4.0]undec-7-eno (DBU) como catalisador; Síntese durante 24h, utilização de *N,N*-dimetilacetamida como solvente Purificação por colunas cromatográficas de sílica gel e clorofórmio como eluente; Rendimentos de 38, 38 e 42% para ftalocianina base livre, metaloftalocianina de zinco e cobalto, respectivamente.
(Shaabani, 1998)	178-195°C	Primeira síntese de metaloftalocianinas sob irradiação de micro-ondas; Metaloftalocianinas de Cu (I), Co(II),Ni (II) e Fe(II); Reação entre os sais metálicos, anidrido ftálico e ureia, a 200°C; Tempo reacional: entre 4,5 e 7 minutos por micro-ondas e entre 360 e 660 minutos reportado para comparação; Rendimentos, após extração Soxhlet, entre 81 e 86%.
(Shaabani et al., 2007)	100-170°C	Síntese de ftalocianina base livre com purificação por extração Soxhlet; Método convencional: ftalonitrilo/hexametildisilazano/sulfato de amônio/dimetilformamida, 140-160°C, 1440min, 72% de rendimento; Ftalonitrilo/sulfeto de sódio/1,2 – propilenoglicol, 160-170°C, 180min, 10% de rendimento; Micro-ondas (900W): ftalonitrilo/hexametildisilazano/sulfato de amônio/dimetilformamida 6 min 75% de rendimento; Ftalonitrilo/sulfeto de sódio/1,2 – propilenoglicol, 5min, 70% de rendimento.
(Zhou et al., 2017)	240°C	Síntese de metaloftalocianina tetrasubstituída (sulfônico) de Co (II); Reagentes: 4-sultoftalato de triamônio, ureia, molibdtato de amônio; Lavagem em etanol e acetona e rendimento de 68%;

Mediante ao exposto, foi realizada uma busca na base de dados internacionais SCOPUS (www.scopus.com) sobre síntese de ftalocianinas e metaloftalocianinas, cujas palavras-chave utilizadas foram "*phthalocyanine synthesis*". Observa-se na Figura 12, que nos últimos 10 anos o número de publicações oscila positivamente e que no ano de 2014 foram publicados 261 artigos científico sobre o referido tema, porém quando se refina a busca para sínteses em uma única etapa, não é encontrado nenhum artigo ou literatura.

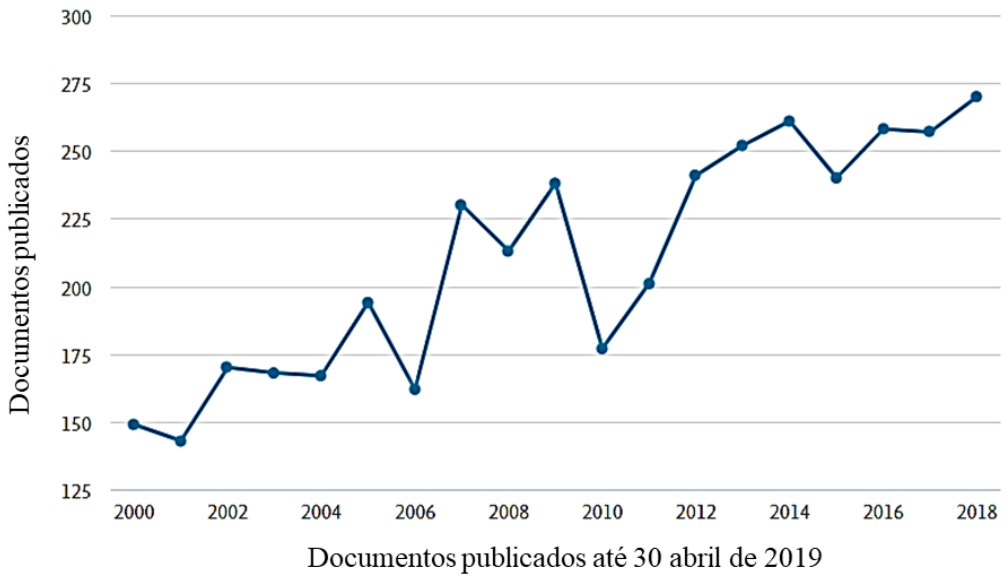

Figura 12: Publicações sobre síntese de metaloftalocianinas desde o ano 2000.

Assim, a tese desenvolvida foi dividida em 3 etapas:

- ✓ **Etapa 1:** a problemática referente à baixa eficiência energética do TiO_2, a possibilidade de promover melhorias dessas propriedades com a imobilização em matrizes inorgânicas e/ou juntamente a utilização de compostos de coordenação macrocíclicos, como metaloftalocianinas e porfirinas. O artigo I apresenta o estudo da obtenção de materiais compósitos aplicado a fotodegradação a base de caulinita/TiO_2/metaloftalocianinas, a fim de aumentar a faixa de absorção energética do novo material, com a finalidade de promover melhorias na conversão de energia, promovendo melhoras na eficiência energética. Com o processo de obtenção espera-se melhorias nas propriedades fotocatalíticas, juntamente a dispersão do TiO_2 na superfície de caulinita, mediante estudos de fotodegradação de prometrina, cafeína e trimetoprim.

- ✓ **Etapa 2:** como visto, argilominerais são bons exemplos para obtenção de materiais adsorventes e, baseado na literatura, observou-se que a modificação com compostos orgânicos e/ou inorgânicos pode promover melhorias significativas nas taxas de remoção. Assim, o artigo II desse trabalho apresenta a obtenção de um material híbrido baseado em laponita funcionalizada biureto e melamina para remoção por adsorção de trimetoprim.
- ✓ **Etapa 3:** devido às condições de síntese e imobilização de MPCs demandarem tempo e energia, o artigo III apresenta o estudo da obtenção de MPC mediante uma nova rota sintética, onde já ocorre a síntese e imobilização *in one step* da MPC na caulinita.

Objetivos do trabalho

Artigo I:

- Obter pelo método sol-gel, utilizando rotas ácida e básica, materiais baseados em Caulinita/TiO_2/Tetracarboximetaloftalocianina de cobalto(II) e caracterizar esses materiais.
- Estudar as propriedades catalíticas e fotocatalíticas frente a reações de oxidação (degradação) das moléculas orgânicas trimetoprim (TMP), prometrina (PMT) e cafeína (CFF).

Artigo II:

- Obter materiais pelo método sol-gel, mediante rota aquosa e não aquosa, baseados em laponita/3-cloropropiltrietoxissilano/(melamina ou biureto), e caracterizar estes materiais.
- Avaliar a adsorção de TMP, frente aos estudos cinético e de equilíbrio.

Artigo III:

- Obter um material baseado em caulinita e metaloftalocianina, aplicando nova rota sintética, e caracterizar este material.
- Confirmar a síntese e imobilização da metaloftalocianina.

Indicadores de calidad de las revistas en las que se han publicado los resultados de esta Tesis Doctoral

Como se ha indicado, los resultados obtenidos en las presente Tesis Doctoral se han recogido directamente en tres artículos científicos. A continuación, se comentan los indicadores de calidad de las revistas en las que se han publicado.

El criterio de calidad más utilizado por la comunidad científica internacional es el factor de impacto (FI). Este índice, elaborado anualmente, mide la frecuencia con la que un artículo de una revista ha sido citado en dicho año en el conjunto de todas las revistas indexadas en un determinado campo científico. Numéricamente, se calcula como el cociente entre el número total de citaciones recibidas en ese año por los artículos publicados en la revista en los dos años anteriores al mismo.

De esta manera, *Thomson Reuters* elabora anualmente el *Journal Citation Reports®,* clasificando más de 8000 revistas en el área de Ciencia y Tecnología. Estas revistas se sitúan en diferentes campos científicos, pudiendo estar una misma revista clasificada en varios campos científicos según sus líneas de investigación prioritarias.

Por su parte, el cuartil es un indicador que sirve para evaluar la importancia relativa de una revista dentro del total de revistas de su área, es decir, es una medida de posición de una revista en relación con todas las de su área. Si dividimos en cuatro partes iguales un listado de revistas ordenadas de mayor a menor índice de impacto, cada una de estas partes será un cuartil, y las revistas serán clasificadas, según su posición, en Q1, Q2, Q3 ó Q4. En los últimos años se han introducido, de forma análoga, las clasificaciones por terciles y deciles, esto es, clasificando las revistas en tres o en diez grupos según el criterio antes indicado, aunque hasta este momento ambas son mucho menos utilizadas que la clasificación por cuartiles.

En la Tabla 6 se presentan los factores de impacto de los últimos 5 años de las revistas en las que se han publicados los resultados directamente derivados de esta Tesis Doctoral, y las posiciones en las que se sitúan dentro de las categorías en las que dichas revistas se encuentran clasificadas.

Tabla 6. Factor de impacto de los últimos cinco años de las revistas en las que se han publicado los resultados de esta Tesis Doctoral, y su posición dentro de las categorías en las que se encuentran clasificadas, así como el cuartil en el que se encuentran.

Año	2014	2015	2016	2017	2018
			DYES AND PIGMENTS		
Factor de impacto	3,966	4,055	3,473	3,767	4,018
Clasificación relativa:					
Química Aplicada	5/72	6/72	11/72	11/72	13/71
Ingeniería Química	10/135	17/135	19/135	25/137	24/138
Ciencias de Materiales, Textiles	1/22	1/23	1/24	2/24	1/24
Cuartil					
Química Aplicada	Q1	Q1	Q1	Q1	Q1
Ingeniería Química	Q1	Q1	Q1	Q1	Q1
Ciencia de Materiales, Textiles	Q1	Q1	Q1	Q1	Q1
			MICROPOROUS AND MESOPOROUS MATERIALS		
Factor de impacto	3,453	3,349	3,615	3,649	4,182
Clasificación relativa:					
Química Aplicada	7/72	10/72	10/72	12/72	12/71
Química Física	40/139	45/144	43/146	51/147	46/148
Ciencias de materiales, Multidisciplinar	44/260	56/271	58/275	66/285	63/293
Nanociencia y Nanotecnología	26/80	31/83	33/87	38/92	37/94
Cuartil					
Química Aplicada	Q1	Q1	Q1	Q1	Q1
Química Física	Q2	Q2	Q2	Q2	Q2
Ciencias de Materiales, Multidisciplinar	Q1	Q1	Q1	Q1	Q1
Nanociencia y Nanotecnología	Q2	Q2	Q2	Q2	Q2
			JOURNAL OF THE BRAZILIAN CHEMICAL SOCIETY		
Factor de impacto	1,129	1,096	1,198	1,444	1,335
Clasificación relativa:					
Química, Multidisciplinar	100/157	110/163	114/166	108/171	122/172
Cuartil					
Química, Multidisciplinar	Q3	Q3	Q3	Q3	Q3

Como se ve, las dos primeras revistas tienen alto índice de impacto, y se sitúan en el primer cuartil al menos en uno de los campos científicos en el que están clasificadas. En cuanto a la última revista, aunque inicialmente era una revista nacional, en los últimos años publica sus artículos en inglés, habiendo aumentado su difusión, estabilizando su índice de impacto por encima de 1,0, y consolidando su posición en el tercer cuartil, lo cual es muy destacable para una revista que no es publicada por ninguna de las grandes editoriales internacionales.

Por otro lado, además de estos tres artículos, los resultados obtenidos en esta Tesis Doctoral se han recogido de forma parcial en otros cuatro artículos, uno publicado en *Dyes and Pigments*, otro en *Applied Clay Science* y dos en *Brazilian Journal of Thermal Analysis* (las primeras páginas de estos artículos se ofrecen en el Anexo 1). La calidad de la primera revista ya ha sido comentada, mientras que *Applied Clay Science* tiene un índice de impacto superior a 3,5 situándose en el primer cuartil en los campos de Ciencia de Materiales y Mineralogía. Por su parte, la revista *Brazilian Journal of Thermal Analysis* no está indexada por el *Journal Citation Reports*®, pero se trata de una revista significativa, implantada en el ámbito regional.

Por tanto, puede afirmarse que los resultados obtenidos en esta Tesis Doctoral han sido divulgados en revistas que presentan un alto factor de impacto y una categoría ampliamente reconocida en los ámbitos de la Catálisis, la Ciencia de los Materiales y las Ciencias Medioambientales.

Referências

Arnab, M., Apte, S.K., Naik, S.D., Sonawane, R.S., Kale, B.B., Baeg, J.O., Antonopoulou, M., Evgenidou, E., Lambropoulou, D., Konstantinou, I., 2014. A review on advanced oxidation processes for the removal of taste and odor compounds from aqueous media. Water Res. 90, 412–414. https://doi.org/10.1111/j.1551-2916.2006.01424.x

Barbosa, L.V., Marçal, L., Nassar, E.J., Calefi, P.S., Vicente, M.A., Trujillano, R., Rives, V., Gil, A., Korili, S.A., Ciuffi, K.J., de Faria, E.H., 2015. Kaolinite-titanium oxide nanocomposites prepared via sol-gel as heterogeneous photocatalysts for dyes degradation. Catal. Today 246, 133–142. https://doi.org/10.1016/j.cattod.2014.09.019

Behera, S.K., Oh, S.Y., Park, H.S., 2010. Sorption of triclosan onto activated carbon, kaolinite and montmorillonite: Effects of pH, ionic strength, and humic acid. J. Hazard. Mater. 179, 684–691. https://doi.org/10.1016/j.jhazmat.2010.03.056

Bethi, B., Sonawane, S.H., Bhanvase, B.A., Gumfekar, S.P., 2016. Nanomaterials-based advanced oxidation processes for wastewater treatment: A review. Chem. Eng. Process. Process Intensif. 109, 178–189. https://doi.org/10.1016/j.cep.2016.08.016

Bobu, M., Yediler, A., Siminiceanu, I., Schulte-Hostede, S., 2008. Degradation studies of ciprofloxacin on a pillared iron catalyst. Appl. Catal. B Environ. 83, 15–23. https://doi.org/10.1016/j.apcatb.2008.01.029

Bokare, A.D., Choi, W., 2014. Review of iron-free Fenton-like systems for activating H2O2 in advanced oxidation processes. J. Hazard. Mater. 275, 121–135. https://doi.org/10.1016/j.jhazmat.2014.04.054

Borsacchi, S., Geppi, M., Ricci, L., Ruggeri, G., Veracini, C.A., 2007. Interactions at the surface of organophilic-modified laponites: A multinuclear solid-state NMR study. Langmuir 23, 3953–3960. https://doi.org/10.1021/la063040a

Brown, M.D., Schoenfisch, M.H., 2018. Catalytic selectivity of metallophthalocyanines for electrochemical nitric oxide sensing. Electrochim. Acta 273, 98–104. https://doi.org/10.1016/j.electacta.2018.03.139

Byrne, C., Subramanian, G., Pillai, S.C., 2018. Recent advances in photocatalysis for environmental applications. J. Environ. Chem. Eng. 6, 3531–3555. https://doi.org/10.1016/j.jece.2017.07.080

Chen, D., Zhu, H., Wang, X., 2014. A facile method to synthesize the photocatalytic TiO2/montmorillonite nanocomposites with enhanced photoactivity. Appl. Surf. Sci. 319, 158–166. https://doi.org/10.1016/j.apsusc.2014.05.085

Cheng, H., Liu, Q., Yang, J., Ma, S., Frost, R.L., 2012. The thermal behavior of kaolinite intercalation complexes-A review. Thermochim. Acta 545, 1–13. https://doi.org/10.1016/j.tca.2012.04.005

Cummins, H.Z., 2007. Liquid, glass, gel: The phases of colloidal Laponite. J. Non. Cryst. Solids 353, 3891–3905. https://doi.org/10.1016/j.jnoncrysol.2007.02.066

de Faria, E.H., Lima, O.J., Ciuffi, K.J., Nassar, E.J., Vicente, M.A., Trujillano, R., Calefi, P.S., 2009.

Hybrid materials prepared by interlayer functionalization of kaolinite with pyridine-carboxylic acids. J. Colloid Interface Sci. 335, 210–215. https://doi.org/10.1016/j.jcis.2009.03.067

Dedzo, G.K., Detellier, C., 2014. Intercalation of two phenolic acids in an ionic liquid-kaolinite nanohybrid material and desorption studies. Appl. Clay Sci. 97–98, 153–159. https://doi.org/10.1016/j.clay.2014.04.038

Do Nascimento, F.B., Manieri, T.M., Cerchiaro, G., Ribeiro, A.O., 2013. Synthesis of unsymmetrical phthalocyanine derivatives and their interaction with mammary MCF7 cells. Dye. Pigment. 99, 316–322. https://doi.org/10.1016/j.dyepig.2013.05.012

Drugbank, n.d. Caffeine and Trimethoprim [WWW Document]. URL https://www.drugbank.ca/ (accessed 10.10.18).

Dumoulin, F., Durmuş, M., Ahsen, V., Nyokong, T., 2010. Synthetic pathways to water-soluble phthalocyanines and close analogs. Coord. Chem. Rev. 254, 2792–2847. https://doi.org/10.1016/j.ccr.2010.05.002

Ebrahimian, A., Zanjanchi, M.A., Noei, H., Arvand, M., Wang, Y., 2014. TiO 2 nanoparticles containing sulphonated cobalt phthalocyanine : Preparation , characterization and photocatalytic performance. J. Environ. Chem. Eng. 2, 484–494. https://doi.org/10.1016/j.jece.2014.01.022

EC-EU, n.d. European Commission - Health and Food Safety [WWW Document]. URL https://ec.europa.eu/info/departments/health-and-food-safety_en (accessed 10.10.18).

Elhalil, A., Elmoubarki, R., Farnane, M., Machrouhi, A., Sadiq, M., Mahjoubi, F.Z., Qourzal, S., Barka, N., 2018. Photocatalytic degradation of caffeine as a model pharmaceutical pollutant on Mg doped ZnO-Al2O3 heterostructure. Environ. Nanotechnology, Monit. Manag. 10, 63–72. https://doi.org/10.1016/j.enmm.2018.02.002

EPA, n.d. United States Environmental Protection Agency [WWW Document]. URL https://www.epa.gov (accessed 10.10.18).

Faria, E.H., 2011. Estudo das Propriedades Luminescentes e Catalíticas de Materiais Híbridos Obtidos pela Funcionalização de uma Caulinita Natural com Complexos de Ácidos Carboxílicos. Emerson Henrique de Faria. Tese (Doutorado em Ciências) 95 - Curso Pós-Graduação Strict. Sensu. Univ. Fr. Fr. 2011. 176.

Gardolinski, J.E., Martins Filho, H.P., Wypych, F., 2003. Comportamento térmico da caulinita hidratada. Quim. Nova 26, 30–35. https://doi.org/10.1590/S0100-40422003000100007

Geissen, V., Mol, H., Klumpp, E., Umlauf, G., Nadal, M., van der Ploeg, M., van de Zee, S.E.A.T.M., Ritsema, C.J., 2015. Emerging pollutants in the environment: A challenge for water resource management. Int. Soil Water Conserv. Res. 3, 57–65. https://doi.org/10.1016/j.iswcr.2015.03.002

González, B., da Silva, T.H., Ciuffi, K.J., Vicente, M.A., Trujillano, R., Rives, V., de Faria, E.H., Korili, S.A., Gil, A., 2017a. Laponite functionalized with biuret and melamine – Application to adsorption of antibiotic trimethoprim. Microporous Mesoporous Mater. 253, 112–122. https://doi.org/10.1016/j.micromeso.2017.06.047

González, B., Muñoz, B., Vicente, M., Trujillano, R., Rives, V., Gil, A., Korili, S., 2018. Photodegradation of 1,2,4-Trichlorobenzene on Montmorillonite–TiO2 Nanocomposites. ChemEngineering 2, 22. https://doi.org/10.3390/chemengineering2020022

González, B., Trujillano, R., Vicente, M.A., Rives, V., De Faria, E.H., Ciuffi, K.J., Korili, S.A., Gil, A., 2017b. Doped Ti-pillared clays as effective adsorbents-Application to methylene blue and trimethoprim removal. Environ. Chem. 14, 267–278. https://doi.org/10.1071/EN16192

Gräfe, M., Singh, B., Balasubramanian, M., 2007. Surface speciation of Cd(II) and Pb(II) on kaolinite by XAFS spectroscopy. J. Colloid Interface Sci. 315, 21–32. https://doi.org/10.1016/j.jcis.2007.05.022

Gürek;, A.G., Hirel, C., 2011. Photosensitizers in medicine, environment, and security, in: Photosensitizers in Medicine, Environment, and Security. Springer, Dordrecht, pp. 1–662. https://doi.org/10.1007/978-90-481-3872-2_2

Huang, H., Gu, X., Zhou, J., Ji, K., Liu, H., Feng, Y., 2009. Photocatalytic degradation of Rhodamine B on TiO2nanoparticles modified with porphyrin and iron-porphyrin. Catal. Commun. 11, 58–61. https://doi.org/10.1016/j.catcom.2009.08.012

Iurascu, B., Siminiceanu, I., Vione, D., Vicente, M.A., Gil, A., 2009. Phenol degradation in water through a heterogeneous photo-Fenton process catalyzed by Fe-treated laponite. Water Res. 43, 1313–1322. https://doi.org/10.1016/j.watres.2008.12.032

Kadish, K., Smith, K.M., Guilard, R., 1999. The porphyrin handbook. Academic Press.

Kaya, E.Ç., Ersoy, S., Durmuş, M., Kantekin, H., 2018. Synthesis of fluorine-containing phthalocyanines and investigation of the photophysical and photochemical properties of the metal-free and zinc phthalocyanines. Heterocycl. Commun. 24, 259–265. https://doi.org/10.1515/hc-2018-0049

Kibanova, D., Trejo, M., Destaillats, H., Cervini-Silva, J., 2009. Synthesis of hectorite – TiO2 and kaolinite – TiO2 nanocomposites with photocatalytic activity for the degradation of model air pollutants. Appl. Clay Sci. 42, 563–568. https://doi.org/10.1016/j.clay.2008.03.009

Kim, H., Sik, Y., Sharma, V.K., 2014. Adsorption of antibiotics and iopromide onto single-walled and multi-walled carbon nanotubes 255, 23–27.

Kudlek, E., 2017. Decomposition of Contaminants of Emerging Concern in Advanced Oxidation Processes. Proceedings 2, 180. https://doi.org/10.3390/ecws-2-04949

Lamastra, L., Balderacchi, M., Trevisan, M., 2016. Inclusion of emerging organic contaminants in groundwater monitoring plans. MethodsX 3, 459–476. https://doi.org/10.1016/j.mex.2016.05.008

Li, C., Sun, Z., Song, A., Dong, X., Zheng, S., Dionysiou, D.D., 2018. Flowing nitrogen atmosphere induced rich oxygen vacancies overspread the surface of TiO2/kaolinite composite for enhanced photocatalytic activity within broad radiation spectrum. Appl. Catal. B Environ. 236, 76–87. https://doi.org/10.1016/j.apcatb.2018.04.083

Li, Z., Hong, H., Liao, L., Ackley, C.J., Schulz, L.A., MacDonald, R.A., Mihelich, A.L., Emard, S.M.,

2011. A mechanistic study of ciprofloxacin removal by kaolinite. Colloids Surfaces B Biointerfaces 88, 339–344. https://doi.org/10.1016/j.colsurfb.2011.07.011

Lorenzo, M., Campo, J., Picó, Y., 2018. Analytical challenges to determine emerging persistent organic pollutants in aquatic ecosystems. TrAC - Trends Anal. Chem. 103, 137–155. https://doi.org/10.1016/j.trac.2018.04.003

Lü, X., Qian, H., Mele, G., Riccardis, A. De, Zhao, R., Chen, J., Wu, H., Hu, N., 2017. Impact of different TiO2 samples and porphyrin substituents on the photocatalytic performance of TiO2@copper porphyrin composites. Catal. Today 281, 45–52. https://doi.org/10.1016/j.cattod.2016.04.027

Lukyanets, E.A., Nemykin, V.N., 2010. The key role of peripheral substituents in the chemistry of phthalocyanines and their analogs. J. Porphyr. Phthalocyanines 14, 1–40. https://doi.org/10.1142/S1088424610001799

Machado, G.S., Groszewicz, P.B., Castro, K.A.D. de F., Wypych, F., Nakagaki, S., 2012. Catalysts for heterogeneous oxidation reaction based on metalloporphyrins immobilized on kaolinite modified with triethanolamine. J. Colloid Interface Sci. 374, 278–286. https://doi.org/10.1016/j.jcis.2012.02.014

Mack, J., Kobayashi, N., 2011. Low symmetry phthalocyanines and their analogues. Chem. Rev. 111, 281–321. https://doi.org/10.1021/cr9003049

Mahdavinia, G.R., Soleymani, M., Etemadi, H., Sabzi, M., Atlasi, Z., 2018. Model protein BSA adsorption onto novel magnetic chitosan/PVA/laponite RD hydrogel nanocomposite beads. Int. J. Biol. Macromol. 107, 719–729. https://doi.org/10.1016/j.ijbiomac.2017.09.042

Marçal, L., de Faria, E.H., Nassar, E.J., Trujillano, R., Martín, N., Vicente, M.A., Rives, V., Gil, A., Korili, S.A., Ciuffi, K.J., 2015. Organically Modified Saponites: SAXS Study of Swelling and Application in Caffeine Removal. ACS Appl. Mater. Interfaces 7, 10853–10862. https://doi.org/10.1021/acsami.5b01894

Martín, J., Orta, M. del M., Medina-Carrasco, S., Santos, J.L., Aparicio, I., Alonso, E., 2018. Removal of priority and emerging pollutants from aqueous media by adsorption onto synthetic organo-funtionalized high-charge swelling micas. Environ. Res. 164, 488–494. https://doi.org/10.1016/j.envres.2018.03.037

Marzouk, S., Heinrich, B., Lévêque, P., Leclerc, N., Khiari, J., Méry, S., 2018. Phthalocyanine-based dumbbell-shaped molecule: Synthesis, structure and charge transport studies. Dye. Pigment. 154, 282–289. https://doi.org/10.1016/j.dyepig.2018.03.017

Mesgari, Z., Gharagozlou, M., Khosravi, A., Gharanjig, K., 2012. Spectrophotometric studies of visible light induced photocatalytic degradation of methyl orange using phthalocyanine-modified Fe-doped TiO2 nanocrystals. Spectrochim. Acta Part A Mol. Biomol. Spectrosc. 92, 148–153. https://doi.org/10.1016/j.saa.2012.02.055

Min, K.S., Kumar, R.S., Lee, J.H., Kim, K.S., Lee, S.G., Son, Y.A., 2019. Synthesis of new

TiO2/porphyrin-based composites and photocatalytic studies on methylene blue degradation. Dye. Pigment. 160, 37–47. https://doi.org/10.1016/j.dyepig.2018.07.045

Molinari, R., Lavorato, C., Argurio, P., 2017. Recent progress of photocatalytic membrane reactors in water treatment and in synthesis of organic compounds. A review. Catal. Today 281, 144–164. https://doi.org/10.1016/j.cattod.2016.06.047

Norman, 2017. Network of reference laboratories, research centres and related organisations for monitoring of emerging environmental substances [WWW Document]. URL http://www.norman-network.net (accessed 10.10.18).

Nyokong, T., Antunes, E., 2010. Photochemical and photophysical properties of metallophthalocyanines, in: Handbook of Porphyrin Science. World Scientific, pp. 247–357. https://doi.org/10.1142/9789814307246_0006

Papoulis, D., Panagiotaras, D., Tsigrou, P., Christoforidis, K.C., Petit, C., Apostolopoulou, A., Stathatos, E., Komarneni, S., Koukouvelas, I., 2018. Halloysite and sepiolite –TiO2 nanocomposites: Synthesis characterization and photocatalytic activity in three aquatic wastes. Mater. Sci. Semicond. Process. 85, 1–8. https://doi.org/10.1016/j.mssp.2018.05.025

Peng, Y., Fang, W., Krauss, M., Brack, W., Wang, Z., Li, F., Zhang, X., 2018. Screening hundreds of emerging organic pollutants (EOPs) in surface water from the Yangtze River Delta (YRD): Occurrence, distribution, ecological risk. Environ. Pollut. 241, 484–493. https://doi.org/10.1016/j.envpol.2018.05.061

Pereira, D.H., Porta, F.A. La, Santiago, R.T., Garcia, D.R., Ramalho, T.C., 2016. New Perspectives on the Role of Frontier Molecular Orbitals in the Study of Chemical Reactivity: A Review. Rev. Virtual Química 8, 425–453. https://doi.org/10.5935/1984-6835.20160032

Petrie, B., Barden, R., Kasprzyk-Hordern, B., 2015. A review on emerging contaminants in wastewaters and the environment: Current knowledge, understudied areas and recommendations for future monitoring. Water Res. 2, 3–27. https://doi.org/10.1016/j.watres.2014.08.053

Pi, Y., Li, X., Xia, Q., Wu, J., Li, Y., Xiao, J., Li, Z., 2017. Adsorptive and photocatalytic removal of Persistent Organic Pollutants (POPs) in water by metal-organic frameworks (MOFs). Chem. Eng. J. 337, 351–371. https://doi.org/10.1016/j.cej.2017.12.092

Pirbazari, A.E., 2015. Sensitization of Tio2 Nanoparticles With Cobalt Phthalocyanine: An Active Photocatalyst for Degradation of 4-Chlorophenol under Visible Light. Procedia Mater. Sci. 11, 622–627. https://doi.org/10.1016/j.mspro.2015.11.096

PubChem, n.d. Open Chemistry Database [WWW Document]. URL https://pubchem.ncbi.nlm.nih.gov.ez249.periodicos.capes.gov.br (accessed 10.10.18).

Rodriguez, O., Peralta-hernandez, J.M., Goonetilleke, A., 2017. Treatment Technologies for Emerging Contaminants in water: A review. Chem. Eng. J. 323, 361–380. https://doi.org/10.1016/j.cej.2017.04.106

Rouquerol, F., Rouquerol, J., Sing, K., 1999. Adsorption by powders & porous solids - principles,

methodology andapplications. Academic Press.

Santos, A.Ma.S., 2016. Impacto do Atomo de Metal nas Propriedades Eletrônicas e Opticas de Ftalocianinas. Universidade de Brasília.

Sevim, A.M., 2017. Synthesis and characterization of Zn and Co monocarboxy-phthalocyanines and investigation of their photocatalytic efficiency as TiO2composites. J. Organomet. Chem. 832, 18–26. https://doi.org/10.1016/j.jorganchem.2017.01.011

Shaabani, A., 1998. Synthesis of Metallophthalocyanines under Solvent-free Conditions using Microwave Irradiation. J. Chem. Res. 0, 672–673. https://doi.org/10.1039/a708858b

Shaabani, A., Maleki-Moghaddam, R., Maleki, A., Rezayan, A.H., 2007. Microwave assisted synthesis of metal-free phthalocyanine and metallophthalocyanines. Dye. Pigment. 74, 279–282. https://doi.org/10.1016/j.dyepig.2006.02.005

Shaposhnikov, G.P., Maizlish, V.E., Kulinich, V.P., 2005. Synthesis and properties of extracomplexes of tetrasubstitued phthalocyanines. Russ. J. Gen. Chem. 75, 1830–1839. https://doi.org/1070-3632/05/7511-1830

Stathatos, E., Papoulis, D., Aggelopoulos, C.A., Panagiotaras, D., Nikolopoulou, A., 2012. TiO2/palygorskite composite nanocrystalline films prepared by surfactant templating route: Synergistic effect to the photocatalytic degradation of an azo-dye in water. J. Hazard. Mater. 211–212, 68–76. https://doi.org/10.1016/j.jhazmat.2011.11.055

Sun, W., Li, J., Mele, G., Zhang, Z., Zhang, F., 2013. Chemical Enhanced photocatalytic degradation of rhodamine B by surface modification of ZnO with copper (II) porphyrin under both UV – vis and visible light irradiation. J. Mol. Catal. A Chem. 366, 84–91.

Szczepanik, B., 2017. Photocatalytic degradation of organic contaminants over clay-TiO2 nanocomposites: A review. Appl. Clay Sci. 141, 227–239. https://doi.org/10.1016/j.clay.2017.02.029

Teodosiu, C., Gilca, A.-F., Barjoveanu, G., Fiore, S., 2018. Emerging pollutants removal through advanced drinking water treatment: A review on processes and environmental performances assessment. J. Clean. Prod. 197, 1210–1221. https://doi.org/10.1016/j.jclepro.2018.06.247

Urbani, M., Grätzel, M., Nazeeruddin, M.K., Torres, T., 2014. Meso-Substituted Porphyrins for Dye-Sensitized Solar Cells. Chem. Rev. 114, 12330–12396. https://doi.org/10.1021/cr5001964

Vrana, B., Smedes, F., Prokeš, R., Loos, R., Mazzella, N., Miege, C., Budzinski, H., Vermeirssen, E., Ocelka, T., Gravell, A., Kaserzon, S., 2016. NORMAN interlaboratory study (ILS) on passive sampling of emerging pollutants - Publications Office of the European Union. https://doi.org/10.2788/6757

Wang, D., Bolton, J.R., Andrews, S.A., Hofmann, R., 2015. Formation of disinfection by-products in the ultraviolet/chlorine advanced oxidation process. Sci. Total Environ. 518–519, 49–57. https://doi.org/10.1016/j.scitotenv.2015.02.094

Weiss, D.S., 2016. The History and Development of Organic Photoconductors for

Electrophotography. J. Imaging Sci. Technol. 60, 305051–3050524. https://doi.org/10.2352/J.ImagingSci.Technol.2016.60.3.030505

Wong, R.C.H., Lo, P.C., Ng, D.K.P., 2017. Stimuli responsive phthalocyanine-based fluorescent probes and photosensitizers. Coord. Chem. Rev. https://doi.org/10.1016/j.ccr.2017.10.006

Yu, M., Li, Y., Zhang, S., Li, X., Yang, Y., Chen, Y., Ma, G., Su, Z., 2014. Improving stability of virus-like particles by ion-exchange chromatographic supports with large pore size: Advantages of gigaporous media beyond enhanced binding capacity. J. Chromatogr. A 1331, 69–79. https://doi.org/10.1016/j.chroma.2014.01.027

Zajac, L., Olszowski, P., Godlewski, S., Bodek, L., Such, B., Jöhr, R., Pawlak, R., Hinaut, A., Glatzel, T., Meyer, E., Szymonski, M., 2016. Self-assembling of Zn porphyrins on a (110) face of rutile TiO2-The anchoring role of carboxyl groups. Appl. Surf. Sci. 379, 277–281. https://doi.org/10.1016/j.apsusc.2016.04.069

Zhao, L., Deng, J., Sun, P., Liu, J., Ji, Y., Nakada, N., Qiao, Z., Tanaka, H., Yang, Y., 2018. Nanomaterials for treating emerging contaminants in water by adsorption and photocatalysis : Systematic review and bibliometric analysis. Sci. Total Environ. 627, 1253–1263. https://doi.org/10.1016/j.scitotenv.2018.02.006

Zhou, W., Zhou, J., Chen, Y., Cui, A., Sun, F., He, M., Xu, Z., Chen, Q., 2017. Metallophthalocyanine intercalated layered double hydroxides as an efficient catalyst for the selective epoxidation of olefin with oxygen. Appl. Catal. A Gen. 542, 191–200. https://doi.org/10.1016/j.apcata.2017.05.029

ARTICLE I

JBCS 30 years

http://dx.doi.org/10.21577/0103-5053.20190178

J. Braz. Chem. Soc., Vol. 00, No. 00, 1-14, 2019
Printed in Brazil - ©2019 Sociedade Brasileira de Química

Article

Kaolinite/TiO_2/cobalt(II) Tetracarboxymetallophthalocyanine Nanocomposites as Heterogeneous Photocatalysts for Decomposition of Organic Pollutants Trimethoprim, Caffeine and Prometryn

Tiago H. da Silva,[a] Anderson O. Ribeiro,[b] Eduardo J. Nassar,[a] Raquel Trujillano,[c] Vicente Rives,[c] Miguel A. Vicente,[c] Emerson H. de Faria[,a] and Katia J. Ciuffi*[,a]*

[a]*Universidade de Franca, Av. Dr. Armando Salles Oliveira, 201, Pq. Universitário, 14404-600 Franca-SP, Brazil*

[b]*Centro de Ciências Naturais e Humanas, Universidade Federal do ABC, 09210-170 Santo André-SP, Brazil*

[c]*GIR-QUESCAT, Departamento de Química Inorgánica, Universidad de Salamanca, 37008 Salamanca, Spain*

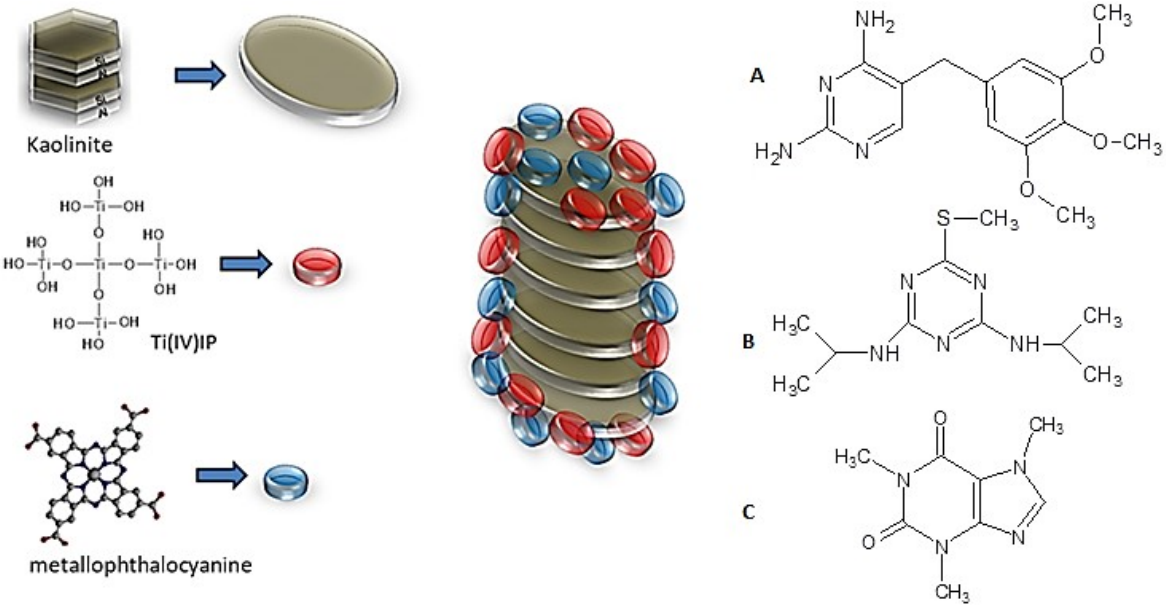

ABSTRACT

São Simão's Brazilian kaolinite has been treated with titanium(IV) isopropoxide and cobalt(II) tetracarboxymetallophthalocyanine under different conditions (acidic or basic), leading, after drying at 100ºC, to new titania-doped Co(II)-metallophthalocyanine/kaolinite solids. These solids were characterised by chemical analysis, powder X-ray diffraction, fourier transform infrared spectroscopy, thermal analyses and nitrogen adsorption. No significant changes were observed by diffractometry, but the specific surface area depended of the synthetic route followed. The ability of these solids for photodegradation of trimethoprim, caffeine and prometryn was evaluated. The photodegradation was followed via mass spectrometry and UV/Vis absorption spectroscopy. The presence of photodegradation by-products was verified in all cases. All the photocatalysts showed high photodegradation rate against prometryn, trimethoprim and caffeine, the degradation efficiencies were 54, 30 and 90%, respectively, when using the heterogeneous photocatalysts. Comparison with commercial TiO_2 (Degusa®) proved that the synthesized photocatalyst based on kaolinite present higher degradation rate than isolated titanium dioxide.

Keywords: Clay minerals; Sol-gel; Heterogeneous Photocatalysis

1. Introduction

The Humankind uses large amounts of chemicals/pharmaceuticals in numerous areas as cosmetics, medicine and industrial.(Grazieli and Collins, 2011; Michael et al., 2013) This excessive consumption could promote an exponential increase in the productive processes of these compounds, which results on the discharge of untreated wastes or partially treated wastewater in natural environments. This incorrect disposal may directly contaminate surface or underground water.(Bethi et al., 2016) In this way, the concern about drinking water should lead to the development of more efficient processes for the treatment of water and wastewater, aiming at environmental preservation. In this context, advanced oxidation process is a promising technology that does not require large cost for up-scaling to technological application and results in higher yields of degradation of organic compounds promoting in some cases the complete mineralization of the pollutants.

Nowadays, the emerging organic pollutants (EOPs) are defined as synthetic or naturally occurring chemicals that are not commonly monitored in the environment, but which have the potential to enter the environment and cause known or suspected adverse ecological and (or) human health effects. More than 700 emerging pollutants, their metabolites and transformation products, have been found in European aquatic environments.(Geissen et al., 2015) These emerging pollutants, and their metabolites and transformation products, have been listed by NORMAN Network (2017).(Norman, 2017)

In this context, trimethoprim [2,4-diamine 5-(3,4,5-trimethoxybenzyl)pyrimidine] (TMP) is a widely used antibacterial drug for treatment of urinary, respiratory or gastrointestinal infections, with application in humans and animals.(Luo et al., 2012; Zhang et al., 2016) However, TMP is incompletely metabolized by humans during the therapeutic process and about 80% is excreted in the pharmacologically active form, which can promote the development of bacterial resistance to this medicine,(Ji et al., 2016; L. Liu et al., 2017; Oros-Ruiz et al., 2013; Zhang et al., 2016) converting this compound in an EOP.

Another example of EOP is caffeine (1,3,7-trimethylxanthine) (CFF), which belongs to the family of methylxanthines and can be classified as an alkaloid; it is consumed regularly around the world, e.g. beverages, pharmaceuticals and products for personal care, becoming a chemical marker of the pollution of surface water and environmental pollution indicator. Caffeine features characteristic stimulant, psychoactive properties, acting on the central nervous system of humans, promoting changes in sleep and agility.(Marçal et al., 2015;

Marques et al., 2013) Large amounts of caffeine occur in the seeds, leaves, and fruits of some plants, the microorganisms existing in the environment cannot metabolize this compound satisfactorily.

Another important pollutant is prometryn (2,4-bis(isopropylamino)-6-(methylthio)-1,3,5-triazine) (PMT), a triazine-class herbicide widely used to control grass and weeds in a range of agro-industrial crops. This class of herbicides, due to their chemical stability, settles in the soil for a large period of time and consequently contaminates water bodies, as groundwater.(Claver et al., 2006; J. Liu et al., 2017) Prometryn is considered a moderately persistent chemical and listed in European Commission Health and Food Safety guidelines as toxic compound,(Claver et al., 2006; Evgenidou et al., 2007; J. Liu et al., 2017) needing the development of methods for its control and remediation.

Considering the great problem of environmental contamination by EOPs, the advanced oxidation processes (AOPs) show a great potential for their elimination. That is, heterogeneous photocatalysis using semiconducting materials emerges as a promising strategy for the protection of the ecosystem and human health because it is effective in the treatment of pharmaceuticals, dyes, herbicides and pesticides, in different concentration ranges, unlike conventional biological treatment processes, which have difficulties for their complete removal.(Alharbi et al., 2017; Araújo et al., 2014; Barbosa et al., 2015; Bethi et al., 2016; Christoforidis et al., 2016; Michael et al., 2013; Patil et al., 2014)

Some materials stand out in photocatalytic processes for environmental remediation, while particles of titanium dioxide (TiO_2) stand out as the most used, functional, versatile and effective photocatalyst, due to its photoelectric properties, low cost, corrosion resistance and non-toxicity.(Deng et al., 2016; Papoulis et al., 2013; Ratnasamy et al., 2004) One of the problems for using of TiO_2 is its low energy efficiency, its energy *band gap* is 3.2 eV, equivalent to the ultraviolet wavelength of 387.5 nm, which corresponds to only 3 to 5% of the solar radiation reaching the Earth surface.(Bethi et al., 2016; Dobrowolska et al., 2012; Mesgari et al., 2012) This problem can be mitigated with some procedures, such as the dispersion on inorganic matrices,(Barbosa et al., 2015; Karamanis et al., 2011; Papoulis et al., 2010) such as clay minerals. Clay minerals are attractive materials for many significant applications, due to their physical and chemical properties, including catalysis/photocatalysis and adsorption,(De Faria et al., 2012; Janíková et al., 2017; Marçal et al., 2015) especially kaolinite, whose layered structure provides the possibility of retention of a great variety of compounds to reduce the energy required for the activation of the semiconductor. Catalyst

improvement via immobilization might also be due to the force field between the support and the TiO_2 particles that inhibits the recombination of electron-hole pairs.(Barbosa et al., 2015)

The metallophtalocyanines molecules consist of aromatic symmetrical macrocycles with benzopyrrole rings connected by nitrogen links that provide a π electron arrangement, providing to the metallophtalocyanines a high absorption coefficient in the ultraviolet/visible region, similar to that of porphyrins, favoring the transfer of energy to the semiconductor.(T. H. da Silva et al., 2016; Kadish et al., 1999; Kimura et al., 2003)

Considering the possibility of improving the catalytic properties of TiO_2 associated to its low energy conversion by dispersion on inorganic matrices along with complexation of organometallic compounds such as metallophtalocyanines, we here report on the preparation of kaolinite/TiO_2/metallophtalocyanines composites, and their application for the degradation of various pollutants, namely, trimethoprim, caffeine and prometryn (Table I.S1).

2. Experimental

2.1. Purification of kaolinite

The kaolinite used in this work was provided by the mining company Darcy R.O. Silva & Cia, located in the city of São Simão (Brazil). The raw clay mineral was purified by the dispersion-decantation method,(de Faria et al., 2010, 2009) and the purified kaolinite was designated Kaol.

2.2. Synthesis of the photocatalysts

The photocatalyst materials were obtained by the sol-gel method, as described by Barbosa *et al.*(Barbosa et al., 2015) A mixture of ethanol (200 mL), kaolinite (38.02 mmol), titanium(IV) isopropoxide (Ti(IV)IP) (8.444 mmol) and cobalt(II) tetracarboxyphthalocyanine (CoMPc) (0.1939 mmol) was submitted to strong magnetic stirring for 24 h at room temperature, in acidic (acetic acid – 17.49 mmol) or basic (sodium hydroxide – 15 mmol) medium, to study the influence of pH on the formation of the material. The hydrolysis/condensation process is schematized in Fig. I.S1.

The samples were denoted as CAR (Composite Acid Route), that is, Kaol-Ti-H^+, a reference solid obtained carrying out the entire process but without the addition of CoMPc, and CAR-CoMPc with the addition of the organometallic compound. Analogously, for the synthesis by the basic route, the solids obtained were denoted CBR (Composite Basic Route, without CoMPc) and CBR-CoMPc with the addition of the metallophtalocyanine, respectively. All the materials were submitted to heat treatment (400ºC) for 3 hours for the removal of solvents and stabilization of the TiO_2 phase, and washed to remove possible non-attached oxides formed during the thermal treatment.

2.3 Photocatalysis study

For the photodegradation reaction studies, a MPDS–Basic system from Peschl Ultraviolet, with a PhotoLAB Batch–L reactor and a TQ150–Z0 lamp (power 150 W), integrated in a photon CABINET, was used. The spectrum is continuous, with the main peaks at 546 nm (φ 5.1 W), 366 nm (radiation flux, φ 6.4 W), 313 nm (φ 4.3 W) and 254 nm (radiation flux, φ 4 W). The reactor is vertically oriented and it is refrigerated by circulating cold water. In each reaction, 750 mg of catalyst was added to a contaminant solution of 25 mg L^{-1} (TMP and CFF) in H_2O and 10 mg L^{-1} of PMT in a 1:1 ethanol:H_2O mixture, due to the

low solubility in water, although the presence of ethanol is not expected to interfere in the catalytic reaction. The concentration of the contaminants was determined by UV–visible spectroscopy at pre-determined time intervals between 15 and 240 min, using a Perkin-Elmer Lambda 35 spectrophotometer. To identify the by–products generated during UV degradation, the solutions were analyzed by mass spectrometry after various treatment times. The equipment used for this purpose was an Agilent 1100 HPLC apparatus coupled to an ultraviolet detector and an Agilent Trap XCT mass spectrometer. These analyses were carried out at Servicio Central de Análisis Elemental, Cromatografía y Masas (Universidad de Salamanca).

2.3.1 Evaluation of photodegradation mechanism

In a typical experiment, a 10 mg L^{-1} aqueous solution of PMT was continuously stirred magnetically through the reactor. A 5 mL aliquot was collected and analyzed by UV-visible spectroscopy (UV/Vis). The effect of chloride ions on the photocatalytic activity was investigated by adding sodium chloride (NaCl) (concentration 16.6 mg L^{-1}) to the initial PMT solution, using the described system.

2.4. Characterization techniques

Chemical analyses were carried out by using a Mass spectrometer with Inductive Coupling Plasma source (ICP-MS) Elan 6000 from Perkin-Elmer Sciex equipped with an autosampler located in a laminar flow hood. The powder X-ray diffraction (PXRD) diagrams of the solids were recorded in a Siemens D-5000 diffractometer operating at 40 kV and 30 mA, using filtered Cu Kα radiation in the 2-65º (2θ) range. All the analyses were carried out at a scan speed of 2º min^{-1}. The thermal analyses were carried out in a TA Instruments SDTQ600 simultaneous DTA-TGA thermal analyzer, at temperatures ranging from 25 to 900ºC, at a heating rate of 10 ºC min^{-1} and under air flow (100 mL min^{-1}). The infrared absorption spectra were recorded in a Perkin. Elmer FTIR Frontier Spectrometer by using a diffuse reflectance accessory, using the KBr pellet technique. The BET specific surface area and porosity data of the solids were calculated from their nitrogen adsorption-desorption isotherms at -196ºC, recorded in a Micromeritics Gemini VII 2390T apparatus. The samples were previously treated at 110ºC under a stream of N_2 for 2 h, in a Micromeritics Flowprep 060 equipment. The absorption spectra in the ultraviolet/visible region were obtained in a Perkin-Elmer Lambda 35 spectrophotometer, coupled to a computer with UV WinLab 2.85

software. Calibration curves were used for the pollutants, verifying that they followed the Lambert-Beer law in the concentration range used in the work. The wavelengths of maximum absorbance were 286 nm for TMP, 273 nm for CFF and 223 nm for PMT, respectively.

3. Results and discussion

3.1. Characterization of the solids

The thermogravimetric curves of the two composites containing the metallophtalocyanines (Fig. I.1) were very similar to those from parent kaolinite and for the composites without metallophtalocyanines (Fig. I.S2). Both CAR-CoMPc and CBR-CoMPc materials showed mass losses related to the elimination of water and solvent close to 60ºC. From this temperature up to ca. 400ºC, removal of organic matter from the precursors was observed as a gently process, followed by the strong mass loss due to dehydroxylation of kaolinite. The dehydroxylation temperature and mass percentage were different from those in parent kaolinite. Thus, for sample CAR-CoMPc the mass loss between 400-900ºC was 13.44%, suggesting the presence of organic matter and/or hydroxyl groups derived from the formation of the polymeric titanium network and immobilized CoMPc, and probably related to the high thermal stability of metallophtalocyanines.(T. H. da Silva et al., 2016) For the CBR-CoMPc solid, this mass loss was 11.69%, suggesting the presence of a lower concentration of hydroxyl groups and CoMPc, probably because of the formation of larger titania aggregates, hindering the immobilization of CoMPc. The thermal curves of composites without CoMPc were very similar, only noting small differences in the mass loss percentages, attributable to differences in the amount of organic matter and of hydroxyl groups. It was also observed that despite very similar amounts of sample were used in the thermal studies, the intensity of the DTA signals was much stronger for sample CAR-CoMPc than for sample CBR-CoMPc, although the mass losses (percentage) were similar in both cases. Due to the low pH value, the carboxylic group was not deprotonated in the acid route (sample CAR-CoMPc) and could react with the titania-kaolinite substrate forming a covalent bond; however, deprotonated carboxylate groups could be coordinated to coordinatively unsaturated (cus) Ti^{4+} cations at the titania surface.

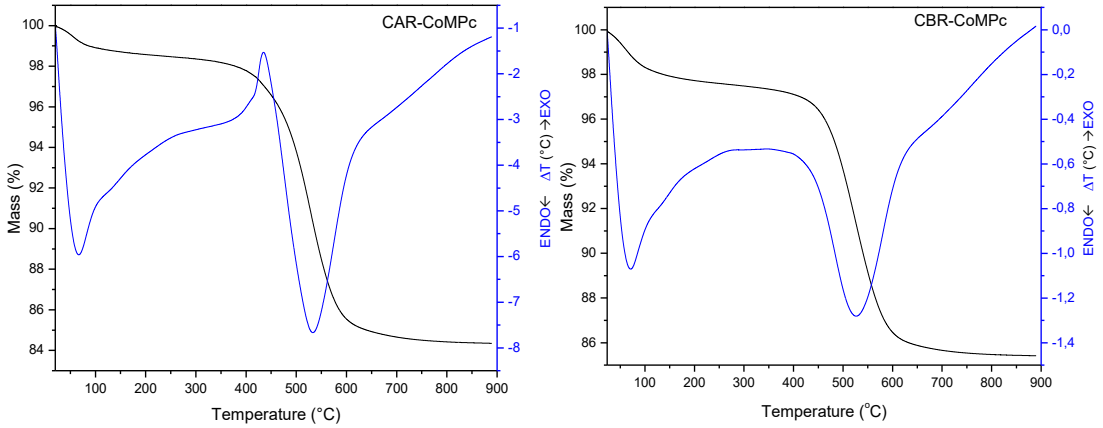

Fig. I.1. TG/DTA Curves of materials derived from kaolinite.

Chemical composition of kaolinite (Table I.1) was very similar to that previously reported,(de Faria et al., 2009) with small differences attributable to isomorphous substitutions. The Si/Al ratio is an important information for kaolinite-derived materials; this ratio is hardly changed, as it would require extreme chemical reactions. The ratio for the parent sample was 1.028. For samples CAR and CBR, this ratio was 1.020 and 1.023, respectively, indicating that the structure of kaolinite was not affected by the incorporation of Ti-species, while for samples CAR-CoMPc and CBR-CoMPc this ratio decreased to 0.999 and 0.962, respectively, suggesting the solubilization of a small amount of silica from the tetrahedral sheet of kaolinite, although a priori it was not expectable that the presence of the metallophtalocyanine may cause this process.(Barbosa et al., 2015; T. H. da Silva et al., 2016)

Table I.1

Chemical composition of the materials, expressed in the free-water form.

	SiO_2	Al_2O_3	Fe_2O_3	MnO	MgO	CaO	Na_2O	K_2O	TiO_2
Kaol	53.02	43.84	1.12	0.01	0.27	0.09	0.06	0.44	1.14
CAR	52.31	43.59	1.09	0.01	0.27	0.08	0.02	0.44	2.19
CBR	48.60	40.39	1.06	0.01	0.26	0.08	1.57	0.42	7.60
CAR-CoMPc	52.00	44.27	1.11	0.01	0.27	0.08	0.02	0.43	1.80
CBR-CoMPc	48.06	42.47	0.99	0.01	0.24	0.08	0.87	0.42	6.86

The content of TiO_2 strongly changed from parent kaolinite to all the composites. The amount of supported TiO_2 was moderate in the composites prepared in the absence of CoMPc (0.6-1.1%), and much higher, 5.7-6.5%, in the presence of this compound, which suggested that the presence of CoMPc strongly affected the hydrolysis of the Ti-precursor; in fact, the Ti precursor can hydrolyze on carboxylate group of CoMPc, as proposed in Fig. I.S1. The presence of so different titania contents could be related to the relative importance of the hydrolysis of the titanium precursor and the condensation steps during the formation of the hybrid materials. Hydrolysis was favored in the acid route (pH close to 4), leading to the formation of a large concentration of Ti-OH units and thus a larger number of small titania clusters would be formed. The basic route (pH close to 12) would give rise to larger precipitation of titania particles, which agglomerate forming large particles.

The acid route promoted the protonation of the alkoxide groups, and preferentially directed the crystalline network to the edges of the kaolinite structure, resulting in a more extended and less branched inorganic polymeric network. Through the basic route, the alkoxide deprotonated, promoting the decrease of the hydrolysis rate, but at the same time improving the condensation kinetics, forming more agglomerated and highly branched species. These facts could explain why the amount of titanium oxide deposited on sample CAR was smaller than on sample CBR.(Brinker and Scherer, 1990)

According to the X-ray diffractograms, the reaction of kaolinite with Ti(IV)IP and CoMPc did not promote any change in the structure of the former (Fig. I.2). Thus, basal spacing of kaolinite remained close to 7.15 Å in all the solids. Kaolinite is usually submitted to a previous swelling treatment with highly polar molecules, e.g., dimethylsulfoxide, to favor intercalation of other species. However, this treatment was not applied in the present case, so it was expectable that the reactions taking place with the other reactants would take place only on the kaolinite surface and on the edges of the crystals and not in the interlayer space, so without swelling of the kaolinite structure.

On other hand, no reflections from Ti-containing species were observed. However, the decrease in the relative intensity of the basal reflection suggested some sort of interaction between kaolinite, CoMPc and TiO_2 (Fig. I.2). This decrease may be caused by the covering of kaolinite surface with titanium alkoxide species, and the attachment of titanium dioxide and CoMPc to the kaolinite layers after hydrolysis and condensation of the alkoxide, interacting with the kaolinite surface.(A. C. da Silva et al., 2016; Dedzo and Detellier, 2014; Letaief et al., 2011; Zbik et al., 2010)

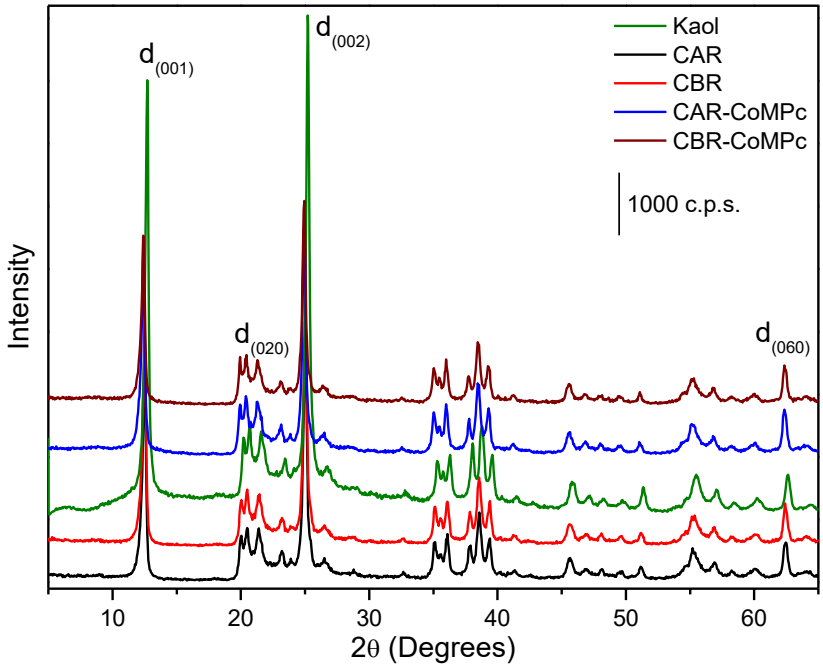

Fig. I.2. Diffractograms of the kaolinite-derived samples.

The intensities of reflections (001) and (002) and also the ratio between their intensities – (001)/(020) – decreased for the derived materials (CAR, CBR, CAR-CoMPc and CBR-CoMPc) (Table I.S2), suggesting that the treatments could promote changes in the stacking of the kaolinite layers. Other evidence was the decrease in the ratio between the intensities of the reflections (020) and (060). This last reflection is characteristic of the *ab* plane; the absence of changes in directions *ab* suggested that this decrease was related to changes in the stacking of plates along the *c*-direction, with a lower number of neatly stacked layered structures.(A. C. da Silva et al., 2016; Dedzo and Detellier, 2014; Letaief et al., 2011; Zbik et al., 2010) These results also demonstrated that the acidic or basic conditions used in the preparation of the samples were not aggressive enough to cause changes in the structure of kaolinite. No peaks due to TiO_2 phases were recorded, although it may be remarked that the characteristic reflections of anatase are very close to those from kaolinite, a fact which made difficult the analysis on these solids.

Based on FTIR spectra (Fig. I.S3), the synthesis of photocatalysts containing TiO_2 and CoMPc did not promote any changes on kaolinite interlayer region, the typical interlayer hydroxyl bands at 3696, 3670, 3654 cm^{-1} (inner surface) and 3621 cm^{-1} (inner) remain intact after reactions in acidic or alkaline media.(Cintra et al., 2019; Da Silva et al., 2014) The presence of CoMPc on solid Kaol/TiO_2 was evidenced by the presence of vibrations at 1400 and 1415 cm^{-1} assigned to C=C units from the aromatic ring, and bands at 1332, 1335 and

1563 cm^{-1} assigned to C-N stretching modes of aromatic amines from the conjugated macrocyclic ring.(Da Silva et al., 2014)

The nitrogen adsorption-desorption isotherms recorded for the solids (Fig. I.S4) were classified as type III.(Barbosa et al., 2015; Thommes et al., 2015) Their similarities confirmed that the texture of the inorganic matrix did not change drastically with the treatments applied. Deposition of TiO_2 and CoMPc on the surface of kaolinite led to small increases in the specific surface area (SSA) values, while porosity remained practically constant (Table I.2). The solids containing metallophtalocyanine showed slightly higher values than the solids without it, which suggested that the presence of CoMPc in the reaction medium could lead to more disperse Ti-species, by the development of sites able to promote the adsorption.(Barbosa et al., 2015; T. H. da Silva et al., 2016)

The band gap of the different solids was estimated from their absorption spectra (Fig. I.S5), by means of the Tauc plot approximation.(Tauc, 1970) This method allowed to determine the band edge by applying the equation 1:

$$\alpha h\nu = A(h\nu - Eg)^{1/2} \quad \text{Equation 1}$$

where α, h, ν, E_g and A denote the adsorption coefficient, Planck constant, radiation frequency, band gap and a constant, respectively. From this equation, a plot of $(\alpha h\nu)^{1/2}$ *vs.* hν, the so-called Tauc Plot, showed a linear region just above the absorption edge whose extrapolation to the photon energy axis (hν) provides the semiconductor band gap value. The presence of CoMPc strongly influenced the band gap, which may induce changes in the absorption ability of the solids and thereof on their photocatalytic properties (Table I.2). The solids containing CoMPc exhibited UV-visible absorption bands at 550-800 nm (Fig. I.S5). These two absorption bands were assigned to Q bands of CoMPc from π-π* transitions which confirmed that the solids containing CoMPc promoted the shift and broadness of the bands to the visible region. Thus, the materials containing CoMPc may inject the electrons to the conduction band (CB) of TiO_2 deposited on kaolinite surfaces, allowing CB to act as electron mediator to transfer them from CoMPc to electron acceptors on TiO_2 surfaces, maintaining intact the valence band (VB).(Pirbazari, 2015)

Table I.2

Textural data and band gap of the materials.

	S_{BET} (m^2/g)	V_P (cm^3/g)	Band gap (eV)
Kaol	23	0.061	4.79
CAR	26	0.063	4.65
CBR	23	0.058	4.75
CAR-CoMPc	29	0.067	1.82
CBR-CoMPc	34	0.065	1.78

S_{BET}: BET specific surface area. V_P: Total pore volume (at $p/p^0 = 0.99$).

Immobilization of TiO_2 in kaolinite modified only slightly its band gap, probably because of the high purity of kaolinite, which did not present any group that could absorb energy for possible transference, and by the low amount of TiO_2 incorporated in these materials, lower than 8% TiO_2 in both cases. However, samples CAR-CoMPc and CBR-CoMPc showed a drastic band gap decrease, assigned to the presence of CoMPc, which may induce the antenna effect interacting with the TiO_2 existing on the kaolinite surface, absorbing energy and transferring it to TiO_2. This is a similar effect to that reported by González *et al*.(González et al., 2017) when using different cations as doping agents in Ti-pillared montmorillonite.

3.2. Photocatalytic degradation of pollutants

Removal of the pollutants TMP, CFF and PMT was estimated by UV-visible spectroscopy. In addition, the by-products formed were identified by mass spectrometry, also aiming to gain information on the degradation route under the reaction conditions used.

Photolysis of TMP was very significant, 72% after 240 min (Fig. I.3), observed by the decrease in intensity/disappearance of the corresponding signals both in UV/Vis and MS.(Ji et al., 2016) The typical molecular ion signal with a mass/charge ratio (m/z) of 291.3 disappeared, indicating that all TMP underwent photodegradation, but not complete mineralization, as fragments with m/z and 243 and 111 were recorded (Fig. I.S6), indicating the formation of by-products/intermediates. These fragments may absorb close to the wavelength used for evaluating TMP (mainly the low degraded fragment with m/z 243), thus leading to false results from UV/Vis. In other words, the remaining TMP amount found may in fact be due to byproducts generated during the photodegradation process.

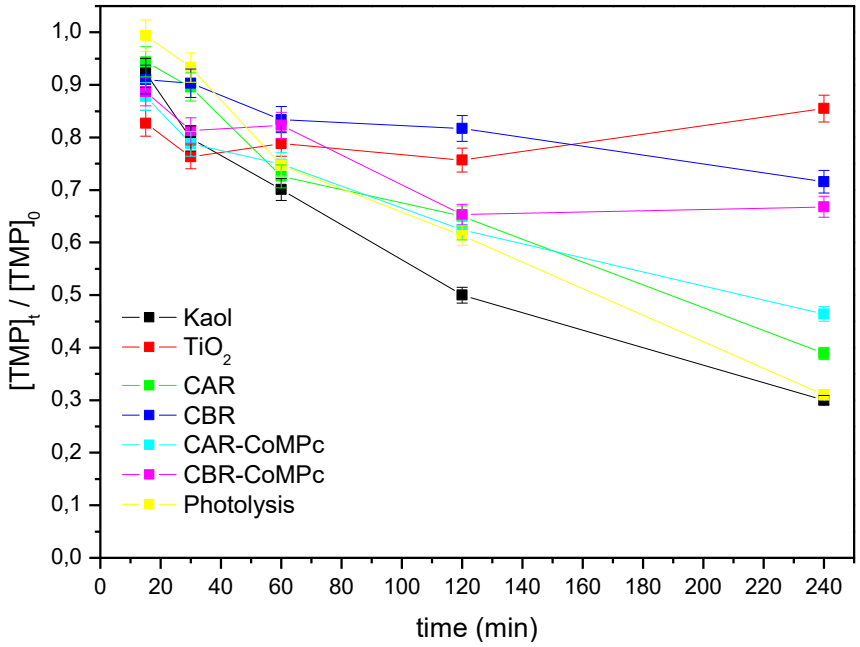

Fig. I.3. Kinetic behavior (C_t/C_0) of the photodegradation of trimethoprim.

Parent kaolinite showed a good efficiency in the photodegradation of TMP, probably due to the presence of active metal species in its structure, Fe^{3+} and Ti^{4+}. It may be remarked that kaolinite adsorbed a small amount of TMP, which in fact may cause the decrease in the intensity of the TMP absorption band in the UV/Vis spectrum.

The composites showed a better photocatalytic behavior than Kaol at short reaction times; however, after 60 min of reaction all the materials showed similar efficiencies, evidencing that a very complex process was involved in TMP photodegradation. This may be limited by the very low amount of TiO_2 in the composites, but also by a blocking effect promoted by CoMPc, hindering the generation of OH• radicals associated to TiO_2 on kaolinite. This effect was actually confirmed, as the amount of TMP photodegraded was higher for the solids without CoMPc than for the solids containing it. This finding strongly suggested that although CoMPc increased the range of light absorption, at the same time CoMPc may difficult the access to active sites from TiO_2. Other possibilities were that the absorbed energy was transferred to Co^{2+} or to the reaction medium, this last hypothesis was supported by the fact that the final temperature after the reaction was 40-45º((*vs.* 25ºC at the beginning of the reaction). Even CoMPc itself may be photodegraded, as suggested by the color change in the catalysts, blue at the beginning of the reaction and almost white at the end.

For the CBR-CoMPc solid, and also for commercial P25 TiO_2, used as reference photocatalyst, the concentration of TMP did not follow the decrease with time pattern observed in photolysis process and for the other catalysts. In these two cases, the concentration of TMP after 240 minutes seemed to be greater than after 120 minutes. This strongly suggested the formation of intermediates that absorbed in the same wavelength region than TMP, and/or of fragments that may slowly recombine in solution. This resulted in complex photodegradation patterns, consequently causing a decrease in the efficiency of generation of hydroxyl (OH•) in the reaction medium.

It is remarkable that the content of TiO_2 in the composites was much lower (between 1.80 and 7.60 %) than the values usually reported in the literature, where contents above 50% or even 90% TiO_2 on inorganic matrices have been used.(Papoulis et al., 2013, 2010) Thus, the performance of our materials was similar to materials with much higher TiO_2 content, being remarkable the fast degradation rate observed at short times of reaction. It may be also considered that no oxidant agent was added to improve the degradation.

Cai and Hu(Cai and Hu, 2017) reported the degradation of sulfamethoxazole and trimethoprim using the photocatalytic system of UVA(LED)/TiO_2, adding H_2O_2 as an oxidizing agent. The system showed satisfactory removal of the antibiotics, and the efficiency was directly linked to the reaction conditions. Approximately 90% of the initial concentration of antibiotics was degraded after 20 min of reaction, forming intermediates which precise nature also depended of the reaction conditions. The initial steps of the degradation should involve the hydroxylation and cleavage of –NH– bonds, resulting in the formation of benzene, aniline and phenol. In fact, these byproducts were evidenced by UV/Vis spectroscopy and confirmed by mass spectrometry. Some signals were found in the MS spectra (Fig. I.S6), their m/z ratios agreed with those reported by Ji *et al*.,(Ji et al., 2016) thus allowing to propose the degradation route included in Fig. I.4. According to this route, fragments with high m/z values were formed, which essentially maintained the structure of the molecule (except the fragment with m/z 111). It was evident that complete mineralization was not achieved under these reaction conditions, but breaking the molecule through different positions may probably provide further degradation.

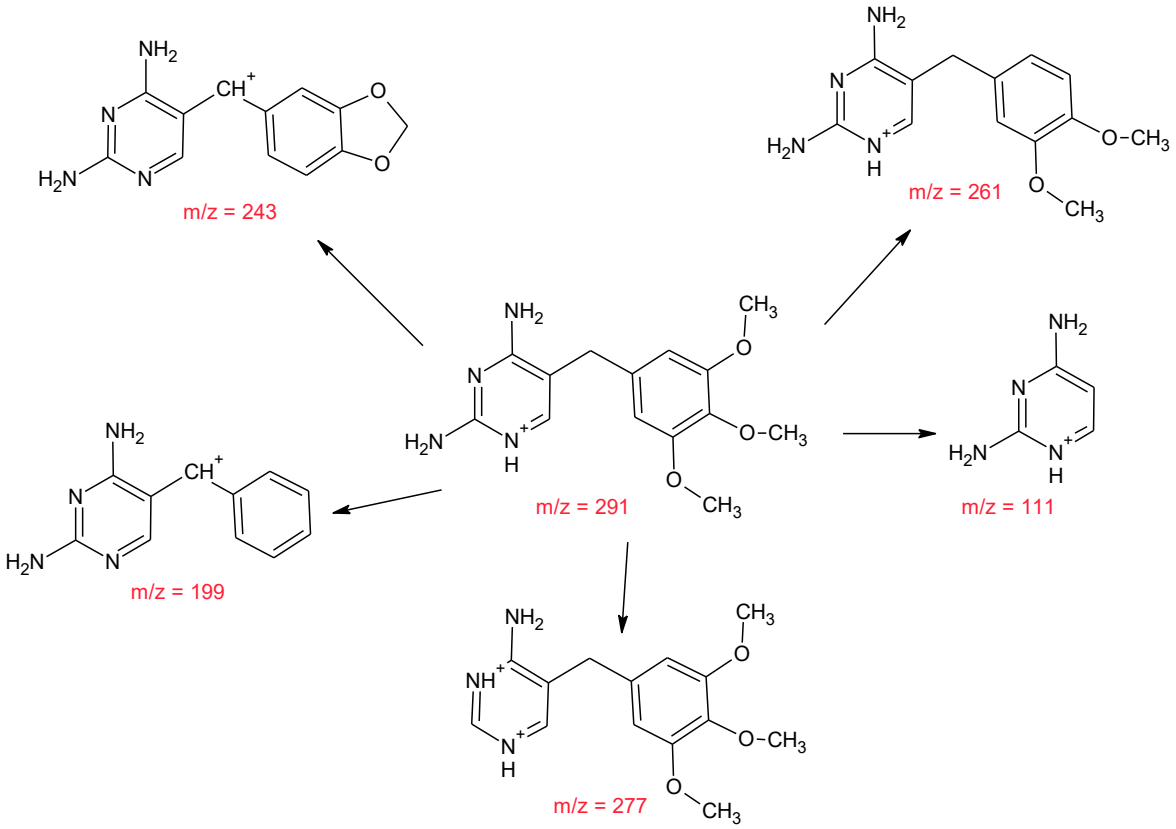

Fig. I.4. Proposal for the photocatalytic decomposition of TMP.

Photodegradation of PMT was also difficult, reaching maximum values close to 40%. Before the degradation study, adsorption tests were carried out (denoted as "Dark experiments" in Fig. I.5); the adsorption was very low for all the solids. In the degradation study, the best results were again found for photolysis and Kaol. In the case of Kaol, the activity could be explained as above for TMP degradation, by the presence of active cations Fe^{3+} and Ti^{4+}. For the four composites, without and with metallophthalocyanine, the degradation efficiency decreased; a finding again attributable to the difficult access to the catalytically active sites or to the formation of stable by-products that may absorb in the same region than TMP in the UV/Vis spectroscopy studies. Although the differences were not very large, the materials obtained through the acid route showed better results, attributable to a better access to the active sites.

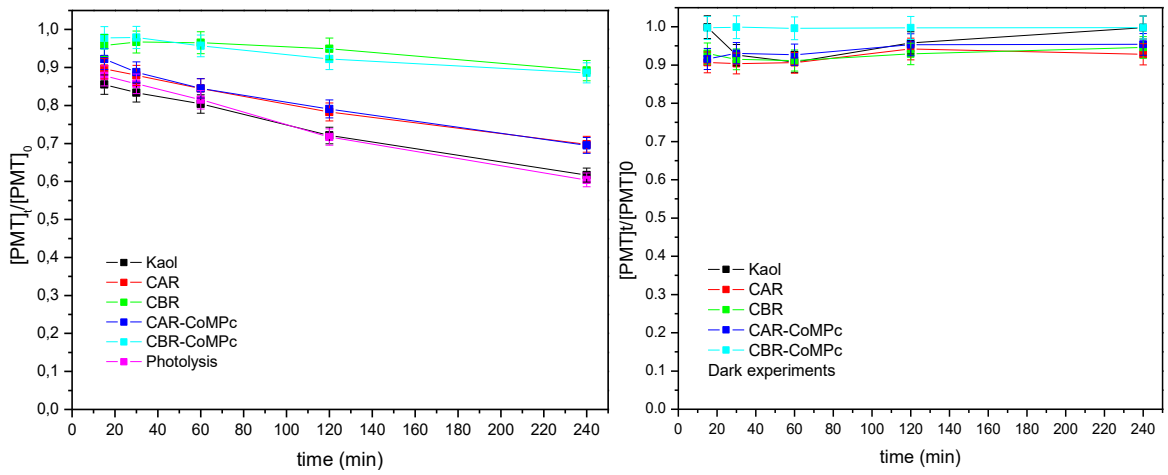

Fig. I.5. Kinetic behavior (C_t/C_0) of the photodegradation of prometryn.

The MS spectra (Fig. I.S7) showed the formation of various by-products after the photocatalytic process, all of them with high m/z values, suggesting that the central ring of the molecule remained unchanged. The fragment with m/z 196 may be particularly stable, as this signal appeared for all materials studied and also in the photolysis runs. The possible structure of the fragments detected by MS is given in Fig. I.6.(Kiss et al., 2007; J. Liu et al., 2017) As indicated, all fragments maintained the chromophoric triazine ring structure, which confirmed the difficulty to quantify the photodegradation of PMT by UV/Vis, because these fragments may absorb very close to the positions of the bands due to the PMT molecule.

Evgenidou *et al.*(Evgenidou et al., 2007) reported PMT degradation using two types of TiO_2 as photocatalysts, demonstrating that Degussa P-25 was more effective than UV-100 Hombikat. Using H_2O_2 and $K_2S_2O_8$ as oxidizing agents, percentages around 70% were reached. These authors claimed the formation of by-products and the difficulty for the complete degradation of the triazine ring.

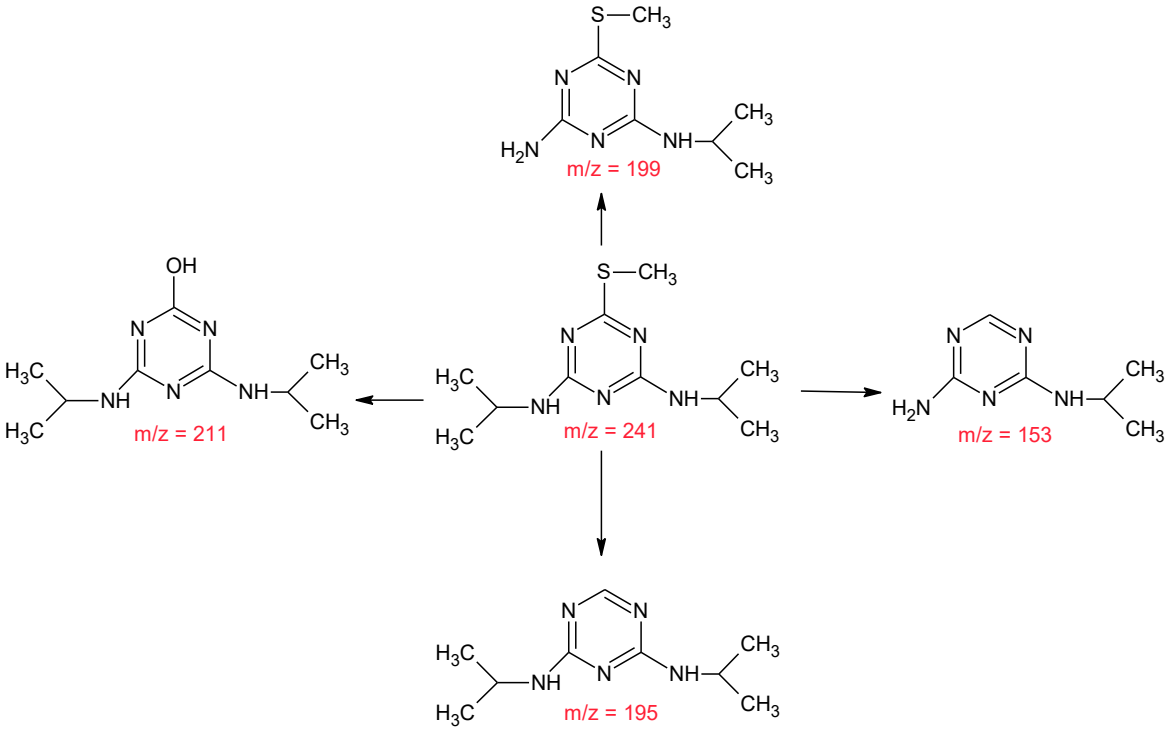

Fig. I.6. Proposal for the photocatalytic decomposition of PMT.

Caffeine was much more sensitive to degradation than trimethoprim and prometryn, reaching values between 85 – 95% (Fig. I.7). Adsorption experiments were also carried out before the photodegradation studies (Fig. I.7, "Dark experiments"), finding that adsorption was low, in some cases almost null and always lower than 10%. Although at the end of the reaction (240 min), the degradation levels were similar for all the materials, it was remarkable that after 120 min photolysis showed the lower degradation degree and the two composites without CoMPc showed a very high (~80%) degradation. Parent kaolinite again showed high activity, demonstrating that it was able to generate photoactive OH• radicals.

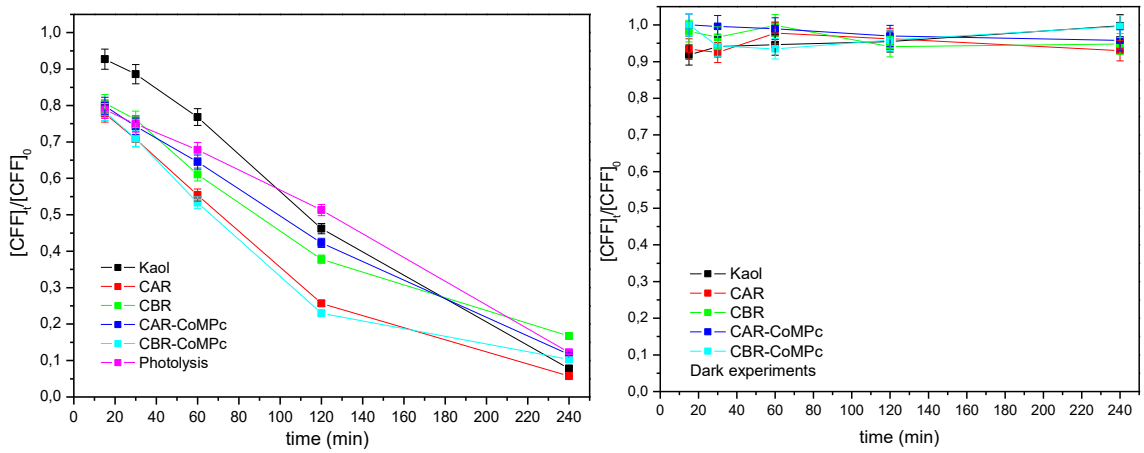

Fig. I.7 Kinetic behavior (C_t/C_0) of the photodegradation of caffeine.

The evolution of CFF under photocatalysis was also analyzed by mass spectrometry (Fig. I.S8). From the m/z values found and comparing with literature reports,(Gracia-Lor et al., 2017; Indermuhle et al., 2013; Lin et al., 2018) its degradation route can be proposed (Fig. I.8). All the fragments detected by MS implied the opening of both the pyrimidine and imidazole rings, except the fragment with m/z 242 that involved only opening of the imidazole ring and oxidation of the terminal resulting groups. The easiness with which these rings can be opened seemed to be a key factor for degradation, and also for its determination by UV/Vis spectroscopy, as the resulting fragments may not absorb close to the absorption bands of CFF.

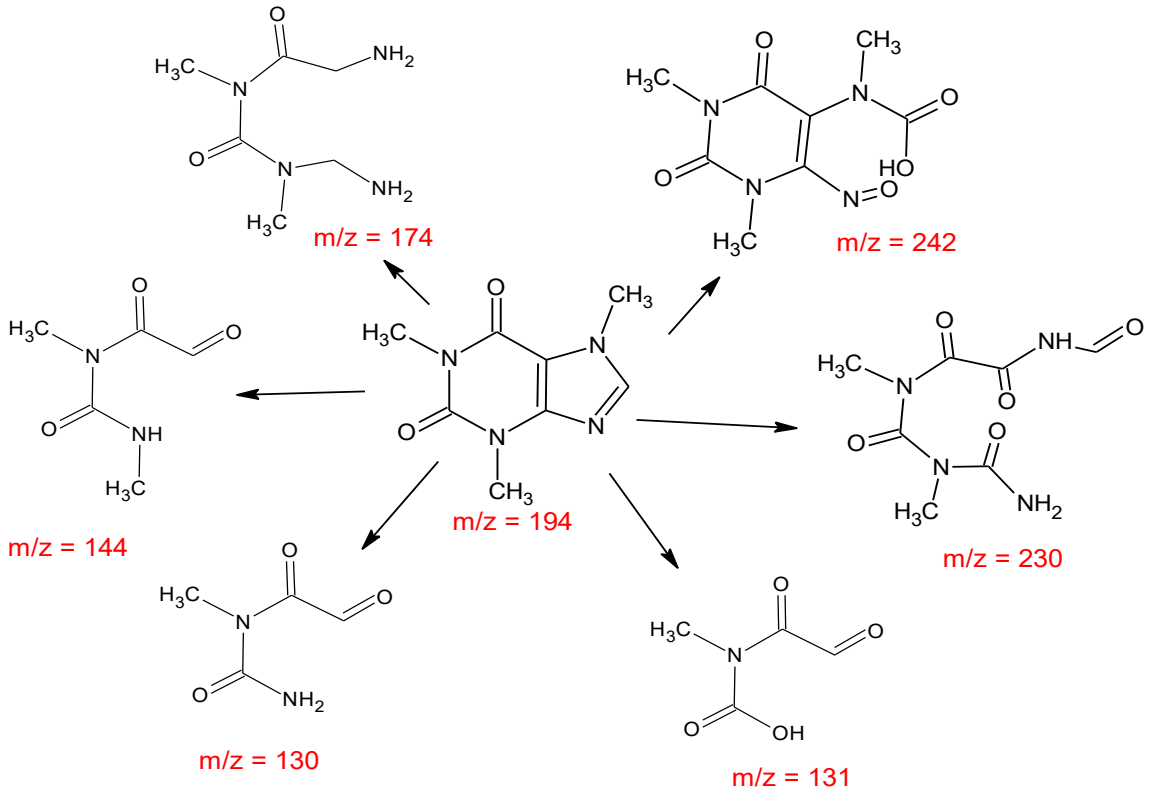

Fig. I.8. Proposal for the photocatalytic decomposition of CFF.

Photodegradation of CFF has been previously reported by Marques *et al.*(Marques et al., 2013) using composites based on acid activated carbon nanotubes and three different Ti-materials (one prepared by sol–gel and two other commercial ones from Evonik and Sigma–Aldrich), reaching 95% degradation ($\lambda > 350$ nm; irradiance ca. 50 mW cm^{-2}; mass of photocatalyst 1.0 g L^{-1}, and time 180 min). The best results were obtained for the composite formed by the carbon nanotubes and Sigma–Aldrich titania, a behavior which has been related to the larger size of the TiO_2 crystallites and the better contact of these particles with carbon nanotubes.

According to Figs. 3, 5 and 7, the solids containing TiO_2-CoMPc promoted different degradation profiles reaching the higher efficiency for the substrate caffeine (90% of CFF, within 240 minutes). Considering the data previously discussed, TiO_2/CoMPc deposited on the kaolinite surface presented a much smaller particle size of semiconductor and a slightly larger surface area than the other materials (Table I.2). However, it is important to remark that these were not key factors in the photocatalytic properties, since, despite these discrete differences, both had the same photocatalytic efficiency. In addition, the results obtained by FTIR before photocatalysis experiments (not shown) evidenced that both samples had residues of synthesis reagents adsorbed on their surface. These residues could compete with the active sites of the photocatalysts, impairing the photocatalysis efficiency. Thus, although photocatalytic efficiency was significant, it could have been even better if the surface of the particles were free of residues of synthesis and organic matter. This effect was confirmed by the reuse experiments, which demonstrated a decrease in the photocatalytic activity during the reuse of the solids.

When the degradation of the EOPs was monitored in relation to time, it was possible to calculate the reaction constant and the half-life time of the processes under study (Fig. I.S9). Equation 2 relates the degradation time to the EOPs concentration:

$$\ln\left(\frac{C}{C_0}\right) = k'.t \qquad \text{Equation 2}$$

where $k' = k\,[SA]$, k is the rate constant of the reaction, $[SA]$ is the concentration of active sites on the catalyst surface, t is the irradiation time: and Co and C represent the concentration of each EOP at the beginning of the reaction and at each time.

The formation of radicals responsible for dye degradation was correlated to high rate constants of the reaction (k') and low half-life times. However, for the constant k' to be high, which will influence the kinetics of degradation, the concentration of available active sites must also be high, since they are directly proportional to each other (Equation 2).

Equation 3 allowed to calculate the time required to reduce to the half the concentration of organic compounds:

$$t^{\frac{1}{2}} = ln\frac{2}{k'} \qquad \text{Equation 3}$$

where $t^{1/2}$ is the half-life time.

According to Equation 2, on plotting $-ln(C/C_0)$ *vs.* t will lead to a straight line which slope is the rate constant of the reaction, k'. In the graphical representation of $-ln(C/C_0)$ *vs.* t

(Fig. I.3, 5 and 7), a first order kinetics can be identified for all cases, indicating that all degradations followed the same mechanism.

Table I.3 contains the values of k' obtained from Fig. I.3, 5 and 7, and their respective half-life times. The reaction presented values of k' and $t_{1/2}$ quite close for TiO_2-CoMPc solids. On the other hand, the values of k' and $t_{1/2}$ for the different substrates were relatively different, a given solid showing higher k' and consequently smaller $t_{1/2}$ for smaller and simple substrate molecules such as CFF, and therefore lower photodegradation rate and much higher $t^{1/2}$ for complex molecules such as PMT and TMP. TiO_2-Co-MPc and TiO_2 deposited on the kaolinite surface using acidic or alkaline routes were therefore equally efficient in the degradation of the different EOPs under study (evidenced by the caffeine study).

Table I.3

First-order kinetic values of k', R^2, and $t_{1/2}$ of the various photocatalysis experiments.

Sample	*First-order kinetics parameters*								
	Trimetoprim (TMP)			Prometryn (PMT)			Caffeine (CFF)		
	k’	R^2	$t^{1/2}$(min)	k’	R^2	$t^{1/2}$(min)	k’	R^2	$t^{1/2}$(min)
Kaol	0.005	0.99	28	0.001	0.99	48	0.011	0.95	20
CAR	0.004	0.98	30	0.001	0.99	48	0.012	0.99	19
CBR	0.001	0.95	48	0.0003	0.90	66	0.007	0.99	25
CAR-CoMPc	0.003	0.98	34	0.001	0.98	48	0.009	0.97	22
CBR-CoMPc	0.001	0.68	48	0.0004	0.97	61	0.009	0.97	22
Photolysis	0.005	0.99	28	0.002	0.99	39	0.008	0.92	23

Literature studies for degradation of TMP(Cai and Hu, 2017), PMT(Evgenidou et al., 2007) and CFF(Marques et al., 2013) have reported that photodegradation was improved by the addition of oxidizing agents or by previous treatments for generation of acid active sites on the materials (Table I.4). In our case, the reaction was carried out in water, without addition of oxidants, and although the degradation level reached was lower than in other studies, all the materials showed good capacity to generate the OH• radicals needed for degradation of the resistant molecules considered.

Table I.4

Comparison of the results obtained in the present work with some literature results for degradation of TMP, PMT and CFF.

Catalyst	Degradation (%)			Oxidant	Reference
	TMP	PMT	CFF		
Kaol	70	38	92		This work
CAR	61	30	94		This work
CBR	28	11	83		This work
CAR-CoMPc	54	30	88		This work
CBR-CoMPc	33	11	90		This work
TiO_2	90			H_2O_2	(Cai and Hu, 2017)
Degussa P-25 and UV-100 Hombikat		70		H_2O_2 and $K_2S_2O_8$	(Evgenidou et al., 2007)
TiO_2/carbon nanotubes			95		(Marques et al., 2013)

Evaluation of Photodegradation mechanism

Zhang *et al.*(Deng et al., 2017; Fida et al., 2015; Ma and Zhang, 2016) have shown the inhibiting effect of inorganic ions, such as chloride, on the photocatalytic degradation of organic pollutants. Most of them have shown that chloride ions existing in the solutions as salts or as degradation by-products, can promote the inhibition of the efficiency during a photocatalytic process. Thus, in order to evaluate the impact of the chloride ions, experiments were conducted with PMT using 16.6 mg/L of NaCl in the initial PMT solution. Fig. I.9 shows the evident inhibition with chloride ions; only around 2.5 % of PMT was degraded in the presence of NaCl, compared to the maximum of 38 % of PMT degradation in the experiments without NaCl.(Bahnemann et al., 2014; Deng et al., 2017; Fida et al., 2015; Ma and Zhang, 2016)

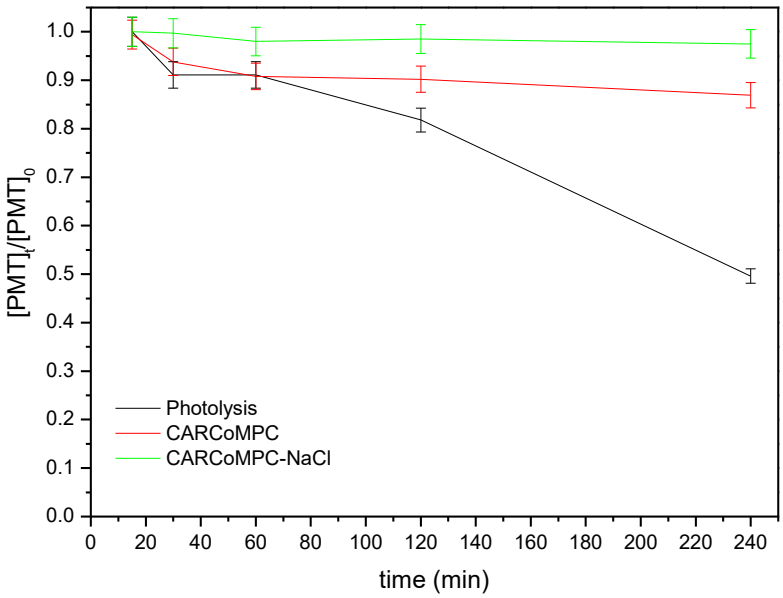

Fig. I.9. Photocatalytic degradation of PMT in the presence of NaCl.

Based on these results, it is confirmed that when a certain concentration of NaCl existed in the reaction system, the degradation of PMT could not be initiated further. Moreover, results in Fig. I.10 showed the inhibiting effect of chloride ions on the constant rates (*k'*) and half-life time ($t^{1/2}$) during PMT degradation. PMT degradation constant decreased from 0.003 on photolysis to 4.7×10^{-4} mg L^{-1} s^{-1} when CAR-CoMPc was used as a catalyst for PMT photodegradation and to 9.7×10^{-5} mg L^{-1} s^{-1} when the same catalyst was used in the presence of 16.6 mg/L NaCl. The kinetic reaction constants in the presence of chloride ions were approximately 5 times lower than for PMT degradation, while the half-life time was 34 min for photolysis, 59 min when using CAR-CoMPc as catalyst, and 85 min when using the same catalyst in the presence of NaCl, in agreement with the evolution of the degradation constants.

Two possible mechanisms have been proposed for the inhibition caused by inorganic ions on the photocatalytic activity of systems containing TiO_2. The first one is a competitive adsorption of inorganic ions on the pristine TiO_2 active surface which blocks adsorption sites for the target molecules. The second one is a possible scavenging effect of the adsorbed inorganic ions which consume photogenerated holes and, therefore, decrease the efficiency of the photocatalytic process. Moreover, according to Zalazar *et al.*(Zalazar et al., 2005) the direct attack of the photogenerated hole is the most significant oxidative step in the photocatalytic oxidation of EOPs, which confirms the great importance of the adsorption ability of the EOPs and the hole quantity for an efficient photocatalytic mineralization.

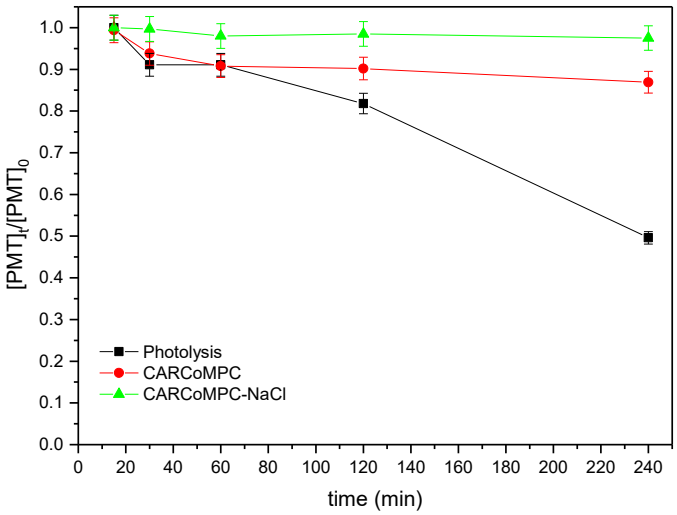

Fig. I.10. Kinetic behavior (C_t/C_0) of the photodegradation of PMT with NaCl.

4. Conclusion

Titanium dioxide and Co(II)-metallophthalocyanine were effectively immobilized on kaolinite surface, using an acid or a basic route for the hydrolysis of the Ti-isopropoxide precursor. The preparation treatments did not alter the basal spacing of kaolinite, but slightly modified the specific surface area and more significantly the band gap of the solid from 4.7 eV in kaolinite based solids containing titanium dioxide to 1.78 eV in solids containing Co(II)-metallophthalocyanine. In the presence of artificial light (from UV to visible), the solids showed moderate photocatalytic activity for removal of trimethoprim and prometryn (54 and 30% total degradation rate), but much higher for caffeine (90% degradation rate) using solids with Co(II)-metallophthalocyanine. In all the photodegradation reactions the presence of by-products was confirmed by mass spectrometry, allowing to identify most of the fragments. In the cases of trimethoprim and prometryn, their rings were not broken, which strongly hindered their degradation, and it may alter the tracing of the process by UV/Vis spectroscopy, as the fragments containing these rings may absorb at the wavelengths used for the determination of the original molecules. In the case of caffeine, their two rings were easily opened, facilitating the degradation of the molecule and also the tracing of the process. The study by mass spectrometry corroborated the different degradation rates obtained by photocatalysis for the three studied molecules.

Acknowledgements

The authors thank a Cooperation Grant jointly financed by Universidad de Salamanca (Spain) and FAPESP (Brasil, 2016/50322-2). This study was financed in part by the Coordenação de Aperfeiçoamento de Pessoal de Nível Superior - Brasil (CAPES) - Finance Code 001. The Brazilian group acknowledges the support from the Brazilian research funding agencies Fundação de Amparo à Pesquisa do Estado de São Paulo (FAPESP) (2017/15482-1,2016/01501–1), CAPES (317/15 and 0274-16) and Conselho Nacional de Desenvolvimento Científico e Tecnológico (CNPq) (305398/2015-6, 302668/2017-9, 311767/2015-0).

Supplementary data

Supplementary Information (molecular structures of organic pollutants, tables from XRD data, chemical reactions, thermal analysis, infrared spectra, N_2 isotherm adsorption-desorption, UV-Visible absorption of nanocomposites solid state analysis, mass spectrometry) is available free of charge at http://jbcs.sbq.org.br.

References

Alharbi, S.K., Kang, J., Nghiem, L.D., Merwe, J.P. van de, Leusch, F.D.L., Price, W.E., 2017. Photolysis and UV / H 2 O 2 of diclofenac , sulfamethoxazole , carbamazepine , and trimethoprim : Identification of their major degradation products by ESI – LC – MS and assessment of the toxicity of reaction mixtures. Process Saf. Environ. Prot. 2, 1–13. https://doi.org/10.1016/j.psep.2017.07.015

Araújo, F.R., Baptista, J.G., Marçal, L., Ciuffi, K.J., Nassar, E.J., Calefi, P.S., Vicente, M.A., Trujillano, R., Rives, V., Gil, A., Korili, S., De Faria, E.H., 2014. Versatile heterogeneous dipicolinate complexes grafted into kaolinite: Catalytic oxidation of hydrocarbons and degradation of dyes. Catal. Today 227, 105–115.

Bahnemann, D.W., Mehle, A., Dražić, G., Štrancar, J., Dillert, R., Krivec, M., 2014. The nature of chlorine-inhibition of photocatalytic degradation of dichloroacetic acid in a TiO2-based microreactor. Phys. Chem. Chem. Phys. 16, 14867. https://doi.org/10.1039/c4cp01043d

Barbosa, L.V., Marçal, L., Nassar, E.J., Calefi, P.S., Vicente, M.A., Trujillano, R., Rives, V., Gil, A., Korili, S.A., Ciuffi, K.J., de Faria, E.H., 2015. Kaolinite-titanium oxide nanocomposites prepared via sol-gel as heterogeneous photocatalysts for dyes degradation. Catal. Today 246, 133–142. https://doi.org/10.1016/j.cattod.2014.09.019

Bethi, B., Sonawane, S.H., Bhanvase, B.A., Gumfekar, S.P., 2016. Nanomaterials-based advanced oxidation processes for wastewater treatment: A review. Chem. Eng. Process. Process Intensif. 109, 178–189. https://doi.org/10.1016/j.cep.2016.08.016

Brinker, C.J., Scherer, G.W., 1990. SOL-GEL SCIENCE - The Physics and Chemostry of Sol-Gel Processing. Academic Press.

Cai, Q., Hu, J., 2017. Decomposition of sulfamethoxazole and trimethoprim by continuous UVA/LED/TiO2 photocatalysis: Decomposition pathways, residual antibacterial activity and toxicity. J. Hazard. Mater. 323, 527–536. https://doi.org/10.1016/j.jhazmat.2016.06.006

Christoforidis, K.C., Montini, T., Bontempi, E., Zafeiratos, S., Jaén, J.J.D., Fornasiero, P., 2016. Synthesis and photocatalytic application of visible-light active β-Fe2O3/g-C3N4 hybrid nanocomposites. Appl. Catal. B Environ. 187, 171–180. https://doi.org/10.1016/j.apcatb.2016.01.013

Cintra, T.E., Saltarelli, M., Salmazo, R.M.D.F., Honorato, T., Nassar, E.J., Trujillano, R., Rives, V., Vicente, M.A., Faria, E.H. De, Ciuffi, K.J., 2019. Applied Clay Science Catalytic activity of porphyrin-catalyts immobilized on kaolinite. Appl. Clay Sci. 168, 469–477. https://doi.org/10.1016/j.clay.2018.12.012

Claver, A., Ormad, P., Rodríguez, L., Ovelleiro, J.L., 2006. Study of the presence of pesticides in surface waters in the Ebro river basin (Spain). Chemosphere 64, 1437–1443. https://doi.org/10.1016/j.chemosphere.2006.02.034

da Silva, A.C., Ciuffi, K.J., Reis, M.J. dos, Calefi, P.S., de Faria, E.H., 2016. Influence of physical/chemical treatments to delamination of nanohybrid kaolinite-dipicolinate. Appl. Clay Sci. 126, 251–258. https://doi.org/10.1016/j.clay.2016.03.023

da Silva, T.H., de Souza, T.F.M., Ribeiro, A.O., Calefi, P.S., Ciuffi, K.J., Nassar, E.J., Molina, E.F., Hamer, P., de Faria, E.H., 2016. New strategies for synthesis and immobilization of methalophtalocyanines onto kaolinite: Preparation, characterization and chemical stability evaluation. Dye. Pigment. 134, 41–50. https://doi.org/10.1016/j.dyepig.2016.06.044

Da Silva, T.H., De Souza, T.F.M., Ribeiro, A.O., Ciuffi, K.J., Nassar, E.J., Silva, M.L.A., Henrique De Faria, E., Calefi, P.S., 2014. Immobilization of metallophthalocyanines on hybrid materials and in-situ synthesis of pseudo-tubular structures from an aminofunctionalized kaolinite. Dye. Pigment. 100, 17–23. https://doi.org/10.1016/j.dyepig.2013.07.019

de Faria, E.H., Ciuffi, K.J., Nassar, E.J., Vicente, M.A., Trujillano, R., Calefi, P.S., 2010. Novel reactive amino-compound: Tris(hydroxymethyl)aminomethane covalently grafted on kaolinite. Appl. Clay Sci. 48, 516–521. https://doi.org/10.1016/j.clay.2010.02.017

de Faria, E.H., Lima, O.J., Ciuffi, K.J., Nassar, E.J., Vicente, M.A., Trujillano, R., Calefi, P.S., 2009. Hybrid materials prepared by interlayer functionalization of kaolinite with pyridine-carboxylic acids. J. Colloid Interface Sci. 335, 210–215. https://doi.org/10.1016/j.jcis.2009.03.067

De Faria, E.H., Ricci, G.P., Marçal, L., Nassar, E.J., Vicente, M.A., Trujillano, R., Gil, A., Korili, S.A., Ciuffi, K.J., Calefi, P.S., 2012. Green and selective oxidation reactions catalyzed by kaolinite covalently grafted with Fe(III) pyridine-carboxylate complexes. Catal. Today 187, 135–149.

Dedzo, G.K., Detellier, C., 2014. Intercalation of two phenolic acids in an ionic liquid-kaolinite nanohybrid material and desorption studies. Appl. Clay Sci. 97–98, 153–159. https://doi.org/10.1016/j.clay.2014.04.038

Deng, F., Zhao, X., Pei, X., Luo, X., Li, W., Au, C., 2016. Sol-Hydrothermal Synthesis of Inorganic-Framework Molecularly Imprinted TiO2 Nanoparticle and Its Enhanced Photocatalytic Activity For Degradation of Target Pollutant. Sci. Adv. Mater. 8, 1079–1085.

Deng, L., Xie, Y., Zhang, G., 2017. Synthesis of C–Cl-codoped titania/attapulgite composites with enhanced visible-light photocatalytic activity. Chinese J. Catal. 38, 379–388. https://doi.org/10.1016/S1872-2067(17)62774-8

Dobrowolska, M., Tivakornsasithorn, K., Liu, X., Furdyna, J.K., Berciu, M., Yu, K.M., Walukiewicz, W., 2012. Controlling the Curie temperature in (Ga,Mn)As through location of the Fermi level within the impurity band. Nat. Mater. 11, 444–9. https://doi.org/10.1038/nmat3250

Evgenidou, E., Bizani, E., Christophoridis, C., Fytianos, K., 2007. Heterogeneous photocatalytic degradation of prometryn in aqueous solutions under UV-Vis irradiation. Chemosphere 68, 1877–1882. https://doi.org/10.1016/j.chemosphere.2007.03.012

Fida, H., Guo, S., Zhang, G., 2015. Preparation and characterization of bifunctional Ti – Fe kaolinite composite for Cr(VI) removal. J. Colloid Interface Sci. 442, 30–38.

Geissen, V., Mol, H., Klumpp, E., Umlauf, G., Nadal, M., van der Ploeg, M., van de Zee, S.E.A.T.M., Ritsema, C.J., 2015. Emerging pollutants in the environment: A challenge for water resource management. Int. Soil Water Conserv. Res. 3, 57–65.

https://doi.org/10.1016/j.iswcr.2015.03.002

González, B., Trujillano, R., Vicente, M.A., Rives, V., De Faria, E.H., Ciuffi, K.J., Korili, S.A., Gil, A., 2017. Doped Ti-pillared clays as effective adsorbents-Application to methylene blue and trimethoprim removal. Environ. Chem. 14, 267–278. https://doi.org/10.1071/EN16192

Gracia-Lor, E., Rousis, N.I., Zuccato, E., Bade, R., Baz-Lomba, J.A., Castrignanò, E., Causanilles, A., Hernández, F., Kasprzyk-Hordern, B., Kinyua, J., McCall, A.K., van Nuijs, A.L.N., Plósz, B.G., Ramin, P., Ryu, Y., Santos, M.M., Thomas, K., de Voogt, P., Yang, Z., Castiglioni, S., 2017. Estimation of caffeine intake from analysis of caffeine metabolites in wastewater. Sci. Total Environ. 609, 1582–1588. https://doi.org/10.1016/j.scitotenv.2017.07.258

Grazieli, C., Collins, C.H., 2011. APLICAÇÕES DE CROMATOGRAFIA LÍQUIDA DE ALTA EFICIÊNCIA PARA O ESTUDO DE POLUENTES ORGÂNICOS EMERGENTES. Quim. Nova 34, 665–676.

Indermuhle, C., Martín de Vidales, M.J., Sáez, C., Robles, J., Cañizares, P., García-Reyes, J.F., Molina-Díaz, A., Comninellis, C., Rodrigo, M.A., 2013. Degradation of caffeine by conductive diamond electrochemical oxidation. Chemosphere 93, 1720–1725. https://doi.org/10.1016/j.chemosphere.2013.05.047

Janíková, B., Tokarský, J., Mamulová Kutláková, K., Kormunda, M., Neuwirthová, L., 2017. Photoactive and non-hazardous kaolin/ZnO composites prepared by calcination of sodium zinc carbonate. Appl. Clay Sci. 143, 345–353. https://doi.org/10.1016/j.clay.2017.04.003

Ji, Y., Xie, W., Fan, Y., Shi, Y., Kong, D., Lu, J., 2016. Degradation of trimethoprim by thermo-activated persulfate oxidation: Reaction kinetics and transformation mechanisms. Chem. Eng. J. 286, 16–24. https://doi.org/10.1016/j.cej.2015.10.050

Kadish, K., Smith, K.M., Guilard, R., 1999. The porphyrin handbook. Academic Press.

Karamanis, D., Ökte, A.N., Vardoulakis, E., Vaimakis, T., 2011. Water vapor adsorption and photocatalytic pollutant degradation with TiO2-sepiolite nanocomposites. Appl. Clay Sci. 53, 181–187. https://doi.org/10.1016/j.clay.2010.12.012

Kimura, M., Kuroda, T., Ohta, K., Hanabusa, K., Shirai, H., Kobayashi, N., 2003. Self-organization of hydrogen-bonded optically active phthalocyanine dimers. Langmuir 19, 4825–4830. https://doi.org/10.1021/la0341512

Kiss, A., Rapi, S., Csutorás, C., 2007. GC/MS studies on revealing products and reaction

mechanism of photodegradation of pesticides. Microchem. J. 85, 13–20. https://doi.org/10.1016/j.microc.2006.06.017

Letaief, S., Leclercq, J., Liu, Y., Detellier, C., 2011. Single kaolinite nanometer layers prepared by an in situ polymerization-exfoliation process in the presence of ionic liquids. Langmuir 27, 15248–15254. https://doi.org/10.1021/la203492m

Lin, K.Y.A., Lai, H.K., Tong, S., 2018. One-step prepared cobalt-based nanosheet as an efficient heterogeneous catalyst for activating peroxymonosulfate to degrade caffeine in water. J. Colloid Interface Sci. 514, 272–280. https://doi.org/10.1016/j.jcis.2017.12.040

Liu, J., Hua, R., Lv, P., Tang, J., Wang, Y., Cao, H., Wu, X., Li, Q.X., 2017. Novel hydrolytic de-methylthiolation of the s-triazine herbicide prometryn by Leucobacter sp. JW-1. Sci. Total Environ. 579, 115–123. https://doi.org/10.1016/j.scitotenv.2016.11.006

Liu, L., Wan, Q., Xu, X., Duan, S., Yang, C., 2017. Combination of micelle collapse and field-amplified sample stacking in capillary electrophoresis for determination of trimethoprim and sulfamethoxazole in animal-originated foodstuffs. Food Chem. 219, 7–12. https://doi.org/10.1016/j.foodchem.2016.09.118

Luo, X., Zheng, Z., Greaves, J., Cooper, W.J., Song, W., 2012. Trimethoprim: Kinetic and mechanistic considerations in photochemical environmental fate and AOP treatment. Water Res. 46, 1327–1336. https://doi.org/10.1016/j.watres.2011.12.052

Ma, Y., Zhang, G., 2016. Sepiolite nanofiber-supported platinum nanoparticle catalysts toward the catalytic oxidation of formaldehyde at ambient temperature: Efficient and stable performance and mechanism. Chem. Eng. J. 288, 70–78. https://doi.org/10.1016/j.cej.2015.11.077

Marçal, L., de Faria, E.H., Nassar, E.J., Trujillano, R., Martín, N., Vicente, M.A., Rives, V., Gil, A., Korili, S.A., Ciuffi, K.J., 2015. Organically Modified Saponites: SAXS Study of Swelling and Application in Caffeine Removal. ACS Appl. Mater. Interfaces 7, 10853–10862. https://doi.org/10.1021/acsami.5b01894

Marques, R.R.N., Sampaio, M.J., Carrapiço, P.M., Silva, C.G., Morales-Torres, S., Dražić, G., Faria, J.L., Silva, A.M.T., 2013. Photocatalytic degradation of caffeine: Developing solutions for emerging pollutants. Catal. Today 209, 108–115. https://doi.org/10.1016/j.cattod.2012.10.008

Mesgari, Z., Gharagozlou, M., Khosravi, A., Gharanjig, K., 2012. Spectrophotometric studies of visible light induced photocatalytic degradation of methyl orange using phthalocyanine-modified Fe-doped TiO2 nanocrystals. Spectrochim. Acta Part A Mol.

Biomol. Spectrosc. 92, 148–153. https://doi.org/10.1016/j.saa.2012.02.055

Michael, I., Frontistis, Z., Fatta-Kassinos, D., 2013. Removal of pharmaceuticals from environmentally relevant matrices by advanced oxidation processes (AOPs), in: Analysis, Removal, Effects and Risk of Pharmaceuticals in the Water Cycle: Occurrence and Transformation in the Environment (Petrovic, M., Barcelo, D., Pérez, S.) Comprehensive Analytical Chemistry. Elsevier B.V., pp. 345–407. https://doi.org/10.1016/B978-0-444-62657-8.00011-2

Norman, 2017. Network of reference laboratories, research centres and related organisations for monitoring of emerging environmental substances [WWW Document]. URL http://www.norman-network.net (accessed 10.10.18).

Oros-Ruiz, S., Zanella, R., Prado, B., 2013. Photocatalytic degradation of trimethoprim by metallic nanoparticles supported on TiO 2-P25. J. Hazard. Mater. 263, 28–35. https://doi.org/10.1016/j.jhazmat.2013.04.010

Papoulis, D., Komarneni, S., Nikolopoulou, A., Tsolis-Katagas, P., Panagiotaras, D., Kacandes, H.G., Zhang, P., Yin, S., Sato, T., Katsuki, H., Nikolopoulou, A., Li, H., Yin, S., 2010. Palygorskite- and Halloysite-TiO2 nanocomposites: Synthesis and photocatalytic activity. Appl. Clay Sci. 50, 118–124. https://doi.org/10.1016/j.clay.2010.07.013

Papoulis, D., Komarneni, S., Panagiotaras, D., Nikolopoulou, A., Li, H., Yin, S., Tsugio, S., Katsuki, H., 2013. Palygorskite–TiO2 nanocomposites: Part 1. Synthesis and characterization. Appl. Clay Sci. 83–84, 191–197. https://doi.org/10.1016/j.clay.2013.09.003

Patil, P.N., Bote, S.D., Gogate, P.R., 2014. Degradation of imidacloprid using combined advanced oxidation processes based on hydrodynamic cavitation. Ultrason. Sonochem. 21, 1770–1777. https://doi.org/10.1016/j.ultsonch.2014.02.024

Pirbazari, A.E., 2015. Sensitization of Tio2 Nanoparticles With Cobalt Phthalocyanine: An Active Photocatalyst for Degradation of 4-Chlorophenol under Visible Light. Procedia Mater. Sci. 11, 622–627. https://doi.org/10.1016/j.mspro.2015.11.096

Ratnasamy, P., Srinivas, D., Knözinger, H., 2004. Active Sites and Reactive Intermediates in Titanium Silicate Molecular Sieves. Adv. Catal. 48, 1–169. https://doi.org/10.1016/S0360-0564(04)48001-8

Tauc, J., 1970. Absorption edge and internal electric fields in amorphous semiconductors. Mater. Res. Bull. 5, 721–729. https://doi.org/10.1016/0025-5408(70)90112-1

Thommes, M., Kaneko, K., Neimark, A. V., Olivier, J.P., Rodriguez-Reinoso, F., Rouquerol, J., Sing, K.S.W., 2015. Physisorption of gases, with special reference to the evaluation of surface area and pore size distribution (IUPAC Technical Report). Pure Appl. Chem. 87, 1051–1069. https://doi.org/10.1515/pac-2014-1117

Zalazar, C.S., Martin, C.A., Cassano, A.E., 2005. Photocatalytic intrinsic reaction kinetics. II: Effects of oxygen concentration on the kinetics of the photocatalytic degradation of dichloroacetic acid. Chem. Eng. Sci. 60, 4311–4322. https://doi.org/10.1016/j.ces.2004.10.050

Zbik, M.S., Raftery, N.A., Smart, R.S.C., Frost, R.L., 2010. Kaolinite platelet orientation for XRD and AFM applications. Appl. Clay Sci. 50, 299–304. https://doi.org/10.1016/j.clay.2010.08.010

Zhang, Y., Wang, A., Tian, X., Wen, Z., Lv, H., Li, D., Li, J., 2016. Efficient mineralization of the antibiotic trimethoprim by solar assisted photoelectro-Fenton process driven by a photovoltaic cell. J. Hazard. Mater. 318, 319–328. https://doi.org/10.1016/j.jhazmat.2016.07.021

SUPPLEMENTARY MATERIALS FOR ARTICLE I

Table I.S1
Chemical structure and formulas of the organic pollutants

Organic pollutants	Chemical structures	Chemical formulas
Trimethoprim (TMP)	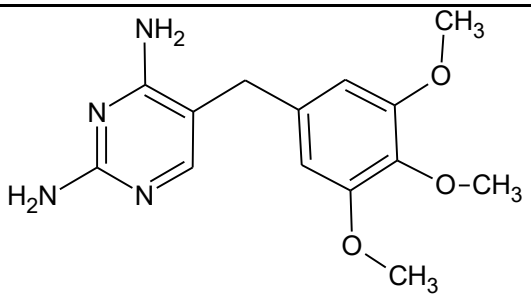	$C_{14}H_{18}N_4O_3$
Prometryn (PMT)	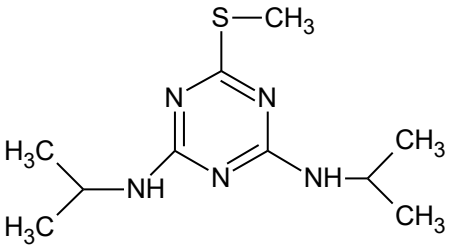	$C_{10}H_{19}N_5S$
Caffeine (CFF)	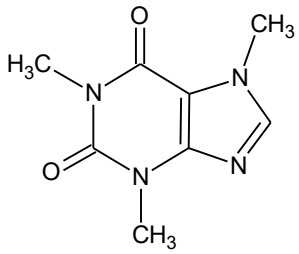	$C_8H_{10}N_4O_2$

Table I.S2
Intensities (cps) of various XRD reflections and ratio between them for different materials.

	$d_{(001)}$	$d_{(020)}$	$d_{(060)}$	$d_{(001)}/d_{(020)}$	$d_{(020)}/d_{(060)}$
Kaol	7184	1481	891	4.85	1.662
CAR	3273	742	635	4.41	1.169
CBR	3135	759	709	4.13	1.071
CAR-CoMPc	3186	838	758	3.80	1.106
CBR-CoMPc	2738	801	666	3.42	1.203

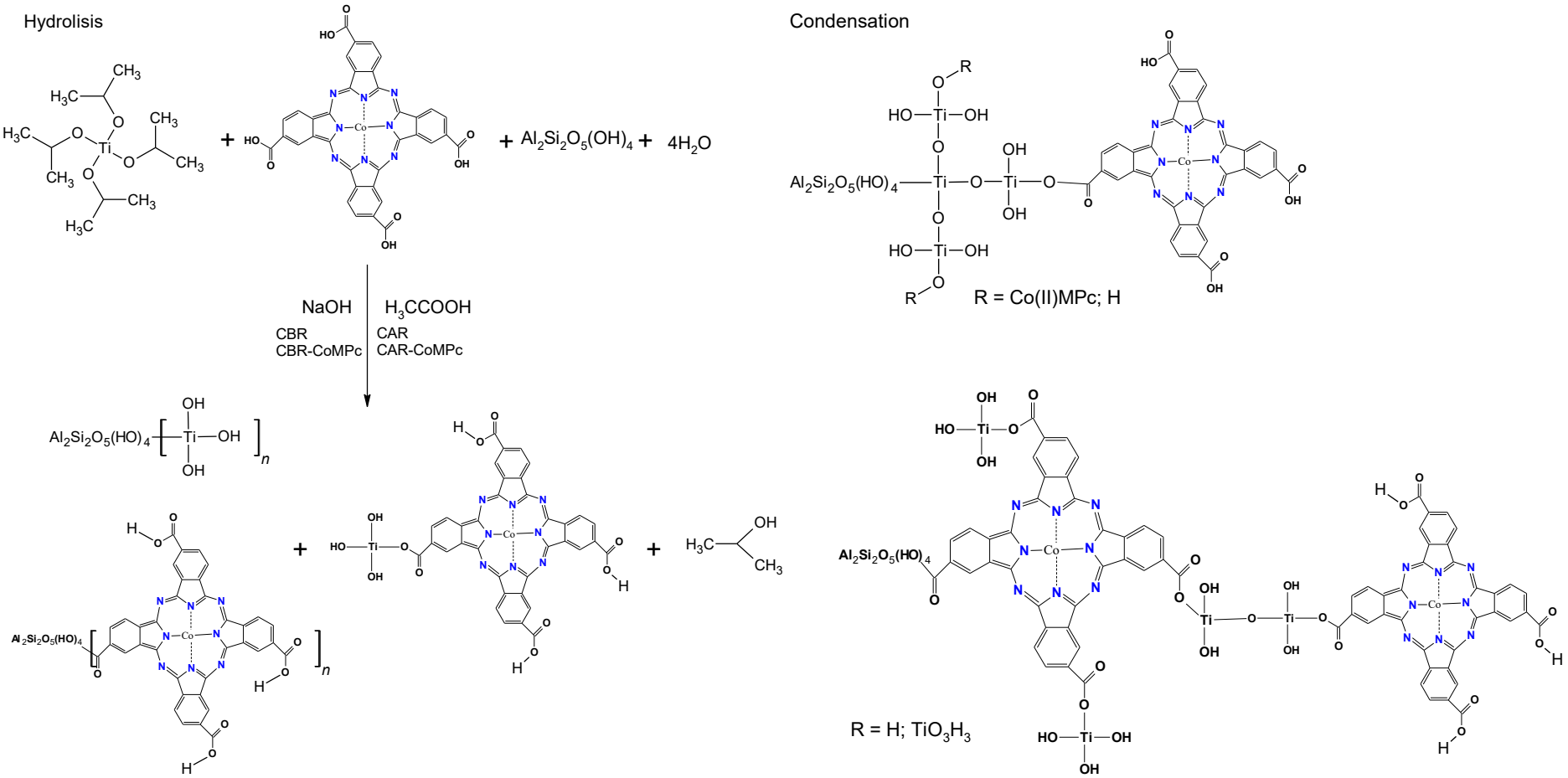

Fig. I.S1. Experimental procedure for the preparation of Kaol/TiO_2/(CoMPC) composites.

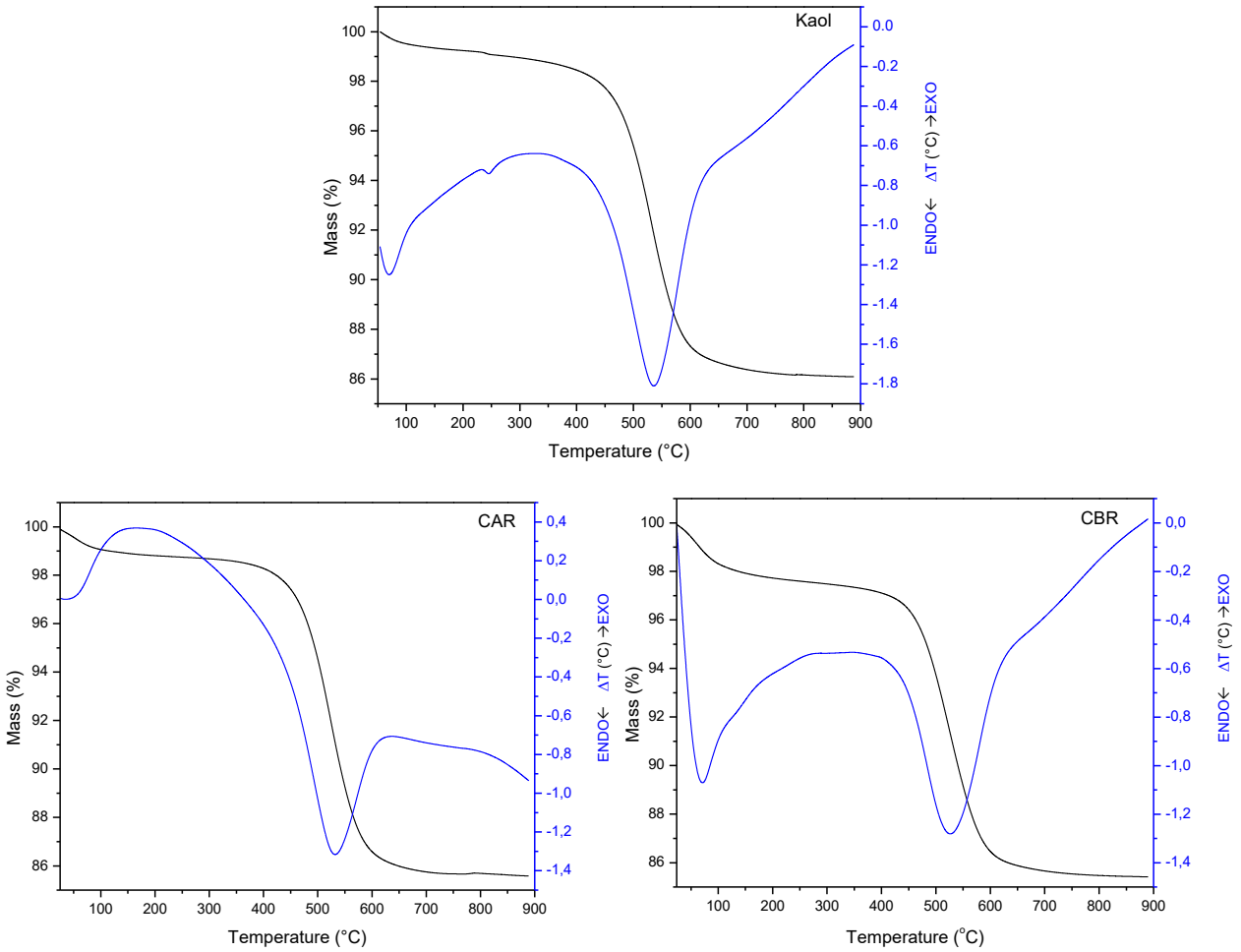

Fig. I.S2. Thermal curves from parent kaolinite and reference samples CAR and CBR.

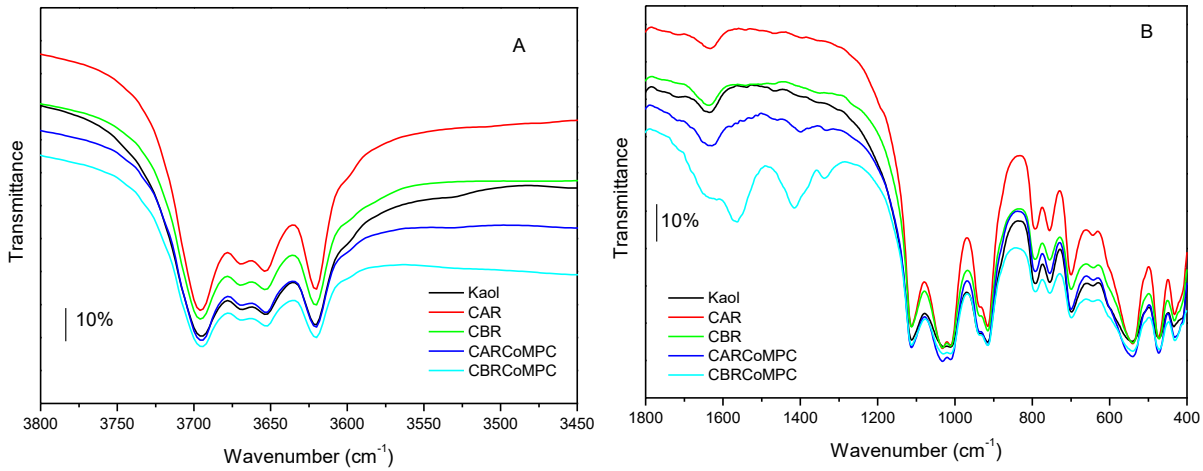

Fig. I.S3: Infrared spectra of the materials based in kaolinite A) region between 3800 and 3450 cm^{-1}; B) region between 1800 and 400 cm^{-1}.

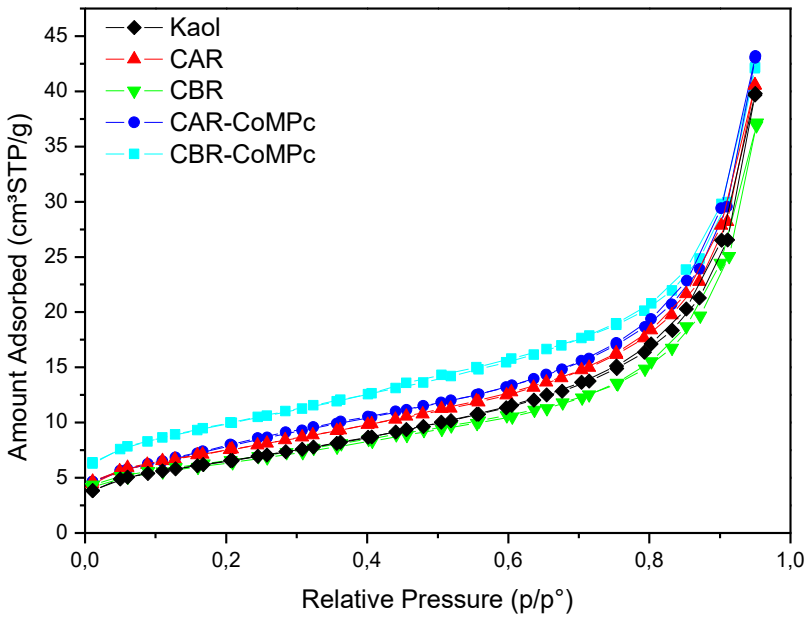

Fig. I.S4. Nitrogen adsorption-desorption isotherms for the different solids.

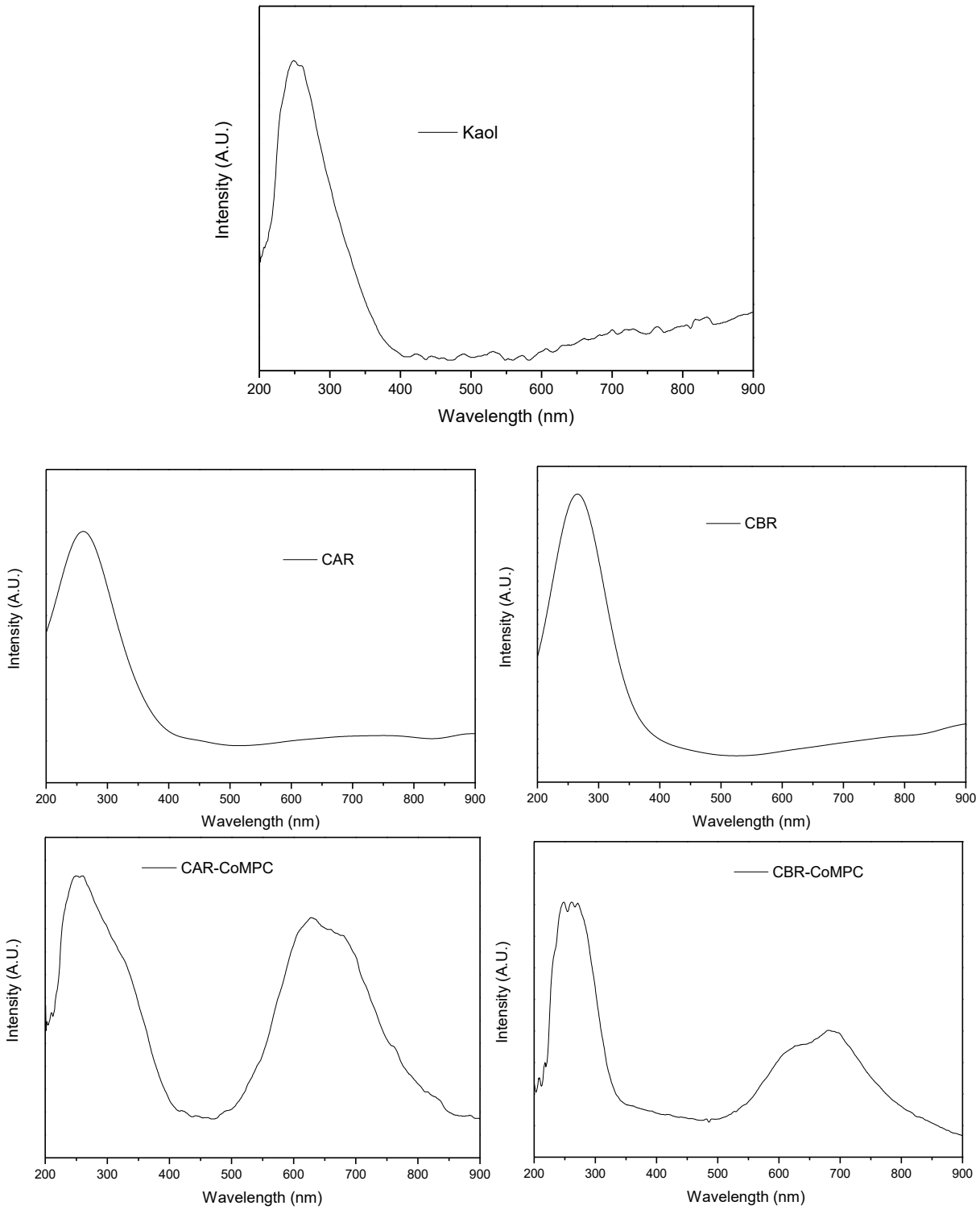

Fig. I.S5: UV-Vis absorption spectra for the materials Kaol, CAR, CBR, CAR-CoMPC and CBR-CoMPC.

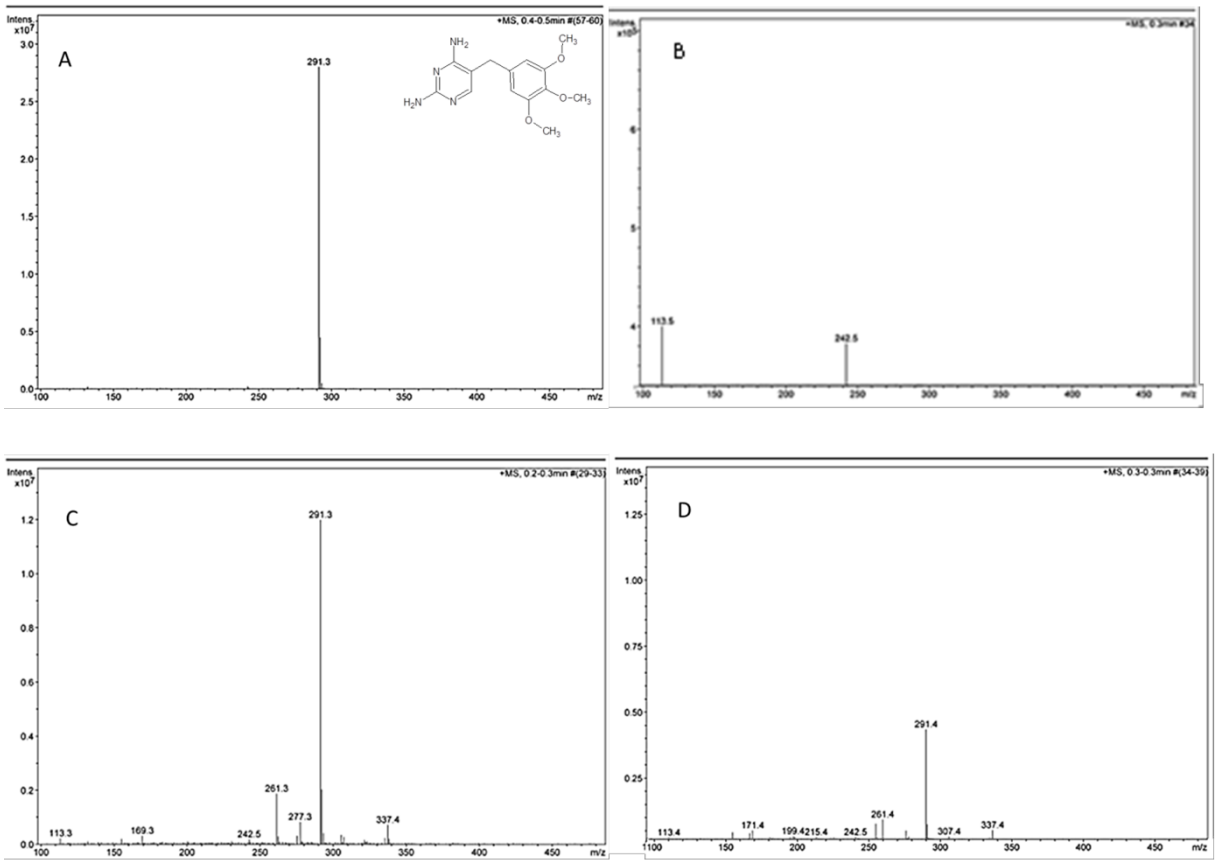

Fig. I.S6. Mass spectra obtained for the following solutions: trimethoprim (A), treated by photolysis for 240 min (B), treated with commercial P25 TiO_2 for 240 min (C) and treated with CAR-CoMPC for 240 min (D).

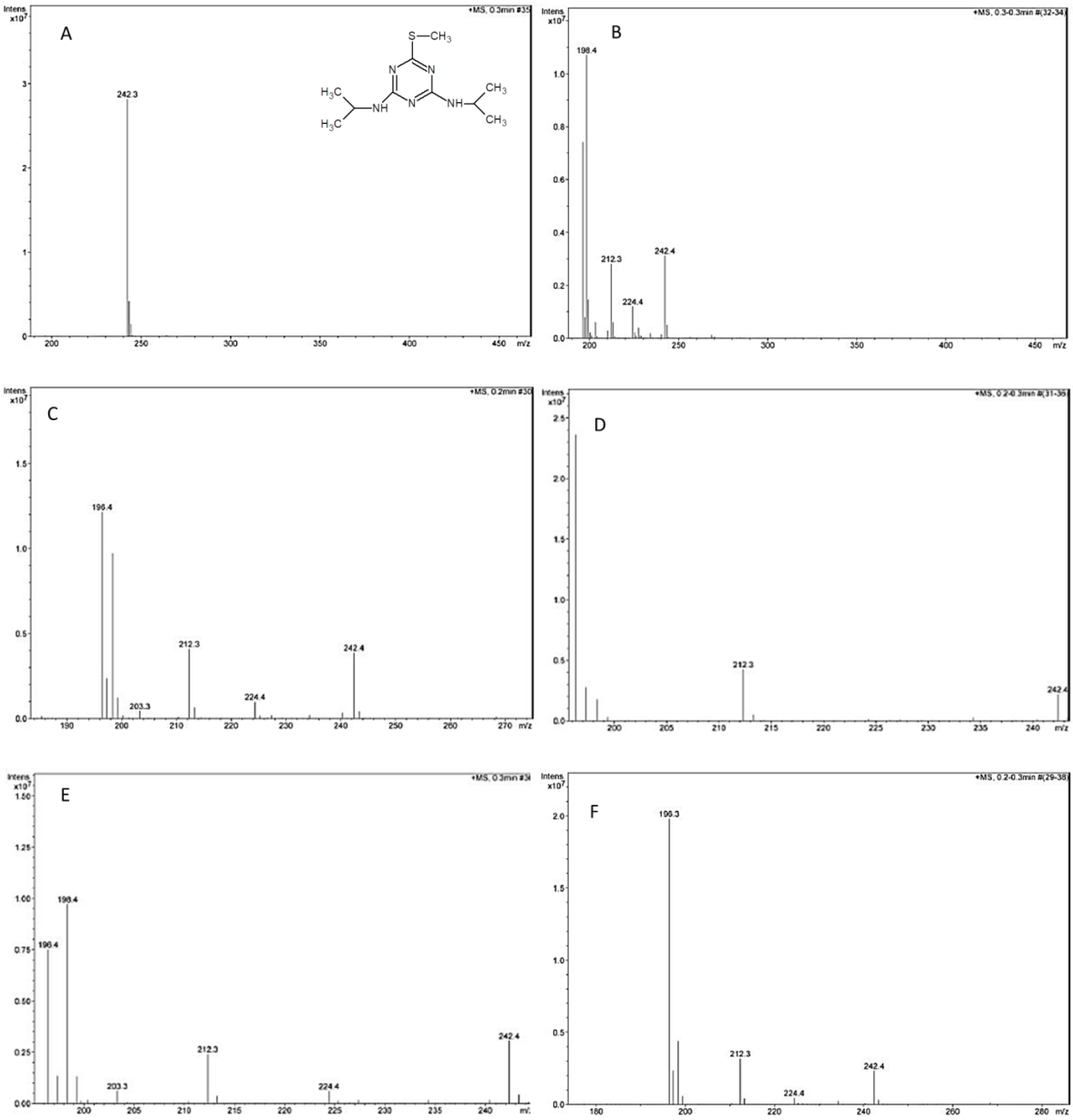

Fig. I.S7. Mass spectra obtained for the following solutions: prometryn (A), treated by photolysis for 240 min (B), treated with CAR for 240 min (C), treated with CBR for 240 min (D), treated with CAR-CoMPC for 240 min (E) and treated with CBR-CoMPC for 240 min.

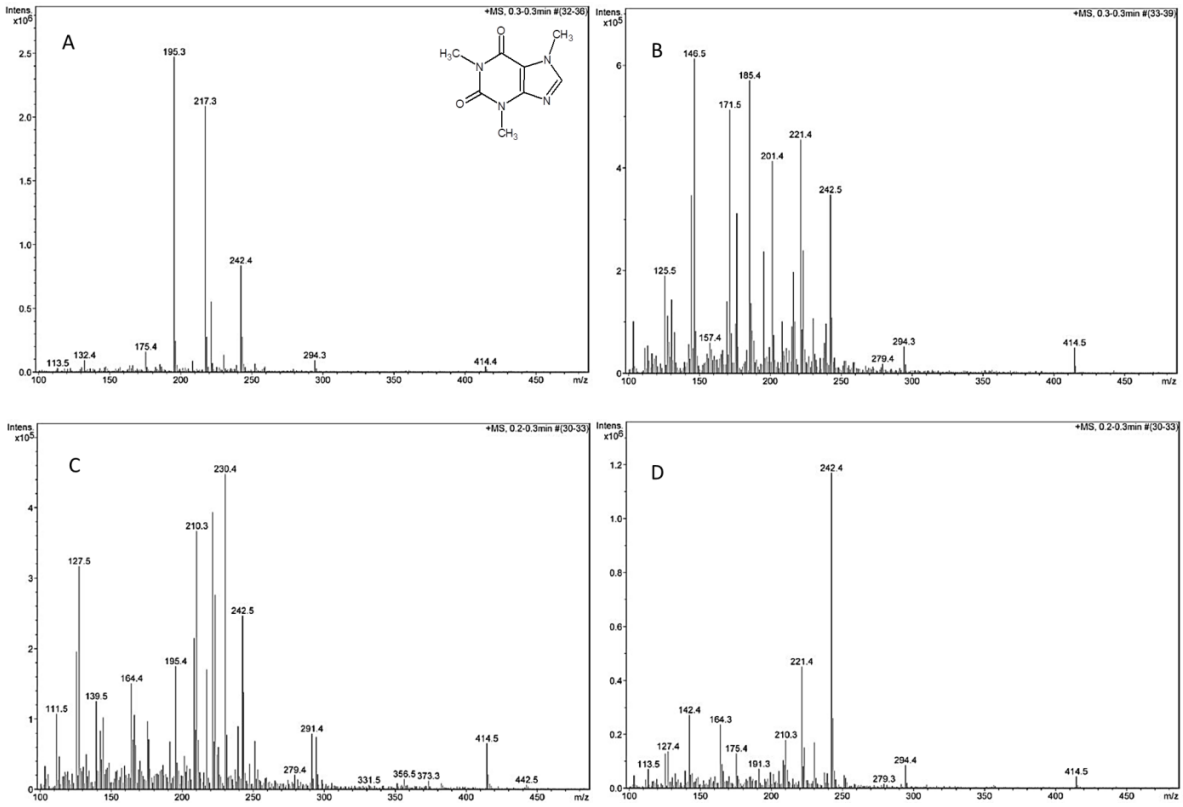

Fig. I.S8. Mass spectra obtained for the following solutions: caffeine (A), treated by photolysis for 240 min (B), treated with CBR for 240 min (C), and treated with CBR-CoMPC for 240 min (D).

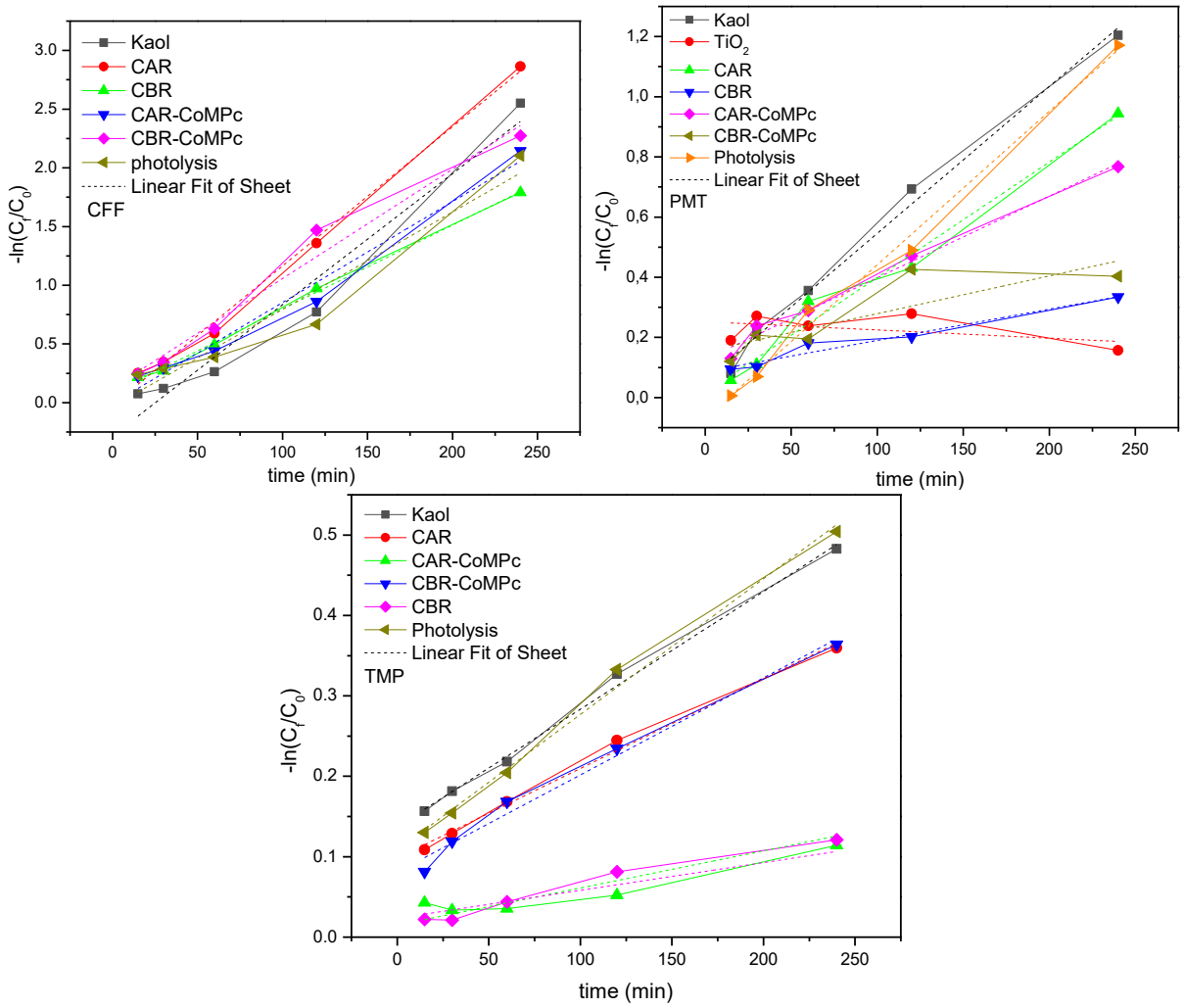

Fig. I.S9: First-order kinetic studies of the various photocatalysis experiments under irradiation.

Article II

Laponite Functionalized with Biuret and Melamine – Application to Adsorption of Antibiotic Trimethoprim.

Microporous and Mesoporous Materials 253 (2017) 112–122

Contents lists available at ScienceDirect

Microporous and Mesoporous Materials

journal homepage: www.elsevier.com/locate/micromeso

Laponite functionalized with biuret and melamine – Application to adsorption of antibiotic trimethoprim

Beatriz González [a], Tiago H. da Silva [b], Katia J. Ciuffi [b], Miguel A. Vicente [a, *], Raquel Trujillano [a], Vicente Rives [a], Emerson H. de Faria [b, **], Sophia A. Korili [c], Antonio Gil [c]

[a] GIR-QUESCAT, Departamento de Química Inorgánica, Universidad de Salamanca, 37008 Salamanca, Spain
[b] Universidade de Franca, Av. Dr. Armando Salles Oliveira, Parque Universitário, 201, 14404-600, Franca, SP, Brazil
[c] Departamento de Química Aplicada, Edificio de los Acebos, Universidad Pública de Navarra, Campus Arrosadía, 31006 Pamplona, Spain

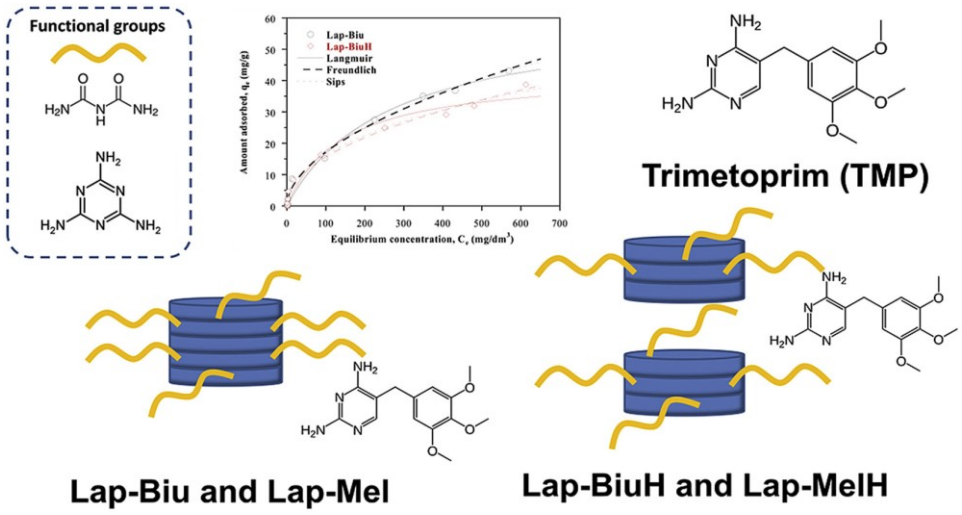

ABSTRACT

Laponite-aminosilane hybrid materials have been prepared by reaction of a chlorosilane, (3-chloropropyl)triethoxysilane, with two aminated compounds, namely, biuret or melamine. The resulting compounds were used for the functionalisation of laponite, using two synthesis procedures. The hybrid materials thus formed were fully characterised, and tested for the adsorption of the antibiotic Trimethoprim (trimethoxybenzyl-2,4-pyrimidinediamine). The characterisation results showed that functionalisation was successful, and the adsorption experiments showed a high affinity of the hybrid materials for the removal of Trimethoprim, with removal percentages larger than 80%.

Keywords: Laponite; Biuret; Melamine; Organophilization; Clay; Trimethoprim adsorption.

1. Introduction

Clay minerals are hydrophilic materials, but for several uses it is even mandatory, to confer their surface an organophilic nature by the incorporation of organic species to favour their interaction with other organic species (polymers, pollutants, etc.) (Christidis, 2013; de Paiva et al., 2008). Among such uses, the formulation of Clay-Polymer Nanocomposites (CNP) is particularly important, but the use of clay minerals in the preparation of paints, cosmetics or personal care products, in the adsorption of pollutants, or as rheological control agents, are other relevant applications that require the clay minerals having an organophilic surface. The organic species incorporated may act as ligands to metal cations, allowing the preparation of catalysts, sensors, luminescent agents, etc. For these reasons, organophilisation of clay minerals has been widely studied.

The strategy for organophilisation is usually fitted to the clay minerals considered. For instance, tetrasubstituted quaternary alkyl-ammonium ions have been mainly used to functionalise swellable smectites, by intercalation in the interlayer region with substitution of their natural occurring charge-balancing exchangeable cations; these preparations are even commercially available (Cloisite®). Grafting of organo-silanes on several clays, particularly silanes containing other functional groups such as amine, mercapto or chlorine, has received increasing interest in the last years, opening new potential applications for these materials (Detellier and Letaief, 2013; Lagaly and Dékány, 2013).

Kaolinite can be organophilised by a multi-step, host-guest displacement method, beginning with small and very polar molecules, and then substituting them by the final functionalising molecules. This special procedure is used because kaolinite has no exchangeable cations and the organophilising species cannot be intercalated by ionic exchange, and swelling of the strongly bonded layers being very difficult (Lagaly et al., 2013).

Laponite is a commercially available synthetic hectorite. It exfoliates very easily in aqueous dispersion, and solid samples do not show a long order in their stacking direction. Its exchangeable cations can be substituted by cationic species, but without intercalation. Functionalisation of laponite has been scarcely studied (Borsacchi et al., 2007) and grafting on the external surface of its layers seems to be the optimal procedure.

Biuret (2-imidodicarbonic diamide), also known as carbamylurea (see its formula in Fig. II.1) results from the condensation of two urea molecules removing one ammonia

molecule. It is the reference for the Biuret reaction, widely used for the identification of proteins and peptides, as peptide bonds react as the biuret molecule does. Biuret is also used to denote the functional group -(HN-CO-)$_2$N-, and can be viewed as the result of the trimerization of isocyanates. Biuret has been used as an alternative to urea as a non-protein nitrogen source for animal feed. Melamine (1,3,5-triazine-2,4,6-triamine, Fig. II.1) can be formally be considered as a trimer of cyanamide; it has fire-retardant properties, and it is widely used to form, by combination with formaldehyde, the resin also known as melamine, used in decorative laminates, insulation (melamine foam) and cement admixture (sulfonated melamine formaldehyde).

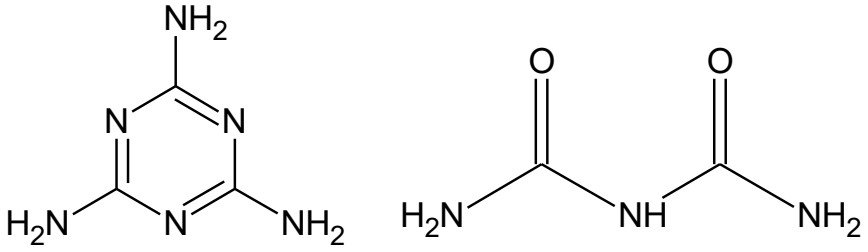

Fig. II.1. Chemical structures for melamine (left) and biuret (right).

In recent years, pharmaceutical products and their derivatives have become of great environmental concern. These compounds may be released to the environment in different ways: disposing of component precursors, disposal of by-products of the manufacturing process, and consumption/elimination of drugs (Bekçi et al., 2007; Molu and Yurdakoç, 2010; Richardson et al., 2005). One of the largest concerns related to this fact is the development of resistant organisms, mainly to antibiotics. Trimethoprim [5-(3,4,5-trimethoxybenzyl) pyrimidine-2,4-diamine] (TMP) is an antibacterial drug used to treat infections, and may inhibit a variety of gram-positive and gram-negative bacteria (Liu et al., 2017), and so being currently used as an antibacterial agent. However, TMP is incompletely metabolised by the human being during the therapeutic process, and about 80% is excreted in its pharmacologically active form (Ji et al., 2016; Liu et al., 2017; Zhang et al., 2016).

Both biuret and melamine contain three amine groups, able to condense with other groups, the three groups being able to condense under appropriate conditions. The chlorosilane (3-chloropropyl)triethoxysilane (abbreviated ClPTES) was chosen for such a condensation reaction. The resulting compounds were used for functionalisation of Laponite, and the functionalised solids, after their complete characterisation, were studied for their ability to adsorb Trimethoprim.

2. Experimental

2.1 Preparation of the hybrid materials

2.1.a. Non-aqueous route. The first step was the condensation between the chlorosilane and the amino derivatives, Fig. II.2. A given mass of the amino precursor (4.31 g, 0.041 mol) of biuret (Biu) or 5.23 g (0.041 mol) of melamine (Mel) was reacted with 10.5 mL (0.041 mol) of (3-chloropropyl)triethoxysilane (ClPTES) using toluene as solvent. The mixture was magnetically stirred in glass flasks for 4 h, under an anhydrous nitrogen atmosphere, at 80 ºC, using a conventional reflux setup. The condensation reaction is schematized in Fig. II.2; one, two or even all three amine groups in each amine molecule can condensate with the silane. *A priori*, it is expected that only one amine group condenses, as the ClPTES:organic compound (Mel or Biu) molar ratio was fixed to 1:1. However, the amine groups could condense also with the silanol groups from the clay, and also the hydroxyl groups from the silane, and so the final condensation degree can change. After 4 hours of reaction, 10.0 g of Laponite were added to each solution and the suspension was maintained under vigorous stirring for 24 h. The resulting materials were washed 3 times with toluene and 5 times with ethanol and oven-dried at 80 ºC; the resulting solids are designated as "Lap-Biu" and "Lap-Mel", respectively.

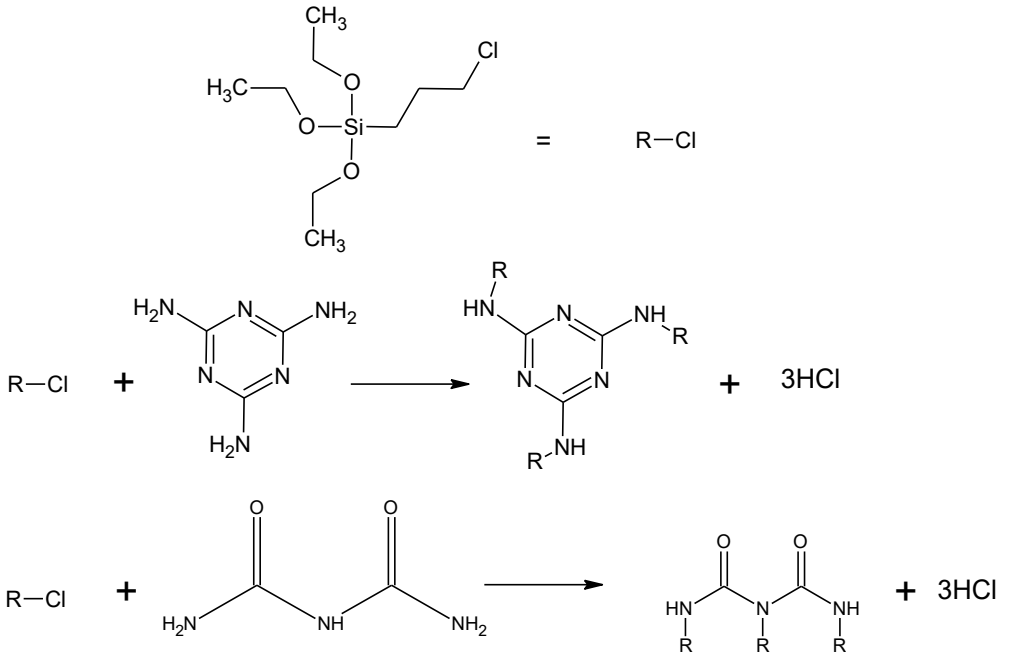

Fig. II.2. Complete condensation reactions between ClPTES and biuret or melamine for the synthesis of new aminosilanes.

2.1.b. Aqueous route. An amount of 10.0 g of Laponite was suspended in 200 mL of water under vigorous stirring to obtain a swollen Laponite gel. Then 10.5 mL (0.041 mol) of ClPTES were slowly added to the suspension and the resulting mixture was vigorous stirred for 1 h at room temperature and then 4.31 g (0.041 mol) of Biu or 5.23 g (0.041 mol) of Mel were added, and the system was maintained under stirring for 24 h at room temperature (ca. 25 ºC). Two drops of HCl were used to initiate the hydrolysis, and more HCl is generated during the process (Fig. II.2). The ClPTES:organic compound (Mel or Biu) molar ratio was fixed to 1:1. The resulting materials were washed and dried as described for the previous method, and they were named as "Lap-BiuH" and "Lap-MelH", respectively.

2.2. Characterisation techniques

Element chemical analyses were carried out at Activation Laboratories Ltd., in Ancaster, Ontario, Canada, using inductively coupled plasma (ICP) for the metallic elements, IR spectroscopy after combustion for C and Kjeldahl method for N determination.

The powder X-ray diffraction (PXRD) diagrams of the solids were recorded in a Siemens D-500 diffractometer operating at 40 kV and 30 mA, using filtered Cu Kα radiation in the 2º to 65º (2θ) range. All the analyses were carried out at a scan speed of 2º/min.

The thermal analyses were carried out in a TA Instruments SDT Q600 simultaneous DTA-TGA thermal analyzer, at temperatures ranging from 25 to 900ºC, at a heating rate of 10ºC/min and under air flow (100 mL/min).

The infrared absorption spectra were recorded in a Perkin-Elmer Spectrum One FTIR spectrometer, using the KBr pellet technique.

The BET specific surface area and porosity data of the solids were calculated from their nitrogen adsorption-desorption isotherms at –196 ºC, carried out in a Micromeritics Gemini VII 2390T apparatus. The samples were previously treated at 110°C under a stream of N_2 for 2 h, in a Micromeritics Flowprep 060 equipment.

Scanning electron microscopy (SEM) was performed using a Carl Zeiss SEM EVO HD25 apparatus with a thermionic LaB_6 filament cannon as the electron source. The samples were coated with a thin gold layer by evaporation using a Bio-Rad ES100 SEN coating system.

2.3. Adsorption of Trimethoprim using the batch method

The adsorption experiments were carried out using the batch method. For all the experiments, the concentration of TMP in the solutions was determined by UV/Visible spectroscopy, using a Hewlett-Packard 8453 Diode Array spectrometer. The absorption was measured at 288 nm, the wavelength corresponding to the maximum absorbance of the molecule under the conditions used. The absorbance at this wavelength showed a linear response, according to the Beer-Lambert law, in the concentration range from 1 to 50 mg/L, which was used in the experiments.

2.3.a. Trimethoprim adsorption kinetics. The kinetics experiments of TMP adsorption onto the adsorbents (Lap-Biu, Lap-Mel, Lap-BiuH and Lap-MelH), were carried out in glass vials by shaking at room temperature a known amount of an adsorbent, typically 50 mg, and 5.0 mL of an aqueous TMP solution with a concentration of 50 mg/L. At pre-determined time intervals between 1 and 150 min, the TMP concentration in the supernatant was analyzed, to calculate the amount of TMP adsorbed onto the solid, according to Equation 1:

$$q_t = \frac{V \cdot (C_i - C_t)}{m} \qquad \text{Equation 1}$$

where q_t (mg/g) is the amount of TMP adsorbed at time t (min), C_i (mg/L) is the initial TMP concentration in the solution, C_t (mg/L) is the TMP concentration in the solution at time t, V (L) is the volume of the solution, and m (g) is the mass of adsorbent used.

Unfortunately, it was not possible to perform the adsorption experiments with the original Laponite, as, when it is immersed in water, a gelation process occurs, making it extremely difficult to separate the liquid from the solid. Thus, it was not possible to compare the results of the hybrid materials with the starting, unloaded Laponite.

2.3.b. Trimethoprim adsorption equilibrium. The equilibrium experiments at 25 °C were carried out in glass vials by shaking for 20 min a known amount of the adsorbent, typically 50 mg, with 5.0 mL of TMP solution at the desired TMP concentration, typically ranging from 1 to 1000 mg/L. Then, the clay was separated from the supernatant by centrifugation at 3500 rpm for 15 min. The concentration of TMP remaining in the

supernatant was determined, and the amount of adsorbed dye was calculated using Equation 2:

$$q_e = \frac{V \cdot (C_i - C_e)}{m} \qquad \text{Equation 2}$$

where q_e (mg/g) is the amount of adsorbed TMP; C_i and C_e (mg/L) are the initial and equilibrium liquid-phase concentrations of the organic compound, respectively; V (L) is the volume of the solution; and m (g) is the amount of adsorbent.

3. Results and discussion

3.1 Characterisation of the adsorbents

The PXRD diagrams of the solids are shown in Fig. II.3. As expected, the diagram for parent Laponite does not show a long order in its basal reflection, but only a shoulder close to 6º (≈ 15 Å). The intralayer reflections, independent of layer stacking, mainly (02,11), ($\bar{2}02$) and (06,33), are, however, clearly evidenced. Incorporation of the aminosilanes leads to noticeable changes in the diffractograms. The changes observed differ depending on the preparation method. In the case of the non-aqueous route, the clay layers are markedly ordered, and the basal reflection is observed as a low intense peak when biuret is used, and as a clear peak, with a basal spacing of 12.5 Å, in the case of melamine. This suggests that grafting of the silane molecules on Laponite induces the layers to orientate parallel between them, thus originating the enhancing of the (001) reflection. The number of stacked layers seems to be larger in the case of melamine, as concluded from the somewhat narrower peak recorded, probably because the melamine molecule is flat itself, and the derived silane may maintain a mostly flat disposition.

When the samples are prepared under aqueous conditions, the stacking is even lower than in original Laponite: the solid obtained using biuret (Lap-BiuH) is completely delaminated, while that one obtained with melamine shows only a residual shoulder due to the basal reflection. So, formation of the aminosilane previously to its interaction with the clay clearly favors ordering of the layers in the resulting solids. Concerning the intralayer reflections, they are weaker in all the treated solids than in parent Laponite, suggesting a certain degradation of the layers, although *a priori* the layers should not be affected by the reaction conditions.

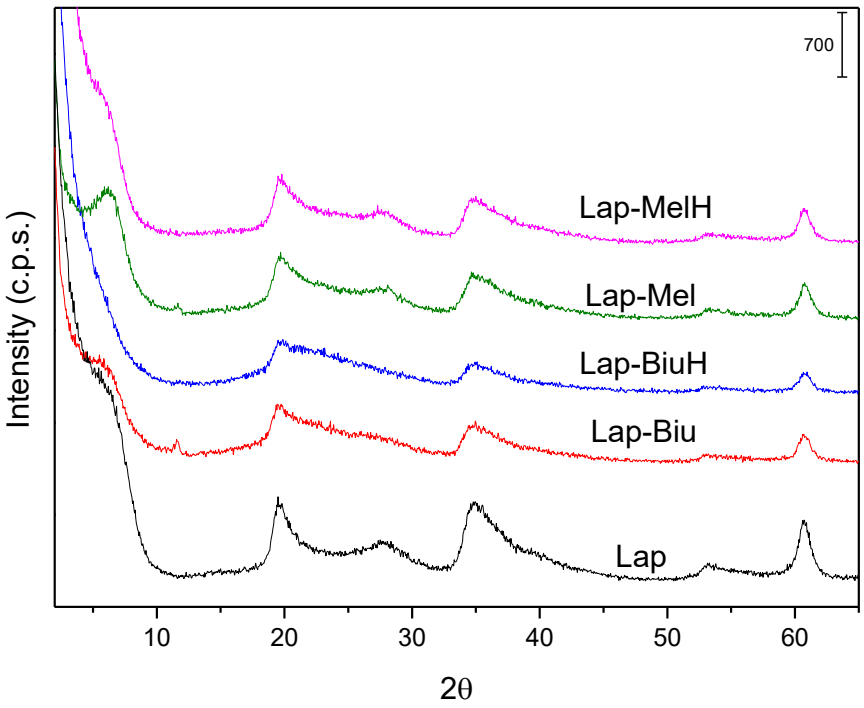

Fig. II.3. PXRD patterns of original Laponite and of the derived solids.

Some differences in the chemical compositions are observed among the grafted materials, and also when they are compared to parent Laponite (Table II.1). As usual for this sort of solids, the chemical composition is given in terms of the oxides of the existing elements and, for the functionalised samples, the content of carbon and nitrogen has been also determined. The solids have different contents of water and organic matter, and consequently the sum of the contents of the metal oxides (in other words, of raw Laponite) was different for each solid. Comparison among the compositions of the solids is difficult; it is observed that fixation of the organic matter produces a significant decrease in the content of MgO, Na_2O and CaO, while no change is observed for Fe_2O_3 and almost constant values were measured for Al_2O_3. The SiO_2 content is similar in all solids, as the relative decrease originated by the fixation of organic matter is somewhat balanced by the increase of silicon content upon fixation of the silane. The content on dry basis, normalising to a value of 100% the sum of the metal oxides content and elemental C and N, is given in Table II.S1 (Supplementary Information), but it is not possible to normalize the composition referred to an "internal standard". The SiO_2 content is usually used as internal standard to analyze the changes in the chemical composition of treated clays, as the tetrahedral layer containing the Si cations is hardly affected by the treatments; however, this is not possible in the current case, because of

the cited increase in silicon content upon incorporation of the silane. The other main component of Laponite, MgO, is very sensitive to acidic conditions, and the results reported in Table II.1 indicate that Mg^{2+} cations from the octahedral layers have undergone lixiviation, so it is not suitable either to be used as an internal reference.

Table II.1

Chemical composition (%w/w) of the samples

Sample	SiO_2	MgO	Al_2O_3	Fe_2O_3	Na_2O	CaO	C	N	Total
Lap	53.90	23.85	0.05	0.03	2.56	0.17	–	–	80.56
Lap-Biu	54.44	14.94	0.06	0.03	0.12	0.12	5.52	0.5	75.73
Lap-BiuH	58.48	12.36	0.06	0.03	0.02	0.02	8.99	0.3	80.26
Lap-Mel	54.43	18.33	0.04	0.03	0.03	0.05	7.10	1.8	81.81
Lap-MelH	52.30	17.62	0.06	0.03	0.02	0.01	5.65	2.7	78.39

Although the results cannot be compared on a reference basis, some effects are remarkable. First of all, the chemical composition of raw Laponite is compatible with literature data (Bandeira et al., 2012; Iurascu et al., 2009). The amount of organic matter fixed (on the basis of elemental C and N) is high, 8-11% in the dry solids, although it is even higher, on considering hydrogen and oxygen from the organic moieties (the hydrogen and oxygen contents have not been determined, as they exist in the solids under different forms, in the layers, as water, in the organic components, hydroxyl groups, etc.). Na^+ and Ca^{2+} cations are almost completely removed, which suggests that the incorporation of the organic matter occurs by a cation exchange reaction. The decrease in the MgO content is very marked, even higher than the relative decrease due to the incorporation of SiO_2 and organic matter, which indicates that part of octahedral Mg^{2+} is actually dissolved in the conditions used to prepare the samples. As commented above, the amount of SiO_2 seems to remain almost constant, but this indicates a significant relative increase that compensates the relative decrease caused by the incorporation of organic matter.

The absence of an internal reference makes not possible to correlate the amounts of SiO_2 (as silane) and of organic matter incorporated during the functionalisation process. However, the amounts of C and N allow to discuss on the degree of condensation between the silane and the aminated molecules, as the molar ratio between these two elements is different depending on the condensation of one, two or the three amine groups of each molecule (see

SI). As indicated, the functionalisation occurs by cation exchange (almost complete removal of sodium and calcium), so the amine groups may be protonated by the HCl molecules generated (Fig. II.2) during the condensation reactions. In addition, in the samples prepared via the aqueus route, the –OEt groups may be hydrolyzed by water. Thus, different final functionalising species are possible.

The C/N mass ratio was 11.0, 29.9, 3.95 and 2.1 for Lap-Biu, Lap-BiuH, Lap-Mel and Lap-MelH solids, respectively. Except for Lap-BiuH, for which the chemical analysis provides a low N content, these results are compatible with the condensation of all the amine groups in the molecules. For instance, in the case of Lap-Mel solid, the experimental C/N mass ratio is 3.95, while the theoretical values are 1.7, 3.0 and 4.3 if one, two or all three amine groups condense (reactions shown in Scheme I, Supplementary Information). It may be even considered that if HCl molecules generated during the condensation produce the hydrolysis of the ethoxide groups, the C/N ratio should slightly decrease, as two C atoms should be removed from the condensated molecule for each hydrolysis step.

So, the functionalisation mainly occurs by cation exchange. The difference between both methods may mainly be the hydrolysis of the ethoxide groups, that may be fast in the aqueous route by the presence of water, and much slower and in a lower extent in the non-hydrolytic method due to the HCl molecules generated by the condensation reaction (Scheme I). The acidic conditions may simultaneously favour the protonation of the amine groups, resulting in protonated species able to exchange the charge balancing cations of the clay.

The FTIR spectra of the solids are included in Fig. II.4. The incorporation of the organic components was clearly concluded from the changes in the spectra, upon comparison with that of parent Laponite. The spectrum for Laponite showed the characteristic stretching bands at 3690 cm^{-1} (MgO-H), 655 cm^{-1} (Mg-O) and 1010 cm^{-1} (Si-O) (Bandeira et al., 2012; Pereira et al., 2008), together with the bands corresponding to stretching and bending modes of water molecules. In the samples functionalised with ClPTES/Biu, intense bands attributed to biuret were observed at 1700, 1630, 1500 and 1340 cm^{-1}, due to vibrations of the C=O, N-H, C-N and C-N-C groups, respectively (Hua-Feng, 2017). In addition, changes were observed in the Si-O region, with bands close to 1000 and 1100 cm^{-1}, attributed to the Si-O vibrations from the clay and new bands from the Si-O bonds derived from the silane. For the melamine-based materials, bands corresponding to the organic molecule were also recorded at 2929, 1545, 1377 and 780 cm^{-1}, attributed to CH groups from the silane, the C=N group of the

central ring of melamine and NH groups from primary or secondary amines (Lagaly and Dékány, 2013; Stolz et al., 2016).

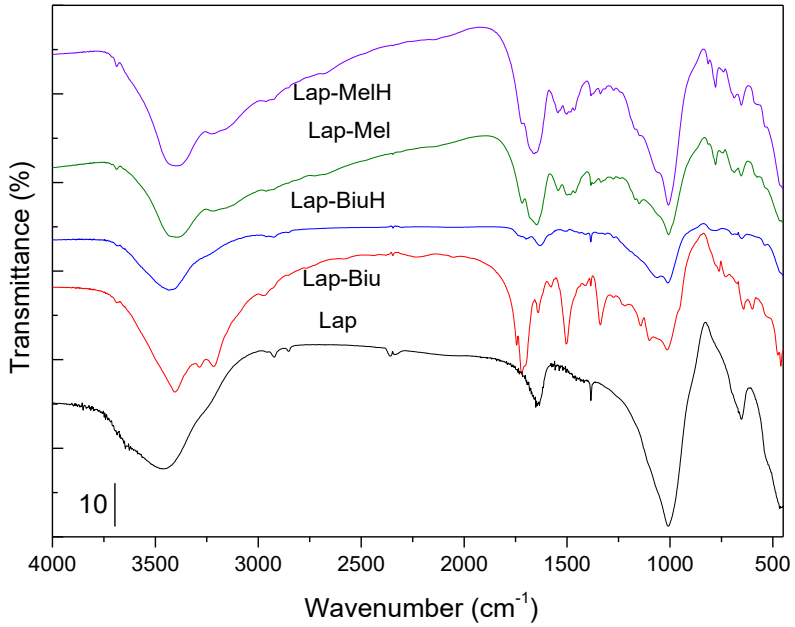

Fig. II.4. FT-IR spectra of both series of solids.

The nitrogen adsorption-desorption isotherms on the solids are shown in Fig. II.5. The isotherms can be classified as Type IV, with a H2 type hysteresis loop, in the case of Lap, Lap-BiuH and Lap-MelH, and as Type IIb, with hysteresis-loop H3, for samples Lap-Biu and Lap-Mel (Pálková et al., 2010; Zid et al., 2017; Zimowska et al., 2016, 2013). The textural properties of the solids are summarized in Table II.2. The BET specific surface area and the pore volume values of Laponite are similar to those reported in the literature (Iurascu et al., 2009; Zid et al., 2017). The synthetic route had a great influence on the evolution of the textural properties, and so the aqueous route promoted a strong increase in the specific surface area and in the pore volume, while the non-hydrolytic route led to a decrease of these values, specially for sample LapMel. This difference may be related to the structural changes undergone by the materials, as concluded from the X-ray diffraction diagrams (Fig. II.3): while the aqueous route led to highly delaminated solids, the non-aqueous route induced a stacking of the layers, where the organic molecules may occupy a large extent or almost the totality of the interlayer space; even it is possible that the organic molecules are simply blocking the access to the interlayer space.

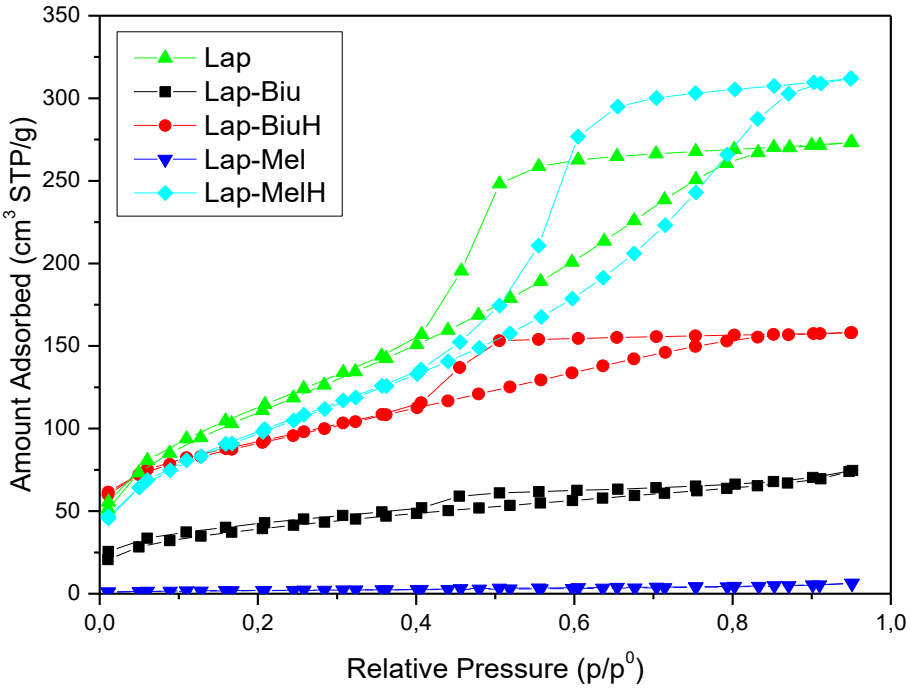

Fig. II.5. Nitrogen adsorption-desorption isotherms at –196 ºC for the solids.

Table II.2

Specific surface area and pore volume of Laponite and its derivatives.

	S_{BET} (m^2/g)	V_p (cm^3/g)
Lap	307	0.245
Lap-Biu	135	0.115
Lap-BiuH	407	0.423
Lap-Mel	7	0.010
Lap-MelH	360	0.482

The aqueous route under acidic conditions promotes the increasing of the basal space of Laponite, suggesting the intercalation of the organomodified alkoxide. As a result, the presence of siloxane and silanol groups and of Mg-OH groups on the interlaminar surface promotes the increase in the specific surface area of the materials prepared by the aqueous route (Table II.2); however, the use of a non polar solvents (toluene) does not promote swelling of Laponite then rendering the attachment of the organomodified alkoxide to the clay external surface resulting in this case in the reduction of the specific surface area, as well as increasing the hydrophobicity of these materials.

The thermogravimetric curves of parent Laponite and of one representative sample, namely, Lap-Biu, are included in Fig. II.6; the curves from the other solids are included in Fig. II.S1; a summary of the mass losses at different temperature intervals for all the samples studied is given in Table II.3. The TG curve for Laponite shows mass losses related to removal of adsorbed water and to dehydroxylation of the layers, amounting 19% of the initial mass of the sample. The first mass loss is associated to an endothermic event centered at 85 °C, while the second mass loss is associated to an endothermic effect at 712ºC, due to the dehydroxylation of the solid and an exothermic event centered at 747°C, due to the subsequent phase change from Laponite to enstatite and silica that occurs immediately after the dehydroxylation.

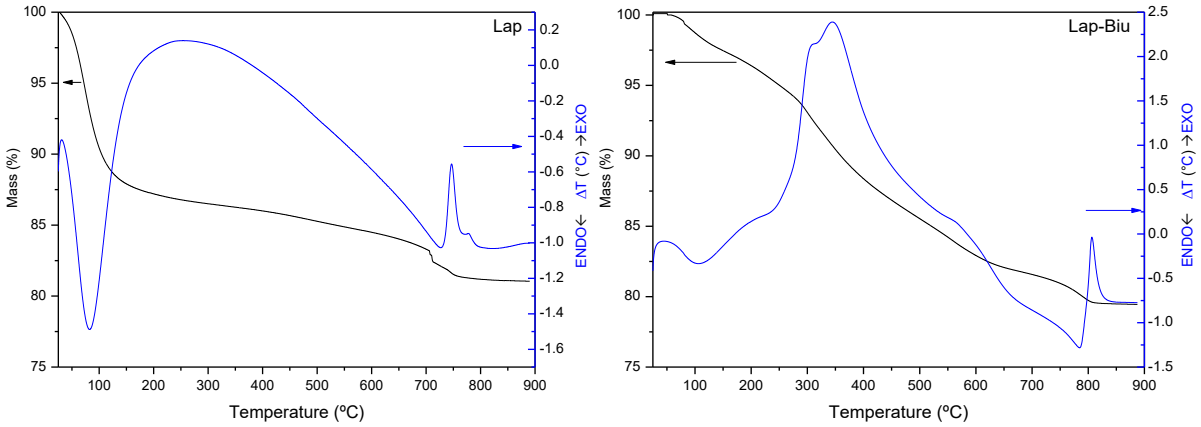

Fig. II.6. Thermogravimetric curves of Lap and Lap-Biu solids.

The curves for all the functionalised samples are composed of an initial mass loss corresponding to the removal of adsorbed water, a central loss of the organic matter, composed of various overlapped effects, and finally the dehydroxylation of Laponite. The first effect is much less intense in the functionalised samples than in parent Laponite, and it accounts only for 1-4% of the initial mass of the solids; the organofunctionalisation process induces hydrophobicity in the solids and strongly decrease the amount of adsorbed water, mainly when the reactions are carried out under non-aqueous conditions and the exchangeable cations are removed. This mass loss is always associated to an endothermic effect, centered between 85 and 106ºC.

The organic matter incorporated in the solids is removed in the temperature range ca. 150 - 650°C. The mass loss is observed in several consecutive, overlapped, steps, without the existence of *plateaux* corresponding to the formation of thermally stable intermediates, in

agreement with the presence of a very broad exothermic effect, also with shoulders corresponding to secondary effects, in the DTA curves. This may be due to the progressive removal of different fragments of the organic molecules, and to the existence of molecules in different environments, retained with different strengths. The process gives rise to a strong exothermic effect, related to combustion of the organic components of the samples. The masses of the final residues were between 74-80% of the initial masses, in agreement with the compositions given by chemical analyses. No significant differences were observed when using biuret or melamine as aminated molecules, the removal of both molecules took place in a similar way and at similar temperatures; the preparation method did not influence significantly the thermal behavior of the solids.

The last mass loss, corresponding to dehydroxylation of Laponite, was considerably delayed, even 90ºC, in the functionalized materials, in comparison with the temperature at which it is recorded for parent Laponite. Thus, this loss was centered at 791-803ºC in the functionalized solids, and was recorded as a broader process than in the natural Laponite, while the associated endothermic effect is also recorded at higher temperatures in the functionalised solids (783-792ºC). This may be mainly due to the "protection" of the clay layers by the SiO_2 formed by the thermal decomposition of the aminosilane incorporated, which may also hinder transmission of heat to the clay layers, and removal of the water generated. Accordingly, the final phase change to form enstatite is also delayed, the associated exothermic effect being centered at 807-809ºC (747ºC for natural Laponite), the higher amount of SiO_2 now available to form the high temperature phase may delay the final phase transformation.

Table II.3

Mass losses (%) in different temperature ranges.

	T_i-150°C	150-650°C	650-T_f	Total
Lap	12.1	3.9	3.0	19.0
Lap-Biu	2.5	15.4	2.6	20.5
Lap-BiuH	3.8	19.7	2.1	25.6
Lap-Mel	2.3	18.0	2.9	23.2
Lap-MelH	3.9	15.1	3.0	22.0

T_i and T_f: Initial and final temperature, respectively

From SEM analysis (Fig. II.7), it is observed that the functionalised solids have a much spongier morphology than parent Laponite (Borsacchi et al., 2007), and among them, the materials obtained by the aqueous route are less spongy than those obtained by the non-hydrolytic route, which showed the spongiest morphology. This confirms that the synthetic route followed influenced the surface structure of the obtained materials.

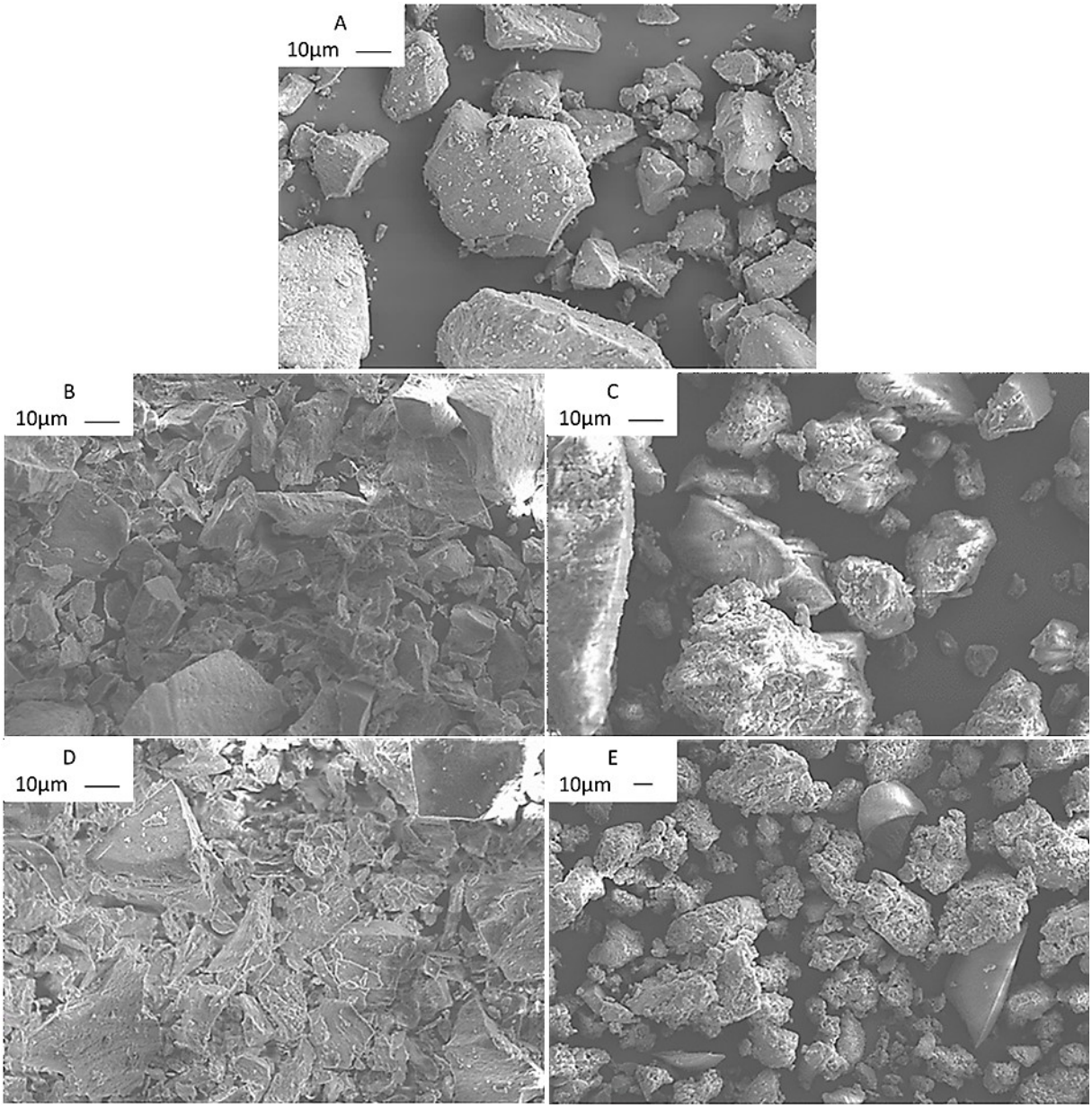

Fig. II.7. SEM micrographs of the solids Lap (A), Lap-Biu (B), Lap-BiuH (C), Lap-Mel (D) and Lap-MelH (E).

3.2. Adsorption study

3.2.a. Kinetics study. Adsorption of TMP (Fig. II.8) was a very fast process and the equilibrium was attained within 20 minutes. Mathematical models (Xi et al., 2010) were applied to the experimental results to determine what of them best described the process. The pseudo-first-order model provided a better fit to the experimental data, and the compounds prepared by the aqueous route showed higher affinity for TMP, with higher rate constants, than the materials obtained by the non-aqueous route. Results reported in the literature for adsorption of TMP on other clay materials (Bekçi et al., 2007; Molu and Yurdakoç, 2010) indicate that the process is best described by the pseudo-second-order mathematical model, where the adsorption rate is controlled by the chemical interaction between the components of the liquid/solid interface, but in Laponite-based materials the pseudo-first-order model shows a better fit (De Carvalho et al., 2010; Qiu et al., 2009).

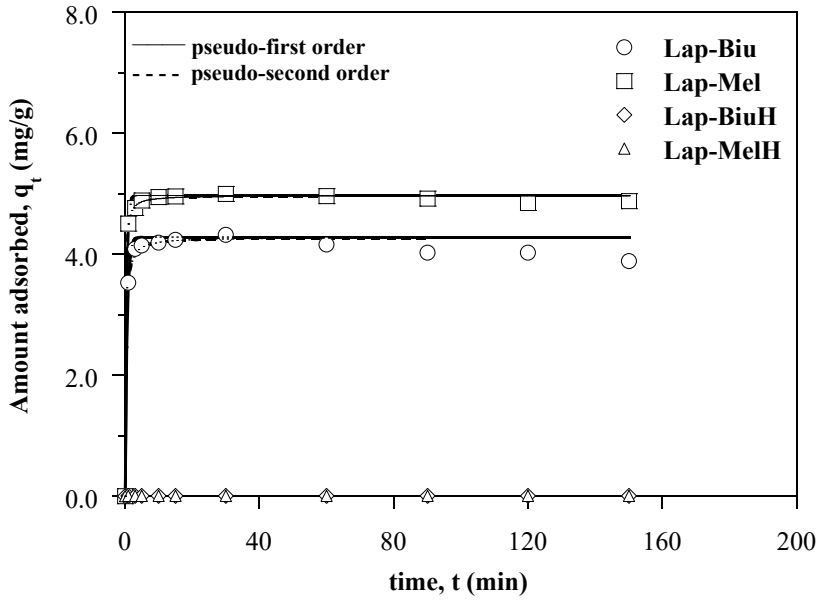

Fig. II.8. Kinetics study of TMP adsorption on Lap-Biu, Lap-BiuH, Lap-Mel and Lap-MelH, and application of the mathematical models of pseudo-first order, pseudo-second order. Symbols: experimental values; lines; fitted model.

To know the adsorption kinetics is a fundamental point in adsorption studies, giving valuable evidences of the possibility of technological application of an adsorbent for a particular separation process. The pseudo-first-order and the second-order kinetic models

were used to elucidate the adsorption mechanism. The pseudo-first-order kinetics model is described by Equation 3 (Lagergren, 1898):

$$q_t = q_e \cdot \left[1 - \exp\left(-k_1 \cdot t\right)\right] \qquad \text{Equation 3}$$

where q_e and q_t (mg/g) are the amounts of adsorbate adsorbed at equilibrium and at time t, respectively, and k_1 is the rate constant (min^{-1}).

The pseudo-second-order kinetic model is described by Equation 4 (Ho and Ofomaja, 2006):

$$q_t = \frac{k_2 \cdot q_e^2 \cdot t}{1 + k_2 \cdot q_e \cdot t} \qquad \text{Equation 4}$$

where q_e is the maximum adsorption capacity (mg/g), q_t is the amount of adsorbate (mg/g) adsorbed at time t (min) and k_2 is the rate constant (g/(mg·min)).

The intra-particle diffusion model, based on the theory by Weber and Morris (Weber and Morris, 1963), was used to identify the applicability of the diffusion mechanism. According to this theory, the adsorbate uptake q_t changes linearly with the square root of the contact time (Equation 5):

$$q_t = k_d \, t^{1/2} + C \qquad \text{Equation 5}$$

where k_d (mg/g·$min^{1/2}$) is a measure of the diffusion coefficient and C is an intraparticle diffusion constant (mg/g) directly proportional to the boundary layer thickness.

The nonlinear chi-square test (χ^2) is a statistical tool necessary to describe the best fit in an adsorption system; it is determined from the sum of the square differences between the experimental and calculated data, with each squared difference divided by its corresponding value (calculated from the theoretical adsorption models), Equation 6. Thus, small X^2 values indicate a good fitting, while a larger value represents deviation of the experimental data.

$$X^2 = \sum_{i=1}^{n} \frac{\left(q_{t_{calc}} - q_{t_{exp}}\right)^2}{q_{t_{exp}}} \qquad \text{Equation 6}$$

The kinetic parameters for the adsorption of TMP on the hybrid materials were calculated from the corresponding plots and are included in Table II.4. The best fit was achieved with the pseudo-first-order kinetic model, evidencing that the adsorption process occurred by a physisorption mechanism.

The acid catalysis in the aqueous route compared to the non-hydrolytic route alters the amount of TMP adsorbed on the clay surface and consequently influences the amount of amine groups attached to the clay. Broadly speaking, the samples prepared by the non-hydrolytic procedure promote removal of TMP until the equilibrium is reached. This fact could be due to the presence of organic units on the clay surfaces and also to the presence of larger amounts of amine groups from melamine or biuret molecules bound to ClPTES. Thus, both the time required to reach the equilibrium and the adsorption capacity could be drastically influenced by the synthetic route followed for organofunctionalization. So, for samples Lap-Biu and Lap-BiuH the kinetics study shows that organofunctionalization modifies the adsorption capacity (q_t = 4.32 mg/g and 0.0043 mg/g, respectively), while for samples Lap-Mel and Lap-MelH the values were q_t = 4.87 mg/g and 0.0050 mg/g, respectively.

Table II.4

Pseudo-first order, pseudo-second order and intraparticle diffusion kinetic parameters for TMP adsorption.

	Lap-Biu	Lap-Mel
Pseudo-first order		
k_1 (min^{-1})	1.72	2.36
q_e (mg/g)	4.28	4.97
χ^2	0.36	0.076
R^2	0.97	0.996
Pseudo-second order		
k_2 (g/(mg·min))	1.15	1.93
q_e (mg/g)	4.28	4.97
χ^2	0.30	0.030
R^2	0.98	0.998
Intraparticle diffusion		
k_d ($mg/(g \cdot min^{1/2})$)	0.068	0.080
C (mg/g)	3.98	4.67
R^2	0.98	0.790

The adsorption capacity q_e at equilibrium calculated for the pseudo-first order kinetics fits very well with the experimental value. This suggests that the pseudo-first order is the predominant mechanism and that the overall rate of TMP adsorption is controlled by the formation of hydrogen bonds between the amine groups in the hybrid materials and TMP, as it has been confirmed by an FTIR study. Fig. II.9 and Fig. II.S2 show the spectra of laponite-functionalized derivatives before and after adsorption of TMP. After adsorption, bands centred around 3358 and 1633 cm^{-1} are observed, in all the cases broader than before adsorption and assigned to the OH stretching and bending modes, respectively, of water molecules. The presence of bands due to hydrogen bonds between TMP and NH_2 groups from solids, which should be recorded in the first region, cannot be definitively confirmed or discarded. The main change induced by the presence of TMP is the shifting and strong enhancement of the hydroxyl band, evidencing the interaction via hydrogen bonding with OH from the clay matrix. The presence of TMP on the surface of the solids was also confirmed by the presence of the bands at 2952 and 2892 cm^{-1}, assigned to C-H stretching modes of aliphatic groups.

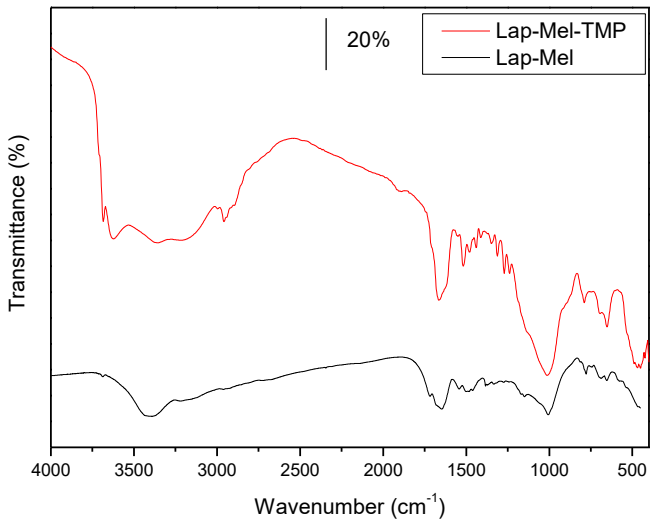

Fig. II.9. FTIR spectra demonstrating the interaction between Lap-Mel and TMP.

The *fractional attainment at equilibrium* is the ratio between the amount of adsorbate removed from solution after a given time (q_t) and that removed when the adsorption equilibrium (q_e) is attained, Eqn. 7.

$$\alpha_e = q_t/q_e \qquad \text{Equation 7}$$

It would be definitely expected that factors such as the number of active adsorption sites on the adsorbate surface and the bulkiness of the adsorbate molecule would affect the rate of adsorption of TMP. However, further more information can be obtained from the fractional attainment at equilibrium. The rate of the attainment of equilibrium may be either film-diffusion controlled or particle-diffusion controlled, even though these two mechanisms cannot be sharply demarcated (Okeimen et al., 1999).

The plot of α_e against time for Lap-Biu and Lap-Mel is shown in Fig. II.10. The adsorbents showed high adsorption capacities in the first stages of the adsorption process, until 5 minutes. The value of α_e for sample Lap-Biu sharply increases in the early steps of the process and converges to one at 15 min. However, for sample Lap-Mel it converges to one even within one minute, confirming the fast removal of TMP from solution. The higher removal rate could be related to the presence of amine groups well dispersed on the clay surface, as evidenced by the lower specific surface area measured for this solid.

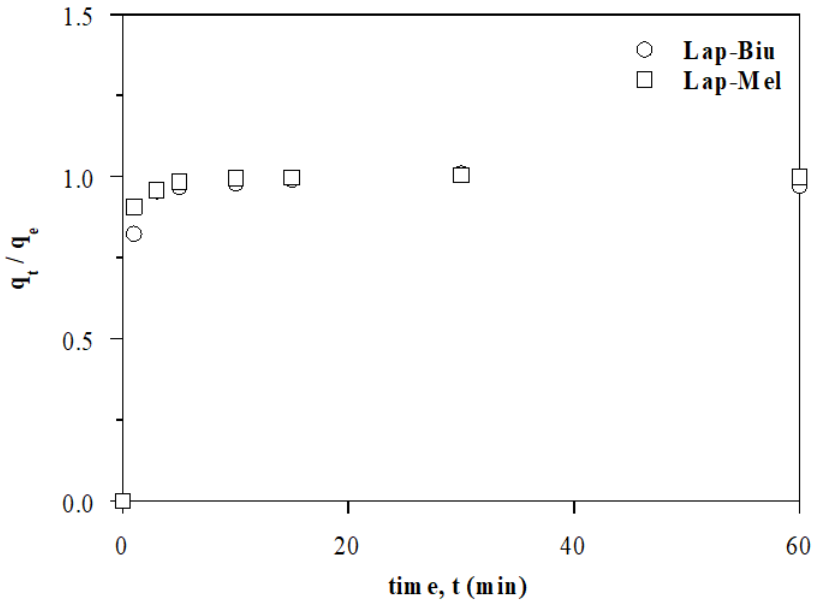

Fig. II.10. Fractional attainment at equilibrium (α_e) against time for TMP uptake by Laponite hybrid materials.

As previously observed with fibrous clays and saponites (Marçal et al., 2015), the presence of organic molecules on the surface may promote a negative effect on the final adsorption capacity. However, the current results suggest that the organic chains from biuret and melamine and the alkoxide groups are well dispersed on the clay platelets in the samples prepared by the non-hydrolytic route and could favor the adsorption of TMP. On the contrary,

the aqueous synthesis in acidic conditions promotes the agglomeration of organic molecules and the possible active sites (amine groups from biuret and melamine) are not available for adsorption of further molecules onto the surface due to their binding to the surface (Fig. II.8). This result agrees well with the previously reported studies on saponite and fibrous clays grafted with amine groups (Marçal et al., 2015; Moreira et al., 2016), where the presence of well-dispersed active sites favors the adsorption process; however if they are in excess, these sites could hinder the adsorption of the target compounds.

3.2.b. Equilibrium study. The data on adsorption at equilibrium of TMP on the organically modified Laponite were fitted by applying the Langmuir, Freundlich, and Sips isotherm models.

The *Langmuir* adsorption model predicts that a monolayer of adsorbate molecules covers the outer surface of the adsorbent; adsorption takes place at specific homogeneous sites of the adsorbent surface, which implies that all adsorption sites are identical and energetically equivalent (Langmuir, 1916). The Langmuir adsorption isotherm has been successfully applied to many adsorption processes involving organic compounds. It equation describing the process can be written as:

$$q_e = \frac{q_L \cdot k_L \cdot C_e}{1 + k_L \cdot C_e} \qquad \text{Equation 8}$$

where both q_L (mg/g) and k_L (dm^3/mg) are Langmuir constants related to the monolayer adsorption capacity.

The *Freundlich* equation is an empirical equation used to describe adsorption on heterogeneous systems. It is usually written as (Freundlich, 1906):

$$q_e = k_F \cdot C_e^{1/m_F} \qquad \text{Equation 9}$$

where k_F and m_F are empirical constants related to the extent of adsorption and its efficacy, respectively.

The *Sips* isotherm is a combined form of the Langmuir and Freundlich models deduced for predicting the adsorption on heterogeneous systems and circumventing the

limitation of the rising adsorbate concentration associated to the Freundlich isotherm model (Sips, 1948). At low adsorbate concentrations, it is simplified to the Freundlich isotherm, while at high adsorbate concentrations, it predicts a monolayer adsorption capacity characteristic of the Langmuir isotherm. The corresponding equation is:

$$q_e = \frac{q_S \cdot k_S \cdot C_e^{m_S}}{1 + k_S \cdot C_e^{m_S}} \qquad \text{Equation 10}$$

where k_S (dm^3/mg) and q_s (mg/g) are the Sips constants representing the adsorption energy and the monolayer adsorption capacity, respectively, and m_S is an empirical constant.

For evaluating the efficiency of the adsorbents, the equilibrium adsorption was studied as a function of the equilibrium concentration (Fig. II.11, Table II.5) applying all three models above described. According to Giles classification (Giles and Smith, 1974), the isotherms were type L4 for Lap-Mel and L3 for the other adsorbents. L-type or Langmuir isotherms are characterized by a non-linear concave inclination with respect to the abscissa axis, indicating a decreasing availability of adsorption sites when the concentration at equilibrium increases (Bekçi et al., 2006; Marçal et al., 2015). Good fitting results were obtained for all samples. Sample Lap-Mel showed the highest adsorption capacity, with q_e = 65.73 mg/g, while the values for samples Lap-Biu, Lap-BiuH and Lap-MelH were q_e = 43.12, 38.73 and 30.75 mg/g, respectively. The regression coefficients were higher than 0.93, and the Sips model (Sips, 1948) showed the best fitting among all models considered.

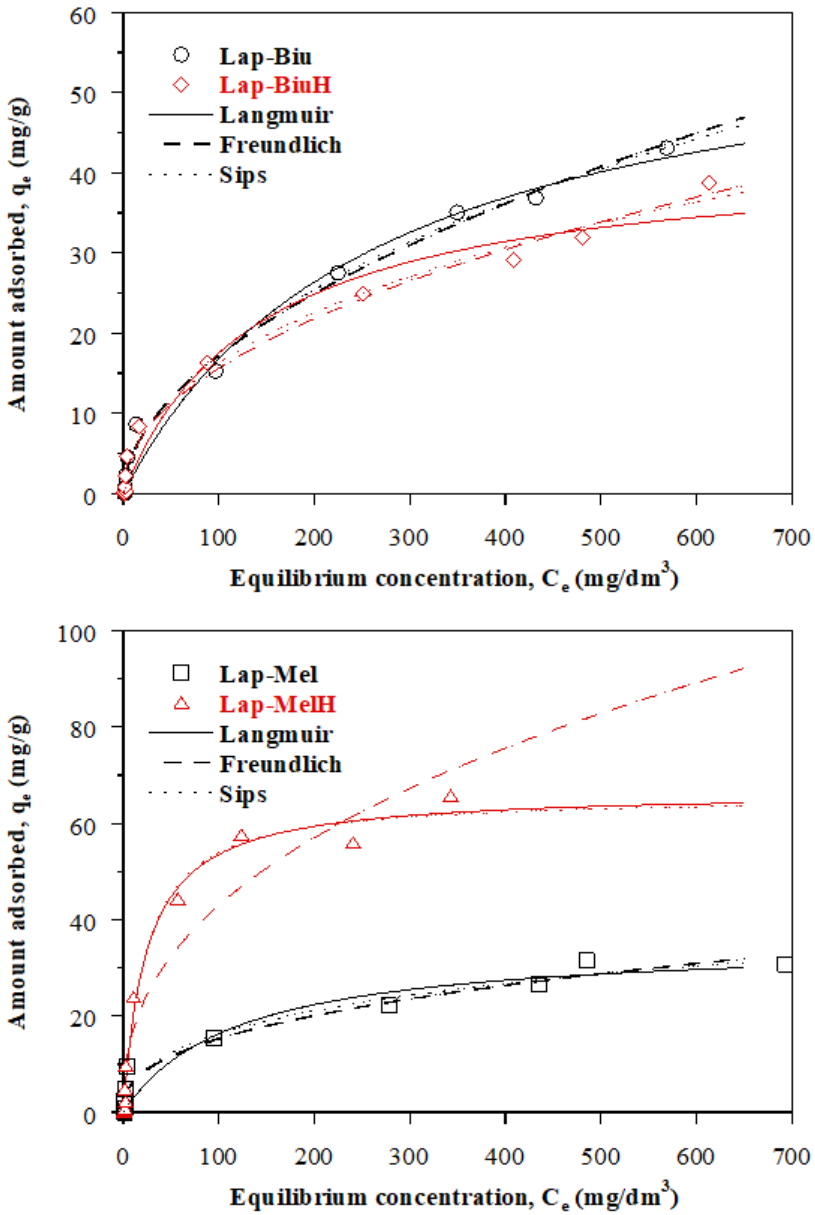

Fig. II.9. Equilibrium study of TMP on Lap-Biu, Lap-BiuH, Lap-Mel and Lap-MelH, and application of the mathematical models of Langmuir, Freundlich and Sips.

Table II.5

Langmuir, Freundlich and Sips equation parameters for the TMP adsorption by modified Laponites.

Adsorbent	Lap-Biu	Lap-BiuH	Lap-Mel	Lap-MelH
Langmuir				
q_L (mg/g)	61	43	35	67
k_L (dm^3/mg)	0.0038	0.0070	0.0086	0.0041
χ^2	53	62	111	102
R^2	0.98	0.970	0.930	0.985
Freundlich				
k_F (mg/g)	1.46	1.71	2.51	6.59
m_F	1.87	2.1	2.5	2.4
χ^2	27	30	67	532
R^2	0.991	0.98	0.96	0.930
Sips				
q_s (mg/g)	226	141	83	66
k_S (dm^3/mg)	0.0055	0.010	0.027	0.038
m_S	0.59	0.55	0.48	1.04
χ^2	26	28	63	101
R^2	0.991	0.98	0.96	0.980

Melamine-derived materials showed the highest percentages of TMP removal, rapidly reaching 99%, which was maintained constant for a long time in the case of the sample prepared by the non-hydrolytic method and slowly decreased for that prepared by the hydrolytic method. After the equilibrium was reached, the desorption process begins (in some cases), a fact that can be attributed to the saturation of the active sites of the solid materials, reducing the efficiency of the process at times larger than the ideal time observed in the kinetic study.

A comparison of the results with those from other adsorbents reported in the literature is given in Table II.6, showing the good performance of the adsorbents studied in this report.

Table II.6

Comparison of the TMP maximum adsorption capacity of the adsorbents prepared in this work with other adsorbents employed in the literature.

Adsorbent	Maximum adsorption capacity (mg/g)	Reference
Lap-Biu	43.12	This work
Lap-BiuH	38.73	This work
Lap-Mel	30.75	This work
Lap-MelH	65.73	This work
Montmorillonite	26.28-46.45	(Molu and Yurdakoç, 2010)
Sewage sludge and fish waste	3.63-6.53 (650 °C) 9.00-13.94 (950 °C)	(Nielsen and Bandosz, 2016)
Activated Carbon activated by phosphorus oxyacids	58.06-78.39	(Liu et al., 2012)

4. Conclusions

New nanohybrid materials based on functionalized derivatives of Laponite were prepared by two routes: organic solvent and aqueous medium under acidic catalysis. The acidic catalysis on hydrolitic method promotes the hydrolysis of the alkoxide, resulting in materials with high specific surface areas. Specifically, Lap-MelH exhibits a larger specific surface area than the starting purified Laponite. All the differences in the physico-chemical properties of the hybrids and in the adsorptive properties of the four materials were carefully evaluated.

The textural characteristics and the presence of the surface functional groups (melamine or biuret) on the Laponite hybrid derivatives strongly depend on the nature of the synthesis route followed, toluene non-aqueous or aqueous under acidic conditions.

The probable interactions of trimethoprim with Laponite nanohybrid derivatives occur by hydrogen bonding and Lewis acid–base interactions and cation exchange. In this sense the presence of organic moieties on the surface or interlayer surface on the Laponite functionalized derivatives also plays an important role.

These strategy synthesis open new possibilities to immobilize important and active molecules such as drugs, catalysts and photocatalysts, among others, on the clay mineral surface or interlayer space.

References for Article II

Bandeira, L.C., Calefi, P.S., Ciuffi, K.J., de Faria, E.H., Nassar, E.J., Vicente, M.A., Trujillano, R., 2012. Preparation of composites of laponite with alginate and alginic acid polysaccharides. Polym. Int. 61, 1170–1176. https://doi.org/10.1002/pi.4196

Bekçi, Z., Seki, Y., Kadir Yurdakoç, M., 2007. A study of equilibrium and FTIR, SEM/EDS analysis of trimethoprim adsorption onto K10. J. Mol. Struct. 827, 67–74. https://doi.org/10.1016/j.molstruc.2006.04.054

Bekçi, Z., Seki, Y., Yurdakoç, M.K., 2006. Equilibrium studies for trimethoprim adsorption on montmorillonite KSF. J. Hazard. Mater. 133, 233–242. https://doi.org/10.1016/j.jhazmat.2005.10.029

Ben Zid, T., Fadhli, M., Khedher, I., Fraile, J.M., 2017. New bis (oxazoline)–vanadyl complexes, supported by electrostatic interaction in Laponite clay, as heterogeneous catalysts for asymmetric oxidation of methyl phenyl sulfide. Micropor. Mesopor. Mater. 239, 167–172. https://doi.org/10.1016/j.micromeso.2016.09.055

Borsacchi, S., Geppi, M., Ricci, L., Ruggeri, G., Veracini, C.A., 2007. Interactions at the surface of organophilic-modified laponites: A multinuclear solid-state NMR study. Langmuir 23, 3953–3960. https://doi.org/10.1021/la063040a

Christidis, G.E., 2013. Chapter 4.1 – Assessment of Industrial Clays, 2nd ed, Developments in Clay Science. Elsevier Ltd. https://doi.org/10.1016/B978-0-08-098259-5.00017-2

De Carvalho, T.E.M., Fungaro, D.A., De Izidoro, J.C., 2010. Adsorção do corante reativo laranja 16 de solução es aquosas por zeólita sintética. Quim. Nova 33, 358–363. https://doi.org/10.1590/S0100-40422010000200023

de Paiva, L.B., Morales, A.R., Valenzuela Díaz, F.R., 2008. Organoclays: Properties, preparation and applications. Appl. Clay Sci. 42, 8–24. https://doi.org/10.1016/j.clay.2008.02.006

Detellier, C., Letaief, S., 2013. Kaolinite-polymer nanocomposites, 2nd ed, Developments in Clay Science. Elsevier Ltd. https://doi.org/10.1016/B978-0-08-098258-8.00022-5

Freundlich, H.M.F., 1906. Over the Adsorption in Solution. Z. Phys. Chem. 57, 385–471.

Giles, C.H., Smith, D., Huitson, A., 1974. A General Treatment and Classification of the Solute Adsorption Isotherm. I. Theoretical. J. Colloid Interf. Sci., 47, 755–765. https://doi.org/10.1016/0021-9797(74)90252-5

Ho, Y.S., Ofomaja, A.E., 2006. Biosorption thermodynamics of cadmium on coconut copra meal as biosorbent. Biochem. Eng. J. 30, 117–123. https://doi.org/10.1016/j.bej.2006.02.012

Hua-Feng, P., 2017. Biuret-assisted formation of nanostructured In_2O_3 architectures and their photoluminescence properties. J. Lumin. 182, 8–14. https://doi.org/10.1016/j.jlumin.2016.10.014

Iurascu, B., Siminiceanu, I., Vione, D., Vicente, M.A., Gil, A., 2009. Phenol degradation in water through a heterogeneous photo-Fenton process catalyzed by Fe-treated laponite. Water Res. 43,

1313–1322. https://doi.org/10.1016/j.watres.2008.12.032

Ji, Y., Xie, W., Fan, Y., Shi, Y., Kong, D., Lu, J., 2016. Degradation of trimethoprim by thermo-activated persulfate oxidation: Reaction kinetics and transformation mechanisms. Chem. Eng. J. 286, 16–24. https://doi.org/10.1016/j.cej.2015.10.050

Lagaly, G., Dékány, I., 2013. Colloid clay science, http://dx.doi.org/10.1016/B978-0-08-098258-8.00010-9; Chapter 8 (pp. 243–345) in: Handbook of Clay Science, 2nd Edition (Bergaya, F., Lagaly, G., Eds.). Elsevier. ISBN 9780080993645

Lagaly, G., Ogawa, M., Dékány, I., 2013. Clay mineral-organic interactions, http://dx.doi.org/10.1016/B978-0-08-098258-8.00015-8; Chapter 10.3 (pp. 435–505) in: Handbook of Clay Science, 2nd Edition (Bergaya, F., Lagaly, G., Eds.). Elsevier. ISBN 9780080993645.

Lagergren, S., 1898. About the theory of so–called adsorption of soluble substances. K. Sven. Vetenskapsakademiens Handl. 24, 1–39.

Langmuir, I., 1916. the Constitution and Fundamental Properties of Solids and Liquids. Part I. Solids. J. Am. Chem. Soc. 252, 2221–2295. https://doi.org/10.1021/ja02268a002

Liu, H., Zhang, J., Bao, N., Cheng, C., Ren, L., Zhang, C., 2012. Textural properties and surface chemistry of lotus stalk-derived activated carbons prepared using different phosphorus oxyacids: Adsorption of trimethoprim. J. Hazard. Mater. 235–236, 367–375. https://doi.org/10.1016/j.jhazmat.2012.08.015

Liu, L., Wan, Q., Xu, X., Duan, S., Yang, C., 2017. Combination of micelle collapse and field-amplified sample stacking in capillary electrophoresis for determination of trimethoprim and sulfamethoxazole in animal-originated foodstuffs. Food Chem. 219, 7–12. https://doi.org/10.1016/j.foodchem.2016.09.118

Marçal, L., de Faria, E.H., Nassar, E.J., Trujillano, R., Martín, N., Vicente, M.A., Rives, V., Gil, A., Korili, S.A., Ciuffi, K.J., 2015. Organically Modified Saponites: SAXS Study of Swelling and Application in Caffeine Removal. ACS Appl. Mater. Interfaces 7, 10853–10862. https://doi.org/10.1021/acsami.5b01894

Molu, Z.B., Yurdakoç, K., 2010. Preparation and characterization of aluminum pillared K10 and KSF for adsorption of trimethoprim. Microporous Mesoporous Mater. 127, 50–60. https://doi.org/10.1016/j.micromeso.2009.06.027

Moreira, M.A., Ciuffi, K.J., Rives, V., Vicente, M.A., Trujillano, R., Gil, A., Korili, S.A., de Faria, E.H., 2016. Effect of chemical modification of palygorskite and sepiolite by 3-aminopropyltriethoxisilane on adsorption of cationic and anionic dyes. Appl. Clay Sci. 135, 394–404. https://doi.org/10.1016/j.clay.2016.10.022

Nielsen, L., Bandosz, T.J., 2016. Analysis of sulfamethoxazole and trimethoprim adsorption on sewage sludge and fish waste derived adsorbents. Microporous Mesoporous Mater. 220, 58–72.

https://doi.org/10.1016/j.micromeso.2015.08.025

Okeimen, F.E., Esther, U.O., David, E.O., 1999. Sorption of Cadmium and Lead ions on modified groundnut husk. Nigerian-Chem. Tech. Biotechnology 31, 97–99.

Pálková, H., Madejová, J., Zimowska, M., Bielańska, E., Olejniczak, Z., Lityńska-Dobrzyńska, L., Serwicka, E.M., 2010. Laponite-derived porous clay heterostructures: I. Synthesis and physicochemical characterization. Microporous Mesoporous Mater. 127, 228–236. https://doi.org/10.1016/j.micromeso.2009.07.019

Pereira, C., Silva, A.R., Carvalho, A.P., Pires, J., Freire, C., 2008. Vanadyl acetylacetonate anchored onto amine-functionalised clays and catalytic activity in the epoxidation of geraniol. J. Mol. Catal. A Chem. 283, 5–14. https://doi.org/10.1016/j.molcata.2007.11.034

Qiu, H., Lv, L., Pan, B., Zhang, Q.Q., Zhang, W., Zhang, Q.Q., 2009. Critical review in adsorption kinetic models. J. Zhejiang Univ. Sci. A 10, 716–724. https://doi.org/10.1631/jzus.A0820524

Richardson, B.J., Lam, P.K.S., Martin, M., 2005. Emerging chemicals of concern: Pharmaceuticals and personal care products (PPCPs) in Asia, with particular reference to Southern China. Mar. Pollut. Bull. 50, 913–920. https://doi.org/10.1016/j.marpolbul.2005.06.034

Sips, R., 1948. On the Structure of a Catalyst Surface. J. Chem. Phys. 16, 490. https://doi.org/10.1063/1.1746922

Stolz, A., Le Floch, S., Reinert, L., Ramos, S.M.M., Tuaillon-Combes, J., Soneda, Y., Chaudet, P., Baillis, D., Blanchard, N., Duclaux, L., San-Miguel, A., 2016. Melamine-derived carbon sponges for oil-water separation. Carbon 107, 198–208. https://doi.org/10.1016/j.carbon.2016.05.059

Weber, W.J., Morris, J.C., 1963. Kinetics of adsorption on carbon from solutions. J. Sanit. Eng. Div. 89, 31–60.

Xi, Y., Mallavarapu, M., Naidu, R., 2010. Preparation, characterization of surfactants modified clay minerals and nitrate adsorption. Appl. Clay Sci. 48, 92–96. https://doi.org/10.1016/j.clay.2009.11.047

Zhang, Y., Wang, A., Tian, X., Wen, Z., Lv, H., Li, D., Li, J., 2016. Efficient mineralization of the antibiotic trimethoprim by solar assisted photoelectro-Fenton process driven by a photovoltaic cell. J. Hazard. Mater. 318, 319–328. https://doi.org/10.1016/j.jhazmat.2016.07.021

Zimowska, M., Gurgul, J., Pálková, H., Olejniczak, Z., Łatka, K., Lityńska-Dobrzyńska, L., Matachowski, L., 2016. Structural rearrangements in Fe-porous clay heterostructures composites derived from Laponite®- Influence of preparation methods and Fe source. Micropor. Mesopor. Mater. 231, 66–81. https://doi.org/10.1016/j.micromeso.2016.05.013

Zimowska, M., Pálková, H., Madejová, J., Dula, R., Pamin, K., Olejniczak, Z., Gil, B., Serwicka, E.M., 2013. Laponite-derived porous clay heterostructures: III. the effect of alumination. Micropor. Mesopor. Mater. 175, 67–75. https://doi.org/10.1016/j.micromeso.2013.02.047

SUPPLEMENTARY MATERIALS FOR ARTICLE II

Table II.S1

Chemical composition (%w/w) of the solids, normalized to water free content, that is the sum of the metallic oxides, C and N being 100% (for the treated solids, the content of elemental C and N was considered, the content of H and O was ignored).

	SiO_2	MgO	Al_2O_3	Fe_2O_3	Na_2O	CaO	C	N	Total
Lap	66.91	29.61	0.06	0.04	3.18	0.21			100
Lap-Biu	71.89	19.73	0.08	0.04	0.16	0.16	7.29	0.7	100
Lap-BiuH	72.86	15.40	0.07	0.04	0.02	0.02	11.20	0.4	100
Lap-Mel	66.53	22.41	0.05	0.04	0.04	0.06	8.68	2.2	100
Lap-MelH	66.72	22.48	0.08	0.04	0.03	0.01	7.21	3.4	100

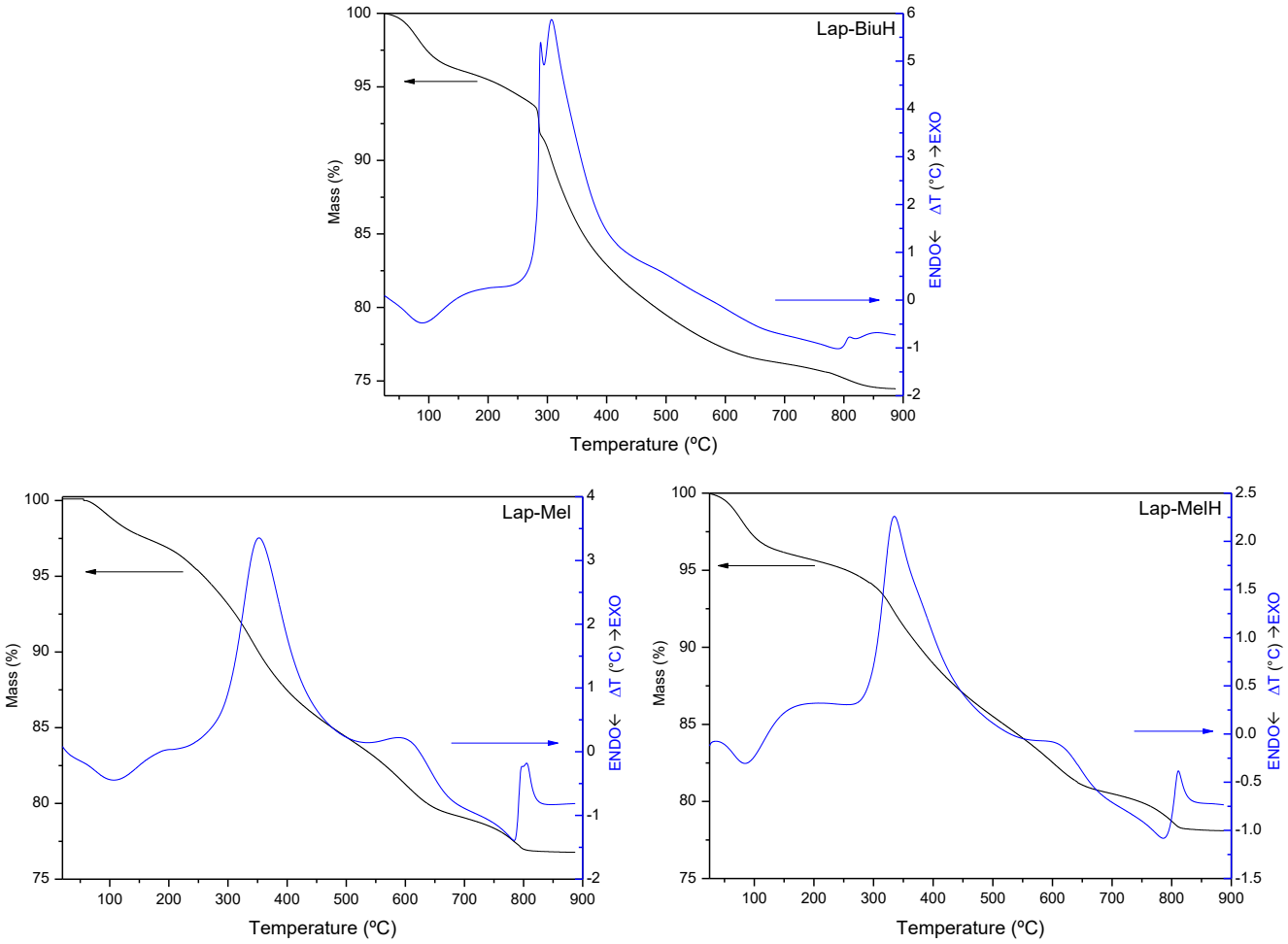

Fig. II.S1. TG and DTA curves of the different materials.

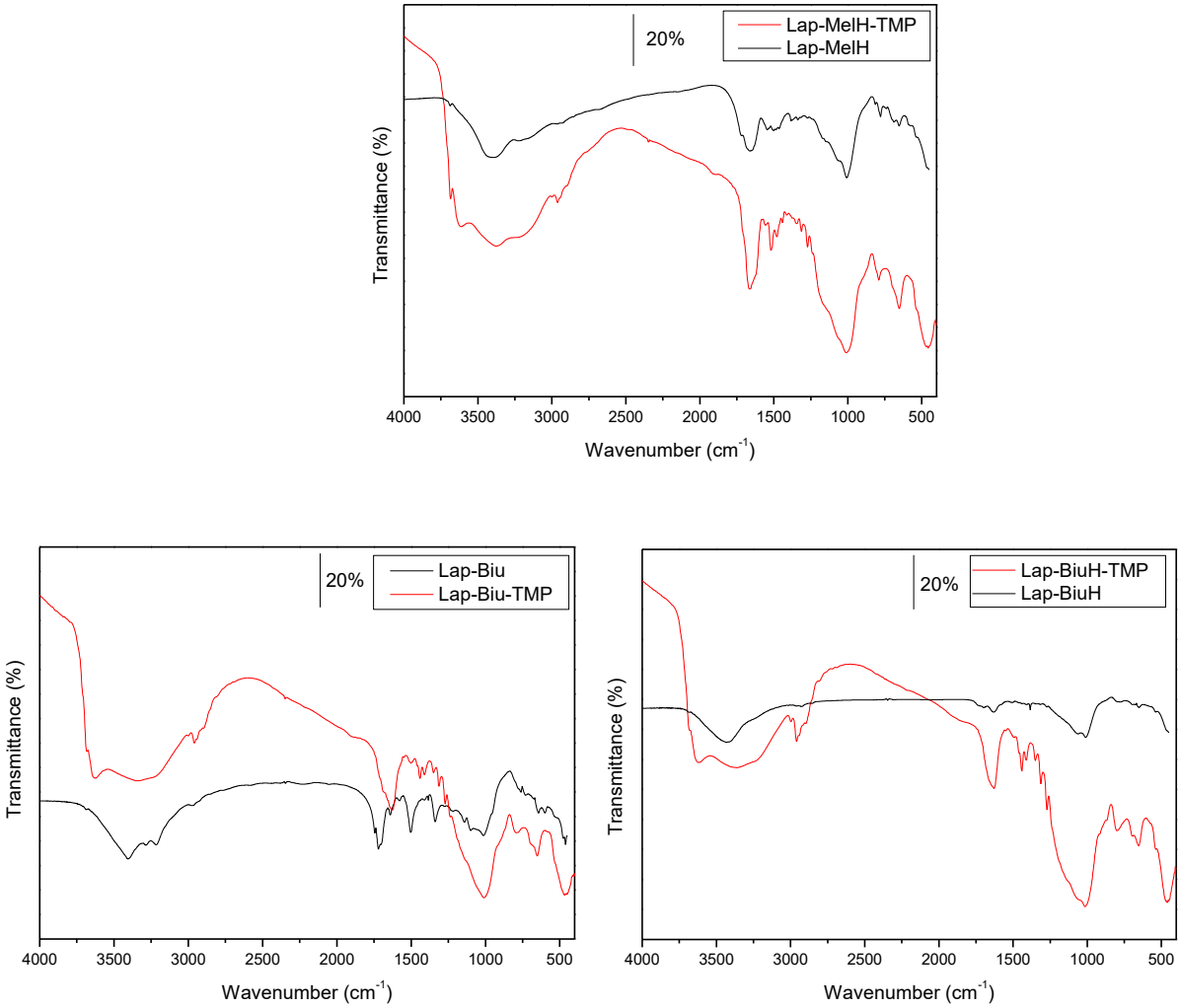

Fig. II.S2. FTIR study of the interaction of Lap-MelH, Lap-Biu and Lap-BiuH solids with TMP.

Scheme I. Probable mechanism involved in laponite functionalization

A. Non-aqueous route

First step: Condensation reaction between the organosilane and each of the amine molecules.

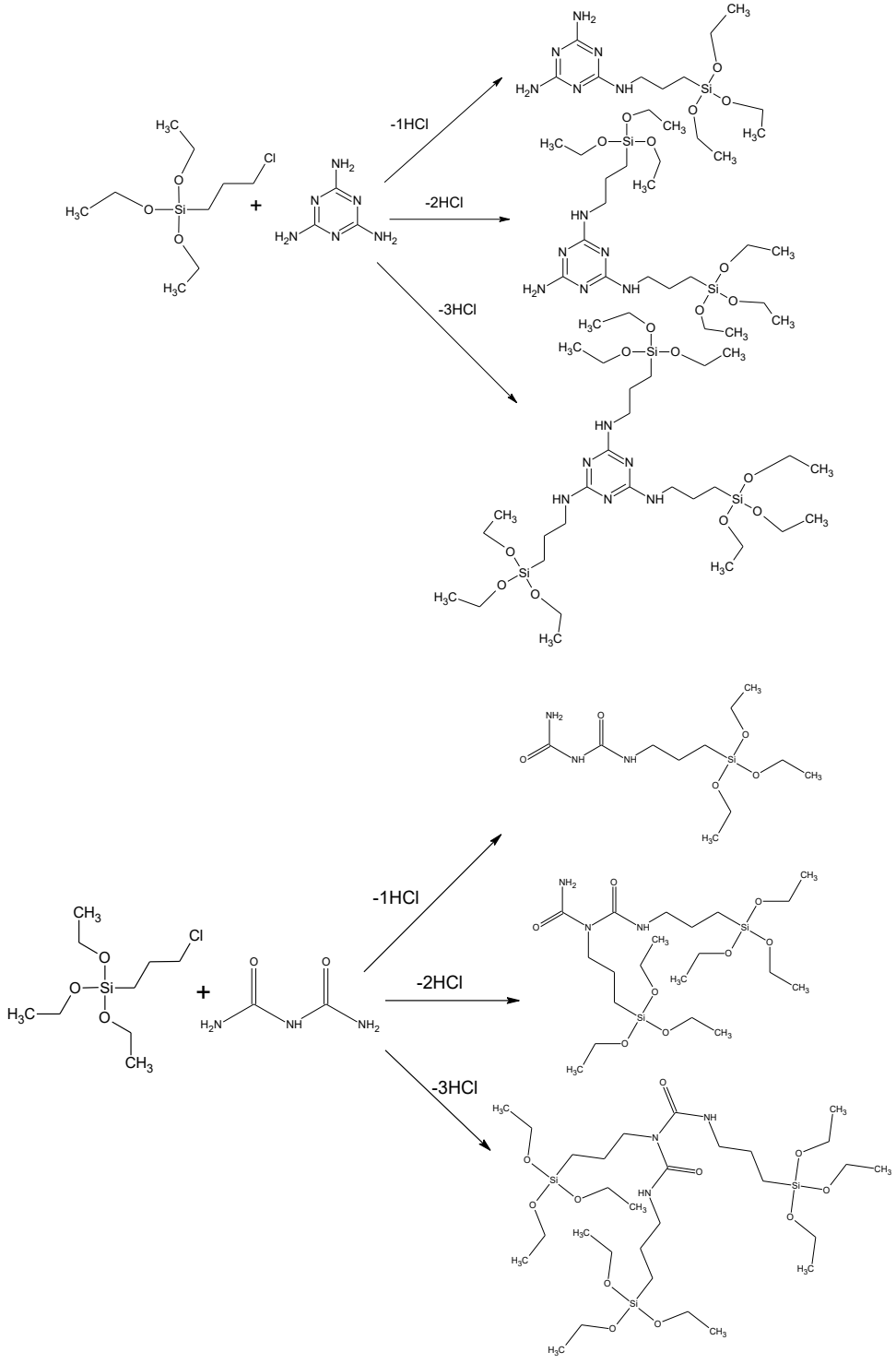

Second step: Condensation with clay silanol groups, hydrolysis and protonation-cation exchange after addition to clay suspension.

B. Aqueous route

First step: Hydrolysis of the alkoxide promoted by water and HCl, and by silanol clay groups.

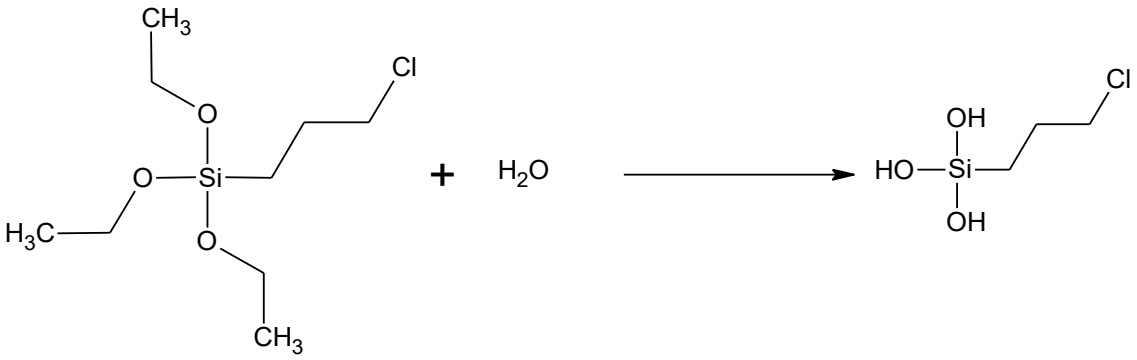

Second step: Condensation of the hydrolyzed alkoxide with the amine molecules.

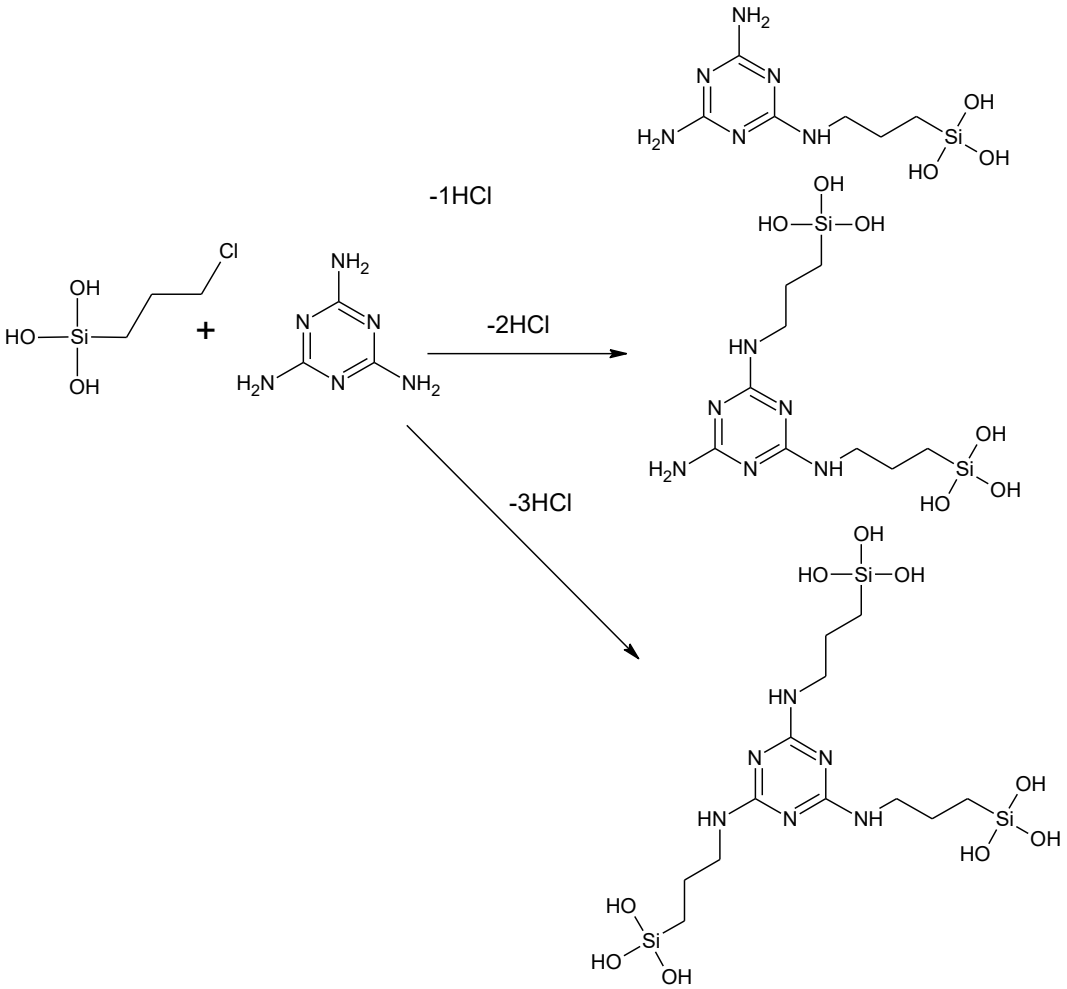

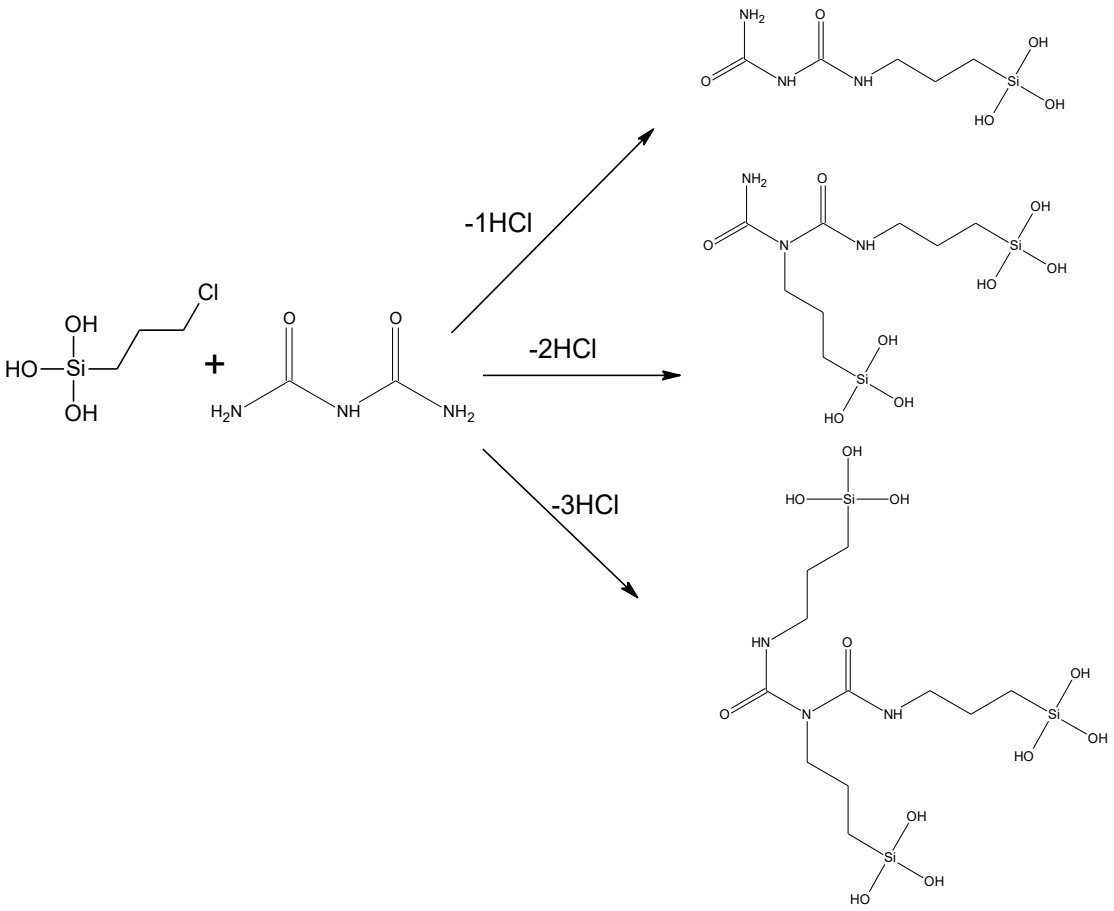

Third step: Condensation with clay silanol groups, and protonation-cation exchange.

Article II

New strategies for synthesis and immobilization of methalophtalocyanines onto kaolinite: Preparation, characterization and chemical stability evaluation.

Dyes and Pigments 134 (2016) 41–50

Contents lists available at ScienceDirect

Dyes and Pigments

journal homepage: www.elsevier.com/locate/dyepig

New strategies for synthesis and immobilization of methalophtalocyanines onto kaolinite: Preparation, characterization and chemical stability evaluation

Tiago Honorato da Silva [a], Thalita F.M. de Souza [b], Anderson Orzari Ribeiro [b], Paulo Sergio Calefi [c], Katia Jorge Ciuffi [a], Eduardo José Nassar [a], Eduardo Ferreira Molina [a], Peter Hamer [d], Emerson Henrique de Faria [a, *]

[a] Gurpo de Pesquisa em Materiais Lamelares Híbridos -GPMatLam – Universidade de Franca, Av. Dr. Armando Salles Oliveira, Pq. Universitário, 201, CEP 14404-600, Franca, SP, Brazil
[b] Centro de Ciências Naturais e Humanas, Universidade Federal do ABC–UFABC, R. Santa Adélia 166, 09210-170, Santo André, SP, Brazil
[c] Instituto Federal de Educação, Ciência e Tecnologia de São Paulo – IFSP, Campus Sertãozinho, Rua Américo Ambrósio, Jd. Canaã, 269, CEP, 14169-263, Sertãozinho, SP, Brazil
[d] Instituto de Química, UNESP-Universidade Estadual Paulista, 14800-900, Araraquara, SP, Brazil

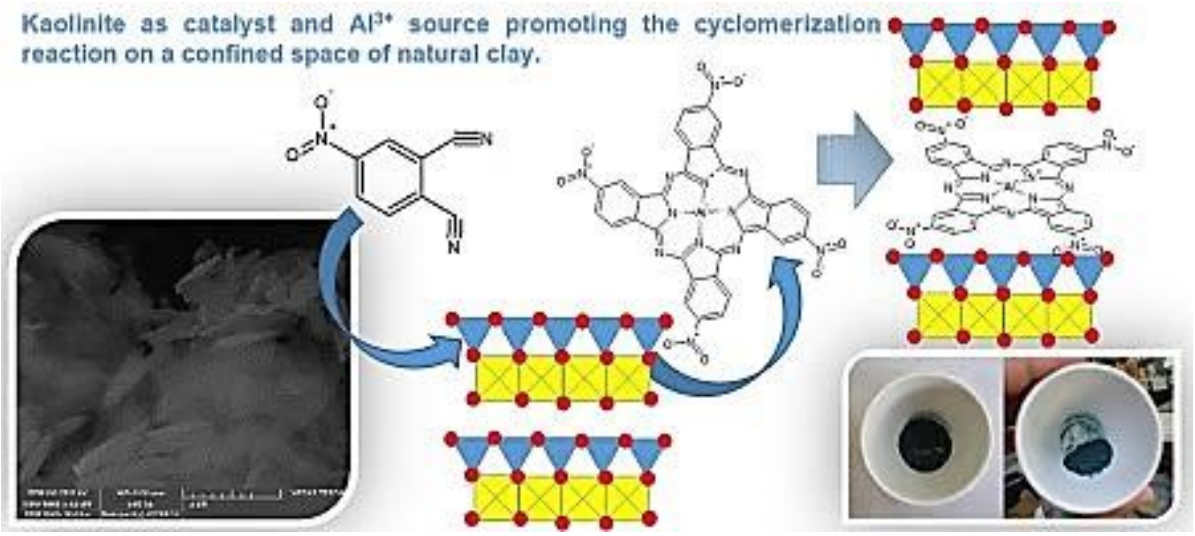

ABSTRACT

This study presents results concerning the one-step synthesis and immobilization of a metallophthalocyanine on kaolinite as support/catalyst. X-ray diffractometry (PXRD), nuclear magnetic resonance (NMR) and infrared (FTIR), UV/Visible (UV/Vis) and X-ray photoelectron (XPS) spectroscopies, thermal analyses and scanning electron microscopy (SEM) aided for the characterization of the materials. The FTIR, XPS and UV/Vis absorption spectra confirmed metallophthalocyanine formation. XRD analysis provided data on the structural disorganization of kaolinite during the synthesis of metallophthalocyanine, corroborated by SEM. NMR revealed that partial dissolution of aluminum from the octahedral kaolinite sheets was possible, which should release Al into the medium and, together with phthalonitrile, promote cyclomerization of the phthalocyanine macrocycle.

Keywords: Phtalocyanines, Immobilization, Hybrid materials, Clays, Nanocomposite

Introduction

Phthalocyanines are symmetric aromatic macrocycles consisting of benzopyrrole rings connected by nitrogen bonds (Kaya et al., 2010; Zawadzka et al., 2014). This arrangement gives rise to a π electron conjugation that provides phthalocyanines with high absorption coefficient in the UV/Visible region, stable electron configuration, and excellent optical properties (Kadish et al., 1999; Kimura et al., 2003).

The first methods developed for the synthesis of metallophthalocyanines involved slow reactions that required high temperatures. In most cases, these conditions culminated in relatively low yields because the reactants underwent degradation and subproducts emerged in the reaction medium (Nyokong and Ahsen, 2012). Over the last decades, new techniques have been developed to increase process yield and make the synthesis of metallophthalocyanines more selective. For example, cyclotetramerization of precursors derived from phthalonitriles, phthalimides, phthalic anhydride, and others has enabled the synthesis of metallophthalocyanines in moderate yields (Lukyanets and Nemykin, 2010; Mack and Kobayashi, 2011).

In aqueous medium, metallophthalocyanines form aggregates that make dispersion difficult. Methalophthalocyanine immobilization on inorganic matrixes minimizes this issue, reaching the atomic molecular scale. Moreover, immobilization increases thermal and chemical stability, improving the properties of metallophthalocyanines (De Oliveira et al., 2008; Ernst and Selle, 1999).

The synthetic routes available to prepare metallophthalocyanines demand significantly long purification steps and excessive amounts of energy. These routes also require the use of a variety of solvents and metallic salts or metals for phthalocyanine cyclomerization, which can contaminate the environment. To meet the principles of green chemistry and sustainability when synthesizing metallophthalocyanines, researchers have searched for new routes that demand less energy and little or no metal or metallic salt as the starting reactant. Other research activities aimed to improve the properties of metallophthalocyanines by immobilizing them on inorganic matrixes (Da Silva et al., 2014).

The use of inorganic matrixes as a source of metallic ions for metallophthalocyanine cyclomerization has become an interesting alternative—matrixes can donate metal ions and

act as support/catalyst for the synthesized metallophthalocyanines, promoting immobilization and enhancing the physicochemical properties of these macromolecules.

Clay minerals have been commonly employed as support to immobilize many substances (Avila et al., 2010; Bhattacharyya and Gupta, 2008; Yang et al., 2012). In this context, kaolinite has stood out for its natural abundance, physicochemical properties, and lamellar structure. Kaolinite constitutes an important industrial raw material for immobilization of metallophthalocyanines (Da Silva et al., 2014), porphyrins (Bizaia et al., 2009; Machado et al., 2012), and other complexes (De Faria et al., 2011), to generate hybrid organic-inorganic materials with interesting properties.

Motivated by the possibility of obtaining metallophthalocyanines by new synthetic routes, in this work we present the preparation and immobilization of metallophthalocyanine on kaolinite in a single step, aiming to save energy, reduce solvent consumption, and comply with the principles of green chemistry and sustainability.

Driven by the ability to synthesize metallophthalocyanines by new synthetic routes, this work shows the study of the aluminum metallophthalocyanines synthesis using kaolinite as aluminium source and support, the immobilization of the synthesized complex in a single step are discussed, aiming energy saving, solvent and while reaching the precepts of green and sustainable chemistry, wherein the aluminium was generated in situ during the synthesis.

The solids could be applied as heterogeneous catalysts, and in photodinamic therapy, photooxidation reactions and photodegradation of pollutants. The great problem in use conventional metallophtalocyanines is the aglomeration of these complexes. However using the complexes imobilized into layered kaolinite we prevent the agregation in the axial position and also increase the activity.

Experimental

The procedures used to purify the clay mineral and to intercalate dimethylsulfoxide (DMSO) into its interlayer space were carried out as described in other literature articles authored by members of our research team (Da Silva et al., 2014; de Faria et al., 2010).

Synthesis and immobilization of metallophthalocyanine on kaolinite

Phthalonitriles, which are precursors of phthalocyanines, bear groups that can interact with groups in the kaolinite structure. This allows immobilization of the precursor on the matrix, followed by metallophthalocyanine formation. One-step synthesis and immobilization of metallophthalocyanines on kaolinite required the use of kaolinite intercalated with DMSO (KaDMSO) and 4-nitrophthalonitrile ($PCNO_2$) at a 3:1 KaDMSO/$PCNO_2$ (m/m) ratio. This mixture was kept at 150 ºC for 48 h. After washing with acetone and separation by centrifugation, the resulting material (designated $KaPCNO_2$) was characterized. Data were compared with the results obtained for aluminum (III) tetranitrometallophthalocyanine (Al(III)TNMPC) obtained by conventional route using solvent and conventional aluminium source from metallic salt according Shaposhnikov (Shaposhnikov et al., 2005), that consisting in react one organic ligand that containing nitro groups (4-nitrophthalonitrile) in contact with metallic specie at temperature near to 210-220 ºC. Fig. III.1 shows a schematic representation of the new synthetic route used to prepare and immobilize metallophthalocyanine on kaolinite.

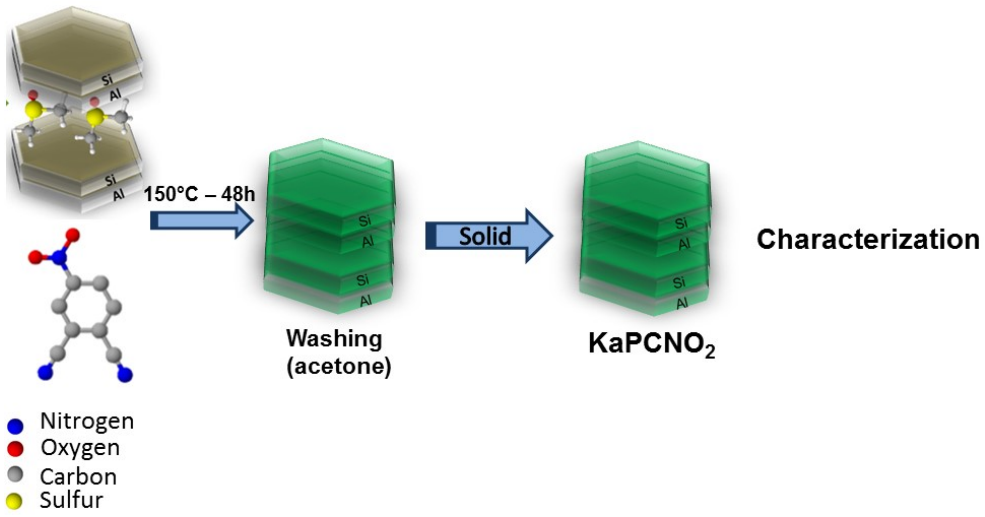

Figure III.1: Schematic representation of the new synthetic route used to prepare and immobilize metallophthalocyanine on kaolinite.

Characterization techniques

The powder X-ray diffractograms (PXRD) of the solids were recorded on a Miniflex II–RIGAKU diffractometer operating at 30 kV and 15 mA (1200 W), using filtered Cu Kα radiation (λ =1.54 Å). The angle 2θ varied from 2 to 65°. All the analyses were undertaken at a scan rate of 2° (2θ) per minute.

Thermal analyses were performed on a TA Instruments–SDT Q600–Simultaneous DTA-TGA analyzer. The samples were heated from 25 to 900 ºC at a heating rate of 20 ºC per minute, in oxidizing (air) atmosphere, at a flow rate of 100 mL/min.

Infrared (FTIR) absorption spectra were acquired on a Perkin Elmer FT-IR Frontier Spectrometer by using a diffuse reflectance accessory. Detailing, 1 mg of each solid were mixed with 100 mg of KBr and finely pulverized until the complete dilution of each solid in KBr. Solids rich in organic ligands (e.g. aluminium metallophthalocyanine were diluted 0.1 mg with 100 mg of KBr. The powder obtained in a typical holder and finally the samples inserted in the FTIR equipment and analyzed The number of scans acquisitions were 32 per spectrum the resolution of 1 cm^{-1} was employed.

For the ultraviolet/visible (UV/Vis) absorption spectra, the samples were placed in cells with 10-mm optical path length. The spectra of liquid and solid samples were recorded on a DiodeArray UV-Vis spectrophotometer HP mod. 8453 and on a OceanOptics Fluorimeter, respectively.

The X-ray photoelectron spectroscopy (XPS) was carried out at a pressure of less than 10^{-7} Pa using a commercial spectrometer (UNI-SPECS UHV). The Mg Kα line was used (hν = 1253.6 eV) and the analyzer pass energy was set to 10 eV. The inelastic background of the Al 2p, Si 2p, N 1s, O 1s and C 1s electron core-level spectra was subtracted using Shirley's method. The binding energy scale of the spectra was corrected using the C 1s hydrocarbon component of the fixed value of 285.0 eV. The spectra were fitted without placing constraints using multiple Voigt profiles.

Nuclear magnetic resonance spectra were registered on a Bruker apparatus model AVANCE III, 9.4 Tesla (400 MHz for hydrogen frequency), equipped with a 4-mm CP/MAS probe for solid samples and a 10-mm BBO probe for liquid samples.

Scanning electron microscopy images were obtained on a TESCAN VEJA 3 SBH apparatus equipped with 30-kV W filament, (3-nm resolution), and SE and BSE detectors.

The textural analyses were accomplished from the corresponding nitrogen adsorption/desorption isotherms at -196°C, obtained in a static volumetric apparatus

(Micromeritics Model ASAP 2020 adsorption analyzer). The samples (0.2 g) were degassed at 150°C for 24 h. The specific surface area (S_{BET}) was obtained by the BET method, and the total pore volume was calculated from the amount of nitrogen adsorbed at a relative pressure of 0.95.

Results and discussion

Characterization of Ka and KaDMSO provided results that agreed with literature data and confirmed the lamellar nature of kaolinite and DMSO intercalation into the clay (Da Silva et al., 2014; de Faria et al., 2010).

UV/Vis absorption spectroscopy

Fig. III.2 shows the UV/Vis spectra of $KaPCNO_2$ and Al(III)TNMPC. These spectra confirmed formation of the metallophthalocyanine.

Both spectra displayed the typical bands of metallophthalocyanines: the Soret band between 300 and 350 nm and the Q band between 600 and 700 nm (Kadish et al., 1999; Kimura et al., 2003). More specifically, these bands were located at 338 and 695 nm in the spectrum of Al(III)TNMPC, respectively, and at 341 and 620 nm in the spectrum of $KaPCNO_2$, respectively. Comparison of the two spectra and the band shifts evidenced formation of the metallophthalocyanine and its immobilization on the functionalized kaolinite.

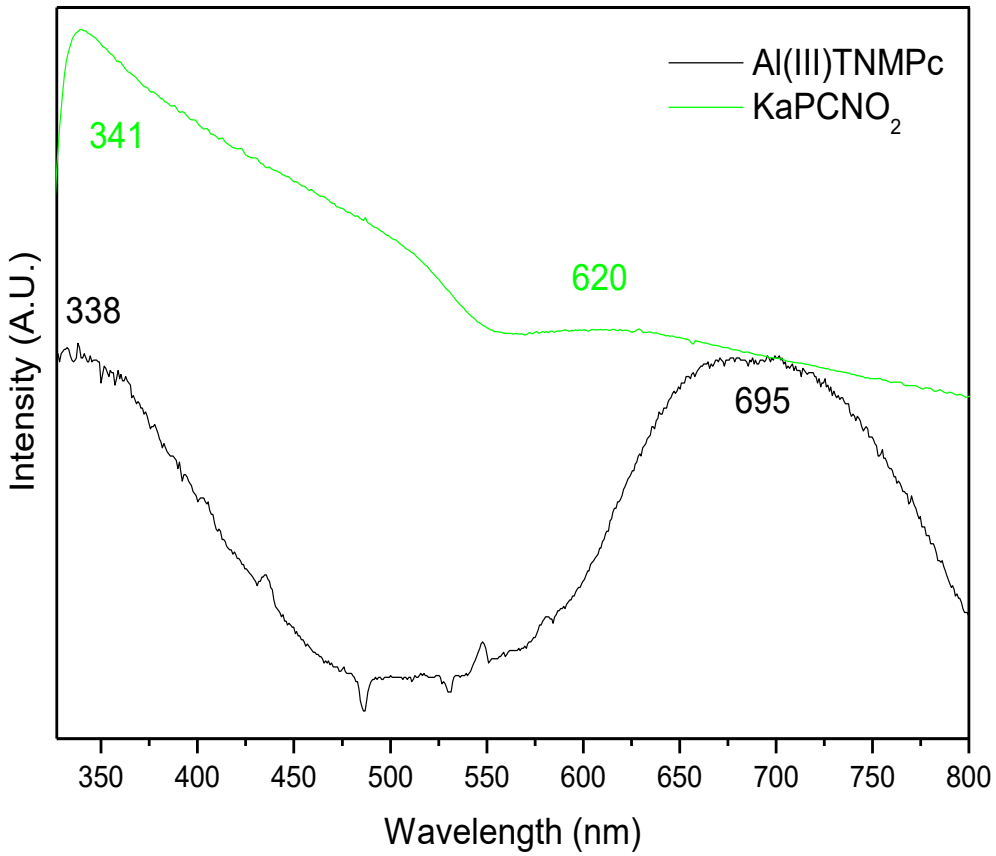

Figure III.2: UV/Vis spectra of Al(III)TNMPC and $KaPCNO_2$.

FTIR spectroscopy

Fig. III.3 and Table III.1 display the FTIR spectra and the major band assignments for Al(III)TNMPC, Ka, $KaPCNO_2$, and $PCNO_2$, respectively.

The FTIR spectra also attested to metallophthalocyanine formation. Bands due to C=N group vibration emerged at 1616 and 1611 cm^{-1} for $KaPCNO_2$ and Al(III)TNMPC, respectively, while the spectrum of the precursor $PCNO_2$ did not contain this band. The vibrations related to the NO_2 group appeared at 1337, 1405, 1520, and 3094 cm^{-1} in the spectrum of Al(III)TNMPC, and at 1344, 1421, 1527, and 3097 cm^{-1} in the spectrum of $KaPCNO_2$. As for $PCNO_2$, the bands due to N=O group vibration arose at 1356, 1411, and 1538 and between 3085 and 3116 cm^{-1} (Bahadoran and Dialameh, 2005; Karaoğlan et al., 2011; Shaposhnikov et al., 2005; Zhou et al., 2009). The changes observed and displacements in the FTIR spectra of the solids compared to kaolinite confirm the interaction of NO_2 groups from Al(III)TNMPC synthesized in situ with kaolinite interlayer hydroxyl groups.

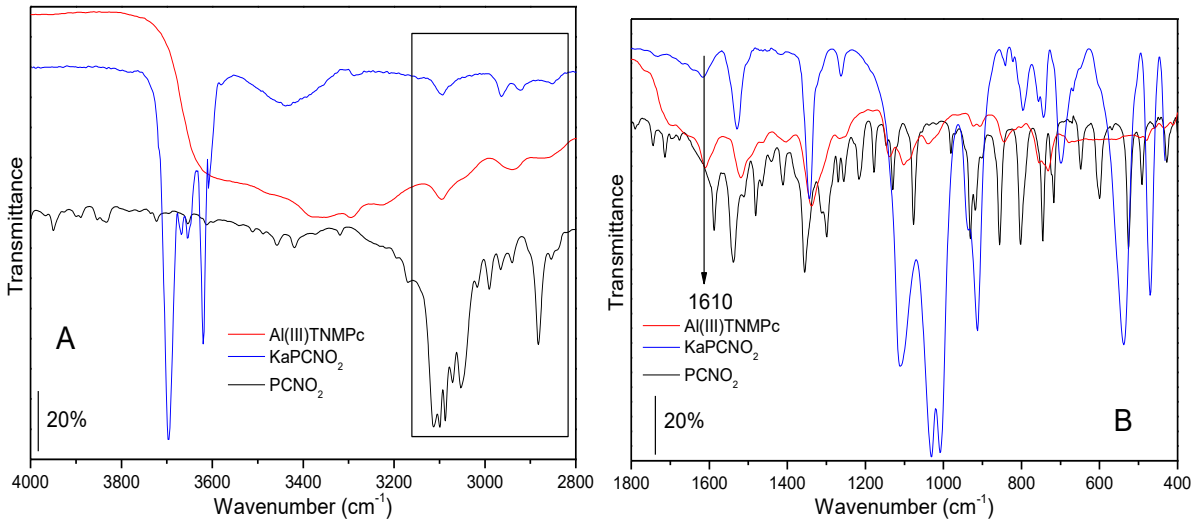

Figure III.3: FTIR absorption spectra of Al(III)TNMPC, Ka, $KaPCNO_2$, and $PCNO_2$ separated by regions: A – from 4000 cm^{-1} to 2800 cm^{-1}; B – from 1800 cm^{-1} to 400cm^{-1}.

Table III.1: Assignment of the main FTIR absorption bands

	Ka (cm^{-1})	Al(III)TNMPC (cm^{-1})	$PCNO_2$ (cm^{-1})	$KaPCNO_2$(cm^{-1})
υOH	3696	-	-	3697
υOH_{inter}	3668, 3654, 3620	-	-	3668, 3654, 3620
υOH_{intra}	-	1337, 1405, 1520, 3094	1356, 1411, 1538, 3085-3116	1344, 1421, 1527, 3097
υN=O	-	1611		1616
υC=N				

XPS analysis

Additional evidence for the formation of aluminum(III) phthalocyanine was obtained by the analysis of XPS N 1s and Al 2p core-level spectra. Fig. III.4a displays the N 1s spectra obtained for the $PCNO_2$ precursor and the $KaPCNO_2$ product. For $PCNO_2$ the component related to nitric oxide, located at 405.5 eV, is separated from the nitrile group (399.2 eV) by about 6.3 eV (Naumkin et al., 2012). The formation of pyrrole-like bonds (C=N-C) induces a shift of the low binding energy component to 398.7 eV (Naumkin et al., 2012). Another indication for the extraction of Al(III) from kaolinite under formation of aluminum(III) phthalocyanine comes from the Al 2p spectra, when comparing kaolinite with $KaPCNO_2$. The spectrum of Ka can be fitted with a single component at 75.3 eV, related to Al of the octahedral sheets bonded to Si occupying the tetrahedral layer (Naumkin et al., 2012). The low energy component (74.2 eV), detected in the spectrum of $KaPCNO_2$, is indicative for Al(III) species in metallophtalocyanine. Taking in account the low sampling depth of XPS of about 5 nm, the noisy Al 2p spectrum of $KaPCNO_2$ results from attenuation effect of kaolinite caused by the wrapping effect of phtalocyanine macromolecules. Furthermore, the quantitative analysis confirmed the nominal composition of TNMPC (61.5 at.% C, 23.1 at.% N, 15.4 at.% O), within an error of ±10%. No signal of sulfur was detected in the spectra, indicating the absence of residual DMSO.

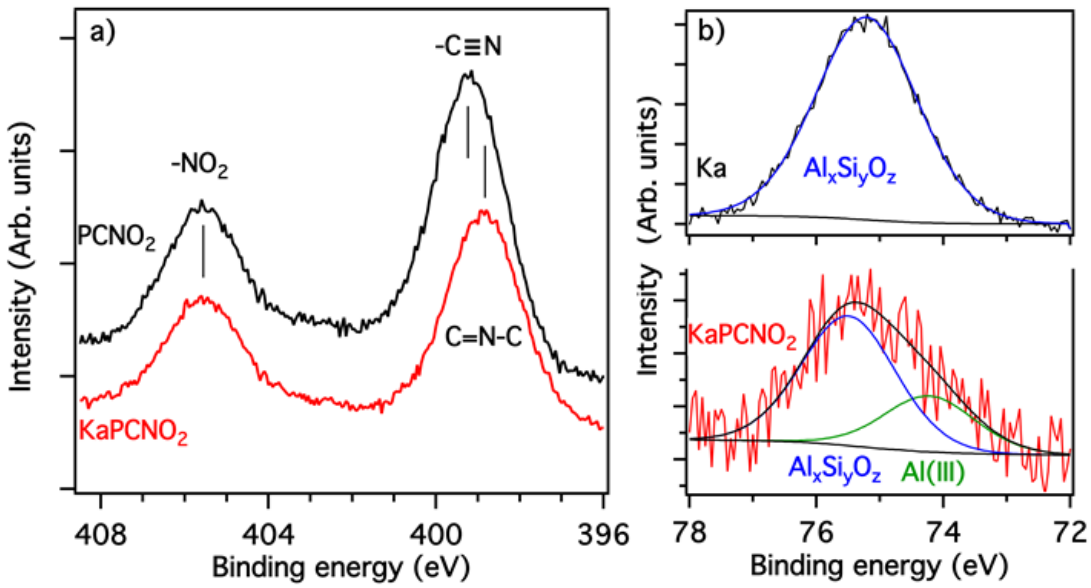

Figure III.4: XPS a) N 1s spectra of $PCNO_2$ and $KaPCNO_2$, b) fitted Al 2p spectra of Ka and $KaPCNO_2$

PXRD analysis

Fig. III.5 depicts the diffractograms recorded for Ka and $KaPCNO_2$. The XRD patterns evidenced the structural modifications that the metallophthalocyanine synthesis promoted in kaolinite.

The diffractograms of KaDMSO and $KaPCNO_2$ were different. Structural modifications experienced by kaolinite during metallophthalocyanine synthesis were evident in the diffractogram of $KaPCNO_2$. Crystalline order decreased during the synthesis—the peaks due to reflections d_{020} and d_{002} broadened, and the peak relative to reflection d_{111} disappeared. Therefore, metallophthalocyanine synthesis made kaolinite more disorganized due to clay exfoliation/delamination and/or partial dissolution (Araújo et al., 2014; Da Silva et al., 2014; Nakagaki et al., 2006; Valášková et al., 2007). The low-intensity peak at $2\theta = 6.12°$, corresponding to a basal spacing of 14.42 Å, was compatible with metallophthalocyanine intercalated into kaolinite interlayer space, obviously this space is not compatible with perpendicular orientation of Al(III)TNMPC, probably this large complex presents parallel orientation in relation to interlayer space of clay. The same effect was previously observed in the previous work using metalloporphryins into grafted clay (Bizaia et al., 2009). Another point that could be emphasized is that treatment removes completely the DMSO molecules from interlayer space of kaolinite and results in the small effect at 14.42 Å assigned to 4-nitrophthalonitrile intercalated and also the parallel orientated Al(III)TNMPC into kaolinite interlayer spaces.

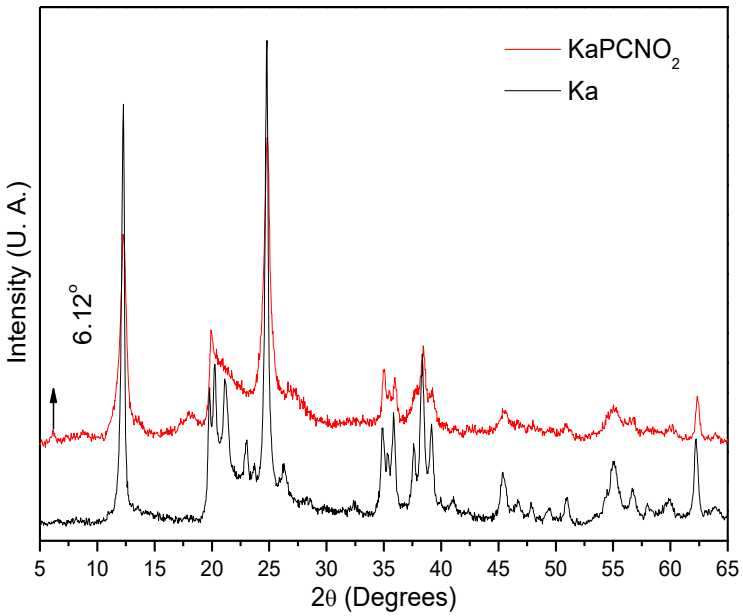

Figure III.5: Diffractograms of Ka and $KaPCNO_2$.

Thermal analyses

Fig. III.6 presents the TG/DTG curves obtained for Ka, $KaPCNO_2$ and Al(III)TNMPC. Comparison of the thermal analyses of Ka and $KaPCNO_2$ revealed that have similar profiles, with small differences due to the presence of the metallophthalocyanine (Al(III)TNMPC).

The TG/DTG curves of Al(III)TNMPC showed a mass loss below 100 ºC, due to moisture water, as well as mass losses relative to metallophthalocyanine degradation at maximum temperatures of 474 and 509 ºC. Comparison of the TG/DTG profiles of $KaPCNO_2$ and Al(III)TNMPC showed that the thermal events occurred at similar temperatures. Because the metallophthalocyanine degradation temperatures were close to the temperature at which kaolinite dehydroxylation took place, the mass losses at 464, 514, and 555 ºC could result from both metallophthalocyanine degradation and the dehydroxylation process. However, analysis of the TG/DTG curves of $KaPCNO_2$ showed that this material contained organic matter—the percent mass loss of purified Ka and $KaPCNO_2$ was 15 and 24%, respectively, and the higher mass loss in the case of $KaPCNO_2$ could be due to the presence of the metallophthalocyanine synthesized in situ on kaolinite.

Based on this mass loss and as demonstrated in the literature (Silva et al., 2012), it was possible to calculate the amount of synthesized metallophthalocyanine—1.05 mol of metallophthalocyanine per mol of kaolinite.

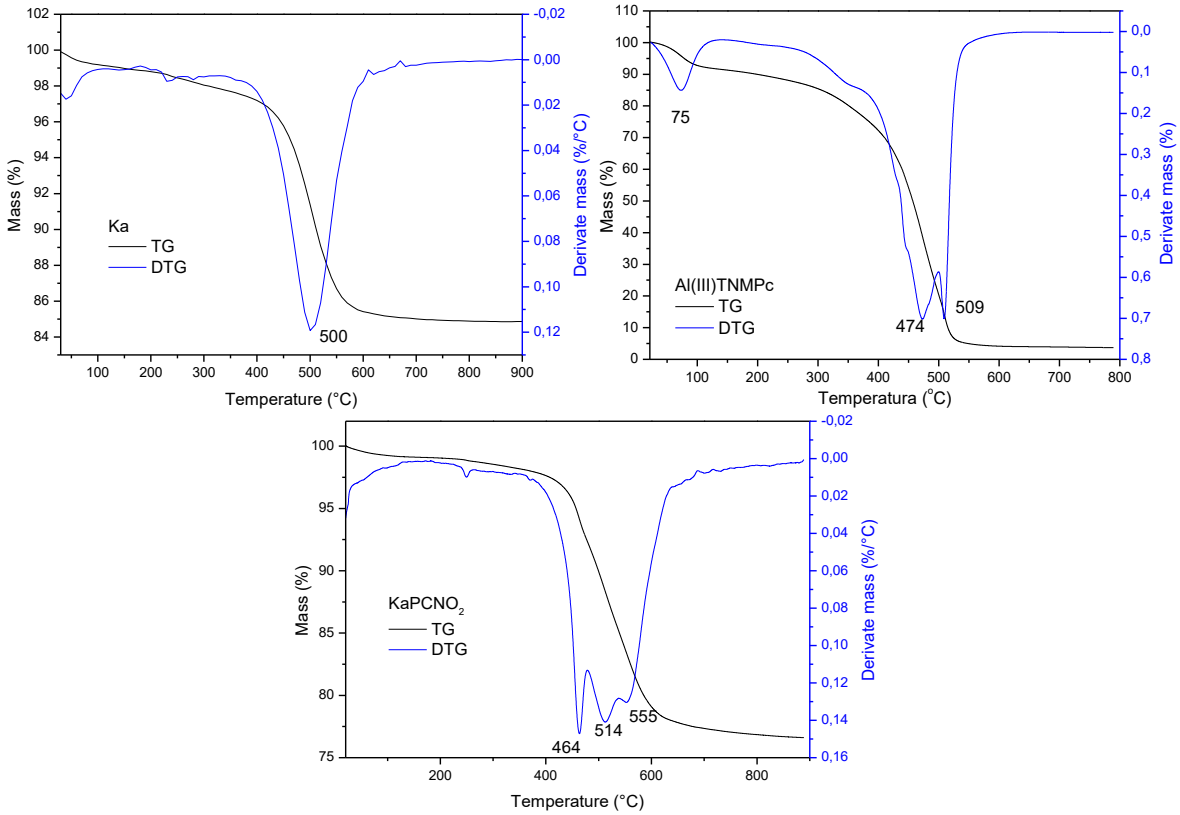

Figure III.6: TG/DTG curves obtained for Ka, Al(III)TNMPC, and $KaPCNO_2$.

The DTA curves (Fig. III.7) obtained for Ka showed an endothermic mass loss at 509 °C, due to kaolinite dehydroxylation. For Al(III)TNMPC, there were two exothermic processes, at 471 and 507 °C, ascribed to aluminum(III) tetranitrometallophthalocyanine. As for $KaPCNO_2$, the kaolinite dehydroxylation temperature decreased (440 °C) as a result of $PCNO_2$ reacting with kaolinite. The temperatures at which exothermic Al(III)TNMPC degradation occurred increased because kaolinite conferred protection to the aluminum complex immobilized on the clay, consequently improving the thermal stability of the metallophthalocyanine.

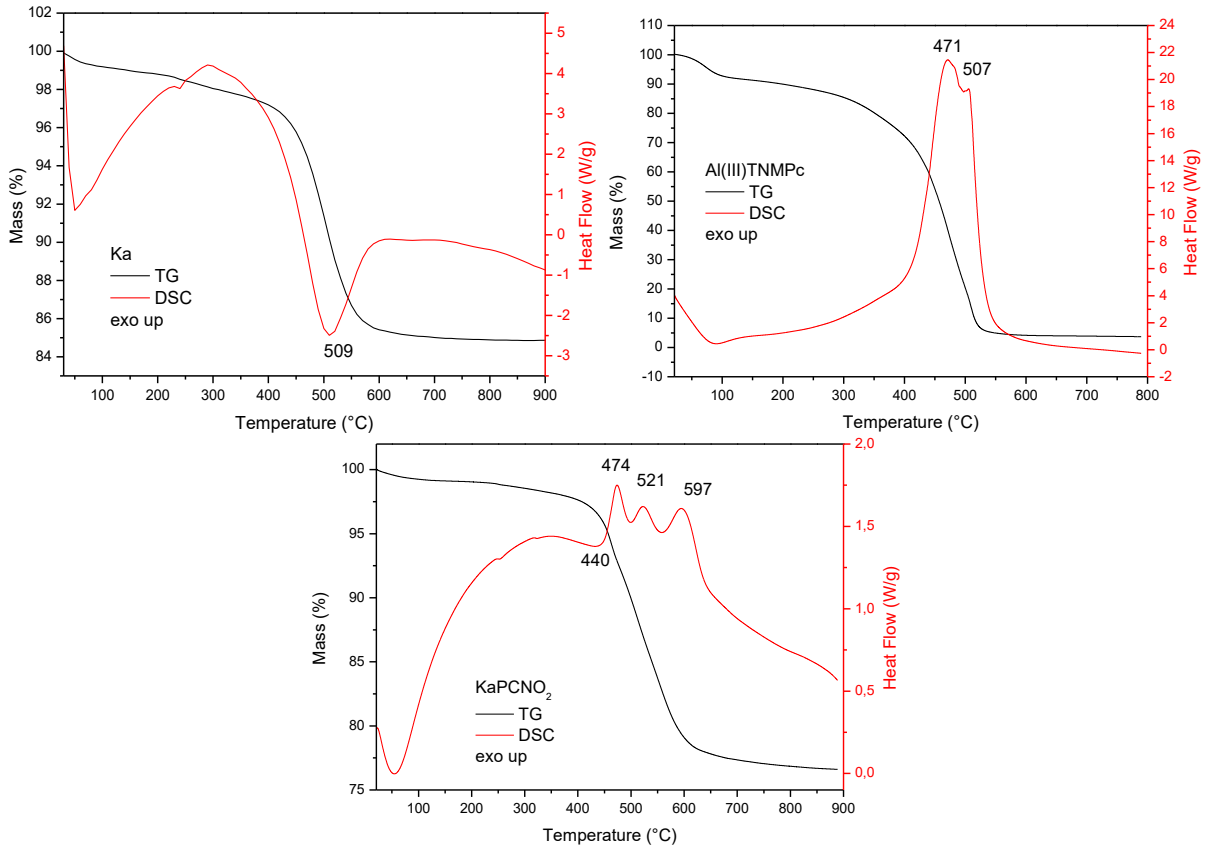

Figure III.7: TG/DTA curves obtained for Ka, Al(III)TNMPC, and $KaPCNO_2$.

^{27}Al NMR analysis

NMR is an important tool to characterize hybrid materials based on kaolinite. This technique evidences changes in the intensities and chemical shifts of octahedral (hexacoordinated) aluminum species, which are coordinated with reaction-prone hydroxyls present in the octahedral sheet (de Faria et al., 2009). Fig. III.8 shows the ^{27}Al NMR spectrum of $KaPCNO_2$.

The peaks with chemical shifts of 1.74 and 8.43 ppm were assigned to hexacoordinated (octahedral) aluminum in the kaolinite octahedral sheet (Fitzgerald et al., 1989; Letaief et al., 2006). Fitzgerald et al. (1989) demonstrated that the relation between octahedral and tetrahedral aluminum (relative intensities in the spectrum) was 400:1 for kaolinite. This was not the case for $KaPCNO_2$—the peaks due to tetrahedral aluminum were practically as intense as the peaks due to octahedral aluminum. Using an average value to calculate the ratio between octahedral and tetrahedral aluminum, the obtained ratio was approximately 1.4:1. These differences between kaolinite and the material synthesized herein may have stemmed from partial dissolution of aluminum present in the octahedral sheet during metallophthalocyanine synthesis, as judged from the chemical shifts at -67.99 and

84.85 ppm, due to tetracoordinated aluminum (Fitzgerald, J. John., 1989; Mantovani et al., 2011). Hence, free aluminum dissolved in the octahedral sheet might exist and participate in the phthalocyanine macrocycle cyclomerization, affording a metallophthalocyanine that bears aluminum as the central ion.

Lyubimtsev et. al. (2015) examinated the reactivity of phthalonitriles derivatives containing diferent terminal groups to promote the phthalocyanine synthesis by conventional routes; for example, the 4-nitrophthalonitrile and 4-aminophtalonitrile, yielding results that demonstrate that the nitro group could influence the reactivity of the composite, the reaction rate is very bigger when use the derivative containing nitro group. Based on this theoretical and experimental result and based on the present s study, we propose that by promoting the reaction of the 4-nitrophthalonitrile with kaolinite, it has the ability to dissolve partially the octahedral sheet of this clay mineral, inducing the leaching of Al^{3+}, consequently promoting the cyclomerization reaction without use conventional presence of metallic salts and solvents.

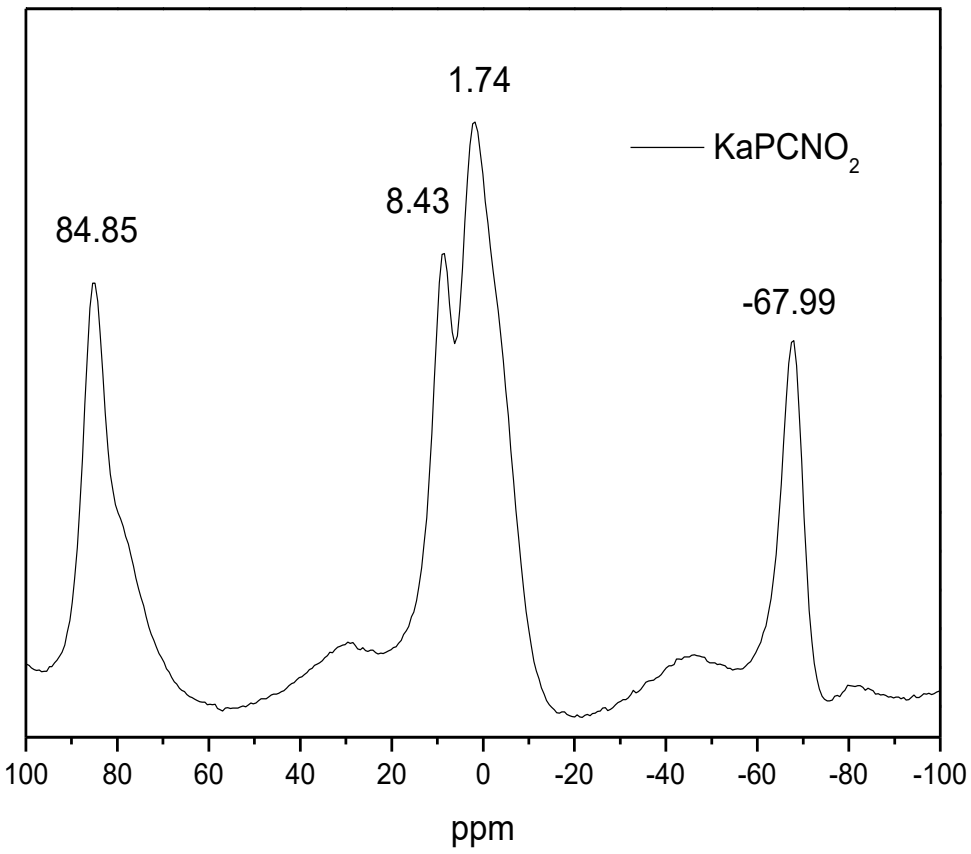

Figure III.8: ^{27}Al NMR spectrum of $KaPCNO_2$.

SEM analysis

SEM provided information about the morphology of the prepared materials. Fig. III.9 presents the SEM images obtained for $KaPCNO_2$ and Ka.

$KaPCNO_2$ was fragmented into poorly aggregated hexagonal sheets, forming a layered material with few pillared layers. Particles were smaller and less ordered as compared with Ka (Fig. III.9A and III.9B). These results agreed with XRD data and indicated that kaolinite was exfoliated/delaminated or even partially dissolved during metallophthalocyanine synthesis.

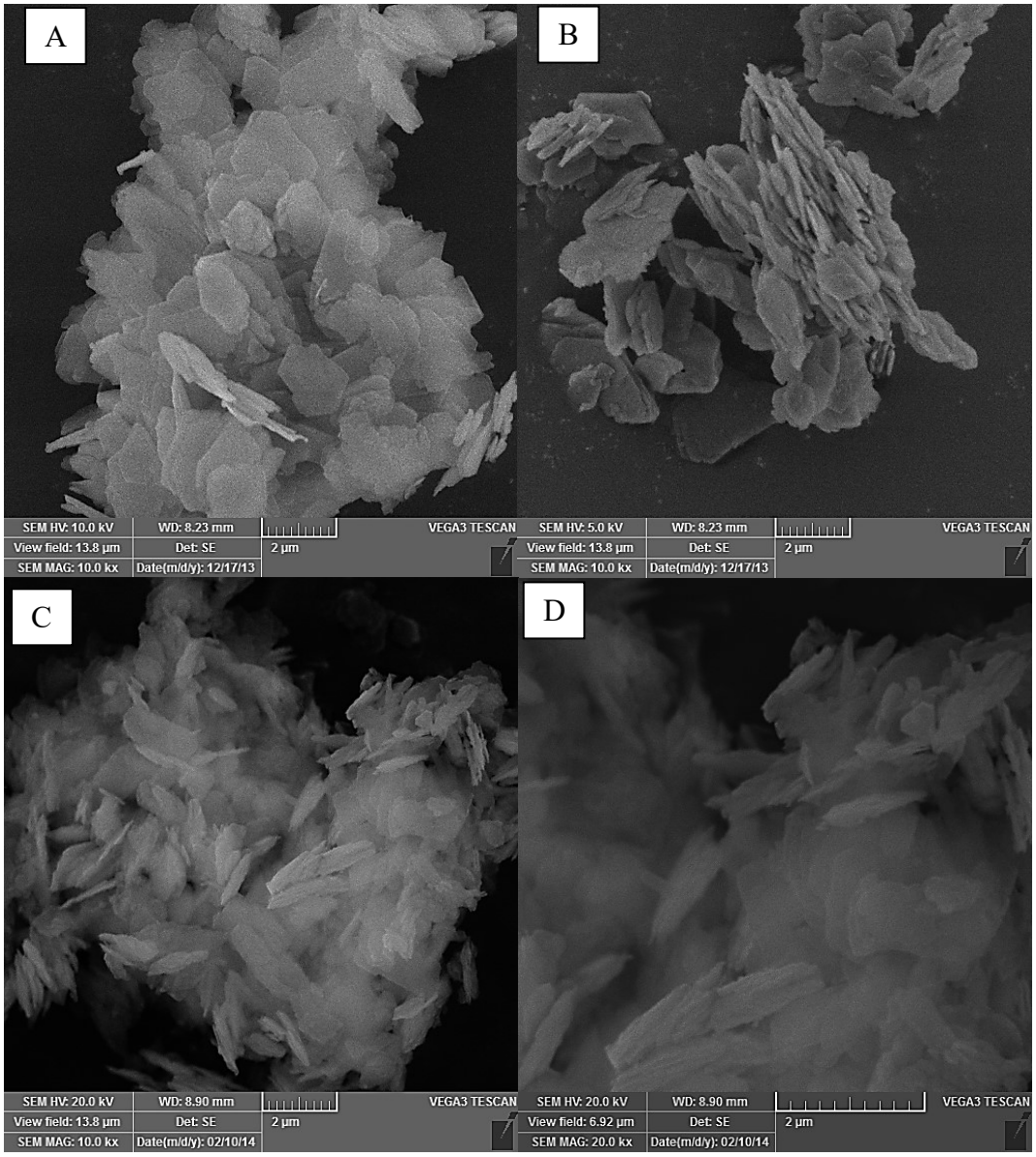

Figure III.9: SEM images of Ka (A and B) and $KaPCNO_2$ at 10kx (C) and 20kx (D) magnification

Mechanism Investigation

The analysis conducted in this study led us to propose a mechanism involving simultaneous metallophthalocyanine synthesis and immobilization on kaolinite. The stages of the proposed process are as follows (Fig. III.10 and III.11):

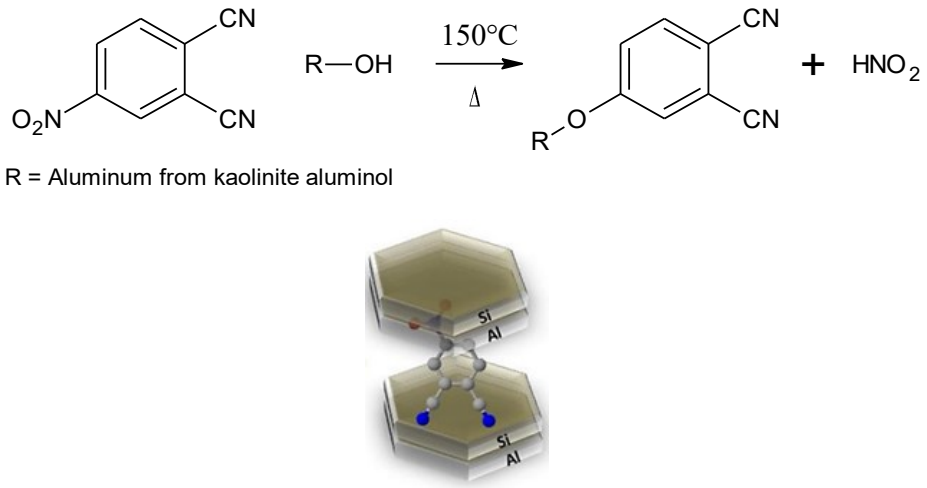

Figure III.10: Schematic representation of the first stage of in situ kaolinite-immobilized metallophthalocyanine synthesis

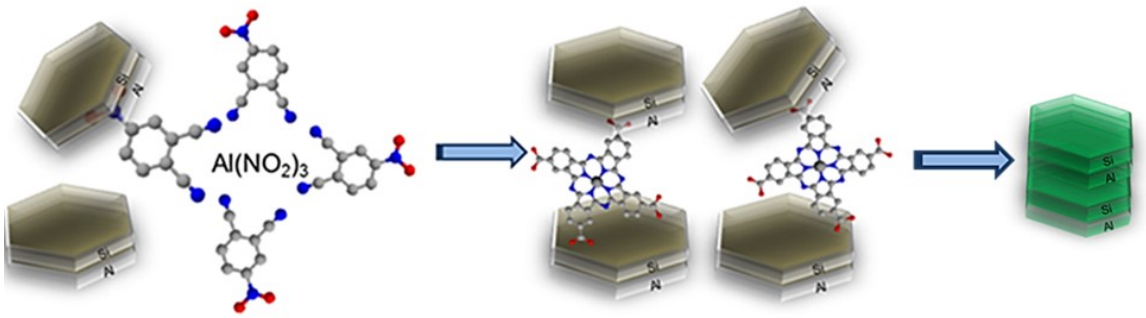

Figure III.11: Schematic representation of the third stage of in situ kaolinite-immobilized metallophthalocyanine synthesis.

1st stage: The nitro group of 4-nitrophthalonitrile reacts with kaolinite, to functionalize part of the kaolinite lamellae with phthalonitrile and to generate nitrous acid as the reaction subproduct.

2nd stage: Nitrous acid reacts with nonfunctionalized aluminol, to dissolve part of the kaolinite octahedral sheets and to generate aluminum nitrite according to the following reaction:

$$Al - OH + HNO_2 \rightarrow Al(NO_2)_3 + H_2O$$

3rd stage: For metallophthalocyanine synthesis to occur, it is necessary to add a metallic salt or a metal to the reaction medium. In the present case, addition of a metallic salt was dismissed because a salt originated in the reaction medium during the metallophthalocyanine synthesis. Indeed, the reaction medium contained kaolinite functionalized with 4-nitrophthalonitrile, nonfunctionalized kaolinite, 4-nitrophthalonitrile (added in excess), and aluminum nitrite (which emerged during the synthesis) (Fig. III.11). This mixture was kept at 150 °C for 48 h, to afford a green solid whose color was typical of metallophthalocyanine (see Fig. III.12)

Figure III.12: Kaolinite functionalized with aluminum(III) tetranitrometallophtalocyanine.

^{27}Al NMR and TG data attested to the synthesis of metallophthalocyanine catalyzed by kaolinite and reinforced our proposal that Al(III)TNMPC synthesis and immobilization occurred simultaneously. Indeed, the metallocomplex decomposed at higher temperature than the phthalonitrile precursor. The amount of metallophthalocyanine was calculated from the residue obtained from the thermogravimetric curve (Silva et al., 2012). The minimum formula based on the molar ratio Ka/Al(III)TNMPC was Ka-$(Al(III)TNMPC)_{1.05.}$ The ratio between the intensities of the typical octahedral and tetrahedral aluminum chemical shifts was 1.4:1, which was completely different from the ratio observed for pure kaolinite (400:1). These results supported the hypothesis that Al(III) was partially removed from the gibbsite octahedral sheet, to induce formation of the aluminum(III) phthalocyanine. In other words, kaolinite served as support, catalyst, and source of Al(III) ions.

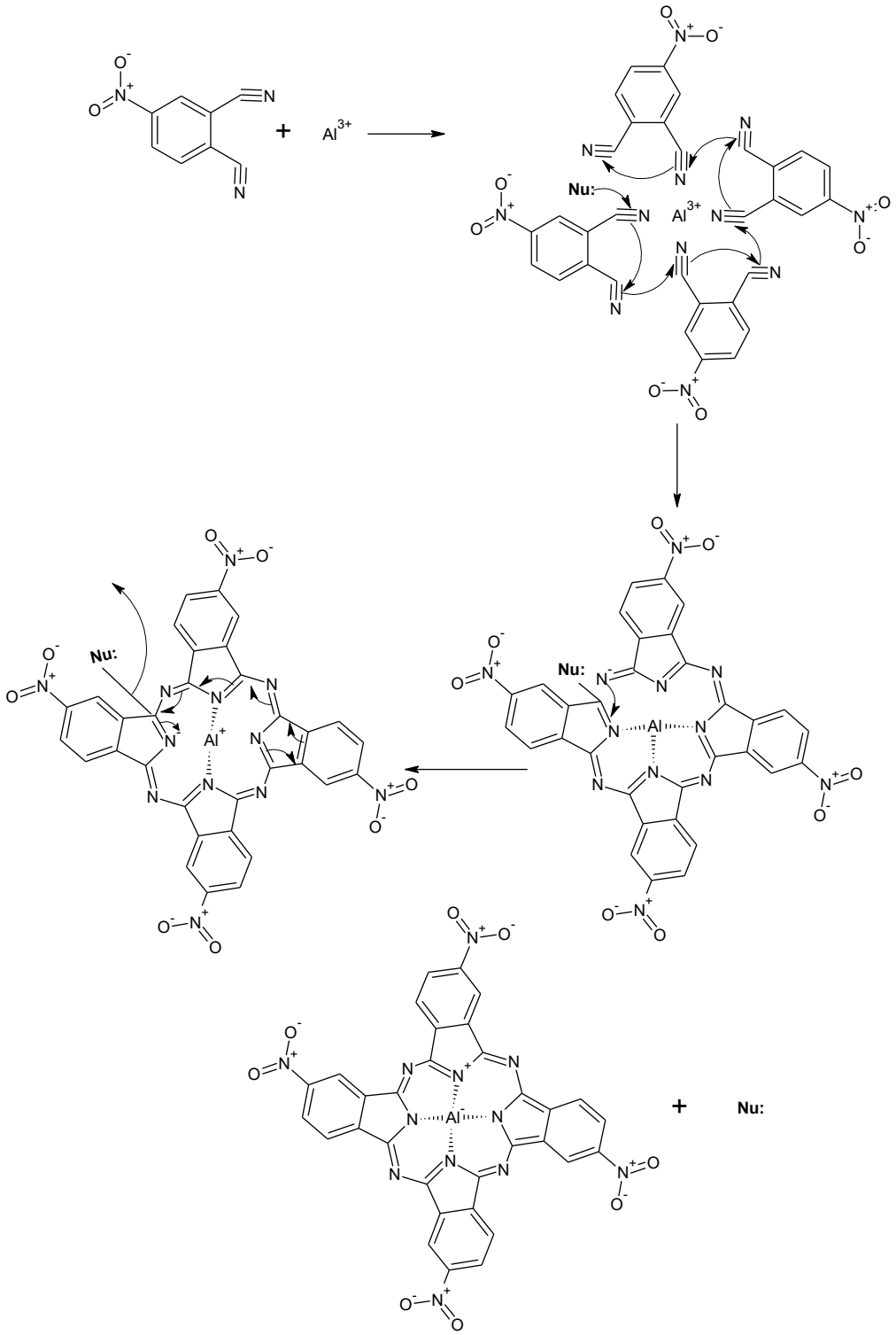

Figure III.13: Cyclization reaction mechanism for aluminum(III) metallophthalocyanine formation

The nitronium group is an intermediate state. The nitronium were generated from nitrosil groups from 4-nitrphthallonitrile precursor, when this specie attack the $Al(OH)_3$ from gibbsite kaolinite layer. The possible mechanism, certainly involves the dissolution of

aluminium from kaolinite promoted by acidic attack of acid specie generated in situ, as represented in the scheme in Fig. III.13. The nitronium group (nucleophile) used at the start of the cyclization oxidizes nitrite to nitrate by donating two electrons to the macrocyclic complex. The resulting nitronium ions undergo aromatic electrophilic substitution at position 4 or combine with another nitronium ion, to produce a nitrogen molecule ($N_{2(g)}$). N_2 then participates in a substitution reaction, to form a nitrate monophthalocyanine and hydrogen gas.

Obviously the nitronium are not stable and could giving a rise to nitrite ion. This oxidation process could be probably induced by kaolinite wich contain many oxides such silicon oxide layer and aluminium oxide hydroxide layer and some impurities such as Ti, Fe and Mn oxides. It´s importante remark that nitronium is one intermediate state and obviously at final we have presente only the nitrite ions.

Textural analysis

Specific surface area calculated by BET (Table III.2) shown that intercalation with DMSO and $PCNO_2$ grafting procedures to generate metallophthalocyanines induces a decreasing of the specific surface area, on other hand the pore size of the grafted compound Ka-$PCNO_2$ is bigger than for purified kaolinite (179 Å) with a value of 730 Å. In this sense the presence of large organic molecules such as Al(III)TNPMPC promotes the exposure of the interlayer hydroxyl groups inducing in all cases the decrease of specific surface area and increase of pore size, probably because the pores that were originated by intercalated DMSO molecules (anchored only by hydrogen bonds) into kaolinite structures were completely removed before $PCNO_2$ grafting. The changes in surface area values may be related to the stacking/restacking of kaolinite and Al(III)TNPMc complexes immobilization in situ and also to delamination of Ka-PCNO platelets that induces the textural changes of kaolinite.

Table III.2: Specific surface area (SBET) and pore size (VpTotal) using the BET method of kaolinite, kaolinite intercalated with DMSO and compound grafted with PCNO2

Sample	$S_{BET}(m^2/g)$	Pore size (Å)
Ka	15,6	179
Ka-DMSO	4,2	806
Ka- $PCNO_2$	0,3	729

Conclusion

FTIR, XPS and UV/Vis spectroscopy confirmed the one-step synthesis and immobilization of a metallophthalocyanine on kaolinite, with the clay serving as support/catalyst. XRD and SEM analyses showed that the kaolinite structure became disorganized during the synthesis. This disorganization was later confirmed by NMR—octahedral Al(III) ions dissolved in the reaction medium and promoted metallophthalocyanine cyclomerization in the presence of pthalonitrile. This process constitutes a new route for metallophthalocyanine synthesis that meets the principles of green chemistry and sustainability.

References for Article III

Araújo, F.R., Baptista, J.G., Marçal, L., Ciuffi, K.J., Nassar, E.J., Calefi, P.S., Vicente, M.A., Trujillano, R., Rives, V., Gil, A., Korili, S., De Faria, E.H., 2014. Versatile heterogeneous dipicolinate complexes grafted into kaolinite: Catalytic oxidation of hydrocarbons and degradation of dyes. Catal. Today 227, 105–115. https://doi.org/10.1016/j.cattod.2013.09.031

Avila, L.R., de Faria, E.H., Ciuffi, K.J., Nassar, E.J., Calefi, P.S., Vicente, M.A., Trujillano, R., 2010. New synthesis strategies for effective functionalization of kaolinite and saponite with silylating agents. J. Colloid Interface Sci. 341, 186–193. https://doi.org/10.1016/j.jcis.2009.08.041

Bahadoran, F., Dialameh, S., 2005. Microwave assisted synthesis of substituted metallo-phthalocyanines and their catalytic activity in epoxidation reaction 163–169.

Bhattacharyya, K.G., Gupta, S. Sen, 2008. Adsorption of a few heavy metals on natural and modified kaolinite and montmorillonite: A review. Adv. Colloid Interface Sci. 140, 114–131. https://doi.org/10.1016/j.cis.2007.12.008

Bizaia, N., de Faria, E.H., Ricci, G.P., Calefi, P.S., Nassar, E.J., Castro, K.A.D.F., Nakagaki, S., Ciuffi, K.J., Trujillano, R., Vicente, M.A., Gil, A., Korili, S.A., 2009. Porphyrin−Kaolinite as Efficient Catalyst for Oxidation Reactions. ACS Appl. Mater. Interfaces 1, 2667–2678. https://doi.org/10.1021/am900556b

Da Silva, T.H., De Souza, T.F.M., Ribeiro, A.O., Ciuffi, K.J., Nassar, E.J., Silva, M.L.A., Henrique De Faria, E., Calefi, P.S., 2014. Immobilization of metallophthalocyanines on hybrid materials and in-situ synthesis of pseudo-tubular structures from an aminofunctionalized kaolinite. Dyes Pigments 100, 17–23. https://doi.org/10.1016/j.dyepig.2013.07.019

de Faria, E.H., Ciuffi, K.J., Nassar, E.J., Vicente, M.A., Trujillano, R., Calefi, P.S., 2010. Novel reactive amino-compound: Tris(hydroxymethyl)aminomethane covalently grafted on kaolinite. Appl. Clay Sci. 48, 516–521. https://doi.org/10.1016/j.clay.2010.02.017

de Faria, E.H., Lima, O.J., Ciuffi, K.J., Nassar, E.J., Vicente, M.A., Trujillano, R., Calefi, P.S., 2009.

Hybrid materials prepared by interlayer functionalization of kaolinite with pyridine-carboxylic acids. J. Colloid Interface Sci. 335, 210–215. https://doi.org/10.1016/j.jcis.2009.03.067

De Faria, E.H., Nassar, E.J., Ciuffi, K.J., Vicente, M.A., Trujillano, R., Rives, V., Calefi, P.S., 2011. New highly luminescent hybrid materials: Terbium pyridine-picolinate covalently grafted on kaolinite. ACS Appl. Mater. Interfaces 3, 1311–1318.

De Oliveira, E., Neri, C.R., Ribeiro, A.O., Garcia, V.S., Costa, L.L., Moura, A.O., Prado, A.G.S., Serra, O.A., Iamamoto, Y., 2008. Hexagonal mesoporous silica modified with copper phthalocyanine as a photocatalyst for pesticide 2,4-dichlorophenoxiacetic acid degradation. J. Colloid Interface Sci. 323, 98–104.

Ernst, S., Selle, M., 1999. Immobilization and catalytic properties of perfluorinated ruthenium phthalocyanine complexes in MCM-41-type molecular sieves. Microporous Mesoporous Mater. 27, 355–363.

Fitzgerald, J.J., Hamza, I.A., Bronnimann, C.E., Dec, S.F. 1989. Solid-state ^{27}Al and ^{29}Si NMR studies of the reactivity of the aluminum-containing clay mineral kaolinite. Solid State Ionics 32/33, 171-378–388. https://doi.org/10.1007/BF02909762

Karaoğlan, G.K., Gümrükçü, G., Koca, A., Gül, A., Avcata, U., 2011. Synthesis and characterization of novel soluble phthalocyanines with fused conjugated unsaturated groups. Dyes Pigments 90, 11–20. https://doi.org/10.1016/j.dyepig.2010.10.002

Kaya, E.Ç., Karadeniz, H., Kantekin, H., 2010. The synthesis and characterization of metal-free and metallophthalocyanine polymers by microwave irradiation containing diazadithia macrocyclic moieties. Dyes Pigments 85, 177–182. https://doi.org/10.1016/j.dyepig.2009.10.021

Kimura, M., Kuroda, T., Ohta, K., Hanabusa, K., Shirai, H., Kobayashi, N., 2003. Self-organization of hydrogen-bonded optically active phthalocyanine dimers. Langmuir 19, 4825–4830. https://doi.org/10.1021/la0341512

Letaief, S., Elbokl, T.A., Detellier, C., 2006. Reactivity of ionic liquids with kaolinite: Melt intersalation of ethyl pyridinium chloride in an urea-kaolinite pre-intercalate. J. Colloid Interf. Sci. 302, 254–258. https://doi.org/10.1016/j.jcis.2006.06.008

Lukyanets, E.A., Nemykin, V.N., 2010. The key role of peripheral substituents in the chemistry of phthalocyanines and their analogs. J. Porphyr. Phthalocyanines 14, 1–40. https://doi.org/10.1142/S1088424610001799

Lyubimtsev, A. V., Zheglova, N. V., Smirnova, E.N., Syrbu, and S.A., Syrbu, S.A., 2015. Reactivity of phthalocyanine precursors. Russ. Chem. Bull. Int. Ed. 64, 1933–1941. https://doi.org/10.1007/s11172-015-1096-y

Machado, G.S., Groszewicz, P.B., Castro, K.A.D. de F., Wypych, F., Nakagaki, S., 2012. Catalysts for heterogeneous oxidation reaction based on metalloporphyrins immobilized on kaolinite modified with triethanolamine. J. Colloid Interf. Sci. 374, 278–286.

Mack, J., Kobayashi, N., 2011. Low symmetry phthalocyanines and their analogues. Chem. Rev. 111, 281–321. https://doi.org/10.1021/cr9003049

Mantovani, M., Escudero, A., Becerro, A.I., 2011. Influence of OH- concentration on the illitization of kaolinite at high pressure. Appl. Clay Sci. 51, 220–225. https://doi.org/10.1016/j.clay.2010.11.021

Nakagaki, S., Machado, G.S., Halma, M., dos Santos Marangon, A.A., de Freitas Castro, K.A.D., Mattoso, N., Wypych, F., 2006. Immobilization of iron porphyrins in tubular kaolinite obtained by an intercalation/delamination procedure. J. Catal. 242, 110–117.

Naumkin, A. V., Kraut-Vass, A., Gaarenstroom, S.W., Powell, C.J., 2012. NIST X-ray Photoelectron Spectroscopy Database [WWW Document]. https://doi.org/http://dx.doi.org/10.18434/T4T88K

Nyokong, T., Ahsen, V., 2012. Photosensitizers in medicine, environment, and security, Photosensitizers in Medicine, Environment, and Security. https://doi.org/10.1007/978-90-481-3872-2

Shaposhnikov, G.P., Maizlish, V.E., Kulinich, V.P., 2005. Synthesis and properties of extracomplexes of tetrasubstitued phthalocyanines. Russ. J. Gen. Chem. 75, 1830–1839. https://doi.org/10.1007/s11176-005-0519-0

Silva, T.H., Reis, M.J., Faria, E.H. De, Ciuffi, K.J., Nassar, J., Calefi, P.S., Franca, U. De, Armando, A., Oliveira, S., Universitário, P.Q., 2012. Study Of Reliability Of Thermal Analysis Technique In The Quantification Of Organic Material In Physical Mixture Of Kaolinite And Tris (Hydroxymethyl) Aminomethane. Brazilian J. Therm. Anal. 01, 15–22.

Valášková, M., Rieder, M., Matějka, V., Čapková, P., Slíva, A., 2007. Exfoliation/delamination of kaolinite by low-temperature washing of kaolinite-urea intercalates. Appl. Clay Sci. 35, 108–118. https://doi.org/10.1016/j.clay.2006.07.001

Yang, S.q., Yuan, P., He, H.p., Qin, Z.h., Zhou, Q., Zhu, J.x., Liu, D., 2012. Effect of reaction temperature on grafting of γ-aminopropyl triethoxysilane (APTES) onto kaolinite. Appl. Clay Sci. 62–63, 8–14. https://doi.org/10.1016/j.clay.2012.04.006

Zawadzka, A., Płóciennik, P., Strzelecki, J., Korcala, A., Arof, A.K., Sahraoui, B., 2014. Impact of annealing process on stacking orientations and second order nonlinear optical properties of metallophthalocyanine thin films and nanostructures. Dyes Pigments 101, 212–220. https://doi.org/10.1016/j.dyepig.2013.09.044

Zhou, X., Li, J., Wang, X., Jin, K., Ma, W., 2009. Oxidative desulfurization of dibenzothiophene based on molecular oxygen and iron phthalocyanine. Fuel Process. Technol. 90, 317–323. https://doi.org/10.1016/j.fuproc.2008.09.002

CONCLUSÕES GERAIS

Nesta tese foi apresentado o desenvolvimento e estudo de novos materiais inorgânico-orgânicos aplicados a adsorção e processos fotocatalíticos e também novas rotas sintéticas na obtenção de materiais de interesse, como as metaloftalocianinas. Segundo as atividades expostas, as principais conclusões do trabalho foram:

Artigo I: as técnicas de caracterização provaram que o dióxido de titânio e tetracarboxiftalocianina de Co(II) foram imobilizados na caulinita; as reações ocorreram na superfície da caulinita, observando a influência da rota sintética (ácida e básica) nas propriedades texturais dos materiais obtidos; a quantidade de TiO_2 incorporado a caulinita foi maior na rota básica, devido a geração de cargas na superfície da argila, facilitando a imobilização; a rota ácida houve menor depósito de TiO_2 devido a geração de menos carga superficial. Frente aos estudos de fotodegradação, trimetoprim (30%) e prometrina (54%) apresentaram maior dificuldade no processo de degradação, já a cafeína apresentou elevada porcentagem de remoção (90%). A espectrometria de massa confirmou que houve a formação de subprodutos e/ou intermediários em todos os casos estudados. Com o estudo para a determinação do mecanismo de fotodegradação, observou-se que a degradação se dá principalmente mediante a geração do radical hidroxila, uma vez que houve a diminuição da porcentagem de degradação de 38 para 2,5%.

Como a cafeína é um marcador ambiental (e houve elevada porcentagem de degradação), sendo possível a presença de outros compostos orgânicos juntamente com a mesma, o estudo apresenta determinada relevância, pois pode ocorrer a degradação tanto da cafeína, quanto de outros compostos orgânicos que estejam no meio.

Vale ressaltar que nos processos estudados, não foram utilizados agentes oxidantes, como comumente é apresentado na literatura, tornado os resultados ainda mais relevantes frente à capacidade dos materiais obtidos serem capazes de gerar espécies que promovam a degradação de compostos orgânicos.

Artigo II: os materiais híbridos baseados em Laponita/3-cloropropiltrietoxissilano/ Melamina ou Biureto foram obtidos com sucesso, utilizando duas rotas sintéticas (hidrolítica e não hidrolítica); as propriedades texturais e a presença dos grupos funcionais (Mel ou Biu) na superfície dos materiais são influenciadas pela rota sintética. No estudo de adsorção de TMP, o tempo necessário para atingir o equilíbrio quanto a capacidade de adsorção pode ser drasticamente influenciado pela rota sintética. Ajustes matemáticos foram aplicados para

compreender o processo de adsorção, sendo que os materiais se ajustam melhor no modelo de pseudo-primeira ordem, evidenciando que o processo de adsorção ocorre por fisissorção, e ao modelo matemático de Sips, que é a combinação dos modelos de Langmuir e Freundlich.

Artigo III: o material híbrido baseado em caulinita/metaloftalocianina foi obtido em uma única etapa, síntese e imobilização; a confirmação da obtenção e imobilização da MPC em caulinita se deu pelas técnicas de FTIR, XPS e UV/Vis, observando bandas características da MPC, principalmente por XPS. A caulinita apresentou-se desorganizada, pois ocorreu o processo de dissolução parcial dos íons de Al(III) hexacoordenados (octaédricos), comprovado por RMN ^{27}Al, pois a relação entre alumínio octaédrico e tetraédrico diminuiu de 400:1, na caulinita, para 1,4:1; o alumínio "livre" dissolvido participar na síntese da ftalocianina, resultando em uma metaloftalocianina com o alumínio como íon central.

PERSPECTIVAS

A tese desenvolvida abre possibilidades na obtenção de novos materiais, compósitos ou híbridos, que sejam multifuncionais e que tenham propriedades específicas, mediante desenvolvimento de:

- Novos catalisadores e fotocatalisadores baseados em matrizes inorgânicas complexadas com macromoléculas orgânicas, para suprir dificuldades e desvantagens da utilização de dióxido de titânio;
- Utilização de radiação visível (natural ou artificial) para utilização de metaloftalocianinas como agentes de transferência de energia (efeito antena) para semicondutores.
- Diferentes rotas sintéticas de imobilização de moléculas de interesse, para obtenção de materiais aplicados à adsorção/dessorção, catálise/fotocatálise baseados em diversos argilominerais naturais e sintéticos, com reações superficiais ou no espaçamento basal;
- Produção de metaloftalocianinas por rotas sintéticas alternativas, utilizando argilominerais como reagentes doadores de íons metálicos, e sua consequente imobilização, diminuindo etapas no processo sintético de híbridos orgânico-inorgânico.

CONCLUSIONES GENERALES

Esta tesis presenta el desarrollo y estudio de nuevos materiales inorgánicos-orgánicos aplicados a procesos de adsorción y fotocatalíticos y también nuevas rutas sintéticas para obtener materiales de interés, como las metaloftalocianinas. Según las actividades expuestas, las principales conclusiones del trabajo fueron:

Artículo I: las técnicas de caracterización han probado que el dióxido de titanio y la tetracarboxiftalocianina de Co(II) fueron inmovilizados en la caolinita; las reacciones ocurrieron en la superficie de la caolinita, observando la influencia de la ruta sintética (ácida o básica) en las propiedades texturales de los materiales obtenidos. La cantidad de TiO_2 incorporado a la caolinita fue mayor en la ruta básica, debido a la generación de cargas en la superficie de la arcilla, facilitando la inmovilización. La ruta ácida produjo una menor fijación de TiO_2 debido a la generación de menos carga superficial. En los estudios de fotodegradación, el trimetoprim (30%) y la prometrina (54%) presentaron mayor dificultad de degradación, mientras que la cafeína presentó un elevado porcentaje de eliminación (90%). La espectrometría de masas confirmó la formación de subproductos y/o intermediarios en todos los casos estudiados. Analizando el mecanismo de fotodegradación se encontró que se produce principalmente mediante la generación del radical hidroxilo, una vez que el porcentaje de degradación disminuyó de 38 a 2.5%.

Dado que la cafeína es un marcador ambiental (y hubo un alto porcentaje de degradación), y la presencia de otros compuestos orgánicos junto con ella es posible, el estudio tiene cierta relevancia, ya que puede haber degradación tanto de la cafeína como de otros compuestos orgánicos que están presentes en el medio.

Es de destacar que en los procesos estudiados, no se utilizaron agentes oxidantes, como se presenta comúnmente en la literatura, lo que hace que los resultados sean aún más relevantes dada la capacidad de los materiales obtenidos para poder generar especies que promueven la degradación de los compuestos orgánicos.

Artículo II: Se obtuvieron con éxito materiales híbridos basados en Laponita/3-cloropropiltrietoxisilano/Melamina o Biuret, utilizando dos rutas sintéticas (hidrolítica y no hidrolítica). Las propiedades texturales y la presencia de dos grupos funcionales (Mel o Biu) en la superficie de los materiales vienen determinadas por la ruta sintética. En la adsorción de trimetoprim, el tiempo necesario para alcanzar el equilibrio también depende drásticamente de la ruta sintética. Se utilizaron ajustes matemáticos para comprender el proceso de adsorción, el cual se ajusta mejor al modelo de pseudo-primer orden, evidenciando que está condicionado por la fisisorción, y al modelo de Sips, que es una combinación de los modelos de Langmuir y Freundlich.

Artículo III: Se obtuvo un material híbrido basado en caolinita/metaloftalocianina en una única etapa de síntesis e inmovilización. La confirmación del proceso se obtuvo por las técnicas de FTIR, XPS y UV/Vis, observando bandas características de MPC, principalmente por XPS. La caolinita apareció desorganizada, debido a la disolución parcial de cationes Al(III) hexacoordinados (octaédricos), comprobado por RMN de ^{27}Al; la relación entre aluminio octaédrico y tetraédrico disminuyó de 400:1 en la caolinita hasta 1,4:1. El aluminio "libre" disuelto de la capa octaédrica puede participar en la síntesis de la ftalocianina, dando lugar a una metaloftalocianina con aluminio como catión central.

PERSPECTIVAS

La Tesis de Doctorado realizada abre nuevas posibilidades en la obtención de nuevos materiales, compuestos o híbridos, que sean multifuncionales y que tengan propiedades específicas, mediante el desarrollo de:

- Nuevos catalizadores y fotocatalizadores basados en matrices inorgánicas complejadas con macromoléculas orgánicas, para salvar las dificultades y las desventajas de la utilización del dióxido de titanio.
- Utilización de radiación visible (natural o artificial) en el uso de metaloftalocianinas como agentes de transferencia de energía (efecto antena) en semiconductores.
- Diferentes rutas sintéticas de inmovilización de moléculas de interés para la obtención de materiales aplicados en adsorción/desorción y en catálisis/fotocatálisis basados en diversos minerales arcillosos naturales y sintéticos, mediante reacciones en su superficie o en su región interlaminar.
- Producción de metaloftalocianinas por rutas sintéticas alternativas, utilizando minerales arcillosos como reactivos dadores de cationes metálicos, con su inmovilización consecuente, disminuyendo las etapas del proceso sintético de materiales híbridos orgánico-inorgánicos.

Anexo I
Artigos publicados

Dyes and Pigments 134 (2016) 41–50

Contents lists available at ScienceDirect

Dyes and Pigments

journal homepage: www.elsevier.com/locate/dyepig

New strategies for synthesis and immobilization of methalophtalocyanines onto kaolinite: Preparation, characterization and chemical stability evaluation

Tiago Honorato da Silva [a], Thalita F.M. de Souza [b], Anderson Orzari Ribeiro [b], Paulo Sergio Calefi [c], Katia Jorge Ciuffi [a], Eduardo José Nassar [a], Eduardo Ferreira Molina [a], Peter Hammer [d], Emerson Henrique de Faria [a, *]

[a] Gurpo de Pesquisa em Materiais Lamelares Híbridos -GPMatLam – Universidade de Franca, Av. Dr. Armando Salles Oliveira, Pq. Universitário, 201, CEP 14404-600, Franca, SP, Brazil
[b] Centro de Ciências Naturais e Humanas, Universidade Federal do ABC–UFABC, R. Santa Adélia 166, 09210-170, Santo André, SP, Brazil
[c] Instituto Federal de Educação, Ciência e Tecnologia de São Paulo – IFSP, Campus Sertãozinho, Rua Américo Ambrósio, Jd. Canaã, 269, CEP, 14169-263, Sertãozinho, SP, Brazil
[d] Instituto de Química, UNESP-Universidade Estadual Paulista, 14800-900, Araraquara, SP, Brazil

ARTICLE INFO

Article history:
Received 9 March 2016
Received in revised form
18 June 2016
Accepted 27 June 2016
Available online 28 June 2016

Keywords:
Phtalocyanines
Immobilization
Hybrid materials
Clays
Nanocomposites

ABSTRACT

This study presents results concerning the one-step synthesis and immobilization of a metallophthalocyanine on kaolinite as support/catalyst. X-ray diffractometry (XRD), nuclear magnetic resonance (NMR) and infrared (FTIR), UV/Visible (UV/Vis) and X-ray photoelectron (XPS) spectroscopies, thermal analyses, textural analyses (BET) and scanning electron microscopy (SEM) aided for the characterization of the materials. The FTIR, XPS and UV/Vis absorption spectra confirmed metallophthalocyanine formation. XRD analysis provided data on the structural disorganization of kaolinite during the synthesis of metallophthalocyanine, corroborated by SEM. NMR revealed that partial dissolution of aluminum from the octahedral kaolinite sheets was possible, which should release Al into the medium and, together with phthalonitrile, promote cyclomerization of the phthalocyanine macrocycle.

1. Introduction

Phthalocyanines are symmetric aromatic macrocycles consisting of benzopyrrole rings connected by nitrogen bonds [1,2]. This arrangement gives rise to a π electron conjugation that provides phthalocyanines with high absorption coefficient in the UV/Visible region, stable electron configuration, and excellent optical properties [3,4].

The first methods developed for the synthesis of metallophthalocyanines involved slow reactions that required high temperatures. In most cases, these conditions culminated in relatively low yields because the reactants underwent degradation and subproducts emerged in the reaction medium [5]. Over the last decades, new techniques have been developed to increase process yield and make the synthesis of metallophthalocyanines more selective. For example, cyclotetramerization of precursors derived from phthalonitriles, phthalimides, phthalic anhydride, and others has enabled the synthesis of metallophthalocyanines in moderate yields [6,7].

In aqueous medium, metallophthalocyanines form aggregates that make dispersion difficult. Methalophthalocyanine immobilization on inorganic matrixes minimizes this issue, reaching the atomic molecular scale. Moreover, immobilization increases thermal and chemical stability, improving the properties of metallophthalocyanines [8,9].

The synthetic routes available to prepare metallophthalocyanines demand significantly long purification steps and excessive amounts of energy. These routes also require the use of a variety of solvents and metallic salts or metals for phthalocyanine cyclomerization, which can contaminate the environment. To meet the principles of green chemistry and sustainability when synthesizing metallophthalocyanines, researchers have searched for new

* Corresponding author.
E-mail address: eh.defaria@gmail.com (E.H. de Faria).

http://dx.doi.org/10.1016/j.dyepig.2016.06.044
0143-7208/

Microporous and Mesoporous Materials 253 (2017) 112–122

Contents lists available at ScienceDirect

Microporous and Mesoporous Materials

journal homepage: www.elsevier.com/locate/micromeso

Laponite functionalized with biuret and melamine – Application to adsorption of antibiotic trimethoprim

Beatriz González [a], Tiago H. da Silva [b], Katia J. Ciuffi [b], Miguel A. Vicente [a, *], Raquel Trujillano [a], Vicente Rives [a], Emerson H. de Faria [b, **], Sophia A. Korili [c], Antonio Gil [c]

[a] GIR-QUESCAT, Departamento de Química Inorgánica, Universidad de Salamanca, 37008 Salamanca, Spain
[b] Universidade de Franca, Av. Dr. Armando Salles Oliveira, Parque Universitário, 201, 14404-600, Franca, SP, Brazil
[c] Departamento de Química Aplicada, Edificio de los Acebos, Universidad Pública de Navarra, Campus Arrosadía, 31006 Pamplona, Spain

ARTICLE INFO

Article history:
Received 8 May 2017
Received in revised form
23 June 2017
Accepted 24 June 2017
Available online 27 June 2017

Keywords:
Laponite
Biuret
Melamine
Organophilization
Clay
Trimethoprim adsorption

ABSTRACT

Laponite-aminosilane hybrid materials have been prepared by reaction of a chlorosilane, (3-chloropropyl)triethoxysilane, with two aminated compounds, namely, biuret and melamine. The resulting compounds were used for the functionalisation of laponite, using two synthesis procedures. The hybrid materials thus formed were fully characterised and tested for the adsorption of the antibiotic Trimethoprim (trimethoxybenzyl-2,4-pyrimidinediamine). The characterisation results showed that functionalisation was successful, and the adsorption experiments showed a high affinity of the hybrid materials for the removal of Trimethoprim, with removal percentages larger than 80%.

1. Introduction

Clay minerals are hydrophilic materials, but for several uses it is even mandatory to confer their surface an organophilic nature by the incorporation of organic species to favour their interaction with other organic species (polymers, pollutants, etc.) [1,2]. Among such uses, the formulation of Clay-Polymer Nanocomposites (CNP) is particularly important, but the use of clay minerals in the preparation of paints, cosmetics or personal care products, in the adsorption of pollutants, or as rheological control agents, are other relevant applications that require the clay minerals having an organophilic surface. The organic species incorporated may act as ligands to metal cations, allowing the preparation of catalysts, sensors, luminescent agents, etc. For these reasons, organophilisation of clay minerals has been widely studied.

The strategy for organophilisation is usually fitted to the clay minerals considered. For instance, tetrasubstituted quaternary alkyl-ammonium ions have been mainly used to functionalise swellable smectites by intercalation in the interlayer region substituting their natural occurring charge-balancing exchangeable cations; these formulations are even commercially available (Cloisite®). Grafting of organo-silanes onto several clays, particularly silanes containing other functional groups such as amine, mercapto or chlorine, has received increasing interest in the last years, opening new potential applications for these materials [3,4].

Kaolinite can be organophilised by a multi-step, host-guest displacement method, beginning with small and very polar molecules, and then substituting them by the final functionalising molecules. This special procedure is used because kaolinite has no exchangeable cations and organophilisation cannot be attained by ionic exchange; moreover, swelling of the strongly bonded layers is very difficult [5].

Laponite is a commercially available synthetic hectorite. It exfoliates very easily in aqueous suspension, and solid samples do not show a long order in their stacking direction. Its exchangeable cations can be substituted by cationic species, but without

* Corresponding author.
** Corresponding author.
E-mail addresses: mavicente@usal.es (M.A. Vicente), emerson.faria@unifran.edu.br (E.H. de Faria).

http://dx.doi.org/10.1016/j.micromeso.2017.06.047
1387-1811/

JBCS 30 yrs

http://dx.doi.org/10.21577/0103-5053.20190178

J. Braz. Chem. Soc., Vol. 00, No. 00, 1-14, 2019
Printed in Brazil - ©2019 Sociedade Brasileira de Química

Article

Kaolinite/TiO_2/cobalt(II) Tetracarboxymetallophthalocyanine Nanocomposites as Heterogeneous Photocatalysts for Decomposition of Organic Pollutants Trimethoprim, Caffeine and Prometryn

Tiago H. da Silva,[a] Anderson O. Ribeiro,[b] Eduardo J. Nassar,[a] Raquel Trujillano,[c] Vicente Rives,[c] Miguel A. Vicente,[c] Emerson H. de Faria[,a] and Katia J. Ciuffi*[,a]*

[a]*Universidade de Franca, Av. Dr. Armando Salles Oliveira, 201, Pq. Universitário, 14404-600 Franca-SP, Brazil*

[b]*Centro de Ciências Naturais e Humanas, Universidade Federal do ABC, 09210-170 Santo André-SP, Brazil*

[c]*GIR-QUESCAT, Departamento de Química Inorgánica, Universidad de Salamanca, 37008 Salamanca, Spain*

São Simão's Brazilian kaolinite has been treated with titanium(IV) isopropoxide and cobalt(II) tetracarboxymetallophthalocyanine under different conditions (acidic or basic), leading, after drying at 100 ºC, to new titania-doped Co(II)-metallophthalocyanine/kaolinite solids. These solids were characterized by chemical analysis, powder X-ray diffraction, Fourier transform infrared spectroscopy, thermal analyses and nitrogen adsorption. No significant changes were observed by diffractometry, but the specific surface area depended of the synthetic route followed. The ability of these solids for photodegradation of trimethoprim, caffeine and prometryn was evaluated. The photodegradation was followed via mass spectrometry and UV-Vis absorption spectroscopy. The presence of photodegradation by-products was verified in all cases. All the photocatalysts showed high photodegradation rate against prometryn, trimethoprim and caffeine, the degradation efficiencies were 54, 30 and 90%, respectively, when using the heterogeneous photocatalysts. Comparison with commercial TiO_2 (Degusa®) proved that the synthesized photocatalyst based on kaolinite present higher degradation rate than isolated titanium dioxide.

Keywords: clay minerals, sol-gel, heterogeneous photocatalysis

Introduction

The humankind uses large amounts of chemicals/pharmaceuticals in numerous areas as cosmetics, medicine and industrial.[1,2] This excessive consumption could promote an exponential increase in the productive processes of these compounds, which results on the discharge of untreated wastes or partially treated wastewater in natural environments. This incorrect disposal may directly contaminate surface or underground water.[3] In this way, the concern about drinking water should lead to the development of more efficient processes for the treatment of water and wastewater, aiming at environmental preservation. In this context, advanced oxidation process is a promising technology that does not require large cost for up-scaling to technological application and results in higher yields of degradation of organic compounds promoting in some cases the complete mineralization of the pollutants.

Nowadays, the emerging organic pollutants (EOPs) are defined as synthetic or naturally occurring chemicals that are not commonly monitored in the environment, but which have the potential to enter the environment and cause known or suspected adverse ecological and (or) human health effects. More than 700 emerging pollutants, their metabolites and transformation products, have been found in European aquatic environments.[4] These emerging pollutants, and their metabolites and transformation products, have been listed by Norman Network (2017).[5]

In this context, trimethoprim [2,4-diamine 5-(3,4,5-trimethoxybenzyl)pyrimidine] (TMP) is a widely used antibacterial drug for treatment of urinary, respiratory or gastrointestinal infections, with application in humans

*e-mail: katia.ciuffi@unifran.edu.br; eh.defaria@gmail.com

Study Of Reliability Of Thermal Analysis Technique In The Quantification Of Organic Material In Physical Mixture Of Kaolinite And Tris(Hydroxymethyl)Aminomethane

Tiago H. da Silva*, Márcio J. dos Reis, Emerson H. de Faria, Katia J. Ciuffi, Eduardo J. Nassar, Paulo S. Calefi*

Universidade de Franca, Av. Dr. Armando Salles Oliveira, PQ. Universitário, 201, Franca-SP, Brasil

Abstract

Usually hybrid materials are characterized by thermal analysis and elemental analysis to determine the ratio of organic/inorganic material. However, statistical errors are usually not taken into account for these techniques. In this work we applied a statistical analysis to determine the reliability of the thermal analysis technique in the quantification of organic material in a mixture of Kaolinite and tris(hydroxymethyl)aminomethane. The results showed that both techniques have a higher degree of reliability depending on the quantity range. The results to organic/inorganic molar ratio 0.52 to 0.62 are better represented by thermal analysis technique, and 0.1 to 0.3 for elemental analysis.

Keywords: : Statistical treatment, hybrid material, kaolinite, functionalization.

1. Introduction

Usually intercalation and/or functionalization of clay are well characterized by X-ray diffraction, but, thermo analytical techniques have been shown to be a very powerful tool for identifying structural changes, thermal stability of the material and also determine stoichiometrycally the relative amount of organic matter in the hybrid material. Functionalized kaolinite has been characterized to determine the ratio of organic/inorganic matter using thermal analysis combined with elemental analysis [1-4]. de Faria et. al. [5] has been used thermal analysis and elemental analysis to verify the thermal stability of a hybrid kaolinite functionalized with pyridine carboxylic acids and determine the ratio of organic/inorganic matter and the results obtained were similar for both techniques. Detellier et. al. [3] have been used thermal analysis coupled with mass spectrometry to identify the processes involved in the decomposition of kaolinite with 3-aminopropyltriethoxysilane and quantifier the fragments released in the decomposition. From the results obtained it was possible to determine the stability resistance for hydrolysis of the materials. Avila et. al. [1] reported the results obtained by thermal analysis to determine the amount of organic matter present in the kaolinite functionalized with organosilanes and from the results obtained, the authors determined stoichiometriccally the formulas of the hybrids.

This work is focused on the quantification of organic matter of mixtures of kaolinite and tris(hydroxymethyl)aminomethane (TRIS) by means of thermal and elemental analysis. A statistical study was done to verify the reliability of the thermal analysis technique by termogravimetric curve and it derivate.

2. Experimental procedures

2.1 Physical mixture of Ka and TRIS

To verify the reliability of the results

* *Corresponding author: Tel.: (+55) 16 3711-8969*
E-mail address: tiagohonoratosilva@hotmail.com and/or pscalefi@unifran.br

Dyes and Pigments 100 (2014) 17–23

Contents lists available at ScienceDirect

Dyes and Pigments

journal homepage: www.elsevier.com/locate/dyepig

Immobilization of metallophthalocyanines on hybrid materials and in-situ synthesis of pseudo-tubular structures from an aminofunctionalized kaolinite

Tiago Honorato da Silva [a], Thalita F.M. de Souza [b], Anderson Orzari Ribeiro [b], Katia Jorge Ciuffi [a], Eduardo José Nassar [a], Marcio L.A. Silva [a], Emerson Henrique de Faria [a], Paulo Sergio Calefi [a,*]

[a] Universidade de Franca, Av. Dr. Armando Salles Oliveira, Pq. Universitário, 201, CEP 14404-600 Franca, SP, Brazil
[b] Centro de Ciências Naturais e Humanas, Universidade Federal do ABC–UFABC, R. Santa Adélia 166, 09210-170 Santo André, SP, Brazil

ARTICLE INFO

Article history:
Received 22 April 2013
Received in revised form
18 July 2013
Accepted 18 July 2013
Available online 26 July 2013

Keywords:
Amino-functionalized kaolinite
Tris(hydroxymethyl)aminomethane
Cobalt(II) tetracarboxyphthalocyanine
Hybrid material
Pseudo tubular
Exfoliated kaolinite

ABSTRACT

The results from a study of the immobilization of cobalt(II) tetracarboxyphthalocyanine on a kaolinite functionalized with tris(hydroxymethyl)aminomethane are presented. The resulting materials were characterized by X-ray diffraction, thermal analyses, infrared and ultraviolet–visible absorption spectroscopy, and scanning and transmission electron microscopy. The detection of some bands typical of cobalt(II) tetracarboxyphthalocyanine by infrared spectroscopy confirmed immobilization of the complex on the amino-functionalized kaolinite and showed that there were no alterations in the interlayer hydroxyl groups of kaolinite, and also evidenced that immobilization occurred via the amine. The X-ray diffraction analysis revealed that the immobilization process prompted a structural change in the functionalized kaolinite, leading to the formation of a non-layered material. Solid state UV–Vis spectroscopy attested to the immobilization of the cobalt(II) tetracarboxyphthalocyanine on the amino-functionalized kaolinite, as verified from the appearance/displacement of some bands characteristic of the metal complex.

1. Introduction

Metallophthalocyanines (MPcs) belong to a class of synthetic compounds that closely resemble natural porphyrins, with the advantage that they are much more chemically and physically stable [1,2].

Some authors [3,4] mention that one disadvantage of MPcs is their poor solubility in an aqueous media and in a number of organic solvents, which limits their use in homogeneous catalysis. This drawback can be overcome by substituting the peripheral groups of MPcs with sulfate or carboxylate, as in the case of cobalt(II) tetracarboxyphthalocyanine (II) (Co(II)MPc, Fig. 1).

However, De Oliveira et al. [5] have reported on the difficult separation of water-soluble MPcs, which restricts their application as photocatalysts and makes their incorporation into inorganic matrices necessary. These authors presented results for phthalocyanine attached to mesoporous silica, which found potential application in pesticide photodegradation. Indeed, excellent catalytic activity was achieved for the immobilized phthalocyanine, with yields increasing from 40 to 90% ongoing from homogeneous to heterogeneous media [5]. Ernst et al. have also published data on the catalytic activity of MPcs immobilized onto molecular sieves, which gave much better yields as compared to the free compound in homogeneous solution [6]. Apart from the aforementioned works there are countless articles describing the advantages of employing MPcs immobilized on various matrices for heterogeneous catalysis. Such advantages include facile separation from the product from the catalyst, recycling, and reuse of these catalysts, not to mention their higher catalytic activity [7,8].

MPc immobilization on an inorganic matrices allows for better dispersion of the macromolecules. This enables better exploration of the MPc properties, since in aqueous medium (and in some other solvents) these complexes form aggregates. Moreover, immobilization provides enhanced stability as well as improved thermal and chemical resistance [5,6]. In this context, layered clay minerals have been widely employed as supports for the immobilization of compounds for a variety of applications [9,10]. Among the clay

* Corresponding author. Tel.: +55 16 3711 8969; fax: +55 16 3711 8878.
E-mail addresses: eh.defaria@unifran.br (E. Henrique de Faria), pscalefi@unifran.br (P.S. Calefi).

0143-7208/$ – see front matter © 2013 Elsevier Ltd. All rights reserved.
http://dx.doi.org/10.1016/j.dyepig.2013.07.019

IIAT Instituto Internacional de Análise Térmica

Available online at www.bjta.iiatbr.org
Braz. J. Therm. Anal. Vol. 4 No. 1-2 (2015) 21 – 27
DOI: 10.18362/bjta.v4.i1-2.57

Brazilian Journal of Thermal Analysis BJTA

Estudo por análises térmicas de compósitos caulim/pigmentos da indústria couro-calçadista

R. R. de Oliveira[1], T. H. da Silva[1], E. H. de Faria[1], L. A. Rocha[1], K. J. Ciuffi[1], P. S. Calefi[2], E. J. Nassar[1]*

[1]*Universidade de Franca, Av. Dr. Armando Salles Oliveira, 201 Pq. Universitário, Franca/SP CEP 14404-60, Brasil.*
[2]*Instituto Federal de Educação,Ciência e Tecnologia de São Paulo, Av. Pastor José Dutra de Moraes, 239.CEP: 15808-305 Catanduva – SP, Brasil.*

Received: 15/11/2014; accepted: 19/02/2015
Available online: 30/06/2015

Resumo

A indústria couro-calçadista utiliza uma variada lista de pigmentos ou combinação deles para promover a coloração aos seus produtos finais, a utilização de dois ou mais pigmentos podem gerar problemas como a homogeneidade da mistura, acarretando diferenças na cor final. Neste sentido, com o intuito de solucionar esse impasse, este trabalho teve como principal objetivo obter compósitos pigmento/caulinita (pigmento amarelo e vermelho) e a sua utilização como cargas pigmentadas na indústria calçadista. Assim, compósitos desses pigmentos foram preparados com uma argila natural caulinita previamente intercalada com dimetilsulfóxido (DMSO), utilizou-se o método do deslocamento na tentativa de substituir as moléculas de DMSO pelos pigmentos. Os compósitos coloridos resultantes foram empregados na confecção de placa de borracha. As técnicas de caracterizações comprovaram que as integridades químicas e físicas dos pigmentos nos compósitos foram preservadas. O produto final obtido com os compósitos apresentou coloração adequada e homogeneidade superior quando comparados aos pigmentos.

Palavras-chave: caulinita, artefatos de borracha, compósitos.

1. Introdução

Pigmentos são substâncias químicas responsáveis pelas colorações de uma variedade de produtos industrializados, podendo ser naturais ou sintéticos, os quais são amplamente utilizados na indústria calçadista. A incorporação desses pigmentos em artefatos de borracha ocorre principalmente através da mistura físicas podendo sofrer influências de vários fatores, tais como: matérias primas empregadas, impurezas, composição, armazenagem, concentração, técnicas de mistura, entre outras.

O Brasil é um dos maiores produtores mundiais de calçados, com as mais diversas cores e estampas que proporcionam um toque sutil para todas as estações do ano, cabe ressaltar as riquezas que o país movimenta em torno das exportações de calçados. Com base nestes dados e nas inúmeras cores produzidas nas indústrias de artefatos de borracha, existe uma dificuldade que impede a obtenção de algumas cores, isso se deve a perda das propriedades dos pigmentos em função da temperatura. A vulcanização da borracha é realizada em temperaturas na ordem de 160 °C e na maioria das vezes são utilizados diferentes pigmentos para conseguir a tonalidade desejada. Nesta temperatura alguns pigmentos podem iniciar um processo de degradação, o que descaracteriza a cor pretendida. Apesar de muitos fabricantes disponibilizarem pigmentos com alta resistência térmica, esses apresentam custo elevado e mesmo assim podem ainda sofrer degradação.

A indústria de artefatos de borrachas utiliza diferentes produtos na sua composição para melhorar suas propriedades, como estabilidade térmica, mecânica, física e química, os quais podem atuar como cargas de reforço, pigmentos e os dois ao mesmo tempo [1-13].

As argilas têm se destacado em vários segmentos industriais apresentando uma diversificação nas aplicações, tais como catalisadores [14-18], argila-corante [19], materiais híbridos [20-23], materiais luminescentes [24] e adsorventes [25].

Nos últimos anos os efeitos da adição de nanopartículas incorporados em matrizes poliméricas, em particular silicatos lamelares organomodificados vem sendo estudado, principalmente relacionadas às suas propriedades termo-mecânicas [26-32]. Apesar de um grande número de artigos publicados com o tema compósitos e polímeros, e conferências especificas sobre o assunto, pouco enfoque tem sido dada à utilização de argilominerais como estabilizante e/ou dispersantes de pigmentos utilizados na indústria calçadista. Em recente pesquisa na literatura, foi encontrado um artigo que estudou a influência da interação pigmento/argila (tioindigo/palygorkite) na cor final do pigmento utilizando a espectroscopia Raman e FTIR, sem a incorporação em artefatos de borracha [33]. A modificação das propriedades físicas e químicas de diversos tipos de polímeros tem sido realizada com a adição de hidróxidos duplos lamelares [34], outros estudos também vêm sendo realizados, como estabilidade de silicone com a adição de

* **Corresponding author:** Tel.: +55 16-3711-8888
E-mail address: eduardo.nassar@unifran.edu.br (E. J. Nassar)

Applied Clay Science 168 (2019) 469–477

Contents lists available at ScienceDirect

Applied Clay Science

journal homepage: www.elsevier.com/locate/clay

Research Paper

Catalytic activity of porphyrin-catalyts immobilized on kaolinite

Thais E. Cintra[a], Michelle Saltarelli[a], Rosangela M. de F. Salmazo[a], Tiago Honorato da Silva[a], Eduardo J. Nassar[a,*], Raquel Trujillano[b], Vicente Rives[b], Miguel A. Vicente[b], Emerson H. de Faria[a], Katia J. Ciuffi[a,*]

[a] Universidade de Franca, Av. Dr. Armando Salles Oliveira, 201 - Pq. Universitário, 14404-600 Franca, SP, Brazil
[b] GIR-QUESCAT, Departamento de Química Inorgánica, Facultad de Ciencias Químicas, Universidad de Salamanca, 37008 Salamanca, Spain

ARTICLE INFO

Keywords:
Ironporphyrin
Kaolinite
Oxidation reactions
Degradation of dyes

ABSTRACT

Two new biomimetic iron-porphyrin heterogeneous catalysts prepared by grafting of iron(III)-5,10,15,20-tetrakis(4-hydroxyphenyl)porphyrin (FeTHPP) on 3-chloropropyltrimethoxysilane (ClPTMS) functionalized kaolinite and on a silica prepared through hydrolysis and condensation of tetraethylorthosilicate (TEOS) and ClPTMS, are reported. The catalysts were characterized and tested for the epoxidation of (*Z*)-cyclooctene and oxidation of cyclohexane using iodosylbenzene as oxygen donor. The position of the Soret band confirmed that the structure of FeTHPP was preserved in the final solids. All catalysts showed a high conversion of the substrates, with total selectivity to the epoxide in the oxidation of cyclooctene, and high selectivity to the ketone in the oxidation of cyclohexane. The catalysts were also used for degradation of dyes in aqueous solutions. The ferroporphyrin-silica catalyst showed the best behavior for (*Z*)-cyclooctene (48% epoxide) and cyclohexane (48% conversion, sum of alcohol and ketone as products) and also for the degradation of the dyes (97% for methylene blue, although with simultaneous adsorption, close to 85% for Orange II and Brilliant Green), while the ferroporphyrin-kaolinite system showed the best behavior for cyclohexane oxidation (48%, with total selectivity to the ketone).

1. Introduction

Heterogeneous catalysts have numerous applications in vital areas such as food production and the pharmaceutical and chemical industries. An estimated 90% of all the chemical processes use heterogeneous catalysts, which are also used in emerging fields like fuel cells, green chemistry, nanotechnology, biotechnology, and biorefineries (Boudart et al., 2008; Zaera, 2013).

Considerable effort has been devoted for improving the technology involved in the production of chemicals through oxidation reactions. Methods to accomplish the selective oxidation of organic substrates with atom economy (i.e., methods that use fewer atoms along the oxidation reaction) have become the largest research field in today chemistry both in the academic and in the industrial fields (Sheldon, 2007; Sheldon and Woodley, 2018).One strategy has been to move from harmful reagents and oxidants to more environmentally friendly substances. Another strategy has been to reduce the amount of energy consumed throughout the oxidation process (Sheldon, 2007; Sheldon et al., 2007; Boudart et al., 2008; Cavani, 2010; Dichiarante et al., 2010). To achieve a higher efficiency in the chemical industry and to ensure the development of greener and more selective catalytic oxidation reactions, more detailed research involving transformation of certain types of molecules is mandatory. Investigations into new heterogeneous catalysts and/or alternative oxidants that will help to enhance reaction selectivity toward the target products still remain a challenge in the area of catalysis (Rothenberg, 2008; Deutschmann et al., 2009; Cavani, 2010; Vidal et al., 2018).

The development of new active, selective, and recyclable catalysts within the context of green chemistry is an urgent matter. The interest in the search for new multifunctional hybrid materials that meet the requirements of Green Chemistry has grown recently. This is because hybrid materials combine maximum usability with environmental compatibility, mimicking Nature.

To attain this goal, a selective heterogeneous catalyst should containing an isolated and well-defined active center resembling the prosthetic group of biological enzymes like the cytochrome P450 monooxygenases P450 (Thomas and Raja, 2006; Goti and Cardona, 2008; Stair, 2008; Jung, 2011), where a protein, globin, isolates the active site of P450, an iron protoporphyrin IX (Groves, 1995; Suslick, 1999; Costas et al., 2000; Meunier et al., 2004; Mansuy, 2007). Among its many features, the "isolated site principle" controls the access of the substrate to the active site and the oxidation reaction selectivity. The

* Corresponding author.
E-mail addresses: eduardo.nassar@unifran.edu.br (E.J. Nassar), katia.ciuffi@unifran.edu.br (K.J. Ciuffi).

https://doi.org/10.1016/j.clay.2018.12.012
Received 21 June 2018; Received in revised form 3 December 2018; Accepted 11 December 2018
Available online 19 December 2018
0169-1317/